TRANSPARENT GLASS-CERAMICS AND

INTERACTION WITH ALKALI METAL VAPOURS

by

John Lau

A thesis submitted for the
degree of Doctor of Philosophy
of the University of Warwick

Department of Physics

July 1980

CONTENTS

List of Figures

List of Tables

To my parents and close friends

for their unfailing support

Acknowledgements

I am grateful to Professor P. W. McMillan for his supervision and generous encouragements throughout the course of this work, and for his assiduity in the reading of this manuscript. I would also like to thank Professor A. J. Forty for making the departmental facilities available to me, for his interest in this work and help on a number of occasions.

I am indebted to Professor J.E. Castle and Mr. R.H. West of the University of Surrey for allowing me to use their ESCA spectrometer, and for their expert advice on the analysis of experimental data. I wish to thank Mr. D.T. Evans and Dr. V. Goddard of Thorn Lighting for the use of the DTA equipment, and for carrying out the prolonged sodium exposure of some of the specimens. Thanks are also due to Dr. R.W.T. Rabbetts of ITT Quartz Crystal Division for the provision of the quartz crystals, Freeman and Procter Welding Engineers of Nuneaton for the skilful welding of the stainless steel crucibles used in this work, and Mr. A.S. Brown for the melting of the sodium silicate and sodium alumino-silicate glasses.

I would like to thank past and present members of the Glass-Ceramics group, and in particular, Ms. L. Heath, Mr. A. Chelibik, Dr. R. Maddison and Dr. R.F. Pettifer for helpful discussions and constructive (or otherwise) comments on this work.

Finally, I would like to thank the technical staff, particularly Mr. G. Smith and Mr. J. Stanley, who have assisted me during the course of this work, and Mrs. C. Parrott for her careful typing of this manuscript.

MEMORANDUM

This dissertation is submitted to the University of Warwick in support of my application for admission to the degree of Doctor of Philosophy. It contains an account of my work carried out principally at the Department of Physics of the University of Warwick during the period October 1976 to September 1979 under the general supervision of Professor P. W. McMillan. No part of this dissertation has been used previously in a degree thesis submitted to this or any other university. The work described is the result of my own independent research except where specifically acknowledged in the text.

July 1980

John Lau.

Abstract

The aims of the project were to investigate the fundamental processes involved when a glass is exposed to sodium vapour, and to examine the different ways of improving the resistance towards sodium attack.

With regard to the interaction of glasses with sodium, the silicates were studied in most detail. The discolouration of the silicate glasses by sodium was treated as a surface phenomenon and techniques such as ESCA, IRRS and ESR were used to investigate the interaction. The results from these various techniques all point to the same conclusion, that the mechanism of sodium attack is the progressive breaking of Si-O bonds to form $Si-O^-$ bonds. The reaction between borate glasses and sodium showed certain similarities with the silicates. This led to the suggestion that the same mechanism of attack might also apply to the borates.

In attempting to improve the resistance of transparent materials towards sodium attack, two methods were considered. The first approach was to change the chemical composition by selecting components of a glass which are inert to sodium. The chemical compatibilities of the components were assessed using an equilibrium thermodynamic argument to consider the possible reactions with sodium, and a number of materials have been suggested to be inert in this way.

The second method of improving the resistance was to rearrange the structure of a glass by crystallisation. The crystallisation behaviour and the microstructures of two glass compositions -

MgBAℓ (3-2) and CAℓ (6) were studied in detail, and transparent glass-ceramics were derived from them. It was found that the improvement in resistance towards sodium attack was only marginal in the case of crystallising the glasses in bulk. However, substantial improvements were observed in the case of surface crystallisation.

CHAPTER 1 : Introduction

1.1.1 Glasses

The term "glass" in normal usage is associated with materials used in the fabrication of bottles, lenses etc. From just everyday experience the diverse properties and consequent utilisation of these materials are already apparent, the different colours of stained glass windows, the resistance of ovenware to thermal shock or the toughness of motor car windscreens are a few examples. Yet there are numerous other less common glasses which are also exploited for their even greater variety of properties. For example neodymium doped glasses in lasers, chalcogenide glasses for their semi-conducting characteristics, or high lead content glasses as radiation shields. Many of the advances made in the past in discovering new glasses were carried out on an empirical basis, whilst systematic investigations were hampered by the fact that over sixty elements in the periodic table in different combinations and proportions can form glasses [Pye (1972)]. However, the immense technical and commercial importance of "glass" has stimulated the need for a more thorough understanding of these materials.

The term "glass" in a scientific context also implies a state of matter - the vitreous state. A state in which the arrangement of atoms or molecules of the material exhibit short range order only, lacking the periodicity or long range order of that of the crystalline state. The most general definition of glass, given by Secrist and MacKenzie (1964), is that it is a non-crystalline solid. As this non-crystalline state can be arrived at via different methods [Rao and Rao (1978)] such as melting, vapour deposition or neutron bombardment, an operative definition for the present work is that glass is a non-crystalline solid

formed from the melt.

In order to understand qualitatively at least, why certain compositions form glasses when melted, it is important to bear in mind certain properties of liquids. Most liquids have a viscosity η which is dependent on the temperature (given by the empirical relationship of the form $\eta = \eta_o \exp[Q/kT]$) i.e. η increases with decreasing temperature. The process of crystallisation in a liquid can only take place via nucleation and the subsequent growth of nuclei (Appendix 1) and the rate of crystal growth is dependent on the reciprocal of viscosity [Turnbull and Cohen (1960)], i.e. if the viscosity of the liquid is high, the diffusion of atoms from the liquid phase to the crystalline phase is restricted, resulting in a slow rate of crystal growth.

Now consider the situation of a "simple" liquid being cooled at a certain rate. When the liquid is cooled below its melting temperature and if care was taken to exclude the presence of any nuclei, or the viscosity is such that the rate of crystal growth is very slow, then the liquid will become supercooled with the liquid still retaining its "liquid-like" structure. As the temperature is lowered, the arrangement of atoms or molecules of the supercooled liquid relaxes to a new configuration in equilibrium with the temperature. This relaxation process involves a characteristic time dependence given by η/G [Rao and Rao (1978)] where G is the shear modulus. Remembering that the viscosity increases with decreasing temperature, the time required for the structure of the supercooled liquid to relax in equilibrium with temperature also increases with decreasing temperature. As cooling continues, a point will be reached when the structure of the supercooled liquid will no longer be able to relax rapidly enough to be in equilibrium with the decreasing temperature. In other words, the viscosity of the supercooled liquid has increased to such an extent (

without crystallising) that its structure has effectively been "frozen in". The temperature at which the structure departs from equilibrium is called the "transformation temperature Tg" and it is dependent on the rate of cooling. For any further cooling below Tg, the supercooled liquid becomes a glass and the viscosity is so large that the glass for all intents and purposes behaves like a solid.

In principle then, any liquid can be supercooled to form a glass provided it can be quenched from the liquidus temperature down to the transformation temperature in a time short compared to that required for nucleation and crystal growth. For more detailed discussions on the subject of glass formation and the properties of glass in general, books by Doremus (1973), Jones (1971), MacKenzie (1960), Pye, Stevens and LaCourse (1972) and Rawson (1967) are referred to.

1.1.2 Glass-Ceramics and Transparent Glass-Ceramics

When a liquid is cooled below its melting temperature in the absence of any nuclei or a glass is heated above its transformation temperature, they are in a supercooled state. This supercooled state from a thermodynamic viewpoint is meta-stable since its Gibbs free energy is higher (because of the higher configurational entropy) than that corresponding to the crystalline state. However, in the presence of nuclei of an adequate size such that crystal growth may proceed, the supercooled state becomes unstable and will have a natural tendency to revert to the lower energy crystalline state. The possibility then exists for a glass to be used as a precursor for derivative materials providing the nucleation and crystallisation processes can be controlled carefully, i.e. through the use of suitable heat treatments. Materials derived from the controlled crystallisation of glasses are known as "glass-ceramics" [McMillan (1979)]. The range of properties obtainable in glass-ceramics

can be potentially much wider than that offered by glasses since they can in principle be varied continuously from those associated with the parent glass to those corresponding to the crystals depending on the proportions and microstructures of the different phases.

One of these diverse properties is that the microstructure of a glass-ceramic can be varied such that it can become either opaque, translucent or transparent to visible light. To explain this property, it is necessary to examine the scattering of light in a medium containing inhomogeneities as in the case of glass-ceramic with crystals embedded in a glassy matrix. If a beam of monochromatic light is incident on such a medium, the scattering of light will occur whenever there are regions or particles having a different refractive index to that of the medium, and as a result the intensity from the main beam will be reduced. If the particles are assumed to be spherical and small compared with the wavelength of light (Rayleigh scattering), then the intensity of light $I(\theta)$ scattered by one of these particles is given by [Beall and Duke (1969)]

$$I(\theta) = \frac{I_o 8\pi^4 a^6}{r^2 \lambda^4} \left| \frac{M^2-1}{M^2+2} \right|^2 (1 + \cos^2\theta) \qquad (1.1.1)$$

where I_o is the intensity of the incident beam, θ is the scattering angle, r is the distance from the scattering centre to the point of observation, a is the radius of the particle, λ is the wavelength of light and M is the ratio of the refractive index of the particles to that of the surrounding medium.

The criterion then for obtaining high transparency is to minimise $I(\theta)$ and can be achieved if either $a \ll \lambda$, or $M \simeq 1$. Therefore, when a glass-ceramic is transparent, either the crystalline phase present is of

a size much smaller than the wavelength of visible light, or there is close matching in the refractive indices between the crystalline phase and the glassy matrix, or both. When a glass-ceramic is translucent or opaque to visible light, this implies either that the size of the crystals is large compared with the wavelength, or there is a large mismatch in the refractive indices between the glass and crystal phase, or both. Whether a glass-ceramic is termed transparent or translucent, the mechanism bringing about the reduction in intensity of transmitted light is the same. The terms transparent and translucent are used for a purely desriptive purpose and any distinction between the two will be of an arbitrary nature. It should also be pointed out that the above equation is not strictly valid for particles large compared with the wavelength (the more general Mie theory [Born and Wolf (1965)] has to be used), but the important parameters, i.e. the particle size and the ratio of the refractive indices, remain the same. Therefore, by controlling the rate of crystal growth, a glass-ceramic can become transparent, translucent or entirely opaque.

The many varied applications and properties of glass-ceramics have been describe in detail by McMillan (1979); and since the processes of nucleation and crystallisation in a supercooled liquid are fundamental to the formation of glass-ceramics, the theory behind these processes has been extracted from a number of authors and it is summarised in Appendix 1 for completeness.

1.2 Review of the Interaction of Glasses with Alkali Metal Vapour

Alkali metals have found many applications in technology. Amongst their proposed uses are those associated with the conversion of energy to

electricity, such as in controlled thermonuclear reactors and high specific alkali-sulphur batteries. In these energy conversion systems, the alkali metals are used either as a coolant or as a conductor. Since the alkali metals present an extremely corrosive environment, particularly at high temperatures (300-700 °C) in which these energy conversion systems operate, stringent requirements are placed upon the materials used for the containment of alkali metals. Any potential containment material must therefore be chemically compatible with the alkali metals at high temperatures whilst maintaining its structural integrity when subjected to large thermal gradients and extensive thermal cycling.

Another use of alkali metals is in the lighting industry, namely in discharge lamps. The low-pressure sodium vapour discharge lamp has high luminous efficacy (>150 lm/W), over two and a half times that of an inert gas filled incandescant lamp [Henderson and Marsden (1972)]. When used in conditions where colour discrimination is not important, such as in street lighting, the sodium vapour lamp presents an extremely economical source. The materials used for the containment of the sodium discharge have a different set of criteria to satisfy apart from the chemical compatibility aspect. The lamp envelope has to be an insulator, the ability to transmit light and its thermal expansion coefficient should match closely with that of the metals used for electrodes and lead wires in order to form a hermetic seal. These specific requirements restrict severely the kind of materials that can be used and glass is probably the most attractive candidate.

The need to find suitable materials for the containment of alkali metals has resulted in extensive research being carried out on the chemical compatibility of refractory metals [Smith and Natesan (1974)] and ceramics [Singh (1976)] with alkali metals. Since the present work

is connected with the lighting industry, the subject of this review is concerned with the interaction of alkali metals with transparent materials, namely glasses.

One of the earliest works reported on the interaction of alkali metals with transparent materials was that by Fonda and Young (1934) in which they exposed hot sodium vapour to a number of different silicate glasses of unknown composition. The glasses were found to discolour after a few hours and the intensity of the discolouration increased with increasing time of exposure. The discolouration which ranged from a yellow, brown or black colour was confined to a film on the surface where it had been exposed to the vapour. In cases where the black discolouration occurred, they attributed that to the chemical disintegration of the glass resulting in the formation of silicon [Hoffman (1933)]. In the case of more resistant glasses where the discolouration is yellow in colour, they found bleaching of the discolouration occurs if the specimens were reheated in a vacuum without the presence of sodium. They tentatively suggested the discolouration may be due to diffusion of sodium atoms into the glass with possible segregation into aggregates of colloidal size. This process is reversible as demonstrated by the bleaching of the discolouration.

Wheeldon (1959) exposed "sodium resistant" glasses, soda lime and borosilicate glasses to sodium vapour under both discharging and non-discharging conditions. He found there was no observable difference between the discolouration. Wheeldon also carried out similar bleaching experiments as Fonda and Young (1934). He found the discolouration did not always disappear, so the discolouration process is not always reversible. From a sodium resistant sample which had been exposed to sodium at 350 °C for 224 hours, he observed that the discolouration advances through the glass surface with a sharp front. This he had taken

to mean an abrupt change in composition and he concluded that the discolouration associated with the absorption of sodium is not a straight forward diffusion process. The thickness of the discoloured layer was estimated to be ~ 5 microns and the concentration of sodium in this layer was estimated to be ~ 2×10^{22} atoms cm^{-3}.

The earliest attempt to study systematically the interaction of alkali metals with glasses is the work by Elyard and Rawson (1962). They studied the effect of exposing glasses of simple composition from different glass forming systems to sodium vapour for the same length of time and the same temperature. By assessing the extent of the discolouration on a colour scale, they were able to draw several general conclusions. They found for a particular glass system, the resistance to sodium attack increases as the ratio of modifying oxide to network forming oxide is increased. For glasses from different systems where the ratio of modifiers to network formers is the same, the glasses in increasing order of resistance to sodium attack are phosphates, silicates, borates, aluminoborates and aluminates. They attributed the mechanism of attack to the chemical reduction of the glasses and used convincing thermodynamic arguments to explain the observed resistance of the various glasses to sodium attack.

At variance with this view is the work by Burns (1965). Burns measured the optical density of vitreous silica capsules containing small amounts of sodium over the temperature range 250-500 °C in situ. The optical density was found to increase with time and temperature. The measured rate of increase of optical density of the discolouration was found to fit satisfactorily equations applicable in a simple diffusion situation. Burns then concluded that the mechanism governing the attack was diffusion controlled. The activation energy for this diffusion mechanism was calculated to be 22 kcal/mole, and the sodium concentration

in the discoloured layer was estimated to be ~ 3×10^{21} atoms cm^{-3}. Burns also speculated that the origin of the discolouration may be due to formation of thin films of silicon monoxide and silicon or trapped electrons at defect sites. Doremus (1977) who carried out similar experiments to Burns on a sodium resistant glass came to the same conclusion. That is, for exposure temperatures below 350°C, the rate of darkening of the glass is controlled by the diffusion of sodium into the glass. The activation energy was calculated to be 27 kcal/mole. Doremus did not speculate on the nature of the discolouration.

An interesting paper by Burggraaf and Van Velzen (1968) in which they discussed the attack of silicate glasses by sodium vapour. They suggested that the attacking or discolouring process occurred in two stages. The first stage is the diffusion of sodium from the vapour phase into the glass producing a yellow-brown discolouration. This first step is reversible as demonstrated by the fact that bleaching in silicate glasses can be observed [Fonda and Young (1934), Ernsberger (1960) and Burns (1965)]. The second stage which is not reversible is the chemical reaction between the diffused sodium and the glass. The authors did not suggest an explanation as to the nature of the discolouration, and they pointed out that in selecting suitable lamp materials, consideration of the thermodynamic factors alone is not sufficient. This was demonstrated by Elyard and Rawson (1962) who found that crystalline quartz was attacked much more slowly (by a factor of 100) than vitreous silica and also by Ihnat (1962) who exposed powdered and very densely sintered alumina to sodium vapour. The powdered alumina was found to react but the densely sintered material remained inert. Burggraaf and Van Velzen (1968) suggested that the packing density and the free volume available have an influence on the kinetic factors and these quantities have to be taken into consideration. The authors who were developing aluminate glasses for lamp envelopes at the time suggested the crystallisation of glasses,

which will lead to more closely packed structures, may have higher resistance to sodium attack than the original glasses.

The most recent paper on the subject is that by Stryjak and McMillan (1979) in which they proposed a possible model for the discolouration in silicate glasses. Their model is based on the idea of colour centre formation being responsible for the discolouration. They envisaged the diffusion or penetration of sodium atoms into the glass, causing the breakage of silicon-oxygen bonds. The electrons from the sodium atoms localise themselves around the negative ion vacancies giving rise to defect centres similar to the E′ centres postulated by Weeks and Nelson (1960). The remaining sodium ions reside in interstitial positions near the vicinity of non-bridging oxygens. In support of this model, the authors exposed samples of a zinc aluminosilicate based glass-ceramic to sodium vapour in a low pressure sodium lamp and to high intensity X-rays which is known to create defects in glasses. They used electron spin resonance spectroscopy to show that both samples gave similar spectra. They then concluded that the defect centres present in both samples were the same.

Other works have also appeared in the literature in connection with the interaction of alkali metal with glasses. It was thought at one time that the exposure of sodium vapour to glasses at elevated temperatures could reveal surface flaws postulated by Griffith (1920). This work was pioneered by Andrade and Tsien (1937) in which they observed crack patterns on the surface of low alkali glasses after treatment with sodium vapour and that the crack patterns could not be attributed to the development of mechanical scratches. This work was followed up by Gordon, Marsh and Parratt (1959) and Argon (1959) on silica, soda lime and Pyrex glasses. However, papers by Nakayama (1959) and Ernsberger (1960, 1962) have shown conclusively that the crack patterns developed only after

cooling to room temperature due to differences in the thermal expansion between the discoloured surface layer and the parent glass substrate.

To summarise the salient features of this survey, consider the situation of a glass being exposed to sodium vapour.

By examining the Gibbs free energy of the possible reactions that can occur and depending on the change in Gibbs free energy between the products and the reactants, it is possible, in principle, to predict whether the glass will react with sodium or not. This thermodynamic argument used by Elyard and Rawson (1962) was found to agree well with the observed results.

In the case where the change in Gibbs free energy is negative, that is the glass can be attacked by sodium, the results of the interaction can be divided into two temperature regimes [Burggraaf and Van Velzen (1968)], a high and a low temperature region. The boundary between these temperature regions is not well defined and will vary for different glass systems. In the high temperature region, the glass is rapidly reduced by the sodium. This results in an intense black discolouration and sometimes flaking at the surface [Fonda and Young (1934)]. In the low temperature region, the sodium attack is manifested by a yellow to brown discolouration. There are some disputes as to the mechanism of this attack. Some authors [Fonda and Young (1934), Burns (1965) and Doremus (1977)] favoured a diffusion controlled process, whilst others [Wheeldon (1959), Elyard and Rawson (1962)] preferred a chemical reduction process where a sharp boundary exists between the discoloured layer and the glass substrate.

There is a great deal of speculation regarding the nature and the mechanism of bleaching of the discolouration [Fonda and Young (1934) and

Burns (1965)]. Only one specific model on the origin of the discolouration has been proposed [Stryjak and McMillan (1979)] which requires further experimental substantiation.

All the authors cited here agreed that the discolouration only occurs at the surface of the glass where it had been exposed to sodium. The thickness of this discoloured layer is typically of the order of a few microns [Wheeldon (1959) and Burns (1965)].

Finally, factors such as the packing density, the free volume available which influence the kinetics of the reaction were introduced [Burggraaf and Van Velzen (1968)] to explain the result that very densely sintered alumina and crystalline quartz are more resistant to attack by sodium than powdered alumina and vitreous silica respectively.

1.3 Aim of the Project

The role of applied science is to utilise the knowledge gained from basic scientific research in practical situations. The direction of this project follows in the same spirit, that is to apply the knowledge gained from studying the interaction of alkali metal with glasses to the ultimate aim of developing suitable transparent materials for the containment of alkali metal. The approach adopted in order to fulfil this general aim has been to investigate the fundamental processes which are involved when glasses are brought into contact with sodium metal vapour and to examine the different ways of improving the resistance to attack by sodium.

The important question of whether a glass will be attacked by sodium was explained by Elyard and Rawson (1962). The predictive value of using a thermodynamic argument depends on knowledge of all the possible

products of the reaction. It is worth pointing out also that the arguments used by the above authors are based on equilibrium thermodynamics. However, glasses in thermodynamic terms are meta-stable systems. Whether it is possible to apply equilibrium thermodynamics to glasses with the same confidence as when applied to crystalline materials is a debatable question.

From the literature survey, it is apparent that the nature of the discolouration mechanism of attack by sodium is not well understood and consequently a great deal of speculation on the subject exists. It is a fact that most authors did not work on comparable glass systems and the conditions of the experiments from which the results were obtained were usually different. These differences were also exacerbated by the complexity of the glass systems studied.

The work of Burggraaf and Van Velzen (1968) suggests that materials which are more densely packed or have more ordered structures could be more resistant to sodium attack than materials which have ill fitting or porous structures. This then give rise to the possibility that materials such as glass-ceramics may be more resistant than the original glass.

The specific goals of this project were to investigate the products of the reactions and to assess the generality of equilibrium thermodynamics when sodium interacts with glasses, to investigate the nature of the discolouration of glasses by sodium, and to examine the effect of crystallisation of suitable glasses with respect to their interaction with sodium. This involved the preparation of glasses and transparent glass-ceramics, investigation of their microstructures, mineralogical constitution and general physical properties with the eventual aim of determining the factors which have to be taken into consideration when developing transparent materials suitable for the

containment of alkali metal.

1.4 Choice of Systems

As mention before, the nature of the discolouration of glasses caused by the interaction with sodium has given rise to a great deal of speculation, even when dealing with a single component glass, namely vitreous silica. The complex multi-component glass systems studied by some authors, despite their commercial value, can serve only to obscure the path of reaching a better understanding. In the hope of gaining a better insight, very simple systems were chosen for the initial stages of the investigation. The systems studied can be divided into three categories,

One component systems:-	Vitreous silica
	Quartz
Two component systems:-	Sodium silicate
	Sodium borate
Three component systems:-	Sodium aluminium silicate
	Magnesium aluminium silicate
	Magnesium aluminium borate
	Calcium magnesium aluminate

There are several reasons why vitreous silica was studied in parallel with quartz. Being single component systems, the origin of the discolouration may be studied without the hinderance of having to consider the effects of the presence of other components. Quartz is a crystalline material, that is, thermodynamically stable and where equilibrium thermodynamics can be applied. Comparison between the behaviour of vitreous silica and quartz when exposed to sodium may enable the assessment of the generality of equilibrium thermodynamics. Also, quartz is known to be more resistant to sodium than vitreous silica [

Elyard and Rawson (1962)]; since these two materials are chemically the same, the difference in their resistance to sodium can only be attributed to the difference in their structure. Closer examination may reveal the importance of the structure with respect to the resistance to sodium.

In the binary and ternary systems the main criterion for the selection of the systems was based on increasing the resistance to sodium to higher temperatures. To realise this, components which are less resistant to sodium were gradually replaced by more refractory components, such as alumina, magnesia and calcia which are known to be very resistant to sodium [Elyard and Rawson (1962), Singh (1976)]. In the binary systems, sodium silicate was chosen since it was found to be more resistant to sodium than silica. Sodium borate was chosen because borates in general are more resistant than silicates and by studying simple borates it was hoped that they might provide clues as to why more complex aluminoborates are so much more resistant to sodium. In addition, the structures of these binary materials are relatively well known which may assist the interpretation of any structural information.

In the ternary systems, small amounts of alumina were substituted for silica in the sodium silicates to assess whether any improvements in the resistance to sodium can be made. Magnesia is very stable with respect to sodium attack, hence magnesium aluminosilicate was studied. This was studied in parallel with magnesium aluminoborate. The general superior resistance to sodium attack of aluminoborates made it an attractive basis to develop transparent glass-ceramics. Finally, calcium magnesium aluminate was chosen because all the components of the glass should be stable with respect to sodium attack. This system was also used to derive transparent glass-ceramics.

1.5 Choice of Experiments and Techniques

From the literature survey, it is apparent that the discolouration of glasses by sodium is a surface phenomenon. Therefore surface sensitive techniques were used to investigate the nature of the discolouration. Infra-red reflection spectroscopy was the major tool used. Electron spectroscopy for chemical analysis (ESCA) was also used, however due to the limited availability of the instrument, the study was restricted to the examination of vitreous silica.

The model proposed by Stryjak and McMillan (1979) predicted the formation of colour centres when silicates are attacked by sodium. Electron spin resonance spectroscopy was used to detect the presence of these paramagnetic centres. Ultra-violet and visible absorption spectroscopy was used to try and locate the presence of any absorption bands, to characterise and compare the extent of the discolouration between glasses.

The thermal changes involved when sodium interacts with the selected systems were studied using differential thermal analysis and the reaction products were traced using X-ray diffraction.

In the preparation of transparent glass-ceramics, the kinetics of nucleation and crystal growth were studied by differential scanning calorimetry and differential thermal analysis. The microstructures and mineralogical constitutions of the resultant transparent glass-ceramics were studied by transmission and scanning electron microscopy and X-ray diffraction. Properties such as the optical transmission, thermal expansion coefficient and the mechanical strength were also measured.

1.6 Plan of Thesis

The thesis is divided into seven chapters and one appendix.

Chapter 2 describes the preparation of glasses and transparent glass-ceramics, details of the techniques and the procedure used to characterise the microstructures and physical properties of the transparent glass-ceramics.

Chapter 3 describes in detail the various techniques and experimental procedure used for the investigation of the interaction of sodium with the glasses and transparent glass-ceramics.

Chapter 4 gives an account of the results obtained from the study of the thermal behaviour, microstructures and physical properties of the transparent glass-ceramics.

Chapter 5 gives an account of the results obtained from the investigation of the interaction of sodium with the glasses and transparent glass-ceramics.

Chapter 6 discusses the findings as a whole and extends the arguments to other alkali metals. A section is devoted to describing materials which are suitable for the containment of alkali metals.

Chapter 7 summarises the salient features of this work and a section is devoted to suggestions for future studies.

Appendix 1 gives an account of the theory of nucleation and crystal growth in a supercooled liquid, essential to the understanding of glass-ceramics.

CHAPTER 2: Materials Preparation and Characterisation

2.1 Introduction

The ultimate aim of this project was to determine the various factors which have to be taken into consideration when developing suitable transparent materials for the containment of alkali metals at elevated temperatures. To fulfil this aim, very simple systems such as vitreous silica and quartz were studied initially in an attempt to understand the basic processes involved when sodium interacts with these materials. This was followed by the study of more complex systems to examine the different ways of improving the resistance to sodium attack at higher temperatures. This was carried out by changing the chemical compositions and by altering the structure by crystallising the glasses.

In order to assess the extent to which the resistance to sodium can be improved by altering the structure, it would be desirable to develop transparent glass ceramics with a varying degree of crystallinity. To achieve this, close studies of the kinetics of nucleation, crystal growth and microstructural details of suitable compositions were carried out.

The present chapter deals with the preparation of glasses and transparent glass-ceramics used for the study of the interaction with sodium. In preparing the transparent glass-ceramics, thermal analytical techniques were used to study the transformation behaviour of suitable compositions. The microstructure and general physical properties were studied in order to characterise these materials. The following sections describe the glass melting process, details of the techniques and experimental procedures used for the development and characterisation of the transparent glass-ceramics.

2.2 Preparation of Glasses

The composition, melting and annealing temperatures of the glasses used to study the interaction with sodium are given in Table 2.2.1.

The vitreous silica used was Spectrosil B, purchased from Thermal Syndicate Ltd. in the form of 1mm thick polished microscope slides. The single crystals of quartz were kindly supplied by the Quartz Division of ITT Components Group. The rest of the glasses were made in 200 gm batches using "Analar" grade reagents. The constituents of the glass were either tumbled or ball-milled for at least three hours prior to melting. The glasses were melted in a platinum 2% rhodium crucible in an electric furnace. The technique of crushing and remelting was used to ensure homogeneity in the glasses. The average melting times for the glasses were approximately 3 hours, except for the calcium magnesium aluminate which was melted for 6 hours.

The melts were cast in an iron mould kept at room temperature. The mould was coated with a graphite suspension to prevent adhesion to the glass. The glasses were annealed for an hour in a muffle furnace before being allowed to cool to ambient temperature over a period of 24 hours.

2.3 Preparation of Transparent Glass-Ceramics

2.3.1 Initial Selection of Suitable Compositions

The basis for the initial selection of suitable compositions for the development of transparent glass-ceramics was to explore compositions which are relatively refractory and at the same time remain resistant to sodium attack.

The aluminoborates are more refractory than borates and in general have better resistance towards sodium attack [Elyard and Rawson (1962)], also magnesium oxide is known to be stable towards sodium [Singh (1976)].

	Composition (Mol %)						Melting Temperature (°c)	Annealing Temperature (°c)
	Na_2O	MgO	CaO	Al_2O_3	B_2O_3	SiO_2		
Vitreous Silica						100	--	--
Quartz (X-cut)						100	--	--
NaS(1)	20					80	1550	700
NaS(2)	30					70	1450	550
NaB(1)	20				80		1200	450
NaB(2)	25				75		1200	450
NaSA1(1)	30			5		65	1400	550
NaSA1(2)	30			10		60	1450	650
MgSA1(8A)		30		20		50	1600	700
MgSA1(8B)		20		13.3		66.7	1650	700
MgBA1(8)		30		20	50		1350	630
MgBA1(3-2)		37		21	42		1350	650
CA1(6)		6	56	38			1600	800

TABLE 2.2.1
Compositions of glasses and crystalline material studied

Therefore, the magnesium aluminoborate system served as a reasonable starting point to develop transparent glass-ceramics. The complete glass forming region was explored systematically. The criterion for glass formation was that the melts, when cooled under the conditions described in section 2.2, should result in homogeneous clear glasses. Promising compositions, that is ones which exhibit relatively high softening temperatures, were subjected to heat treatments.

A two stage heat treatment programme was used for the crystallisation of the glasses [Appendix I] where the first stage is used for inducing the formation of nuclei and the second stage is used for the subsequent growth of the nuclei. The heat treatment programmes used at this stage were developed very much on an intuitive basis. However, they served to pinpoint certain suitable compositions. Suitable compositions are ones which can be crystallised at a certain temperature for a "reasonable" length of time without substantial deformation. A few compositions were found to satisfy these requirements, but one composition labelled MgBAl (3-2) was found to be outstanding. This composition was used for further studies and the information required for refining the heat treatment programme was obtained from differential scanning calorimetry measurements.

The aluminates were found to be the most resistant to sodium attack out of the glasses studied [Elyard and Rawson (1962)]; combined with their high temperature properties, they present an extremely attractive proposition. A series of compositions in the calcium magnesium system was tried. Their ability to form glasses using the methods described in section 2.2 were found to be very sensitive to compositional changes. From the melts attempted, only one composition labelled CAl (6) was found to form a glass readily.

Upon heat treatment, CA1 (6) was found to exhibit surface crystallisation only. This implies a heterogeneous nucleation process in which nucleation sites were present at the surface for crystal growth. It follows that the condition of the surface, whether "pristine" or otherwise, has an important bearing on the microstructure of the surface crystallised layer. In order to standardise the surface, 2mm thick slides of CA1 (6) were polished on both sides to a 1 micron diamond finish. The specimens (~ 5 x 20 x 1.5 mm) were vibrated in 80 mesh silicon carbide for a known length of time to induce a "certain amount" of surface flaws and they were handled with plastic tweezers thereafter. The samples were heat treated using a single stage heat treatment programme to induce crystal growth. Refinements on this programme were carried out on a trial and error basis.

2.3.2 Thermal Analysis

When a material transforms from one phase to another, due to the difference in the Gibbs free energies of the phases, heat is either evolved or absorbed. This evolution or absorption of heat can be measured directly or as a change in temperature. To make use of this behaviour two kinds of thermal analytical techniques were used to study the kinetics of nucleation and crystal growth of the selected materials, labelled MgBA1 (3-2) and CA1 (6). They were differential thermal analysis (DTA) and differential scanning calorimetry (DSC). Due to the limitations of the instrument used, DSC was carried out on MgBA1 (3-2) only.

2.3.2.1 Differential Thermal Analysis (DTA)

The principle of DTA involves the measurement of the temperature difference between two samples as a function of temperature as both are heated

simultaneously. If one sample is an inert reference material, a temperature difference will show up as the sample of interest undergoes a transformation.

Although the basic principle of DTA is simple, in practice, it is important to remember that it is a comparative technique and it involves the measurement of temperature. Any asymmetries in the apparatus such as the positions of the sample wells in the heating block, the position of the heating block with respect to the furnaces and the shape of the crucibles, have to be eliminated. In order for the temperature of the sample to increase, there must be an input of heat from a body which is at a higher temperature; therefore, a temperature gradient exists. Depending on where the measurements of temperature are being made, the results can be misleading. The increase in temperature of the sample also depends on the specific heat and the thermal conductivity which vary as a function of temperature. Hence, the choice of reference materials is important. The thermal conductivity varies widely, depending on the way in which the sample (usually in the form of loose particles) is packed in the crucible, and due consideration must be given to what happens during heating. For instance, glass particles usually fuse together when heated beyond the transformation temperature. This causes a shrinkage in volume and may then result in an apparent endothermic reaction. Other parameters, such as the heating rate and the atmosphere in which the samples are being heated, can affect the rate of reaction and, therefore, must be taken into consideration when interpreting the results.

The subject of DTA has been studied extensively and detailed discussions on both the theoretical and practical aspects of the technique can be found in Smothers and Chiang (1958), Mackenzie and Mitchell (1962), Melling, Wilburn and McIntosh (1969), Ware (1971) and

and McIntosh, Turnock and Wilburn (1974). Despite the stringent experimental conditions and the difficulty in the interpretation of results, DTA has been used successfully to study the crystallisation behaviour of glasses. Short reviews on the applications of DTA in the study of glasses can be found in Gregory and Veasey (1972) and McMillan (1979).

A method of studying the kinetics of crystallisation, which is of particular interest to the present study, was described by Thakur and Thiagarajan (1966). The general theory can be derived as follows:

If w is the concentration of the reactants at any time t and the reaction is of n^{th} order, then

$$-\frac{dw}{dt} = Kw^n$$

where K is the reaction rate constant and it is related to the absolute temperature through the Arrhenius equation.

$$K = A \exp\left[-\frac{E}{RT}\right]$$

where A is the frequency factor and E is the activation energy per mole which includes all the activated steps in crystallisation. By substitution and differentiation

$$\frac{d^2w}{dt^2} = -A \exp\left[-\frac{E}{RT}\right][nw^{n-1}]\frac{dw}{dt} - Aw^n \exp\left[-\frac{E}{RT}\right]\left[\frac{E}{RT^2}\right]\frac{dT}{dt}$$

If the heating rate dT/dt is constant, put $dT/dt = \beta$ and substitute for dw/dt. Then

$$\frac{d^2w}{dt^2} = -A \exp\left[-\frac{E}{RT}\right][nw^{n-1}]\frac{dw}{dt} + \frac{dw}{dt}\frac{E}{RT^2}\beta$$

By assuming that the reactions vessels are infinite cylinders, that the thermal properties of the material do not change significantly before and after the reaction and that the weight loss is negligible, the maximum rate of reaction was found to coincide with the exothermic peak temperature in DTA [Akita and Kase (1968)]. Therefore, at the maximum rate of reaction, $d^2w/dt^2 = 0$, and if the peak temperature is denoted by Tm, then

$$A \exp\left[-\frac{E}{RT}\right][nw^{n-1}] = \frac{\beta E}{RT_m^2} \qquad (2.3.1)$$

In the case of a first order reaction, n = 1. By taking log to the base e, equation (2.3.1) becomes

$$\ln\left[\beta/T_m^2\right] = \ln\left[\frac{AR}{E}\right] - \frac{E}{R}\left(\frac{1}{T_m}\right) \qquad (2.3.2)$$

Hence, a plot of $\ln\left[\beta/T_m^2\right]$ versus $1/T_m$ should give a straight line if the reaction is of 1^{st} order and the activation energy E can be calculated.

All the DTA experiments were carried out at Thorn Lighting lamps research laboratory on a Stanton-Redcroft 67/4 DTA apparatus. The two selected glasses MgBA1 (3-2) and CA1 (6) were crushed and sieved into three groups of particle sizes, coarse (500-170 μm), medium (150-100 μm) and fine (< 50 μm). DTA traces were obtained from particles of different sizes over a range of heating rates from 4°c/min. to 16°c/min. The conditions of the experiments were normalised by using the method of packing recommended by the manufacturer of the DTA apparatus, the same weights (70 ± 0.05 mg) of samples were used throughout under the same atmospheric conditions (static air). The inert standard used was alumina which was also divided into three particle sizes to match the samples.

2.3.2.2 Differential Scanning Calorimetry (DSC)

DSC is similar to DTA in that both are comparative techniques, the main difference lies in their schemes of detecting heat changes. In DSC, the rate of heat evolved or absorbed by a sample (when compared with an inert standard) whilst undergoing a phase transformation is measured directly either as a function of temperature or time. The results are much more reproducible than in DTA since many of the problems associated with the measurement of temperature are removed. The measurement of heat content enables the evaluation of the specific heat which is the single most important thermodynamic parameter. Knowledge of the specific heat as a function of temperature enables other quantities such as the enthalpy, entropy and Gibbs free energy to be calculated. The measurement of heat content as a function of time enables the kinetics of phase transformations to be studied.

However, most commercial differential scanning calorimeters have a top temperature limit of between 700-800°c; this restricts the study of refractory glasses severely. Studies of transformations in glassy materials by DSC, which have appeared in the current literature, are concentrated on the chalcogenide glasses [Das, Platakis and Bever (1974), Thornburg and Johnson (1975)] and metallic glasses [Chou and Turnbull (1975), Bagley and Vogel (1975), Scott (1978)]. In the present work, DSC could only be used on the composition MgBAl (3-2). The main objectives were to devise a suitable heat treatment programme for this composition and to study the kinetics of crystallisation in more detail, hence DSC in this instance was used to measure heat changes as a function of time.

The results obtained were analysed in terms of the generalised theory of phase transformations [Christian (1975)]:

If a material is undergoing a phase transformation isothermally from phase α to phase β, and the fraction of material transformed $^{\beta}X(t)$ at time t can be expressed by

$$^{\beta}X(t) = 1 - \exp\left[- kt^{n}\right] \qquad (2.3.3)$$

This is known as the Johnson-Mehl-Avrami equation, where k is a rate constant and n is called the Avrami exponent which need not be an integer. The value of the Avrami exponent may, in favourable situations such as constant nucleation rate and linear growth, give some information about the shapes of the transformed phase. Equation (2.3.3) can be written as

$$\ln\left[\ln\left[\frac{1}{1 - {}^{\beta}X(t)}\right]\right] = \ln k + n\ln t \qquad (2.3.4)$$

thus n can be calculated from the gradient of a plot of $\ln[\ln[{}^{1}/_{1-}{}^{\beta}X(t)]]$ versus ln t.

In an experiment, the rate of change of heat dH/dt is measured as a function of time at constant pressure, i.e.

$$\frac{dH}{dt} = {}^{\beta}H'(t)$$

and this is related to $^{\beta}X(t)$ by

$$\frac{1}{\beta_{H\infty}} \int_{0}^{t} {}^{\beta}H'(t)\, dt = {}^{\beta}X(t) \qquad (2.3.5)$$

where $^{\beta}H\infty$ is the total heat evolved due to the transformation.

Figure 2.3.1 shows schematically a typical experimental curve. It can be seen that there is a drift in the base line. This is due to the change in specific heat of the glass due to crystallisation. In order to calculate $^{\beta}H\infty$, a straight line is drawn as a first approximation

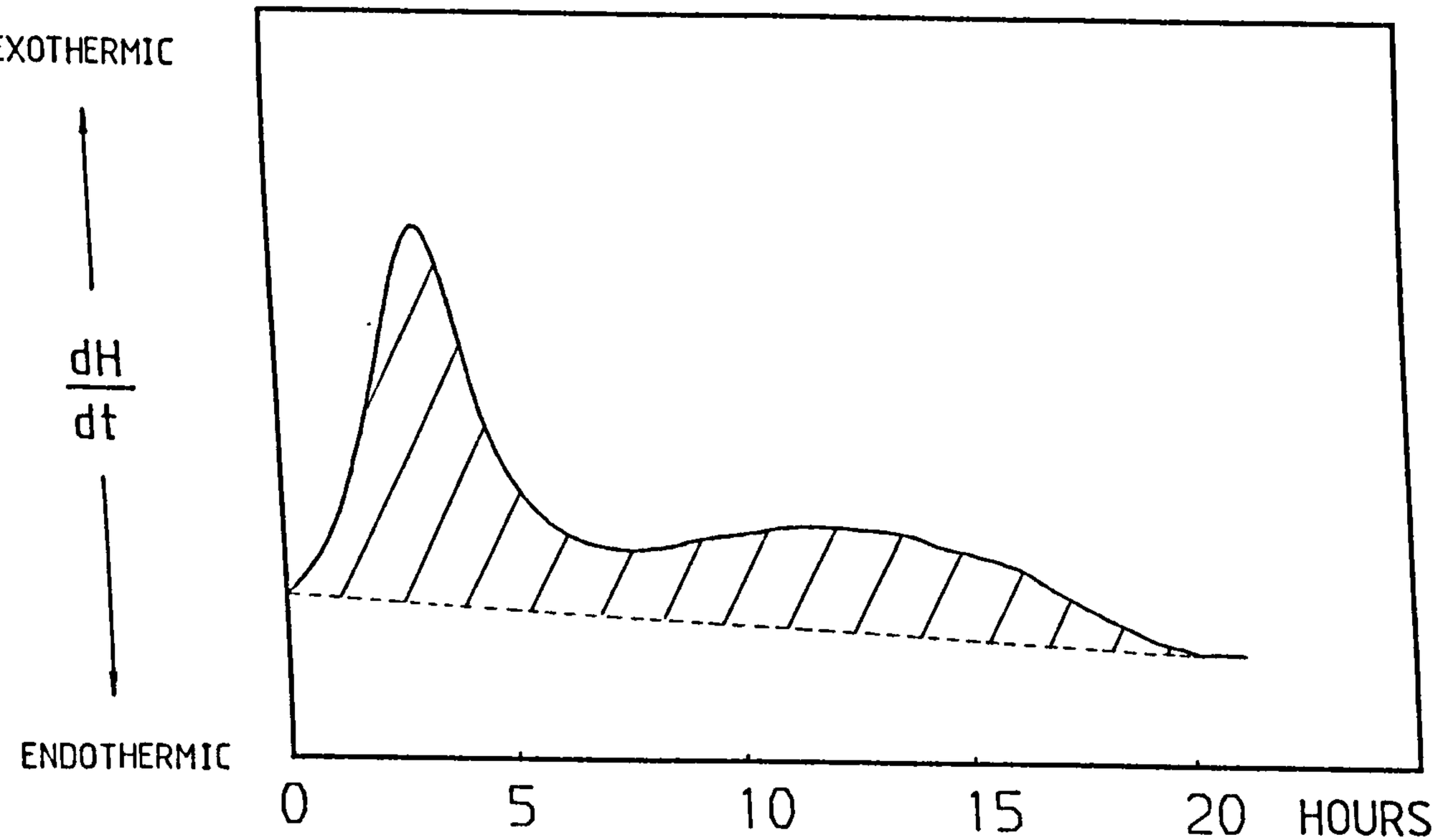

FIGURE 2.3.1

Schematic diagram of a typical DSC experimental trace for the crystallisation of a glass.

between the initial and final point of the transformation. The total area enclosed (shaded portion) is proportional to $\beta_{H\infty}$. A computer programme was written to carry out the integration by dividing the area enclosed by the curve into 500 strips. By assuming the strips to be trapeziums, the area of each strip was calculated and $\beta_{H\infty}$ was obtained by summing the areas of all the strips.

The experiments were carried out using a Setaram DSC. Two platinum crucibles were used which were matched in weight to better than 1 part in 250. All the samples used have roughly the same dimensions (2x5x10 mm) weighing about 200mg. They were washed with acetone and thereafter handled with tweezers. The samples were placed in one of the crucibles and ran against the other empty crucible acting as a reference.

2.4 Microstructures of Transparent Glass-Ceramics

The use of thermal analytical techniques gave details concerning the kinetic behaviour of nucleation and crystal growth in the selected glass compositions. In particular, the results from DSC measurements could be manipulated to give indications about the shapes and the volume fraction of the transformed phases. However, for more quantitative microstructural information, the use of electron microscopy is more appropriate. From electron micrographs, quantities such as the volume fraction, the surface area per unit volume and the particle size distributions of the transformed phases can be calculated. In the present work though, the aim is to develop transparent glass-ceramics with different degrees of crystallinity; therefore the quantity of interest is the volume fraction.

The microstructures of crystallised samples of MgBAl (3-2) and CAl (6) were studied by scanning electron microscopy (SEM) and transmission electron microscopy (TEM). The volume fractions of the crystals formed were calculated from the electron micrographs. Finally, the mineralogical

constitutions of the transparent glass-ceramics were studied by X-ray powder diffraction.

2.4.1 Electron Microscopy

Electron microscopy is nowadays a routine research tool in the science of materials. The term electron microscopy embodies a host of different techniques and far too many to discuss individually here. However, an excellent introductory text by Bowen and Hall (1975) describes the principles and applications of most of the modern microscopic techniques with ample references for further reading, whilst some applications of electron microscopy to the study of glasses and glass-ceramics are described by McMillan (1979). In the present work, SEM was the major tool used supplemented by TEM where high resolution (< 20nm) was required, and the following discussion is restricted to the sample preparation aspects of these two techniques.

A problem always encountered in TEM is the preparation of thin samples (~ 100nm) which are transparent to electrons. When this can be achieved, the question of whether the specimens are representative of the bulk material arises. Two factors contribute to this uncertainty. One is the small volume of materials that is being examined and the other is the method used in thinning the specimens. For example, the generation of heat during grinding and polishing the specimens could modify the microstructure. On the whole, these ambiguities can be clarified by the laborious methods of sampling different areas of a bulk specimen and employing different sample preparation techniques to compare any common features. The use of SEM overcomes most of these problems by having a large depth of field and ease of sample preparation. The technique can be applied to examining large areas (~ $1cm^2$) and in favourable cases specimens can be examined without any special sample preparation. In

general though, SEM has an upper limit of useful magnification of about 50K. Therefore, whenever high resolution is required (< 20nm), the use of TEM is unavoidable.

SEM was used to examine the fractured surfaces of crystallised samples of MgBAl (3-2) and CAl (6). A technique of chemically etching the aluminoborates was developed to enhance image contrast, whilst etching was found to be unnecessary for the aluminates. Very little exploratory work was carried out on the different methods of preparing thin specimens for TEM. A mechanical thinning technique was used; this method, apart from minor details, is similar to that described by Hing and McMillan (1973) and Stryjak and McMillan (1978). These authors have found the technique of thinning specimens by ion bombardment produced sufficiently thin areas which are transparent to electrons and, at the same time, creating no observable artifacts due to the thinning technique. TEM was used to study crystallised samples of MgBAl (3-2) only. No attempt was made to study the composition CAl (6) which only showed surface crystallisation. The following two sections are devoted to the sample preparation procedures for SEM and TEM.

2.4.1.1 Sample preparation for SEM

MgBAl (3-2) specimens for SEM were prepared from bulk samples in the form of small bars (2 x 5 x 20 mm) which had been heat treated. These bars were cracked in half in a three point bend arrangement and thereafter handled with plastic tweezers. The fractured specimens were etched in 4% HF diluted with water in an ultrasonic bath. It was necessary to agitate the specimens in the ultrasonic bath to remove any fluoride compounds formed on the fractured surfaces during etching. The etching time required in order to show good image contrast was found to vary from 10 minutes, for a fairly glassy sample, to 30 seconds for a highly crystallised

sample. The specimens were washed thoroughly with deionised water after etching and then rinsed with acetone. They were mounted on aluminium stubs with a conducting paint (Silverdag) such that the fractured surfaces could be examined. Finally a thin layer of gold (~50Å) was sputtered on to the surfaces of the specimens to prevent charging in the electron beam.

The preparation of CA1 (6) specimens were carried out in exactly the same way except without the etching process.

A Cambridge scanning electron microscope was used; typical operating conditions were at 30 kV with sample currents around 120 μA.

2.4.1.2 Sample preparation for TEM

The specimens of MgBA1 (3-2) for TEM were prepared from bulk samples which had been heat treated. Thin slices (~ 250 microns) were cut from the bulk samples using a diamond saw. The thin slices were mounted on a brass block using a thermoplastic resin (Lakeside resin) and were thinned down to about 150 microns using 800 grit silicon carbide paper and water as a lubricant. 3mm diameter discs were drilled out from these slices using an ultrasonic drill while still mounted on the brass block. The discs were removed from the brass block by dissolving the resin with acetone. Each was abraded with a stream of 9 micron alumina particles (carried in compressed N_2) directed at the centre until a small perforation just appeared.

The discs were washed with acetone in an ultrasonic bath before transferring to an Edwards MAI argon ion-beam machining equipment for the final thinning. The discs were mounted at an angle of about 20° away from the direction of incidence of the sputtering ions. The sputtering time was found to vary for different samples, but typical conditions were at an

accelerating potential of 6 kV, with an ion current of 30 μA for 4 hours. The final assessment of whether the specimens were sufficiently thin was by looking for interference fringes around the perforation with an optical microscope at 400 times magnification. Finally, a thin layer of carbon (estimated to be between 5–15 nm in thickness) was deposited on to the discs to prevent charging in the electron beam.

A JEM 200 transmission electron microscope operating at 200 kV was used.

2.4.2 Quantitative Analysis - Volume Fraction

In this section, the analysis of the microstructure of the transparent glass-ceramics is restricted to the determination of phase proportions.

Consider a material of phase α which contains a randomly dispersed second phase β. The principle used in determining the volume fraction of β-phase in a specimen can be summarised by

$$V_f = \frac{V_\beta}{V} = A_f = \frac{A_\beta}{A} = L_f = \frac{L_\beta}{L} = P_f = \frac{P_\beta}{P} \qquad (2.4.1)$$

where V_f = Volume fraction of β-phase

V_β = Volume of β-phase in the specimen

V = Total volume of the specimen

A_f = Area fraction of β-phase

A_β = Area of β-phase in a random planar section

A = Total area of the random planar section

L_f = Linear fraction of β-phase

L_β = Linear fraction of β-phase in a random linear line

L = Total length of the random linear line

P_f = Point fraction of β-phase

P_β = Number of points falling in the β-phase

P = Total number of points sampled

This relationship has been proved by Delesse (1848) and Rosiwal (1903) and it implies the volume fraction can be obtained by either areal analysis, lineal analysis or by point counting, as shown in figure 2.4.1. The efficiency of each method, that is, the method which gives the smallest error for the least effort, has been investigated by Hilliard and Cahn (1961) and by DeHoff and Rhines (1968). These authors have shown that the systematic point counting method is the most efficient, providing the phase of interest is randomly dispersed and the spacing between the regular points laid down is greater than the maximum intercept length of this phase.

From an initial assessment of the SEM micrographs, the above conditions could be satisfied. Hence the systematic point counting method was used to calculate the volume fraction. A square array of 18 x 18 points was projected on to the micrographs and the number of points falling on the crystallised phases were counted manually.

It is worth considering that in any practical situation, only a finite number of observations can be made and an error will be introduced as a result. Gladman and Woodhead (1969) have shown that for P number of observations, the error introduced is given by

$$\frac{\sigma_{V_f}}{V_f} = \left[\frac{1}{P_\beta}\left(1-V_f\right)\right]^{\frac{1}{2}} = \left[\frac{1}{P_\beta} - \frac{1}{P} \right]^{\frac{1}{2}} \qquad (2.4.2)$$

where σ_{V_f} is the standard deviation of V_f. Equation (2.4.2) also implies

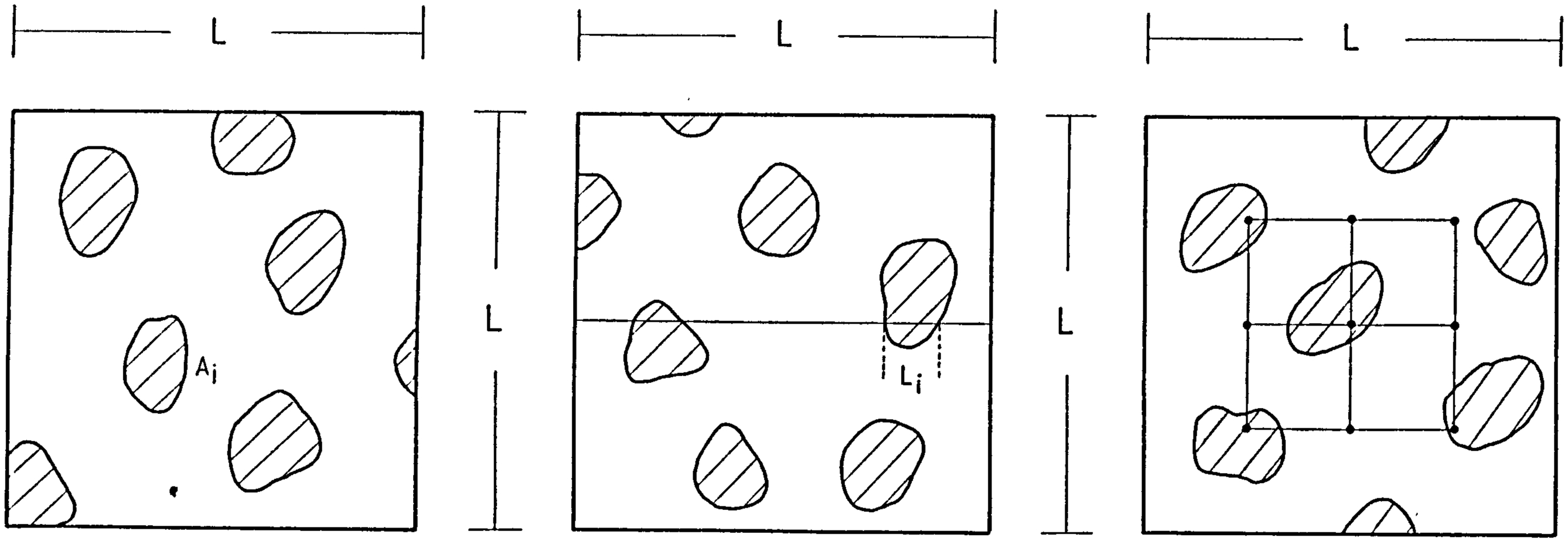

$$A_f = \frac{\sum_i A_i}{L^2} \qquad L_f = \frac{\sum_i L_i}{L} \qquad P_f = \frac{4}{9}$$

(a) (b) (c)

FIGURE 2.4.1

Illustration of three basic methods for estimating the volume fraction of a phase: a) the area fraction, b) the lineal fraction and c) the point count.

that for a chosen standard deviation at different volume fraction, the total number of observations P required can be determined. Standard nomograms have been constructed [Blank and Gladman (1970] so that the inter-relationships between P, V_f and σ_{V_f} can be determined conveniently.

In addition to the errors associated with counting with a finite number of points, there are experimental errors to be considered. These are sectioning errors and errors due to the limit of resolution of the microscope. The relationships in equation (2.4.1) assume measurements or sampling are being carried out on a planar, flat section randomly cutting the three dimensional structure. In practice, it is often not possible since specimens are usually etched (as in the present work) or preferentially polished so that the phases are in relief. As can be seen from figure 2.4.2, the observed volume fraction is always equal to or greater than the true volume fraction. Providing the relief height or etch depth t is small, and that no particles are removed during etching and polishing, the true volume fraction V_f can be expressed by [Pickering (1975)]

$$V_f = V_f' - \frac{S_v t}{4} \qquad (2.4.3)$$

where V_f' is the observed volume fraction, S_v is the surface area of β-phase per unit volume in the specimen,

$$S_v = \frac{2N}{L} = 2N_L .$$

where N is the number of β-phase boundaries in a linear traverse of length L and N_L is the average number of β-phase boundaries per unit length. S_v can be measured readily using lineal analysis.

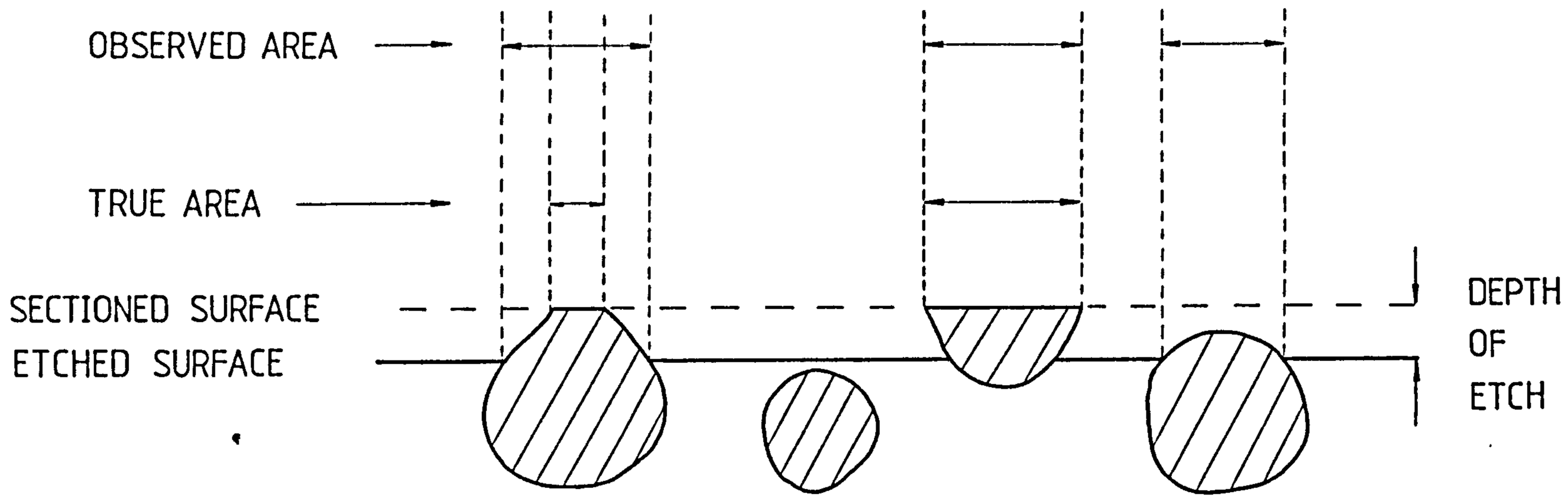

FIGURE 2.4.2

Diagrammatic representation of sectioning errors.

In cases where the particle sizes of the β-phase are approaching the resolution of the microscope, considerable errors can be introduced due to the inability to distinguish the boundaries between phases. An estimate of the relative error $[S_{V_f}/V_f]$ caused by the resolution of an optical microscope was given by Pickering (1975) and it is

$$\frac{S_{V_f}}{V_f} = \frac{\pi N_L}{2V_f} \left[\frac{\lambda}{2(N.A.)} \right] \qquad (2.4.4)$$

where λ is the wavelength of light and (N.A.) is the numerical aperture of the microscope. The quantity $[\lambda/2(N.A.)]$ is the resolution of the microscope. To demonstrate the effect of particle size on this error, assume the β-phase to be consisting of spheres of diameter D, then equation (2.4.4) can be written as

$$\frac{S_{V_f}}{V_f} = \frac{3\pi}{2D} \left[\frac{\lambda}{2(N.A.)} \right] \qquad (2.4.5)$$

In a typical scanning electron microscope, provided the specimens are properly coated to prevent charging, the resolution owing to electrical noise is usually limited to about 20 nm. The variations of particle size with the relative error by substituting the noise limit of 20 nm for $[\lambda/2(N.A.)]$ in equation (2.4.5) are shown in table 2.4.1. The error due to the lack of resolution becomes insignificant for particles greater than about 5 μm.

Diameters of β-phase particles (μm)	Relative Error (%)
0.1	94
0.5	19
1.0	9.4
5.0	1.9
10.0	0.1

TABLE 2.4.1

Relative error as a function of particle size assuming a microscope resolution of 20 nm.

2.4.3 X-Ray Diffraction

The crystalline phases present in the transparent glass-ceramics were identified using X-ray diffraction which is a very well established technique and, therefore, will not be mentioned further, but an excellent text by Klug and Alexander (1974) describes comprehensively the theory and practice of various X-ray diffraction techniques currently employed.

In the present work, a Debye-Scherrer powder camera was used. The samples were prepared by crushing the glass-ceramics and then passing the resultant powder through a 300 mesh (~ 50 micron) sieve. The powders obtained were mounted on thin Pyrex glass fibres (~ 0.1 mm diameter) using a mixture of Sellotape glue dissolved in chloroform. The diffraction patterns were obtained using radiation from a copper target and recorded on film.

The identifications were carried out by comparing with standard A.S.T.M. powder diffraction data.

2.5 General Physical Properties of Transparent Glass-Ceramics

Some of the physical properties of the transparent glass-ceramics derived from the MgBAl (3-2) and CAl (6) compositions were measured. The aim was to characterise the transparent glass-ceramics and to assess the potential of these materials for use as envelopes for sodium vapour lamps.

In considering any materials for lamp envelopes, apart from the chemical compatibility aspect, other equally important properties have to be taken into account. They are:

1) Transparency

The material has to be able to transmit visible light for obvious reasons. The degree of transparency will affect the overall

efficiency of the lamp, hence a highly transparent or translucent material is desirable.

2) Sealing to metals

The material has to be able to form a hermetic seal with metals which are used as supporting wires and external contacts. Common metals used in sodium vapour lamps are tungsten, molybdenum and niobium. In order to form a hermetic seal, one of the essential requirements is that there should be close matching of thermal expansivity between the material and the metal. The generation of excessive stresses caused by large differential expansion or contraction during thermal cycling may result in failure of the seal.

If the material to be used is a glass, then the viscosity characteristics have to be such that the glass is workable during sealing.

3) Electrical resistivity.

The material has to remain a good insulator of electricity at the operating temperature of the lamp.

4) Mechanical Strength

If the material possesses good mechanical strength, then the walls of the envelope could be made thinner. Apart from the saving in the quantity of material used, this would lead to a higher degree of transparency and more flexibility in the design of the lamp. Hence a strong material is desirable.

In the present work, the optical transmission (200-700 nm), the linear thermal expansion coefficient (30-550°C) and the maximum failure stress determined in 4-point bending were measured. Other properties such as viscosity and electrical measurements, although

they are important, were not carried out due to the lack of time. It should also be emphasised that no attempt was made to correlate the physical properties measured with the microstructures for the same reason. In the following sections, details of the experimental procedures used for the different physical properties measurements are given.

2.5.1 Optical Transmission

The optical transmission of the glasses and transparent glass-ceramics of MgBAl (3-2) and CAl (6) were measured using a Cecil double beam spectrophotometer in the wavelength range 200-700 nm.

For the MgBAl (3-2) samples, specimens for the optical measurements were prepared by heat treating 2 mm thick slices of the original glass and then by polishing down to a 9 micron alumina finish on both sides. The final thicknesses of the specimens used were 1.5 ± 0.1 mm.

The preparation of specimens of CAl (6) for heat treatments have been described in section 2.3.1 and it was found that the heat treated samples only exhibit surface crystallisation. The transmission measurements were carried out on these samples without further polishing. The thickness of the samples used were 1.5 ± 0.1 mm.

2.5.2 Thermal Expansion

The linear thermal expansion coefficients of the glasses and glass-ceramics were measured using a vitreous silica dilatometer. The dilatometer consisted of a silica rod inside a vertically mounted silica tube with a closed end. The specimen about 5 cm long was placed inside the tube with the rod just resting on top of it, and the whole arrangement was inserted inside a tube furnace. The temperature of the silica tube

at the point where it was mounted was kept constant by circulating water at 30°C. The relative extension between the rod and the tube was measured using a linear variable displacement transducer (LVDT) with a sensitivity of 4.32 mV/micron. The temperature of the specimen was raised at the rate of 2°C/min. and measured using a chromel-alumel thermocouple. The dilatometer was calibrated by using vitreous silica and platinum as standards.

Four specimens of each material were measured and the relative thermal expansion coefficient α is given by

$$\alpha = \frac{\Delta L}{L_o (T-T_o)}$$

where L_o is the initial length of the specimen at temperature T_o and ΔL is the extension at temperature T. Therefore, from the gradient of a plot of the relative expansion versus temperature, α can be calculated. The gradients of the plots were calculated by the method of least squares. The relative expansion coefficient was corrected by adding the calibrating value of the dilatometer in the temperature range of interest to obtain the absolute value.

2.5.3 Mechanical Strength - 4-Point Bending

The maximum failure stresses of the glass and glass-ceramics of MgBAl (3-2) were measured only. This is due to the difficulty in preparing specimens of CAl (6) for strength determinations within the time available for this work.

Rods of MgBAl (3-2) with diameters ranging from 1.3 - 2.5 mm were drawn from the melt and cut into 5 cm lengths. The dimensions of the rods were closely controlled by rejecting rods which had more than 0.03 mm variation in their diameters and more than 0.2 mm taper over the 5 cm

lengths. The rods were subjected to appropriate heat treatments and then allowed to cool down to ambient temperatures overnight.

The mechanical strengths of glasses depend very much on the conditions of the surfaces and the chemical environment during test. In order to normalise the surfaces of the specimens, an abrasion treatment was used. The treatment used was somewhat arbitrary but the same procedure was used throughout the experiment. The rods were vibrated in fresh 80 mesh silicon carbide for 30 minutes and thereafter handled with plastic tweezers. The rods were rinsed in acetone and then tested within an hour of the abrasion treatment. The relative humidity was recorded before and after the experiment.

A 4-point bending jig with a span of 4 cm between the outer knife edges and a 1 cm separation between the inner knife edges was used on an Instron. The tests were carried out at room temperature with a loading speed of 0.02 cm/min. The maximum load before failure and the diameters of the rods where they had fractured were recorded. Fifteen specimens were measured for each material and the maximum failure stress σ_{max} for a rod was calculated by [Holloway (1973)]

$$\sigma_{max} = \frac{2Pd}{\pi r^3}$$

where P is the maximum load, r the radius of the rod and d the spacing between the outer and inner knife edge.

CHAPTER 3: Interaction with Sodium Metal Vapour

3.1 Introduction

The approach adopted in this project was first of all to study the interaction of sodium with relatively simple systems. The aim was to gain a better insight into the nature of the discolouration and to determine the factors which govern whether a material will interact with sodium. Different methods of improving the resistance were then explored by changing the compositions of the systems gradually and by altering the structure of some of the selected glasses by crystallisation. The preparation of these systems has already been described and the present chapter is concerned with the interaction of sodium metal with these glasses and transparent glass-ceramics.

Different methods of exposing the specimens to sodium vapour were attempted and the most versatile technique was to expose the samples in an evacuated "bomb" containing sodium. The advantages and shortcomings of this method are discussed and details of the routine used for specimen preparation and exposure to sodium are given.

When the specimens had been exposed to sodium vapour, a method of quantifying the extent of the attack was necessary in order to assess the degree of resistance to sodium for different systems. This was carried out by measuring the optical transmission.

The reactions of crystalline and glassy materials with sodium were studied by differential thermal analysis and X-ray powder diffraction. The results obtained from this investigation were used to assess the generality of equilibrium thermodynamics.

From the literature survey, it is apparent that when sodium interacts with a glass, the resultant discolouration is confined to the first few

microns beneath the surface. To study the nature of the discolouration, infra-red reflection spectroscopy (IRRS) and X-ray photoelectron spectroscopy (XPS or ESCA) which are sensitive to this sub-surface region were used. Finally, electron spin resonance (ESR) was carried out on some of the specimens to investigate the model concerning the origin of the discolouration proposed by Stryjak and McMillan (1979).

3.2 Exposure to Sodium Metal Vapour

3.2.1 Techniques of Exposure

The methods described below all relied on the exposure of glasses and transparent glass-ceramics to the saturated vapour of liquid sodium. The different practices used by previous authors [Elyard and Rawson (1962), Burns (1965), Stryjak and McMillan (1979)] were attempted but each method was found to have its limitations. The final technique used was developed through experience with these different methods.

The most convenient ways of exposing specimens to sodium vapour have been to seal the sodium metal and the specimens in an evacuated ampoule made from glass tubing with a sodium resistant glaze (ply tubing) or to seal sodium metal in an ampoule made from the material under investigation. In the former method, the sodium resistant glaze in the ply tubing softens at around 450°C. This then represents the maximum temperature that can be used. If the specimens under test were extremely resistant to sodium, in order to observe any discolouration, the exposure times would have been necessarily long. A more serious problem was that specimens were found to discolour unevenly. This was caused by temperature gradients in the specimens, since only a small part of the specimens was in contact with the

walls of the tubing. The ampoule method of exposure is useful only in situations where the material of interest can be drawn into tubes and where the analytical techniques used to investigate the nature of the discolouration do not require specimens of a specific shape.

Another method used was to expose specimens inside a commercial low pressure sodium lamp. This was carried out with the co-operation of Thorn Lighting Lamps Research Laboratory. Apart from the limited number of specimens that could be exposed, the greatest limitation was that the lamps can only operate at around 280-300°C. This meant exposure times were typically of the order of a few thousand hours for relatively sodium resistant specimens.

By far, the most versatile technique was to expose the specimens inside an evacuated "bomb". A stainless steel bomb was constructed and it is shown in figure 3.2.1. The merits of this technique are that the bomb can be used over a wide temperature range (up to 600°C in the present work), it is reusable and up to six specimens can be exposed at once. The specimens can be baked out and hence they are in a "cleaner" condition before exposing to sodium vapour. To alleviate the problem of uneven discolouration of the samples, the specimen tray was designed such that three sides of the tray were in thermal contact with the walls of the bomb. Although the thermal conductivity of stainless steel is not particularly high (~ 8 times smaller than copper, but ~ 50 times greater than glass), any thermal gradients present across the width of the tray and hence the specimens, which were laid flat on the tray, were expected to be small. This was borne out in practice even on large specimens (25 x 20 x 1 mm), the discolouration was found to be even over the entire surface.

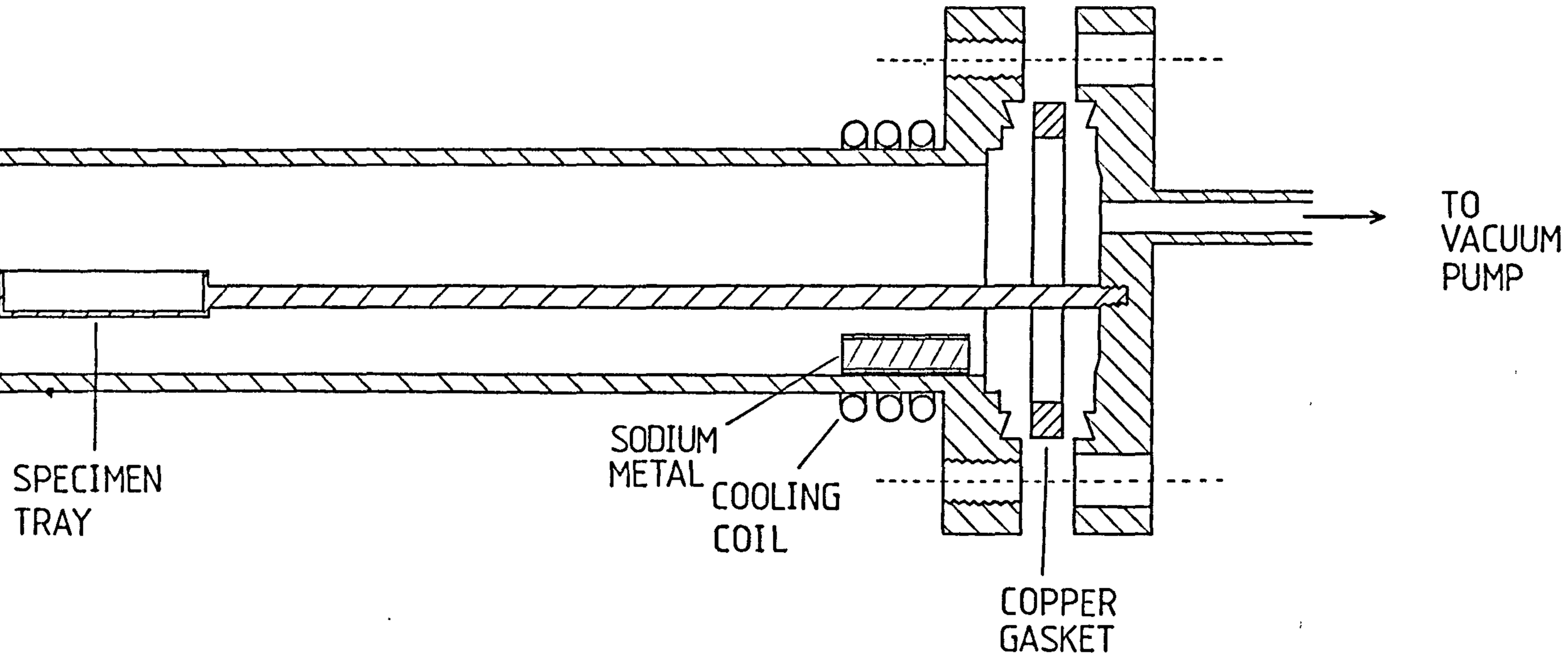

FIGURE 3.2.1

CROSS SECTIONAL VIEW OF THE STAINLESS STEEL BOMB USED FOR SODIUM VAPOUR EXPOSURE

One disadvantage of this method was the existence of a temperature gradient along the length of the bomb, with the result that sodium metal vapour tended to condense at cooler parts. At exposure temperatures of up to 450°C for a duration of 3 hours, the loss of sodium metal in the hot zone (where the specimens were situated) through evaporation was not significant. However, beyond this temperature, the problem became more acute. To compensate for this evaporation, extra sodium metal (~ 1 gm) was used. The bomb was also tilted to about 30° from the horizontal during exposure, in the belief that when sufficiently large droplets of sodium metal were formed in the cooler regions, they would run down to the hotter parts again.

3.2.2 Procedure of Exposure

The vitreous silica and quartz supplied were already polished and they were used as received. The rest of the glasses and transparent glass-ceramics were cut into the appropriate size (~ 20 x 5 x 2 mm) on a diamond saw. The samples were polished on both sides using a slurry of 9 micron alumina particles and water. In cases where the glasses were known to be hygroscopic or react with water [NaS(1), NaS(2), NaB(1), NaB(2)], paraffin was used as a lubricant.

Before exposing to sodium vapour, the samples were washed with deionised water where possible, then rinsed in dried acetone and methanol in an ultrasonic bath. The specimens were handled with tweezers thereafter.

The samples were placed in the specimen tray of the bomb and a short length (~ 3 cm) of stainless steel tubing filled with standard laboratory reagent grade sodium metal (~ $\frac{1}{2}$ gm) was placed at the mouth of the bomb near the cooling coil. The bomb was sealed and evacuated to ~10^{-6} torr and inserted inside a tube furnace. The samples were baked out at 500°C

(where possible) for an hour at $\sim 10^{-6}$ torr, whilst the sodium metal was kept cold by the cooling coil. The bomb was then brought to the desired temperature of exposure and the specimens were allowed to reach thermal equilibrium over a period of 12-24 hours. The cooling coil was removed and the bomb was isolated from the vacuum system just before exposure. The bomb was tilted so that the tube containing the sodium metal slid down the bomb below the specimen tray.

After exposure, the bomb was removed from the furnace and quenched to room temperature to prevent the sodium metal vapour from condensing on the specimens. The bomb was opened in a dried nitrogen atmosphere and the samples were kept in either a nitrogen atmosphere or evacuated desiccators to prevent contamination by oxygen or water vapour.

This routine for cleaning and exposure was used for all the glasses and transparent glass-ceramics studied. Owing to the complexities of glass surfaces, whether the routine used for preparing, cleaning and exposing the specimens to sodium was an ideal one is debatable. However, it was felt there is a need to standardise the surface treatments to eliminate "irregularities" which would invalidate any comparisons between specimens.

3.3 Characterisation of Discolouration by Sodium

In the present work, the different glasses and transparent glass-ceramics studied were directed at determining factors which would improve the resistance of a material towards sodium attack. In order to assess whether a material with a particular chemical composition or structure is more resistant than another, it was necessary to have some means of quantifying the resistance to sodium attack so that a comparison can be made.

The most prominent feature of a glass having been attacked by sodium is the appearance of a discoloured layer on the surface. Materials which

are not very resistant such as vitreous silica showed a black discolouration after being exposed to sodium at 400°C for 3 hours, whilst a more resistant material such as sodium silicate (30 mol.% soda content) showed a light yellowish colour after undergoing the same exposure conditions. The colour of the attacked surface then reflects how resistant a material is towards sodium. To make use of this phenomenon, the optical transmission spectra of the discoloured glasses and transparent glass-ceramics were measured from 200-700 nm.

In an ideal situation, if the discolouration showed a distinct absorption band within the range of frequencies measured, then the resistance of a material towards sodium attack could be related directly to the magnitude of this absorption band. However, in all the cases studied here, the discolouration showed a broad absorption band which extends over the entire range of frequencies measured. Typical absorption spectra obtained for a material which has been exposed to sodium at various temperatures for a fixed time are shown in figure 3.3.1. At low temperatures of exposure the specimen can be seen to absorb strongly in the ultraviolet end with the tail of the absorption edge extending into most of the visible region. As the temperature of exposure is increased, the absorption edge gradually shifts to longer wavelengths. At the highest temperature of exposure, the discolouration absorbs strongly over most of the visible region with the result that the absorption band could only be measured sensibly over a short range of frequencies.

An attempt to characterise these absorption bands was made using Urbach's rule [Mott and Davis (1971)] which is given by the following empirical relationship.

$$\alpha = \alpha_o \exp\left[\frac{\gamma'(\hbar\omega - E_o)}{kT}\right] \qquad (3.3.1)$$

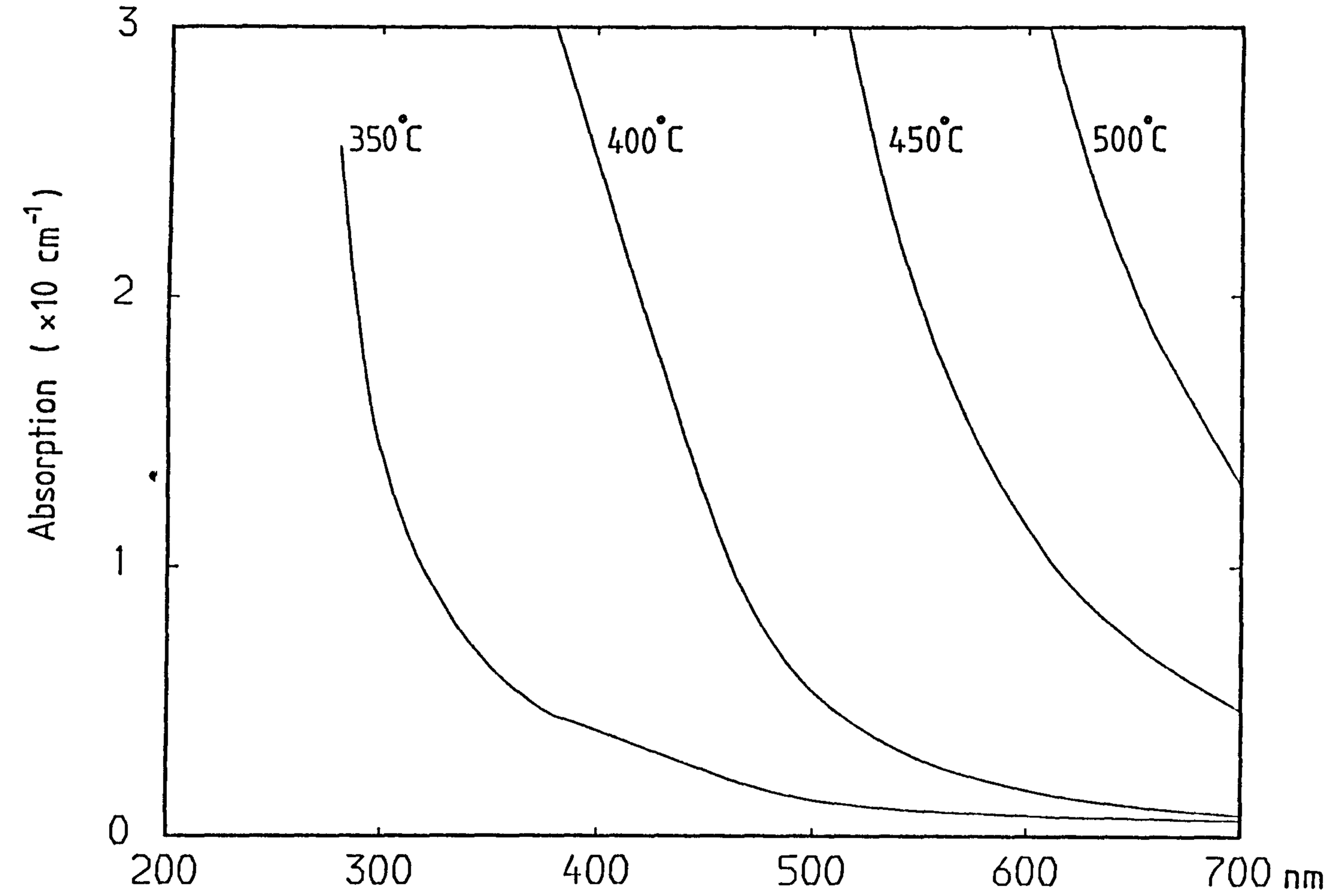

FIGURE 3.3.1

Typical absorption spectra of a silicate glass which has been exposed to sodium at various temperatures for a fixed time of 3 hours.

where α is the absorption coefficient, $\hbar\omega$ is the photon energy, E_o is the energy of the "Urbach" edge, T is the absolute temperature, k is the Boltzmann constant, γ' and α_o are constants. The parameters α_o, γ' and E_o can be adjusted to fit the experimental data which, in turn, can be used to characterise the absorption bands. However, the measured values of α at low temperatures of exposure did not obey an exponential relationship with the photon energy, and at high temperatures of exposure, insufficient experimental data did not permit a satisfactory fit to equation (3.3.1).

A different approach was to assume the absorption coefficient at a particular wavelength $\alpha(\lambda)$ is proportional to the total amount of sodium M which has diffused into the material i.e.

$$\alpha(\lambda) \propto M \qquad (3.3.2)$$

In a simple diffusion situation, the total amount of sodium which has diffused into the material after a time t is [Doremus (1962)]

$$M = 2C_o \left[\frac{Dt}{\pi}\right]^{\frac{1}{2}}$$

where C_o is the concentration of sodium at the surface and D is the diffusion coefficient. The appropriate values of D were extracted from a review paper on ionic diffusion in glasses by Terai and Hayami (1975). By assuming the surface concentration C_o is equal to the concentration of sodium atoms in the vapour phase and that the vapour behaves ideally, then

$$C_o = N_a \frac{n}{V} = \frac{P}{RT}$$

where n/v is the number of moles per unit volume, N_a is the Avogadros' number, P is the vapour pressure of sodium and R is the gas constant. The vapour pressure P at a particular temperature can be obtained from standard tables. Hence, at temperature T for a time t, the total amount of sodium diffused into the material is given by

$$M = \frac{2P}{RT}\left[\frac{Dt}{\pi}\right]^{\frac{1}{2}} \qquad (3.3.3)$$

and

$$\alpha(\lambda) \propto \frac{P}{T}(Dt)^{\frac{1}{2}}.$$

However, a plot of $\alpha(\lambda)$ versus $P(Dt)^{\frac{1}{2}}/T$ failed to give a straight line. It would seem that the simple diffusion argument was not applicable.

Finally, a qualitative approach was adopted as a last resort to describe the discolouration. From the Beer-Lambert law for a particular wavelength λ

$$I(\lambda) = I_o \exp[-\alpha(\lambda)X]$$

where $I(\lambda)$ is the intensity of the transmitted radiation, I_o is the intensity of the incident radiation, $\alpha(\lambda)$ is the absorption coefficient at λ and X is the thickness of the absorbing material. If $\alpha(\lambda)$ is assumed to consist of two contributions, i.e.

$$\alpha(\lambda) = \alpha_g(\lambda) + \alpha_c(\lambda)$$

where $\alpha_g(\lambda)$ and $\alpha_c(\lambda)$ are the absorption coefficients for the unexposed material and for the discolouration respectively. Then the intensity of transmitted radiation for the unexposed material is given by

$$I_g(\lambda) = I_o \exp[-\alpha_g(\lambda)X] \qquad (3.3.4)$$

The measured absorption coefficient is an average result which does not distinguish between discolouration concentrated at the surface or distributed evenly throughout the thickness of the sample. Hence, for an exposed material, the transmitted intensity can be written as

$$I_c(\lambda) = I_o \exp\ [-(\alpha_g(\lambda) + \alpha_c(\lambda))\ X] \qquad (3.3.5)$$

Combining equations (3.3.4) and 3.3.5)

$$I_c(\lambda) = I_g(\lambda)\ \exp\ [-\alpha_c(\lambda)\ X] \qquad (3.3.6)$$

or $$\frac{1}{X}\ \ln\left[\frac{I_g(\lambda)}{I_c(\lambda)}\right] = \alpha_c(\lambda)$$

Therefore, a plot of $\alpha_c(\lambda)$ at a particular wavelength versus temperature of exposure for a fixed time would give an idea of the resistance of different materials with respect to the sodium treatment. The wavelength was chosen to be 500 nm which is about the centre of the optical region. This method of characterising the discolouration is fairly arbitrary, However, the qualitative results obtained seemed to show good agreement with infra-red reflection measurements which are described later in this chapter.

The optical transmissions of the specimens were measured using a Cecil double beam spectrophotometer in the range 200-700 nm at room temperature. To avoid contamination of the samples by oxygen or water vapour during measurements, the specimens were placed inside a silica liquid sample holder with an air-tight stopper whilst in a dried nitrogen atmosphere. The measurements were carried out with an empty liquid sample holder in the reference-beam of the spectrometer.

3.4 Thermal Investigation of the Reaction with Sodium Metal Vapour

3.4.1 Introduction

On the question of whether a glass will be attacked upon exposure to sodium vapour, an explanation based on equilibrium thermodynamics was first introduced by Elyard and Rawson (1962). The arguments these authors used are as follow. If vitreous silica is exposed to sodium, a likely reaction is

$$4Na + SiO_2 \rightarrow 2Na_2O + Si \qquad \Delta G > 0$$

The change in free energy of the reaction is positive, so the reaction is not likely to occur. However, subsequent reaction of Na_2O with excess SiO_2 present, resulting in the formation of a sodium silicate, will give a negative change in free energy. For example

$$4Na + SiO_2 \rightarrow 2Na_2O + Si \qquad \Delta G > 0$$

$$2Na_2O + 4SiO_2 \rightarrow 2Na_2Si_2O_5 \qquad \Delta G < 0$$

and

$$4Na + 5SiO_2 \rightarrow 2Na_2Si_2O_5 + Si \qquad \Delta G < 0$$

Hence the reduction of vitreous silica by sodium is to be expected.

A similar argument is also applicable to vitreous B_2O_3; the reaction

$$6Na + B_2O_3 \rightarrow 3Na_2O + 2B \qquad \Delta G > 0$$

is not likely to occur, but further reaction of Na_2O with excess B_2O_3 resulting in a sodium borate will give a negative change in free energy. So the reduction of vitreous B_2O_3 by sodium is also to be expected.

Both vitreous SiO_2 and vitreous B_2O_3 are attacked by sodium, but whether the reduction processes indeed result in the formation of sodium silicate or borate has not been confirmed experimentally. It is clear though, from the above examples, that if a thermodynamic argument is to

be applied to predict whether a glass will react with sodium, full knowledge of the possible pathways of the reaction is necessary. Another factor to bear in mind is the generality of equilibrium thermodynamics when applied to meta-stable systems such as glasses. Whether the difference in thermodynamic properties between a glassy material and its crystalline counterpart affects the overall outcome of a reaction predicted by an equilibrium argument remains an open question.

The aim of the present work was to investigate the reaction of sodium with the selected glasses. Differential thermal analysis was carried out to study the heat changes of any reactions and the temperatures at which they occurred. Vitreous silica and quartz were closely examined when reacted with sodium under identical conditions, in the belief that a comparison between the behaviour of the two materials might provide a means of assessing the generality of an equilibrium thermodynamic argument. X-ray powder diffraction was carried out to investigate whether any crystalline products were formed during the reaction with sodium. The identification of the reaction products may then provide clues as to how the glasses were attacked.

3.4.2 Differential Thermal Analysis (DTA).

The principle and the practice of DTA have already been discussed in section 2.3.2 , thus the following description is concerned with the details of the experiment.

The aim was to measure the heat changes involved as the glasses were heated in an environment of sodium. This was carried out by sealing the sample and the sodium metal inside an evacuated capsule. The capsules in a cylindrical form were made of stainless steel;

they measured about 3 cm high and 6 mm in diameter so as to fit into the sample cell of the Stanton-Redcroft 67/4 DTA apparatus. To maximise the sensitivity the walls of the capsules were made as thin as possible ($\sim$ 0.2 mm in thickness) and a recess (or indentation) of about 4 mm deep and 2 mm in diameter was made at the bottom of the capsule to accommodate the thermocouple of the DTA apparatus.

The procedure of the experiment was to place a known weight of sample (0.1000 $\pm$ .0002 gm, in the form of 100-150 micron particles) and sodium metal ($\sim$ 0.12 gm) inside the capsule. The capsules were connected to a vacuum system and evacuated to $\sim 10^{-6}$ torr. They were then sealed about 1 cm from the top by resistance welding whilst still under vacuum. The thermal analysis was carried out at a heating rate of $\sim 8^{\circ}C$/min using 100-150 micron alumina particles in a similar capsule as reference and in a nitrogen atmosphere to prevent the capsules from oxidising.

3.4.3 X-Ray Powder Diffraction

X-ray powder diffraction was used to investigate whether any crystalline products were formed when sodium interacts with the selected glasses.

A Debye-Scherrer powder camera was used. The powder samples were prepared by crushing the glasses and passing the resultant powder through a 300 mesh ($\sim$ 50 microns) sieve. The glass powders were placed loosely on the specimen tray of the stainless steel bomb (figure 3.2.1) and they were exposed to sodium vapour using the procedure described in section 3.2.2. After exposure to sodium, the powders are extremely reactive, therefore they were handled in a dried nitrogen atmosphere whenever possible. The problem of contamination by oxygen or water

vapour during exposure to X-rays was overcome by sealing the sodium exposed powders inside Pyrex glass capillaries (0.5 - 0.8mm in diameter).

The diffraction patterns were obtained using radiation from a copper target and they were recorded on film. The identifications were carried out by comparing with standard A.S.T.M. powder diffraction data.

3.5 Surface Sensitive Studies

3.5.1 Introduction

To summarise the work on the interaction of sodium with glasses by previous authors (see section 1.3), the results of the interaction were conveniently divided into a high and a low temperature regime. At high temperatures of exposure the glass is reduced rapidly by sodium. Whereas at low exposure temperatures, the attack by sodium is manifested in the formation of a yellow to brown discoloured layer on the surface of the glass where it has been exposed to the vapour. Various possibilities have been suggested concerning the nature of the discolouration, such as the formation of silicon monoxide [Burns (1965)], colour centres [Stryjak and McMillan (1979)] or aggregates of sodium of colloidal size [Fonda and Young (1934)]. Apart from some experimental evidence on the formation of colour centres, the other possibilities have not been borne out experimentally.

All the authors agreed that the discolouration of the glasses by sodium is essentially a surface phenomenon and that the thickness of the discoloured layer was estimated to be a few microns. To study the nature of the discolouration, then, any chosen technique has to be sensitive to this region of the surface. For the present work, the techniques employed to investigate the nature of the discolouration

PAGE
MISSING
IN
ORIGINAL

provide information about the chemical states or structures of the glass. This is illustrated by the work of Trickler et. al. (a.1974, b.1974) on iron containing calcium phosphates and borates, and Bruckner et. al. (1978) on the structure of alkali silicates and alumino-silicates. The other area of research is concerned with the glass surface such as protective tin coatings [Budd (1975)], compositional changes at the surface of hydrogen reduced lead silicates [Bates et. al. (1972)] and leached soda lime silicates [Escard and Brion (1975)]. In the present section, a brief discussion of ESCA is given, followed by details of the experiment carried out.

As a spectroscopic tool, ESCA is extremely versatile [Clark (1977)], amongst its many virtues is the capability of studying the electronic structures of solids, liquids and gases. It can be used as an analytical tool for elemental identification; when applied to solids, it is a surface sensitive technique and with the possibility of analytical depth profiling. Much of the interest in ESCA has been stimulated by the discovery that the core level binding energies of an element change depending on the chemical environment [Siegbahn (1967)]. This is similar to the chemical shift in NMR and gives rise to the possibility of identification of oxidation states and structures.

The fundamental processes occurring in ESCA are depicted in figure 3.5.1. If a solid is irradiated with monoenergetic photons of a sufficiently high energy ($\sim$ 1-2 KeV), the emission of electrons will occur as a consequence of the absorption of photons. The kinetic energy of the emitted electrons (or photoelectrons) is given by Einstein's relationship:

$$E_k = h\upsilon - I_k \qquad (3.5.1)$$

where $h\upsilon$ is the energy of the incident photon, I_k and E_k are the binding

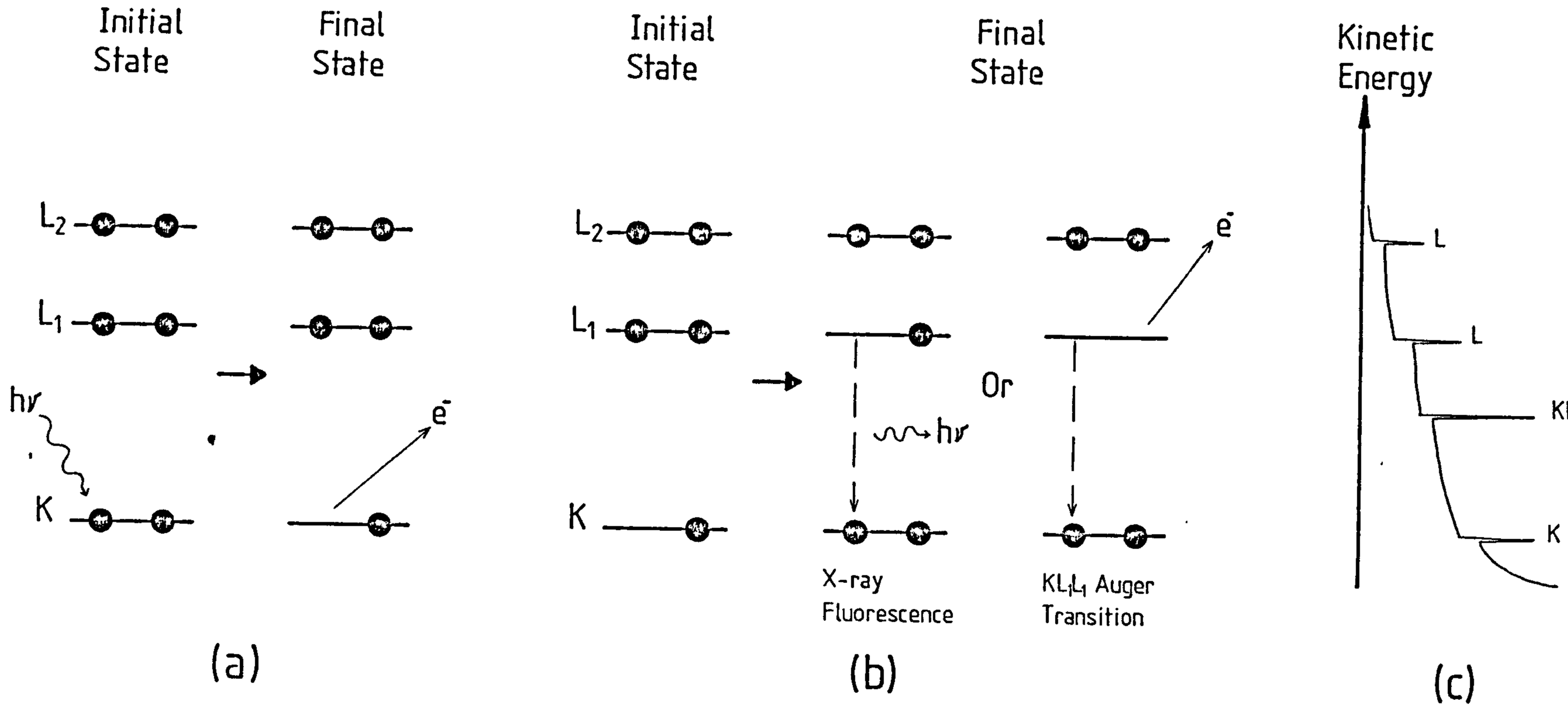

FIGURE 3.5.1

Schematic diagram of the fundamental processes occurring in an atom during an ESCA experiment. (a) Ejection of a core electron by a high energy photon, leaving a vacant "hole" in the core. (b) Relaxation of the atom having a vacant core state. (c) The measured kinetic energy spectrum of ejected electrons. The high background at low kinetic energies is due to electrons which had been inelastically scattered.

and kinetic energy respectively of the k^{th} species of electrons in the material. Since the energy levels occupied by the electrons are quantised, the analysis of the distribution of kinetic energies of photoelectrons will show a series of discrete bands. The positions (in energy) of these bands is related to the binding energies of the core levels of the material through equation 3.5.1. The ejection of electrons produce vacant "holes" in the core levels and the atoms in the material can subsequently relax by one or two means (Figure 3.5.1b). That is by X-ray fluorescence or by emission of secondary electrons via an Auger process. Hence, additional peaks are observed in the kinetic energy spectrum due to the emission of Auger electrons.

The surface sensitivity of the technique is attributed to the fact that electrons travelling through a solid will have a high probability of being inelastically scattered by locally bound electrons. Therefore only photoelectrons which are produced near the surface have a high probability of emerging from the surface (and to the detector) and appear in the kinetic energy spectrum with their original characteristic energy. The rest of the ejected electrons having undergone inelastic collisions contribute to the continuous background at lower kinetic energies (Figure 3.5.1c). The surface sensitivity of the technique can be described by a "mean escape depth", and it represents the depth from which $1/e$ of the photoelectrons produced can escape without a loss of energy. The mean escape depth is strongly dependent on the kinetic energy and the material in question, but typical values are tens of angstroms in the energy range 10-1000eV [Brundle (1974)].

The ejection of electrons leaves a net positive charge on the specimen and subsequent electrons leaving the surface will have a lower kinetic energy. There are two ways in which the specimens can neutralise this charge. One is if the sample is in electrical contact

with the spectrometer (earthed) where electrons can be taken up as required or the capture of stray electrons from the vacuum system. In the study of insulators such as inorganic glasses where the specimen cannot be earthed, and if the rate of arrival of stray electrons is less than that ejected, the specimen will have a net positive charge. This renders the measurement of absolute binding energy and hence core level shifts inaccurate.

To circumvent this charging problem in the present work, a quantity called the "Auger parameter" [Wagner and Biloen (1973)] was measured. The Auger parameter α^* is the relative separation (in energy) between the strongest Auger peak and a particular core level where both occur in the same spectrum. For example

$$\alpha^* = E_{KE}\ (KLL) - [h\upsilon - E_{BE}(2P)] \qquad (3.5.2)$$

or $$\alpha^* = E_{KE}\ (KLL) - E_{KE}(2P)$$

where E_{KE} (KLL) is the kinetic energy of the KLL Auger line and $E_{BE}(2P)$ and $E_{KE}(2P)$ are the binding and kinetic energies of the 2P level. The Auger parameter is independent of charging and since Auger peaks are also subjected to "chemical shifts", α^* varies for different chemical environments. An inconvenient feature of the Auger parameter however can be seen from equation 3.5.2, α^* is dependent on $h\upsilon$, the energy of the exciting photons. Therefore α^* will be different for different X-ray sources used. Recently Wagner, Gale and Raymond (1979) have introduced a "modified Auger parameter" which is independent of $h\upsilon$, given by

$$\alpha^{**} = E_{KE}\ (KLL) + E_{BE}(2P) \qquad (3.5.3)$$

where E_{KE}(KLL) and E_{BE}(2P) are measured on the same spectrum. This is a much more useful quantity since it is now independent of outside variables and is a characteristic property of the element in a particular chemical environment. The Auger parameter for many compounds has been measured by Wagner et. al. (1977, 1979) and by Castle and West (1979) and their results will be used for comparison with the present work through the modified Auger parameter.

Vitreous silica which has been exposed to sodium vapour, as described in section 3.2 at various temperatures, was studied by ESCA. The aim was to establish whether there are any changes in the oxidation states of silicon, oxygen and sodium. The experiment was carried out at room temperatures in a V.G. ESCA3 spectrometer using a 260W aluminium X-ray source ($h\upsilon$ = 1486.6eV) and a hemispherical electron analyser. The spectrometer was equipped with a V.G. 3000 data system for handling the results and wide sweeps (0-1200eV) of the kinetic energy spectrum and narrow scans (20eV wide) of the individual peaks were taken and computer averaged over 5 sweeps. The acquisition time was 300 seconds per sweep and the analyser energy was 50eV.

3.5.3 Infra-Red Reflection Spectroscopy (IRRS)

Infra-red spectroscopy is concerned with the interaction of electromagnetic radiation with the vibrational and rotational modes of molecules or molecular groups. The conditions for interaction are that the energy of the radiation is equal to the difference in energy between transitional states and that the radiation can be coupled to the molecules. Coupling can be achieved if the molecules or the vibrations (and rotations) of the molecule exhibit an electric moment. The vibrational and rotational spectra obtained are characteristic of the

molecules concerned and suitable analyses can give information about the shapes of the molecules and bond strengths between atoms in the molecule. In cases where the intermolecular interactions are important, as in solids, the rotational modes are usually smeared out and the vibrational spectra are modified depending on the structure. Hence, careful analysis of the vibrational modes can, in favourable cases, give information about the structure of the solid.

Infra-red spectroscopy has become very much a routine technique and it will not be discussed further as many comprehensive texts on the subject already exist [Herzberg (1945), Nakamoto (1978), Houghton and Smith (1966)]. The volume of literature available on the infra-red studies of inorganic oxide glasses is also extensive and a resume of the current advances in the field is beyond the scope of the present section. Instead reviews by Simon (1960), Wong and Angell (1971, 1976) and Donald and McMillan (1978) on infra-red transmitting materials are referred to. The present section will concentrate on the technique working in the reflection mode and its application to the study of surface phenomena.

The majority of infra-red studies are carried out in the transmission mode, but measurement of the reflectivity can also be used to locate the vibrational modes of a solid. To illustrate this, consider a simple solid with N molecules per unit volume and an effective charge n_e on each molecule. If the molecules are represented by damped harmonic oscillators and the solid is subjected to the influence of a varying electric field E of frequency ω, then the polarisation $\hat{P}$ of the lattice is given by [Ziman (1964)]

$$\hat{P}(\omega) = \frac{Nn_e e^2 E}{M(\omega_o^2 - \omega^2 + i\omega\Gamma)} \qquad (3.5.4)$$

where e is the electronic charge, M the reduced mass of the atoms in the molecule, ω_o is the resonant frequency of a particular vibrational mode of the solid and Γ the damping factor. The symbol $\sim$ is used to denote a complex quantity. From classical theory,

$$\hat{\epsilon}(\omega) = 1 + \frac{\hat{P}(\omega)}{\epsilon_o E} \qquad (3.5.5)$$

and $$\hat{\epsilon}(\omega) = \hat{n}(\omega)^2$$

or $$\epsilon_1 + i\epsilon_2 = (n + ik)^2 \qquad (3.5.6)$$

where ϵ_o is the permittivity of free space, $\hat{\epsilon}$ the dielectric constant, $\hat{n}$ the refractive index and k is known as the extinction coefficient. By combining equations (3.5.4) and (3.5.5) and separating into real and imaginary parts,

$$\epsilon_1 = 1 + \frac{S\omega_o^2(\omega_o^2-\omega^2)}{[(\omega_o^2-\omega^2)^2+\omega^2\Gamma^2]}$$

$$\epsilon_2 = \frac{S\omega_o^2\omega\Gamma}{[(\omega_o^2-\omega^2)^2+\omega^2\Gamma^2]}$$

where $$S = \frac{Nn_e e^2}{\epsilon_o M}$$

and S is related to the strength of interaction between the solid and the applied field [Loudon (1973)] and from equation (3.5.6)

$$n = [\tfrac{1}{2}(\epsilon_1^2+\epsilon_2^2)^{\frac{1}{2}} + \epsilon_1]^{\frac{1}{2}}$$

$$k = [\tfrac{1}{2}(\epsilon_1^2+\epsilon_2^2)^{\frac{1}{2}} - \epsilon_1]^{\frac{1}{2}}$$

The reflectance R is the quantity measured and it is related to the refractive index through Fresnel's formula for reflection from a plane boundary. At normal incidence, the reflectance is given by

$$R = \frac{(n-1)^2 + k^2}{(n+1)^2 + k^2}$$

The variations of ϵ_1, ϵ_2, n, k and R as functions of ω for a particular choice of S and Γ through the resonant frequency ω_o are shown in figure 3.5.2. As it can be seen, the reflectance increases sharply near the region of ω_o but neither maxima of the reflectance nor the extinction coefficient (the quantity measured in transmission) coincide with the resonant frequency. The reflectance peak does not follow a Lorentzian or a Gaussian line shape and it can be distorted beyond recognition depending on S and Γ.

The analysis of the reflectance spectra can be quite involved, this has tended to encourage the use of the more straight forward transmission method. However, in situations where the materials under study are strongly absorbing and the preparation of thin films is necessarily difficult, then measurements in the reflection mode are more convenient. The reflection method has the advantage that the optical constants (n and k) can be calculated separately from the reflectance data using either a graphical procedure described by Simon (1951) or by Kramers Kronig analysis [Andermann, Caron and Dows (1965)]. The technique can also be applied to the study of surfaces since the thickness of the material examined is restricted to the penetration depth. At 0° angle of incidence, the penetration depth d is given by [Born and Wolf (1965)]

$$d = \frac{\lambda_o}{4\pi nk}$$

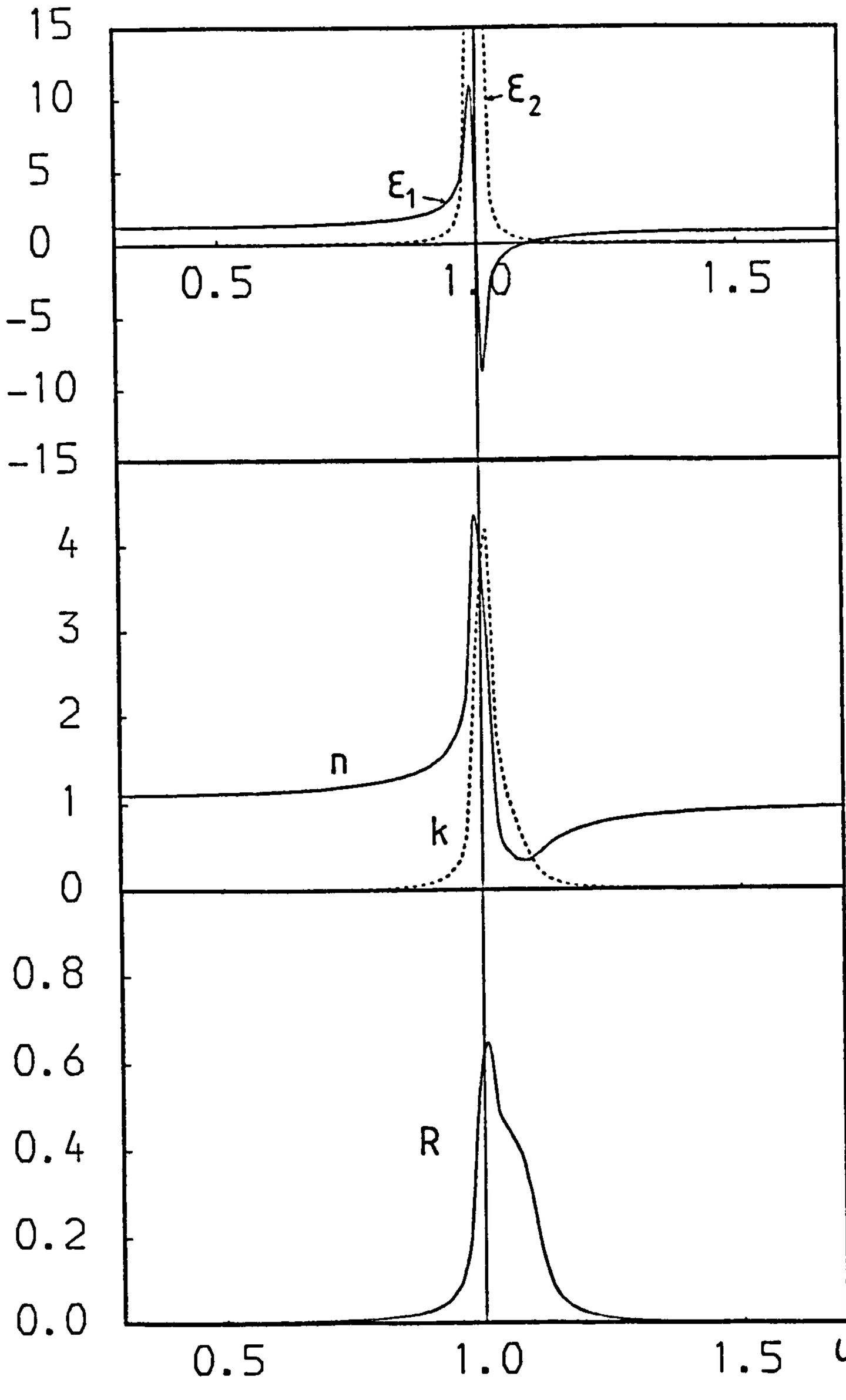

FIGURE 3.5.2

Variation of (a) the dielectric constants with frequency, (b) the refractive index and extinction coefficient with frequency and (c) the percentage reflectance with frequency through the resonant frequency ω_o. $S = 0.2$ and $\Gamma = \omega_o/20$.

where λ_o is the wavelength of the incident radiation. Given that λ_o = 10 micron, then for a silicate glass with n ~ 1.5 and k ~ 1, d is of the order of 0.5 microns. IRRS has been applied successfully to the study of leached glass surfaces [Sanders, Person and Hench (1972)] and the general merits of the technique have been discussed by Hench (1975).

For the present work, IRRS was used as a surface sensitive technique to examine the vibrational modes of the glasses which have been exposed to sodium. The structural information deduced from the changes in the vibrational spectra was analysed on a qualitative basis and this analysis relied heavily on the work of previous workers [Jellyman and Procter (1955)]. All the glasses and transparent glass-ceramics described in chapter 2 were studied and the preparation of the samples has already been described in section 3.2. The specimens were exposed to sodium at various temperatures for a fixed time of 3 hours and thereafter handled with tweezers. Infra-red reflection spectra were taken at room temperature in the wavelength range 5 - 25 microns. The measurements were carried out on a Grubb Parsons Spectromaster double beam spectrometer using a vertical reflectance attachment with a fixed angle of incidence of 15°; the standard used was an aluminised mirror. To prevent the specimens from being contaminated, the reflectance measurements were carried out as soon as possible (~ a few minutes) after exposure to sodium and an enclosure was built such that the sample compartment of the spectrometer could be flushed with dried nitrogen during measurement.

3.6 Electron Spin Resonance (ESR)

Any atomic system which possesses a net angular momentum has a permanent magnetic moment associated with it and it is, therefore, paramagnetic. The net angular momentum arises from incompletely

filled orbitals or unpaired electrons (spins). If such a paramagnetic system in its ground state is placed in a magnetic field, the ground state will split into a set of discreet energy levels due to the Zeeman interaction, which may be further modified by other interactions, e.g. hyperfine interaction. The separation in energy between these discreet levels falls in the microwave region and ESR is concerned with transitions between these levels. The fundamental principle of ESR are well treated in books by Orton (1968), Pake (1962), Slichter (1963) and Feynman (1965), and will not be discussed further.

ESR has found applications in many areas, the utility of the technique lies in the possibility of identifying the paramagnetic centres, their valence state and the environment in which they reside. Of interest to the present work is the study of radiation induced defects in inorganic oxide glasses. Both theoretical and experimental investigations in this area are extensive, and details can be found in reviews by Bishay (1970), Wong and Angell (1976) and Griscom (1973/4, 1978). The main conclusions drawn can be summarised in a schematic form shown in figure 3.6.1. The prevalent defects induced by irradiation are electrons trapped in oxygen vacancies (E' centres) and holes trapped on both bridging and non-bridging oxygens. To explain the origin of the discolouration in silicate glasses caused by the exposure to sodium, Stryjak and McMillan (1979) proposed a model in which they suggested the discolouration is due to the formation of E' centres [see section 1.2]. This is a result of sodium atoms having diffused into the surface of the glass and caused breaking of some Si-O bonds. Their model was deduced from the observation that both X-ray irradiated and sodium exposed specimens produced the same kind of ESR spectrum.

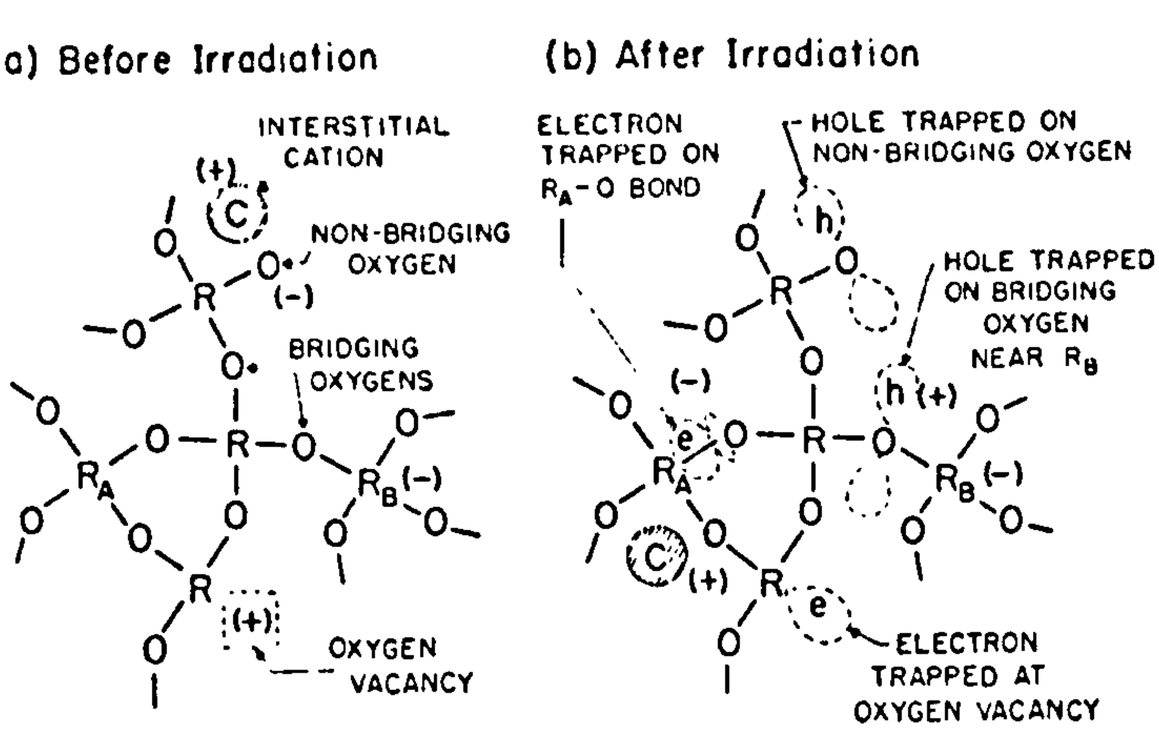

FIGURE 3.6.1*

Schematic diagram of an oxide glass showing several types of radiation-induced paramagnetic centers in their relationships with pre-existing defects such as an oxygen vacancy, a non-bridging oxygen, and substitutional impurities. Dashed 'balloons' enclose regions of high probability density for the trapped electrons (e) or trapped holes (h). This figure illustrates the locally charge-compensated nature of the trapped species. It should be noted, however, that the individual trapped holes and electrons are assumed to be much more distant from one another than shown here.

* Extracted from the paper by Griscom (1973/4).

The purpose of the present work is to pursue a similar line of investigation starting with vitreous silica and then gradually increase the complexity of the glasses in order to establish a certain trend. All the silicate glasses listed in table 2.2.1 were studied and the preparation of the specimens has been described in section 3.2. The specimens were exposed to sodium at various temperatures for a fixed time of 3 hours and thereafter handled with tweezers. The experiments were carried out at room temperature on a Decca X1 ESR spectrometer operating at 9.27 GHz. The ESR spectra were obtained as the first derivative of absorption of microwave power versus magnetic field and carbon (coke) was used as a g-marker for the free electron resonance. To prevent contamination during measurement, the specimens were sealed inside the sample tube of the ESR apparatus with a rubber bung in a dried nitrogen atmosphere.

CHAPTER 4: Microstructural and General Properties of Transparent Glass-Ceramics

The present chapter is concerned with results obtained from the characterisation of transparent glass-ceramics derived from the glass compositions MgBAl (3-2) and CAl (6) [Table 2.2.1], and it is divided into three sections. Under the heading of thermal analysis, details of the heat treatment programmes used to crystallise the glasses and the kinetics of crystallisation of these glasses studied by DTA and DSC are given. The second section presents the microstructures of the resultant transparent glass-ceramics studied by SEM and TEM. Results of the quantitative analysis of the transformed fractions and their mineralogical constitution are also included and the third section deals with the results of some of the general properties of the transparent glass-ceramics.

4.1 Thermal Analysis

4.1.1 Heat Treatments

A two stage heat treatment programme was used to crystallise the glass MgBAl (3-2) where the first stage was used to induce the formation of nuclei and the second stage was used to promote the subsequent growth of the nuclei. The second stage heat treatment temperature was chosen such that the glass could be crystallised in a reasonable length of time ($\sim$ a few hours) without substantial deformation. This temperature was arrived at on a trial and error basis, and for this particular composition, the optimum "crystallisation temperature" was about 730°C.

In order to develop transparent glass-ceramics with appreciable volume fractions of crystals, a high density of nuclei is required. Therefore, it is necessary to choose a temperature in the first stage of the heat

treatment for which the rate of nucleation is a maximum. This temperature was determined by DSC.

Figure 4.1.1 (a) shows the heat evolved measured as a function of time at the crystallisation temperature of 730°C for samples of MgBAl(3-2) which have been heat treated at different "nucleation temperatures" for a fixed period of 4 hours. All the curves showed a change in slope after the first few hours indicating the "fully" crystallised material probably contains two crystalline phases. From observations made in other heat treatments, most specimens became almost opaque after about 4 hours at 730°C. Therefore the portion in figure 4.1.1 (a) that is of interest to the development of transparent glass-ceramics is the first few hours. It should also be added that for a sample of MgBAl (3-2) which had not received any nucleation treatment, the amount of heat evolved at the crystallisation temperature of 730°C (not shown in figure) over a period of 24 hours was not significant. This implies that the curve for the rate of nucleation (see Appendix 1) is sufficiently far removed from the crystallisation temperature of 730°C.

By considering an arbitrary time of say 3 hours in figure 4.1.1 (a), the amount of heat evolved for the specimen which had been nucleated at 670°C for 4 hours is the highest. This implies the highest volume fraction of crystals transformed which, in turn, suggests the highest density of nuclei. Hence, the optimum nucleation temperature for MgBAl (3-2) was about 670°C. Figure 4.1.1 (b) shows the effect of varying the "nucleation time" at 670°C. For the sample which had been nucleated for 12 hours, the increase in the amount of heat evolved after say 3 hours is substantial, indicating an even higher density of nuclei, as expected.

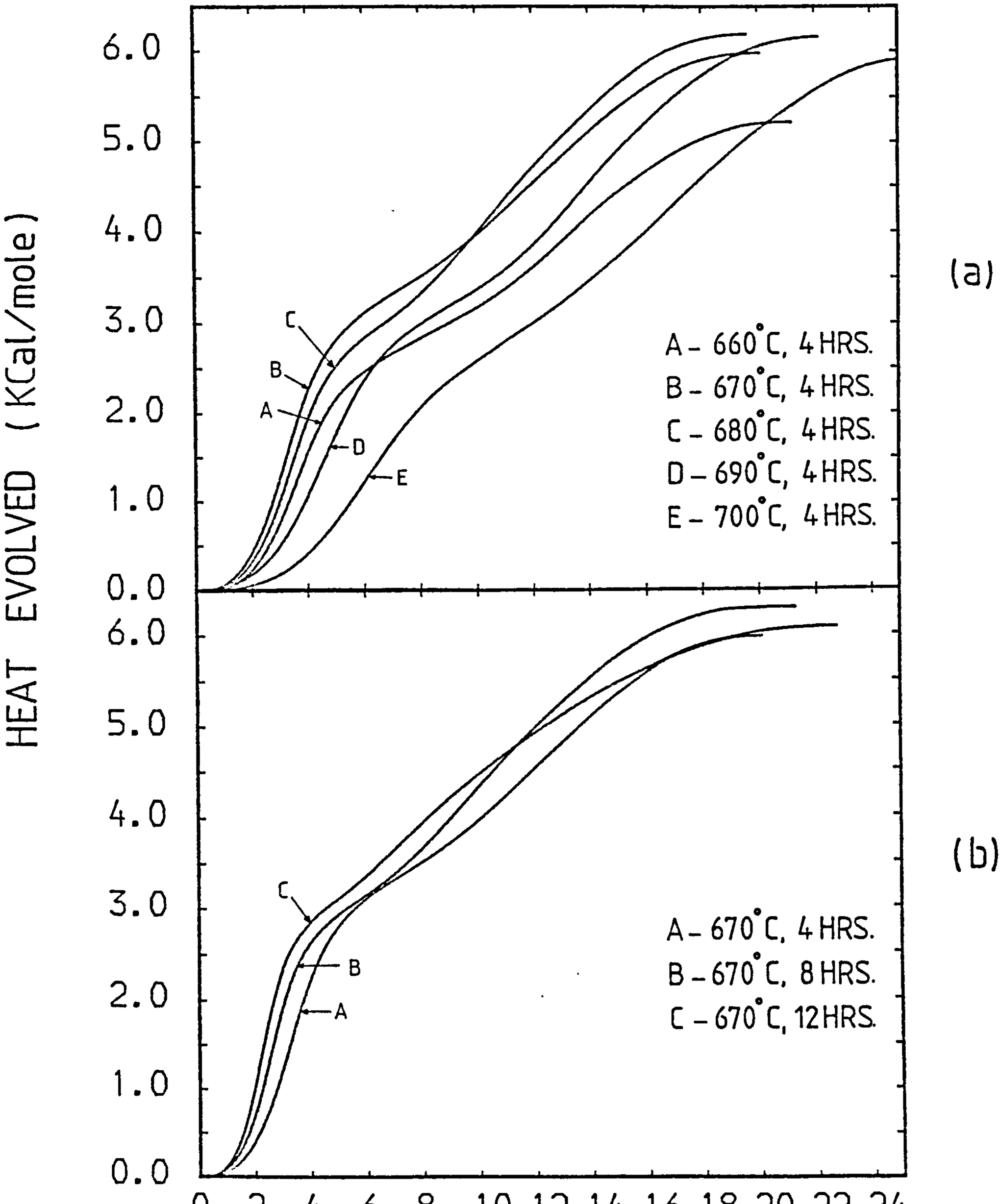

FIGURE 4.1.1

Heat of crystallisation as a function of time at 730°C for the composition MgBA1 (3-2) nucleated at (a) different temperatures for a period of 4 hours and (b) the same temperature of 670°C for different times.

As already mentioned in section 2.3.1, the composition CA1(6) showed surface crystallisation only and that an abrasion treatment was used to standardise the surface. SEM micrographs demonstrating the effect of this abrasion treatment are shown in figure 4.1.2. For the sample which had not received any abrasion, relatively sparse "islands" of crystals were formed. For the samples which had been abraded, the overall effect is that there is greater enhancement in crystal growth, and in particular the sample which had been abraded for 2 hours. There is a higher density of crystals formed which are apparently more uniform in size. Since an appreciable volume fraction of crystals is desired, all the specimens used for the preparation of transparent glass-ceramics were abraded for 2 hours before any heat treatments.

A single stage heat treatment programme was used to crystallise CA1(6). The choice of crystallisation temperature was based on the same criterion as that for MgBA1 (3-2), that is, the growth of crystals should proceed at a controllable rate without significant deformation of the sample. The optimum crystallisation temperature for the composition CA1 (6) was found to be 880°C.

The heat treatment programmes used to crystallise MgBA1 (3-2) and CA1 (6) are summarised in table 4.1.1.

4.1.2 Differential Thermal Analysis (DTA)

DTA was carried out on MgBA1 (3-2), both on the glass and the glass which had been nucleated at 670°C for various times. The results are shown in figure 4.1.3. For the sample which did not receive any nucleation treatment, a single crystallisation peak occurred, with perhaps a weak shoulder appearing on the low temperature side of the

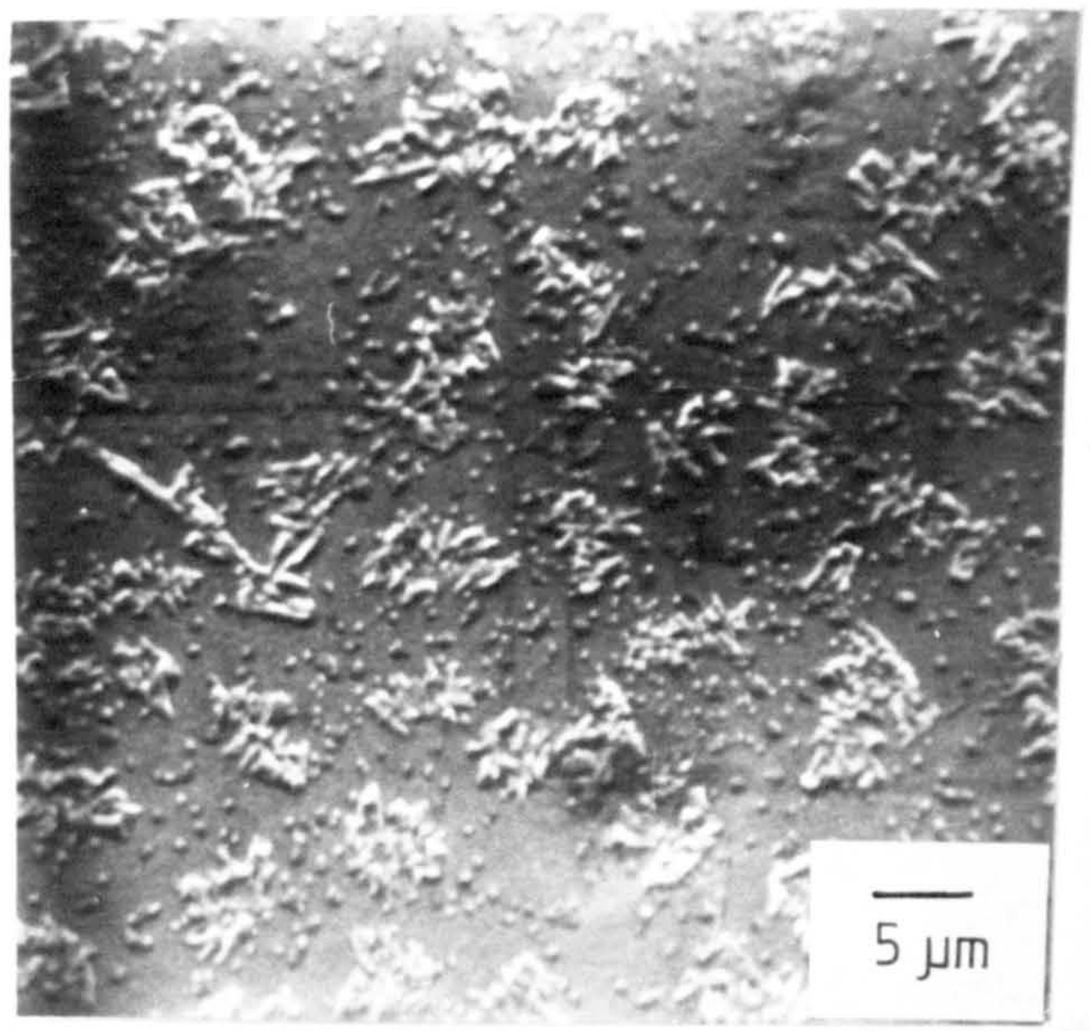

No abrasion.

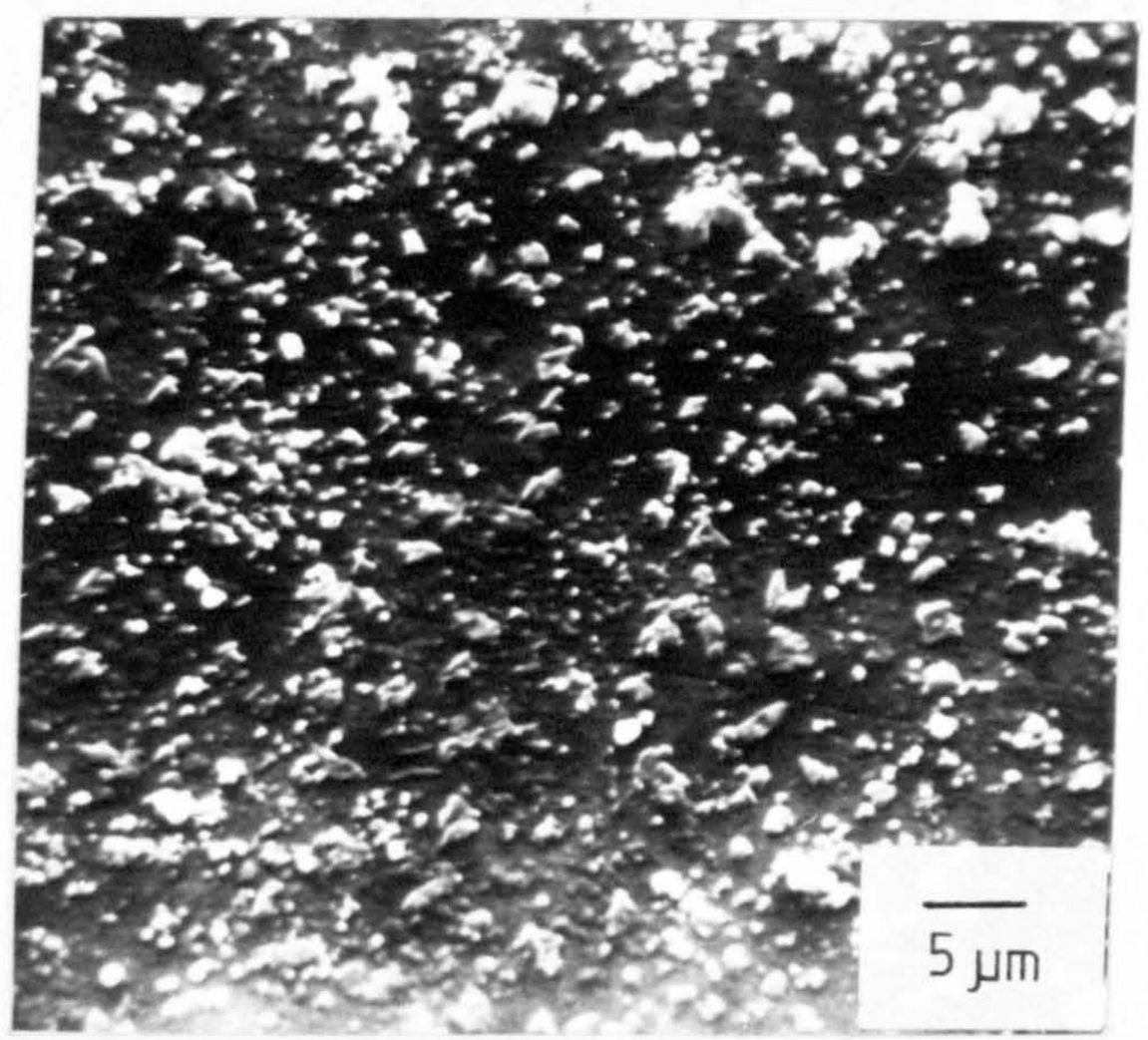

Abraded for $\frac{1}{2}$hr.

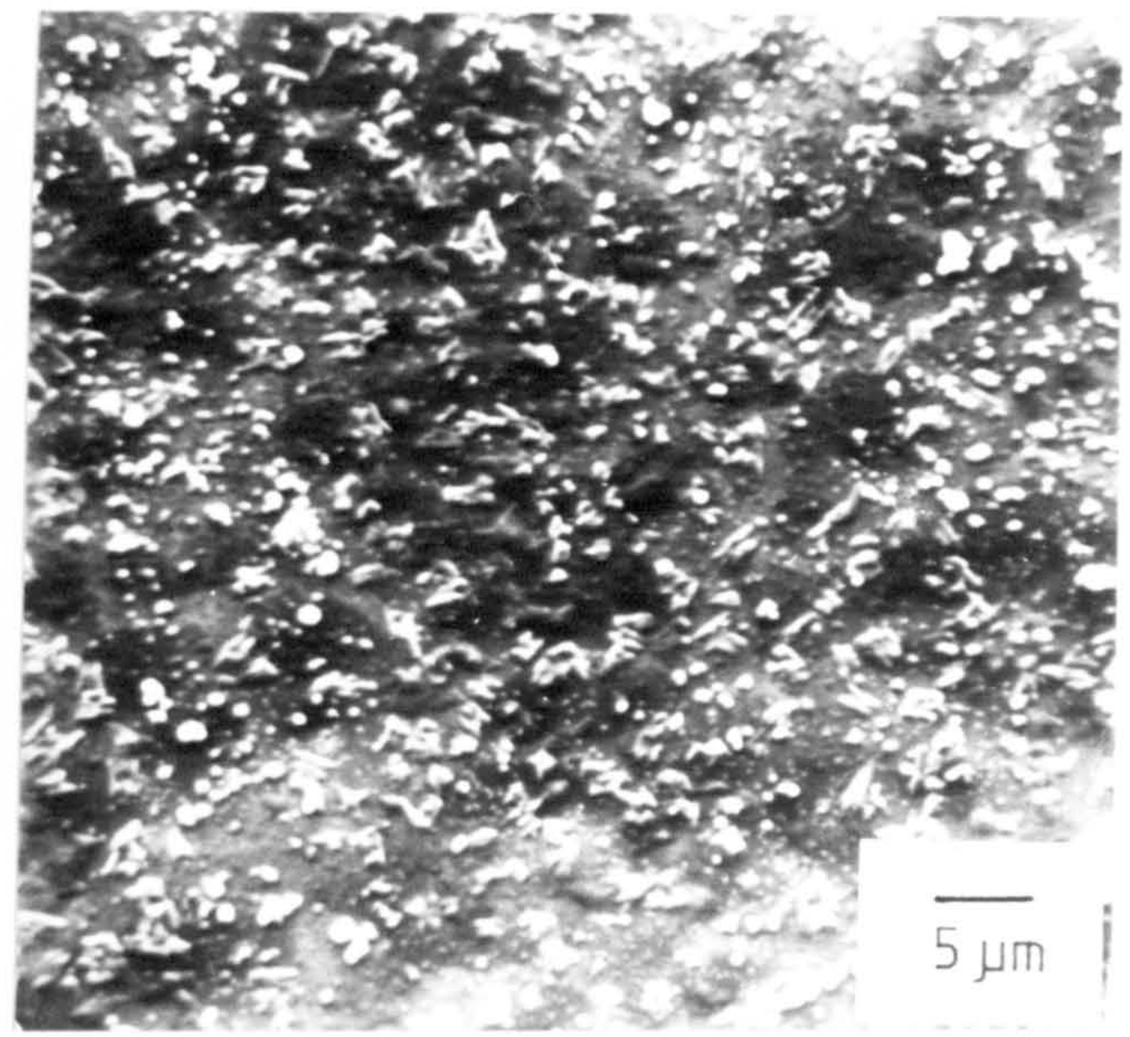

Abraded for 2hrs.

Figure 4.1.2

Effect of the abrasion treatment on CAl(6)
heat treated at 880°c for $\frac{1}{4}$hr.

Glass	Nucleation Conditions	Crystallisation Conditions
MgBAl(3-2)	From ambient to 670°C at 5°C/min. Hold for either 4 or 8 or 12 hours.	From 670°C to 730°C at 2°C/min. Remove samples at hourly intervals up to 5 hrs.
CAl(6)	Specimens polished to 1 micron diamond paste finish initially, then tumble in fresh 80 mesh silicon carbide for 2 hours.	From ambient to 880°C at 5°C/min. Remove samples at 2 hourly intervals up to 6 hrs.

TABLE 4.1.1

Heat treatment programmes for the compositions MgBAl(3-2) and CAl(6).

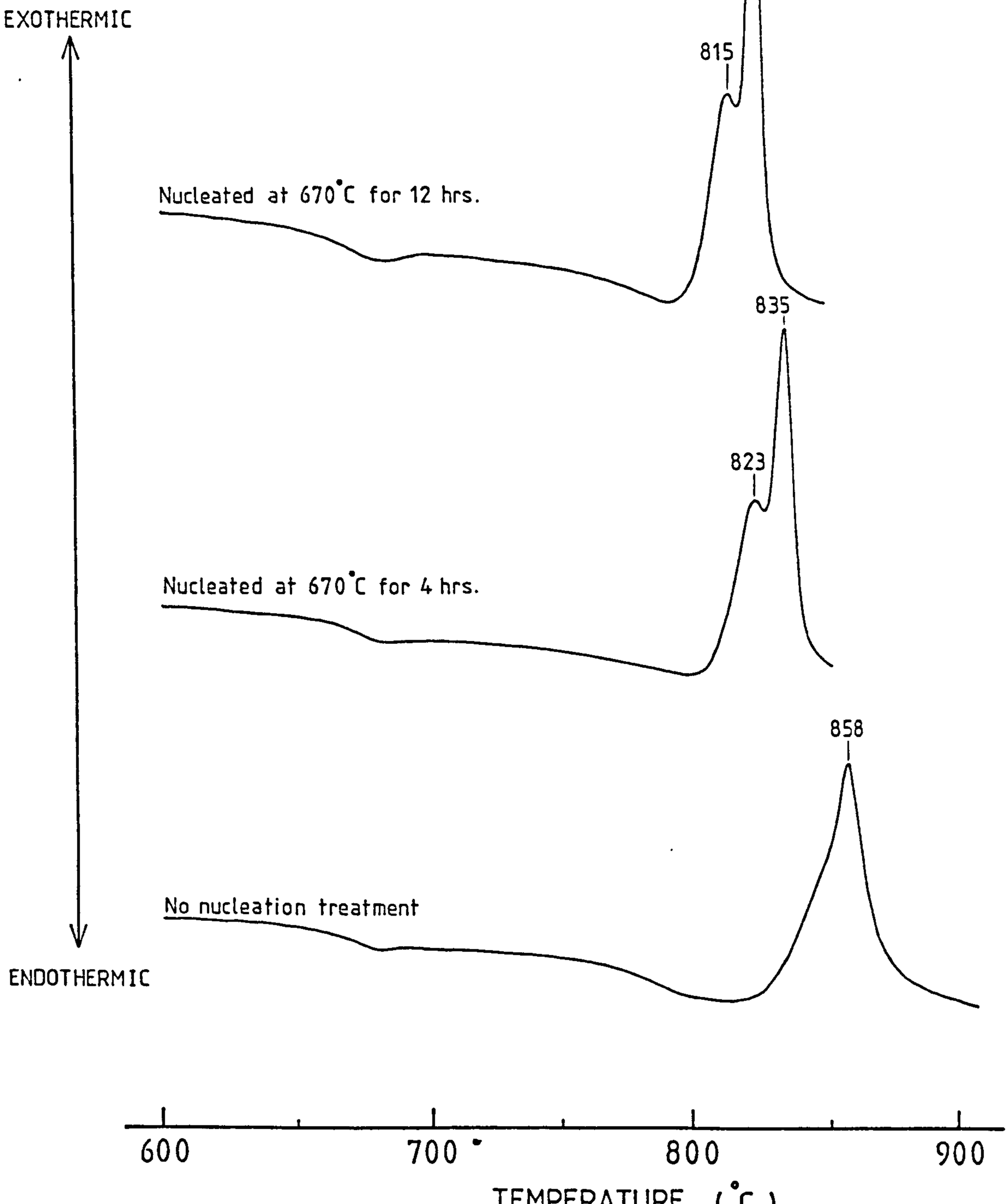

FIGURE 4.1.3

DTA traces of the composition MgBAl (3-2) with different nucleation treatments. Measurements were made at ~ 8°C/min; all samples had equal weights (70 mg) and particle sizes (100 - 150 microns).

peak. For samples which had been nucleated, two distinct crystallisation peaks can be seen and they appeared at lower temperatures.

The appearance of the two crystallisation peaks confirms the earlier belief that two crystalline phases were being formed, and it is possible to correlate these peaks with the curves for the amount of heat evolved measured as a function of heat treatment time by DSC (shown in figure 4.1.1). In the DTA traces, the lower temperature crystallisation peak emerged as a direct result of the nucleation treatment, and in the DSC curves, the initial rate of heat evolved (up to $\sim$ 5 hours) is also very sensitive to the nucleation treatments. This leads to the conclusion that the lower temperature peak in the DTA traces and the initial gradient in the DSC curves correspond to the same crystalline phase being formed. It follows that the higher temperature peak in the DTA traces corresponds to the crystalline phase being formed at the shallow gradient (from $\sim$ 5 - 24 hours) in the DSC curves.

The effect of the nucleation treatment is interpreted as having induced more nuclei, consequently promoting the growth of a larger number of crystals of the "lower temperature phase" relative to the number of crystals of the "higher temperature phase". The result is the appearance of an exothermic peak which becomes resolvable from the peak corresponding to the higher temperature crystalline phase.

The reason why the two crystallisation peaks have shifted to lower temperatures with nucleation treatment can be explained qualitatively in terms of the presence of nuclei. The crystallisation of a glass takes place via the processes of nucleation and subsequent crystal growth, and each one of these processes contains two activation energies, termed the thermodynamic barrier and the kinetic barrier to either nucleation or crystal growth (see Appendix 1). If the transformation from the glassy phase to the crystalline phase is viewed as a whole,

it is possible to sum these activation energies and refer to them as the complex activation energy. For a glass which had been nucleated or contains nuclei, this complex activation energy for the transformation is composed of the thermodynamic and kinetic barriers for crystal growth only and it is less than that for a glass without any nuclei. Therefore less energy is required to surmount this barrier to transformation and hence the crystallisation peaks in the DTA traces occurred at lower temperatures. If more nuclei were present as in the case of a longer nucleation time, a greater number of crystals are formed. Whether the growth mechanism for these crystals is interface controlled or diffusion controlled, the crystals will either impinge on each other earlier or the constituents of the crystal remaining in the residual glass phase will be depleted sooner than if less crystals were present. This effect is manifested as a further lowering of the peak temperature.

It was observed that the particle size of the sample has an influence on the positions (in temperature) of the crystallisation peaks and this can serve as a method of distinguishing between bulk and surface crystallisation. The arguments are as follow. In the case of surface crystallisation, crystal growth proceeds from nucleation sites present at the surface, and for a particular type of surface the number of nucleation sites is proportional to the surface area. If DTA is carried out on the coarse and the fine particles of a glass in which surface crystallisation is the predominant transformation mechanism; because of the extra surface present in the fine particles, there is a larger number of nuclei, then the exothermic peak due to crystallisation should occur at a temperature lower than that corresponding to the coarse particles. However, if bulk crystallisation is the dominant transformation mechanism, then the exothermic peaks of both the coarse

and the fine particles should occur at more or less the same temperature.

DTA traces (a) and (b) for the fine (< 50 microns) and the coarse (500-170 microns) particles respectively of MgBal(3-2) nucleated at 670°C for 12 hours are shown in figure 4.1.4. For the coarse particles, two distinct crystallisation peaks can be seen, but for the fine particles the higher temperature crystallisation peak has shifted to a lower temperature and has merged with the lower temperature crystallisation peak. Another feature is that the lower temperature peak for both the coarse and the fine particles has remained at approximately the same temperature. Using the above arguments, these observations imply the lower temperature peak is due to bulk crystallisation, but the higher temperature peak corresponds to that of surface crystallisation.

To further this view, DTA was carried out with the fine particles in the sample cell and the coarse particles in the reference cell [This is equivalent to superposing traces (a) and (b) together.] and the result is shown by trace (c) of figure 4.1.4. The lower temperature crystallisation peak has more or less been cancelled indicating bulk crystallisation. The higher temperature peak in the case of the fine particles showed a real drop in temperature, indicating surface crystallisation.

DTA experiments with different particle sizes similar to that outlines above were also carried out for the composition CA1 (6), and the results are shown in figure 4.1.5. DTA traces (a) and (b) for the fine and coarse particles respectively showed a single crystallisation peak indicating only one crystalline phase is being formed. Trace (c),

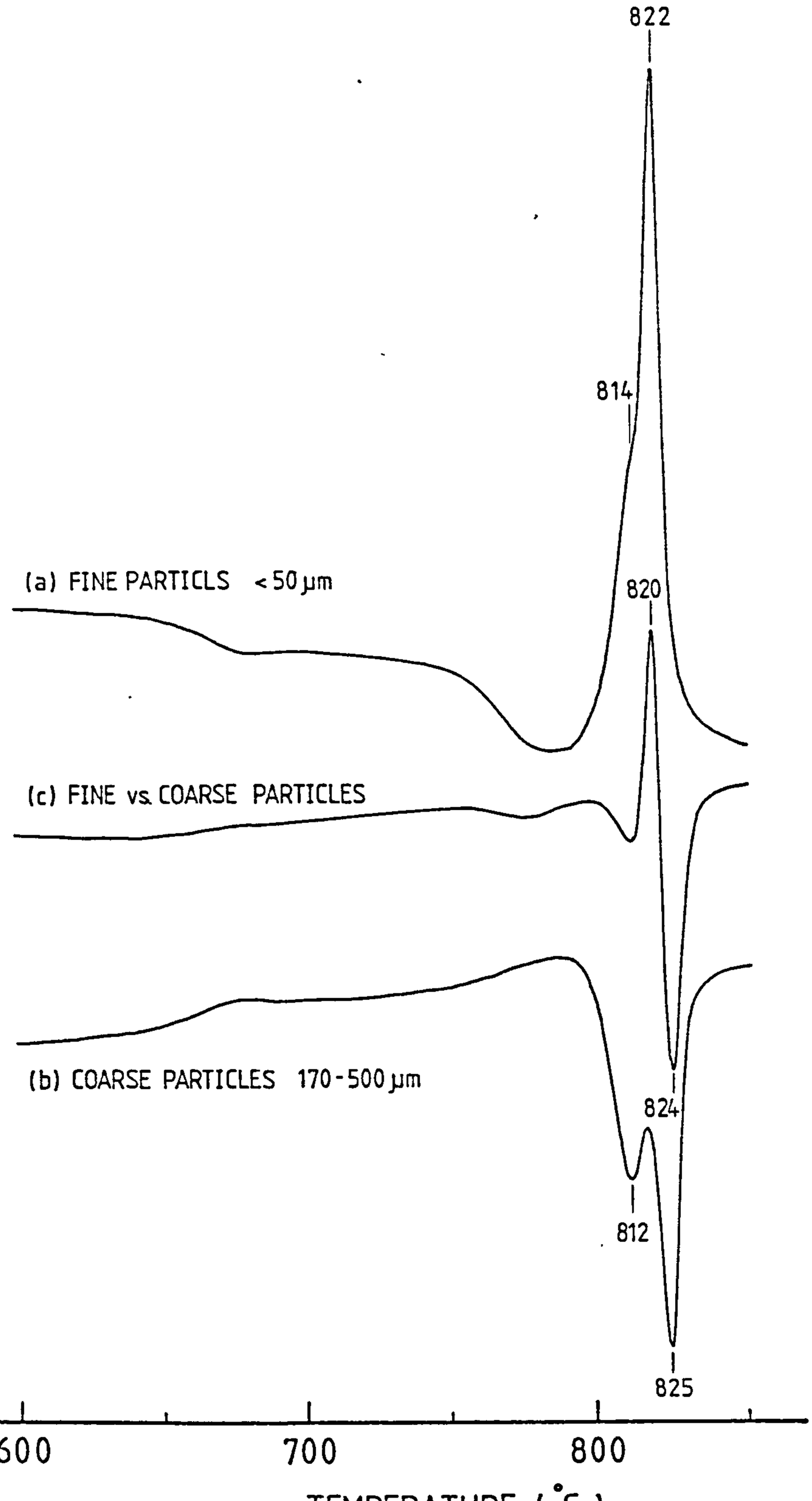

FIGURE 4.1.4

DTA traces of samples of MgBAl (3-2) nucleated at 670°C for 12 hours having different particle sizes. Trace (a) was measured in the normal way. Trace (b) was measured with the sample in the reference cell and the alumina reference in the sample cell. Trace (c) was measured with the fine particles in the sample cell and the coarse particles in the reference cell. All measurements were carried out at ~ 8°C/min with samples having equal weights.

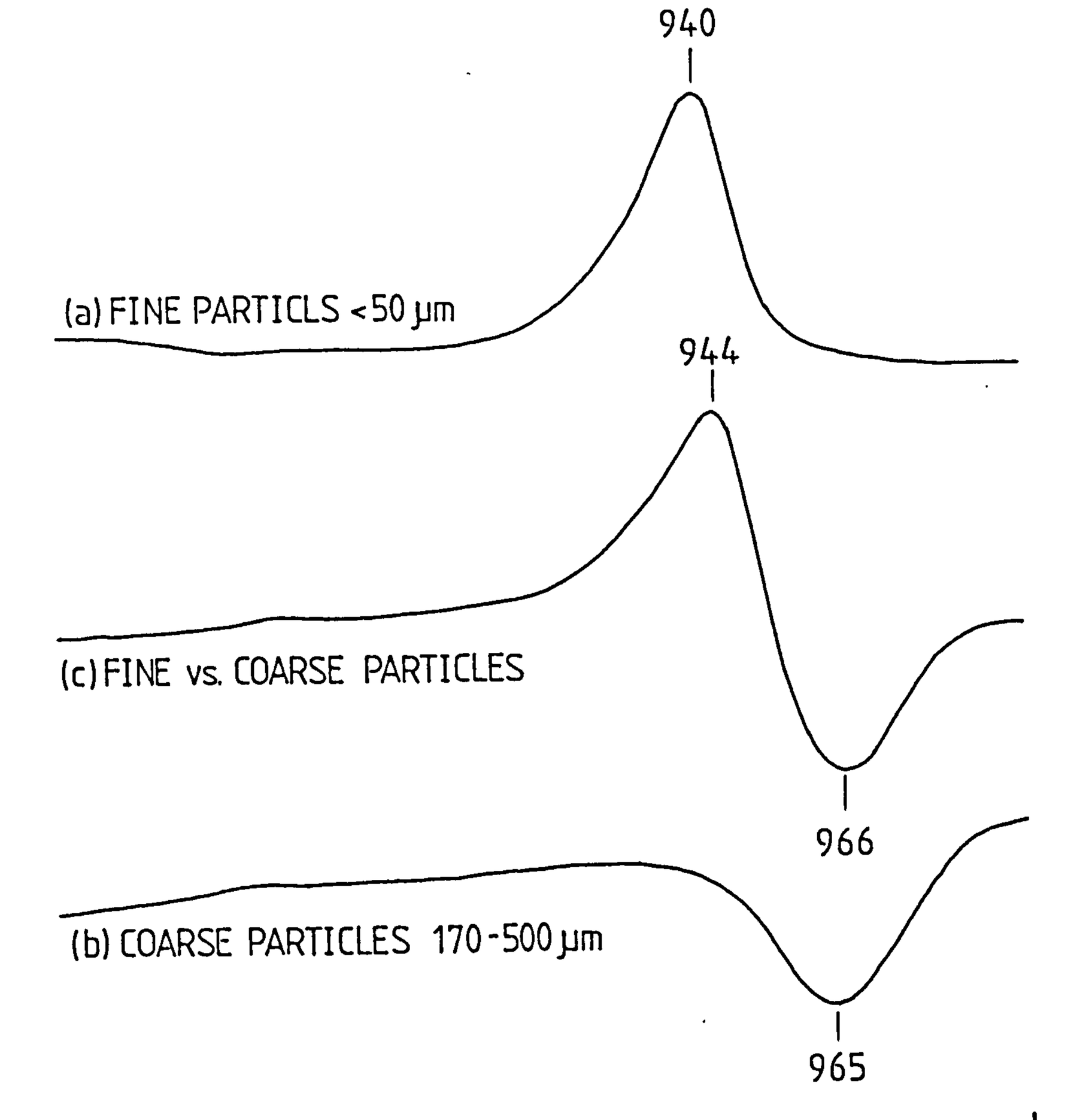

FIGURE 4.1.5

DTA traces of samples of CA1(6) having different particle sizes. Trace (a) was measured in the normal way. Trace (b) was measured with the sample in the reference cell and the alumina reference in the sample cell. Trace (c) was measured with the fine particles in the sample cell and the coarse particles in the reference cell. All measurements were carried out at ~ 8°C/min with samples having equal weights.

obtained by placing the fine and coarse particles in the sample and reference cells respectively, showed a large difference of 22°C between the peak temperatures for the fine and the coarse particles [compared with a 4°C drop for MgBAl (3-2)]. This suggests the transformation mechanism for CAl (6) is strongly surface dependent, in agreement with the observations made during heat treatment that CAl (6) exhibits surface crystallisation only.

DTA was also carried out at different heating rates (in the range 4 - 16°C/min) and the positions of the peak temperatures were found to change accordingly, i.e. higher rates of heating resulted in higher peak temperatures. Using the theory outlined in section 2.3.2.1, by plotting $\ln[\beta/T_m^2]$ versus $1/T_m$ where β is the heating rate and T_m is the peak temperature, a straight line should result if the transformation is a first order reaction. The gradient of the line gives the activation energy for all the activated steps involved in crystallisation.

Using the method of least squares, both crystallisation peaks for the glass MgBAl (3-2) nucleated at 670°C for 12 hours gave poor fits to straight lines with standard errors in the gradients in excess of 10%. It follows then that the transformation is not a first order reaction. Results for the composition CAl (6) are shown in figure 4.1.6. The error bars shown are estimated from the accuracy with which the peak temperatures can be determined and it is $\sim 2°C$. The fit to a straight line (by least squares) is relatively good with a standard error of about 5% in the gradient. The tentative conclusion (since there are only 5 data points) is that the transformation of CAl (6) follows a first order reaction and the activation energy was calculated to be 123 ± 6 KCal/mole.

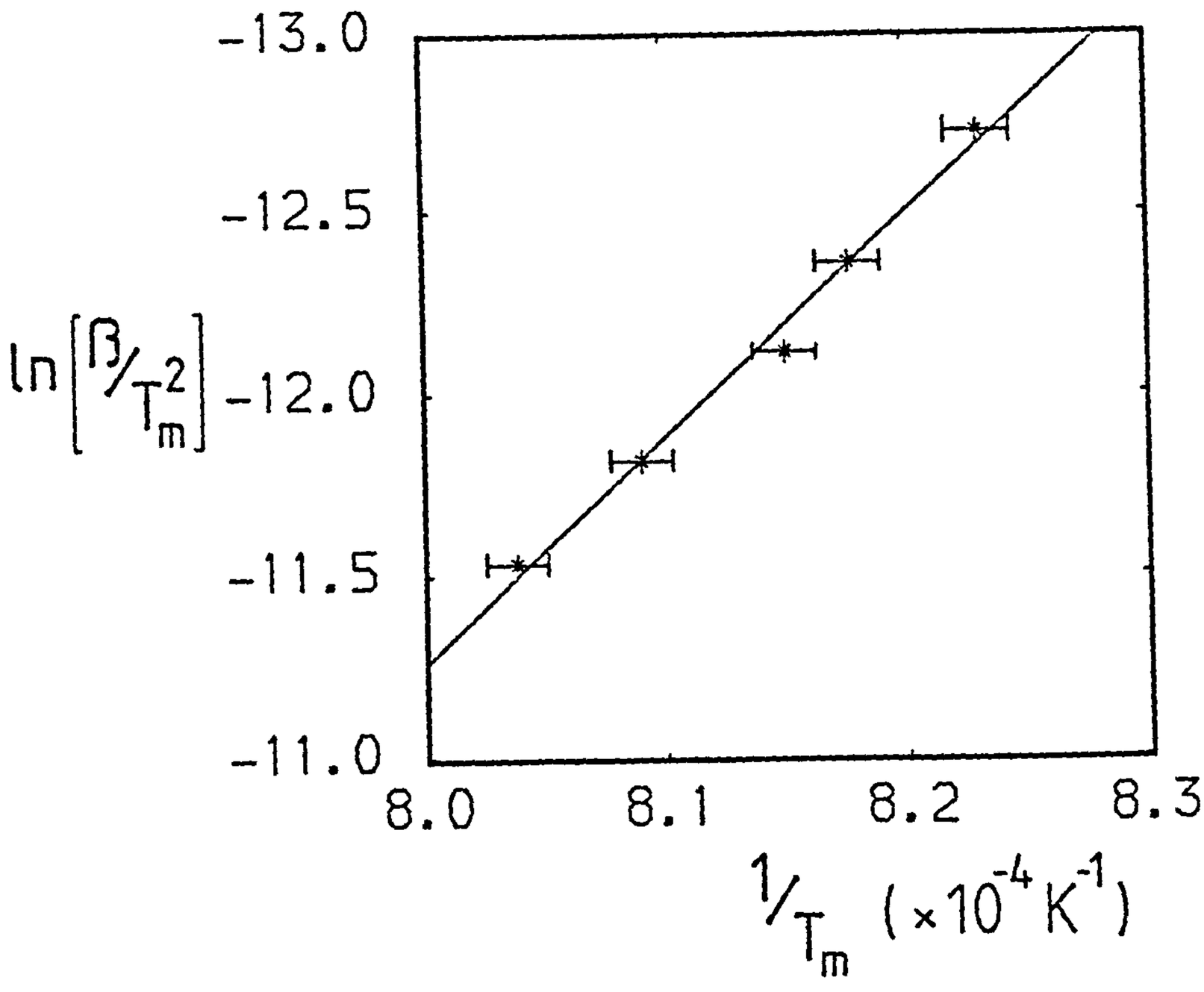

FIGURE 4.1.6

Plot of $\ln[\beta/T_m^2]$ versus $1/T_m$ for the composition CA1(6)

4.1.3 Differential Scanning Calorimetry (DSC)

The isothermal transformation behaviour of samples of MgBA1 (3-2) having different nucleation treatments was investigated by DSC at 730°C. Using the method of integration described in section 2.3.2.2, the results given as heat evolved as a function of time have already been presented in figure 4.1.1. These results were analysed in terms of the generalised theory of phase transformations (also described in section 2.3.2.2). Using equation 2.3.4, plots of $\ln[\ln[1/(1-X(t))]]$ versus $\ln t$ were carried out and typical results are shown in figure 4.1.7. Two distinct gradients can be seen indicating two phases were being formed, and for the sake of convenience these gradients were labelled α and β (as shown in figure 4.1.7) corresponding to phase α and phase β being formed. The Avrami exponents n for these phases were calculated from the gradients and they are summarised in table 4.1.2.

The Avrami exponents for the α-phase for all the samples lie in a narrow range of values from 2.8 → 3.2. This implies, irrespective of the nucleation treatment, that all the samples undergo a similar type of transformation. It is possible to glean more information about the glass from the values of the Avrami exponent and with the aid of observations made from other experiments. For example, from the SEM micrographs shown in figure 4.2.2, for the sample which had been nucleated at 670°C for 12 hours, it is estimated that the crystals impinged on each other after about $3\frac{1}{2}$ hours. This corresponds fairly well with the time when the curve of heat evolved (shown in figure 4.1.1b) undergoes a change in gradient, indicating the termination of the growth of the α-phase. This suggests the growth of the α-phase is limited by the impingement of the crystals and it is therefore an interface controlled process. Table 4.1.3 is extracted from the

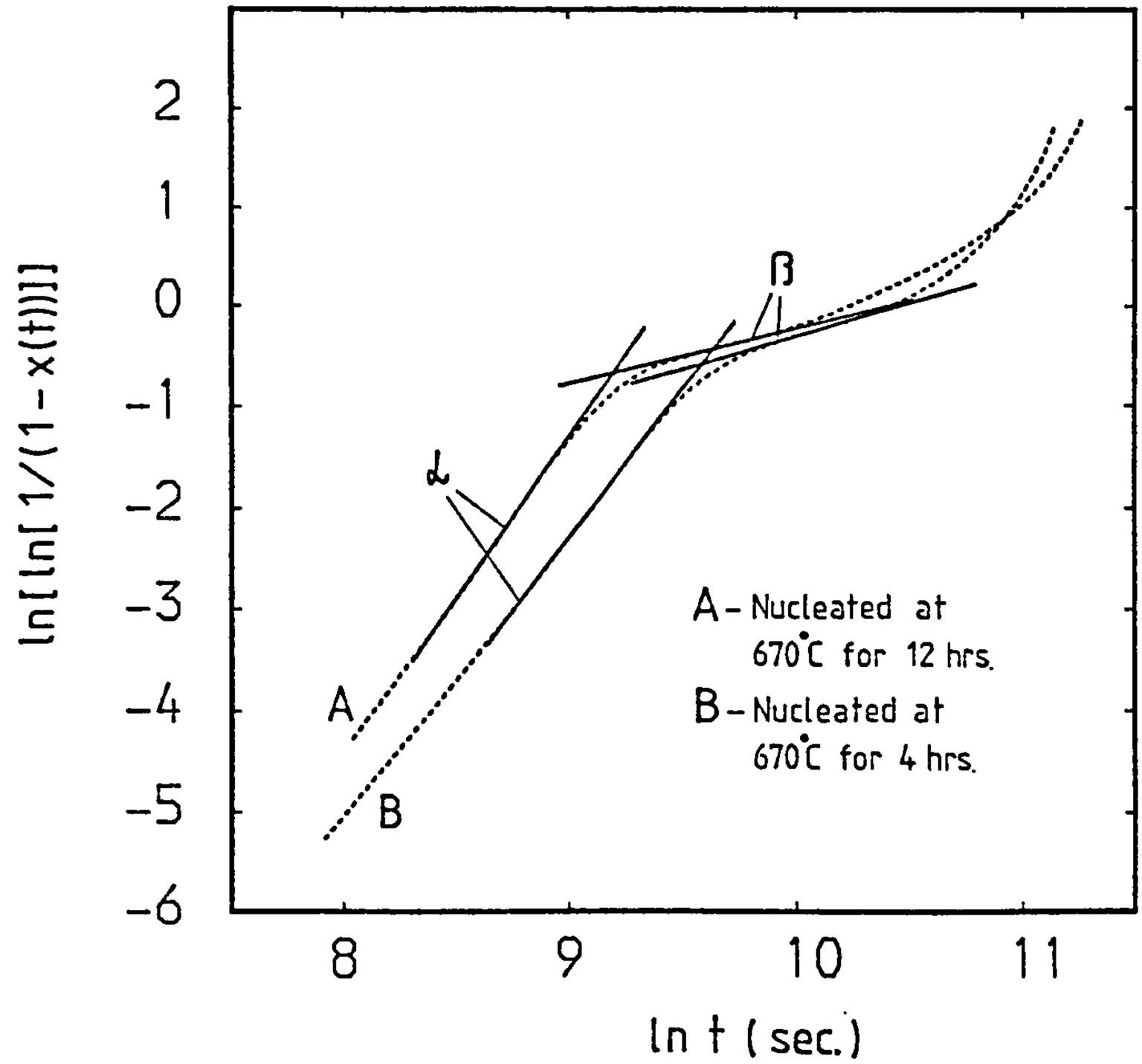

FIGURE 4.1.7

Typical plots of ln[ln[1/(1 - X(t))]] versus ln t for samples of MgBA1 (3-2) having received different nucleation treatments and then isothermally transformed at 730°C.

Sample	Avrami Exponent n	
	α phase	β phase
MgBal(3-2)		
Nucleated at 660°C for 4 hrs.	3.15 ± 0.10	0.71 ± 0.10
Nucleated at 670°C for 4 hrs.	2.93 ± 0.10	0.67 ± 0.10
Nucleated at 670°C for 8 hrs.	2.96 ± 0.10	0.59 ± 0.10
Nucleated at 670°C for 12 hrs.	3.21 ± 0.10	0.56 ± 0.10
Nucleated at 680°C for 4 hrs.	2.99 ± 0.10	0.75 ± 0.10
Nucleated at 690°C for 4 hrs.	2.81 ± 0.10	0.79 ± 0.10
Nucleated at 700°C for 4 hrs.	2.95 ± 0.10	1.16 ± 0.10

TABLE 4.1.2

Avrami exponents of samples of MgBAl(3-2)
isothermally transformed at 730°C.

TABLE 4.1.3*

VALUES OF n IN KINETIC LAW $\zeta = 1 - \exp(-kt^n)$

Polymorphic changes, discontinuous precipitation, eutectoid reactions, interface controlled growth, etc.

Conditions	n
Increasing nucleation rate	>4
Constant nucleation rate	4
Decreasing nucleation rate	3–4
Zero nucleation rate (saturation of point sites)	3
Grain edge nucleation after saturation	2
Grain boundary nucleation after saturation	1

Diffusion controlled growth

Conditions	n
All shapes growing from small dimensions, increasing nucleation rate	$>2\frac{1}{2}$
All shapes growing from small dimensions, constant nucleation rate	$2\frac{1}{2}$
All shapes growing from small dimensions, decreasing nucleation rate	$1\frac{1}{2}$–$2\frac{1}{2}$
All shapes growing from small dimensions, zero nucleation rate	$1\frac{1}{2}$
Growth of particles of appreciable initial volume	1–$1\frac{1}{2}$
Needles and plates of finite long dimensions, small in comparison with their separation	1
Thickening of long cylinders (needles) (e.g. after complete end impingement)	1
Thickening of very large plates (e.g. after complete edge impingement)	$\frac{1}{2}$
Precipitation on dislocations (very early stages)	$\sim\frac{2}{3}$

* Extracted from Christian (1975)
"The Theory of Transformations in Metals and Alloys"
Part 1, p. 542.

book by Christian (1975) and it gives the Avrami exponents for a variety of situations. If the α-phase is assumed to be interface controlled with $n \sim 3$ (see table 4.1.2), then according to table 4.1.3, the rate of nucleation is zero. This implies the rate of nucleation for the α-phase at 730°C is zero, which is consistent with the observations made during heat treatment, that is, the glass did not crystallise to any appreciable extent at 730°C if no nucleation treatment was used.

With regard to the β-phase, the Avrami exponents varied from $\sim 0.5 \rightarrow 1.2$. To enlarge on these results, once again the specimen which had been nucleated at 670°C for 12 hours (with $n \sim \frac{1}{2}$) is used as an example. No microscopy information is available because of the lack of time. However, from DTA results given earlier, the β-phase corresponds to the "higher temperature phase" and the transformation takes place via surface crystallisation. This is in agreement with observations made by cracking the specimens in half the prolonged heat treatments at 730°C for various times; a crystal layer is formed at the surface which gradually thickens. From table 4.1.3, if a diffusion controlled growth mechanism is assumed, the situation corresponding to $n = \frac{1}{2}$ is the thickening of very large plates. This fits in very well with the above observations and suggests the growth mechanism for the β-phase is probably diffusion controlled. For samples with different nucleation treatments, the Avrami exponents can be as high as 1. Using the idea of a diffusion controlled growth mechanism, the thickening of long cylinders or needles for the phase β is to be expected (from table 4.1.3). This is purely speculative though, since no experimental information is available for these samples.

4.2 Microstructure of Transparent Glass-Ceramics

4.2.1 Electron Microscopy

The present investigation is concerned with the glass-ceramics of MgBAl(3-2) and CAl(6) derived using the heat treatment programmes given in table 4.1.1. The preparation of samples for electron microscopy has already been described in section 2.4.1, and in the case of glass-ceramics of MgBAl(3-2), the bulk of the materials was examined by SEM and TEM, whilst for glass-ceramics of CAl(6), only the surface regions were examined by SEM.

Figure 4.2.1 shows SEM micrographs illustrating the effect of varying the nucleation time on MgBAl(3-2). The crystals formed correspond to the α-phase or the lower temperature phase described in the previous sections. The crystals are distributed randomly throughout the bulk of the material and as expected, the number of crystals increased with increasing nucleation time. These observations are in accordance with both the DTA and DSC results.

SEM micrographs showing the growth of the α-phase with time at 730°C for samples of MgBAl(3-2) having different nucleation treatments are given in figure 4.2.2. The crystals which appear as "ellipsoids" can be seen to grow with time until a point is reached where they impinged on each other and beyond that form a kind of "interlocking structure". It was noted that for a particular specimen, the ellipsoids appeared to be relatively uniform in size. A plausible explanation for this observation would be if the rate of crystal growth is assumed to be sufficiently slow at the nucleation temperature of 670°C as to be insignificant. Remembering that the rate of nucleation is zero at the crystallising temperature of 730°C (from DSC results), the combined

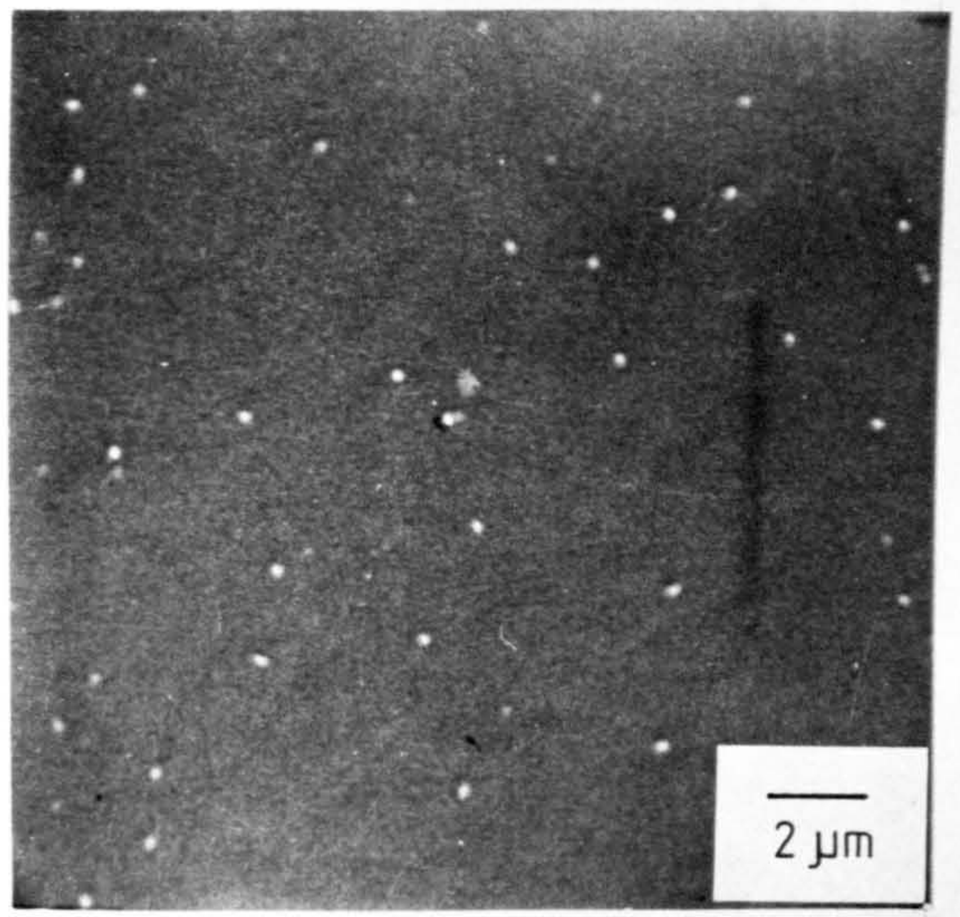

670°C 4hrs.
730°C 1hr.

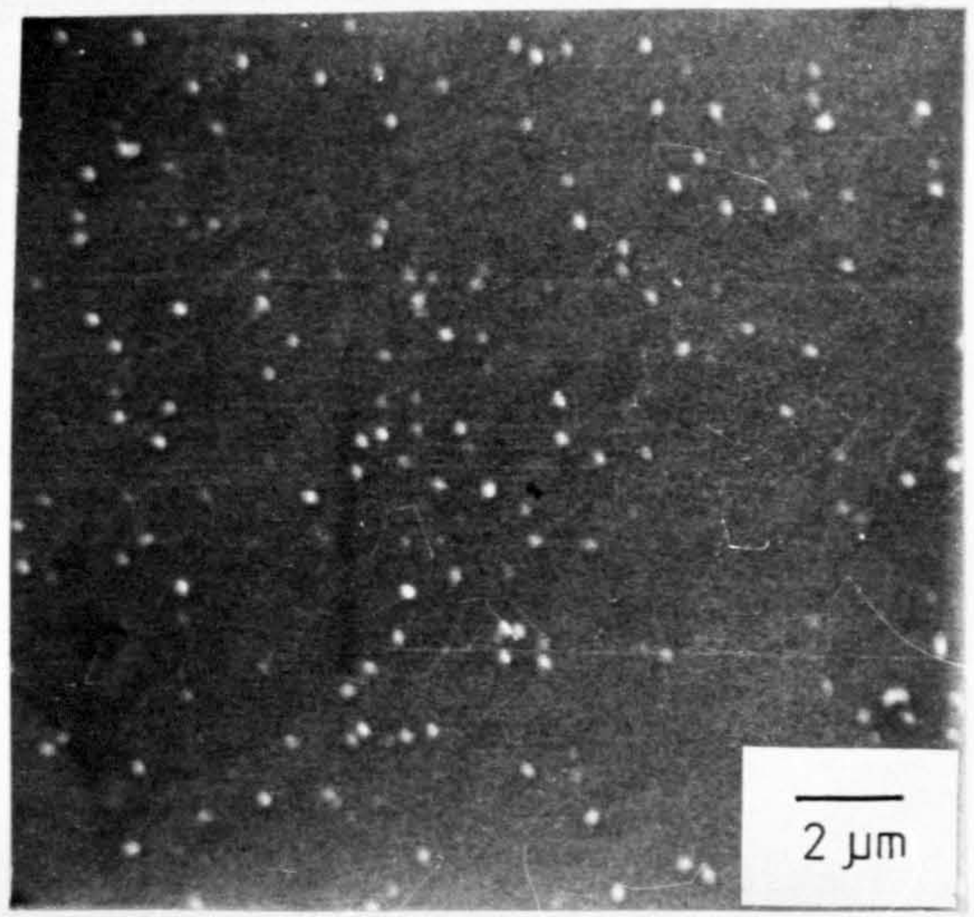

670°C 8hrs.
730°C 1hr.

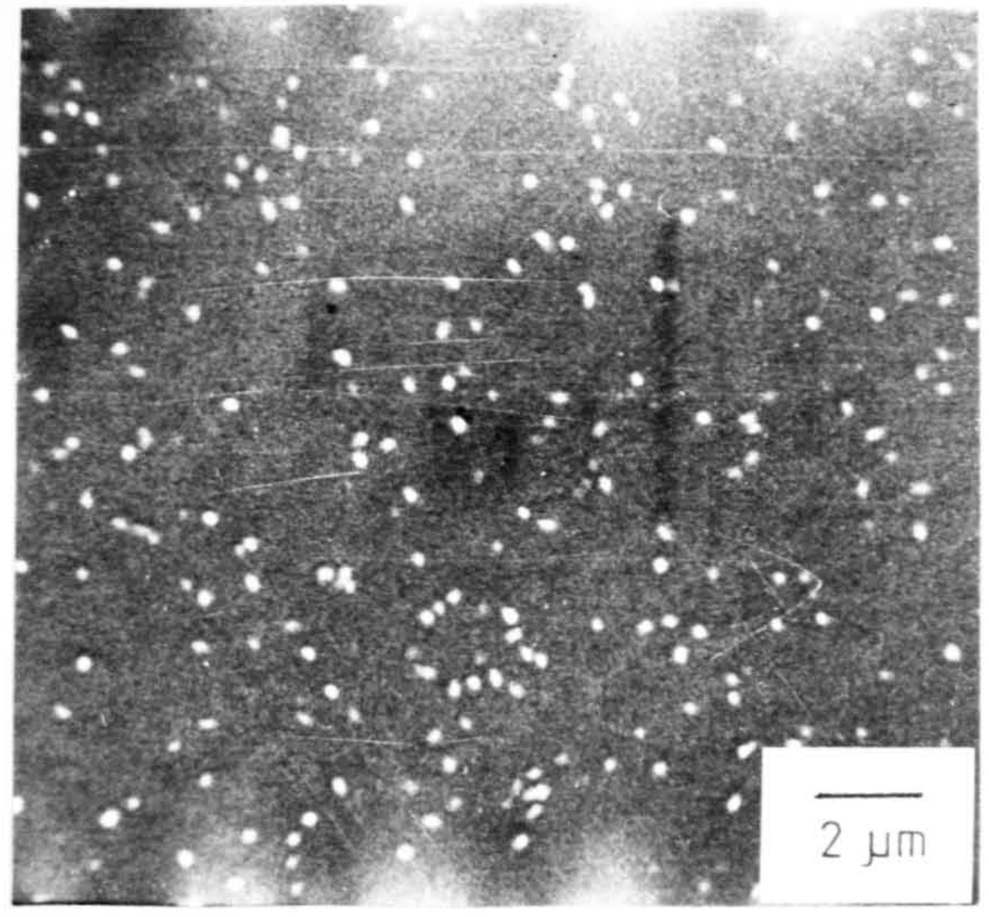

670°C 12hrs.
730°C 1hr.

Figure 4.2.1.

Effect of nucleating MgBAl(3-2) at the same temperature for varying lengths of time.

At 670°C for 4hrs

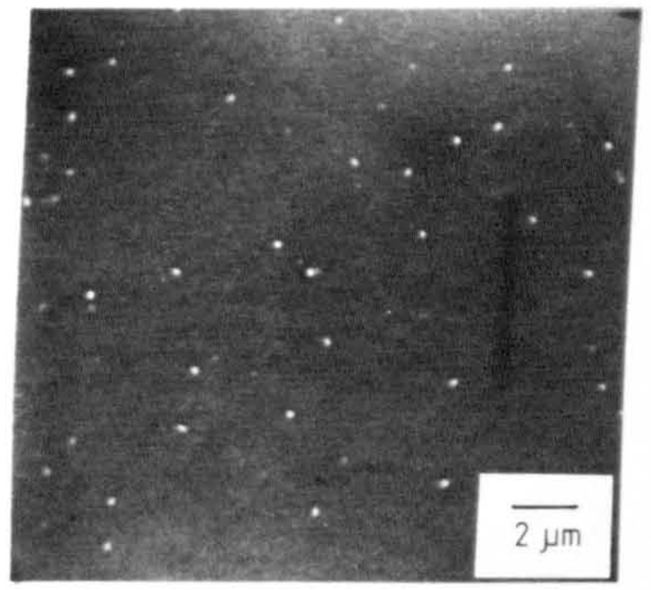

1hr

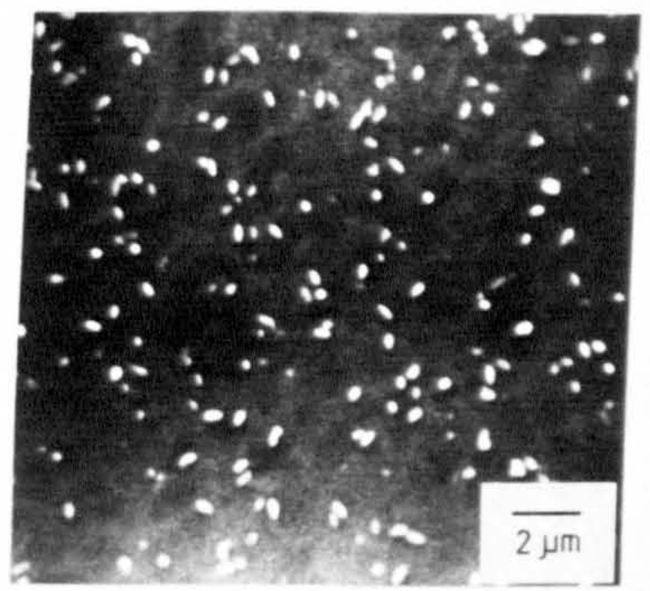

2hrs

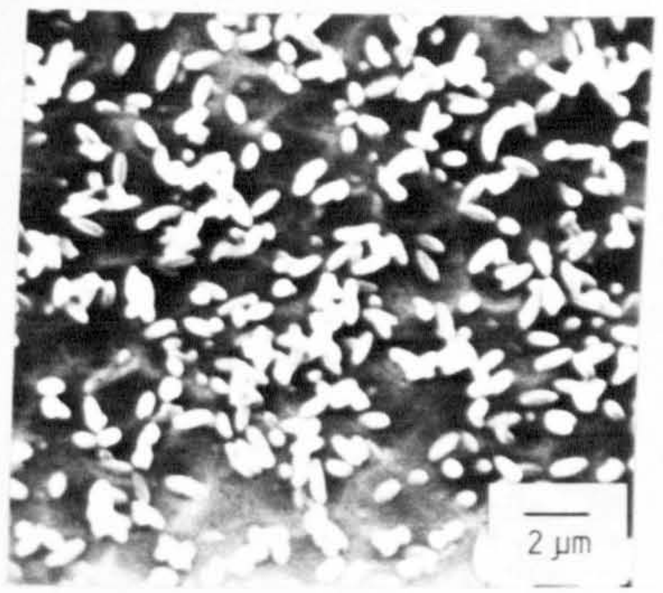

3hrs

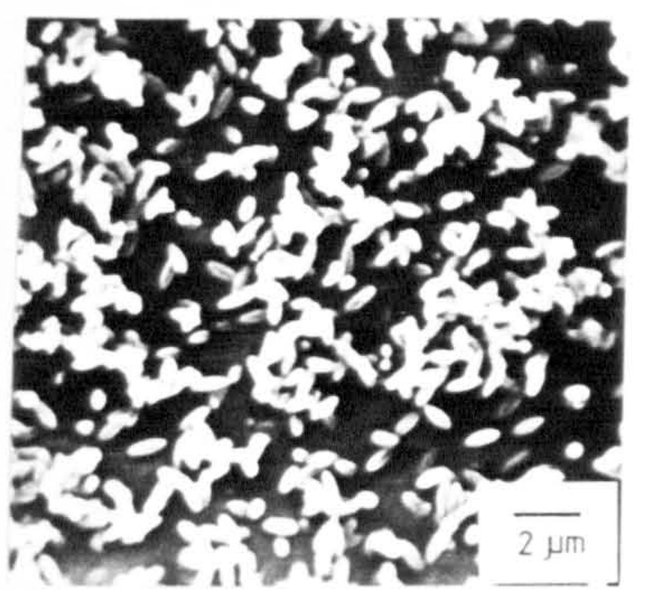

4hrs

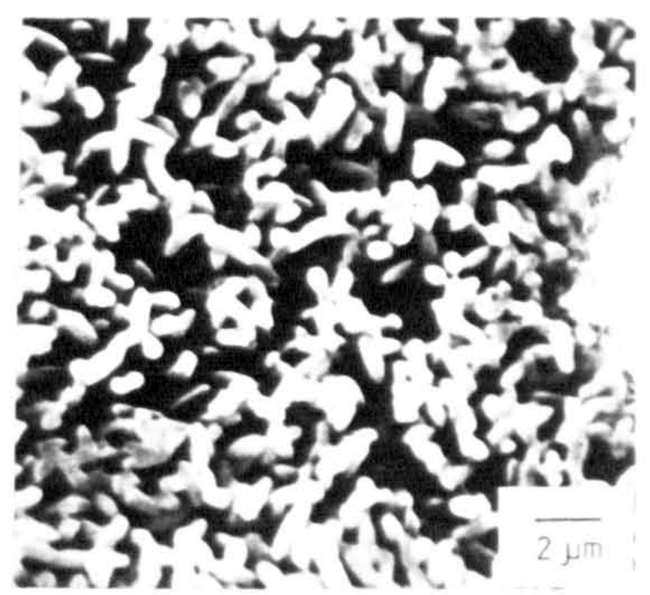

5hrs

At 730°C

At 670°C for 12hrs

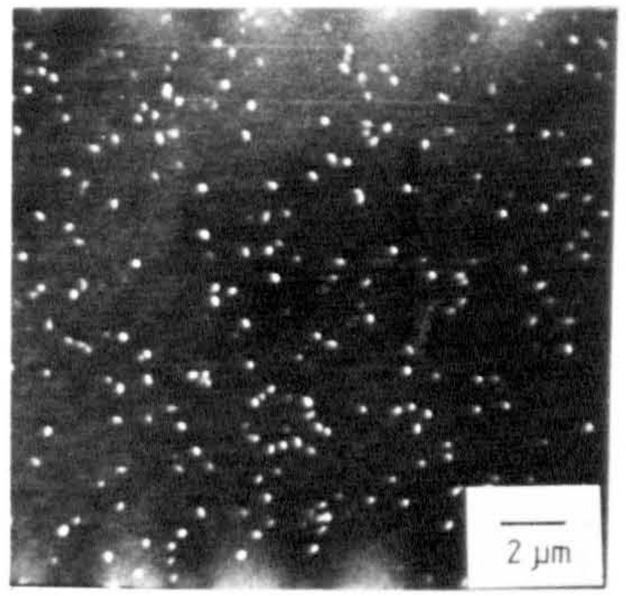

1hr

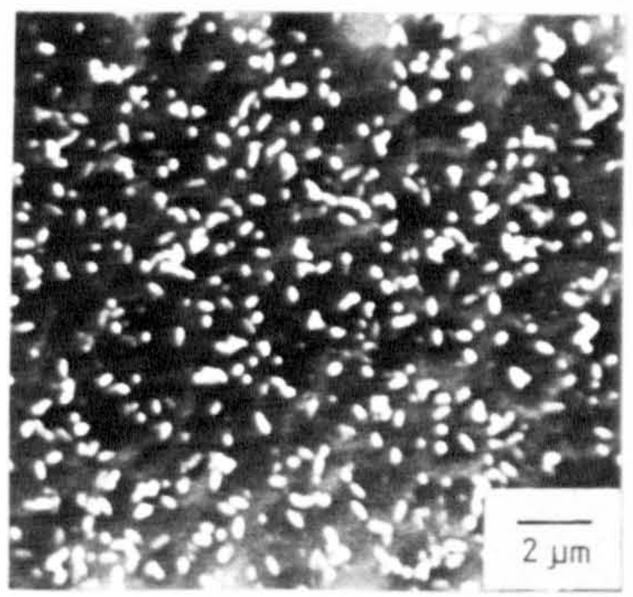

2hrs

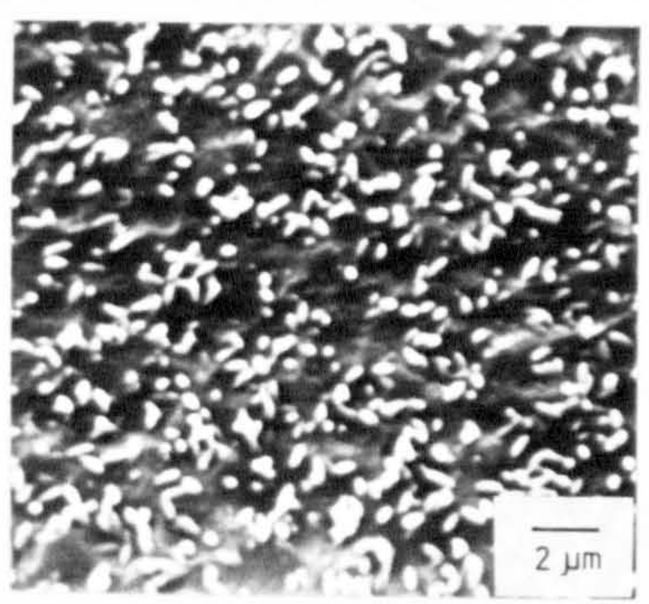

3hrs

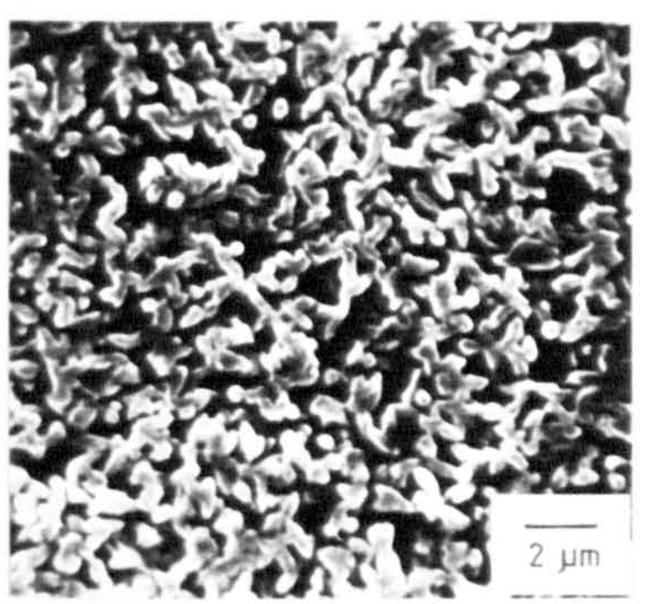

4hrs

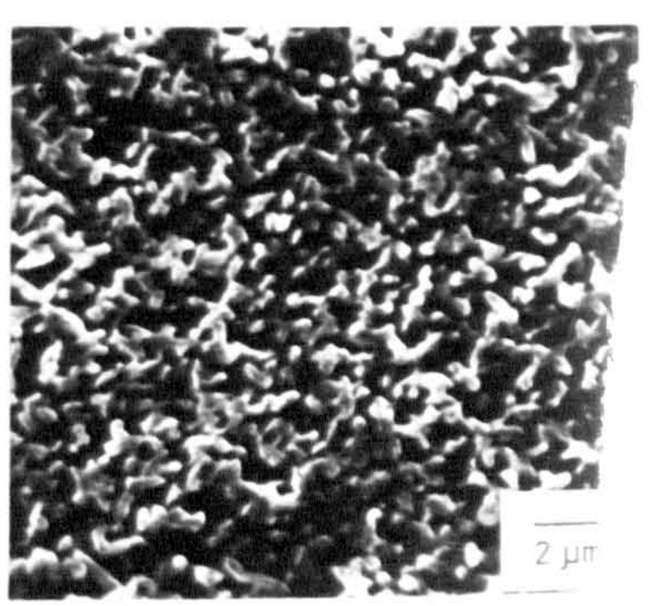

5hrs

At 730°C

Figure 4.2.2

Effect of crystallising MgBAl(3-2) at the same temperature for varying lengths of time.

effect is that nuclei are formed at 670°C, but the rate of crystal growth is sufficiently slow that the nuclei do not grow appreciably. When the temperature of the material is raised to 730°C at 2°C/min, and therefore in a time short compared to the nucleation time, very few "extra" nuclei are formed. At 730°C the rate of nucleation is zero and the situation is that the majority of the nuclei of more or less the same size start growing at the same rate and hence the observed uniform size of the crystals. The initial assumption that the rate of crystal growth is insignificant at the nucleation temperature is supported by observations in as far as the material after prolonged heat treatments (~ 24 hours) appeared glassy, but there is no other experimental evidence to substantiate this.

With regard to the question of whether the samples examined are indeed representative of the material, figure 4.2.3 shows TEM micrographs of samples of MgBAl (3-2) heat treated for various times. These micrographs compare very well with the SEM micrographs shown in figure 4.2.2, and in particular the sample which had been heat treated for 5 hours where "elliptical shaped" crystals can be clearly seen. The method of preparing samples for SEM and TEM are very different, where the former is a chemical etching technique and the latter is a mechanical thinning technique; both however give similar microstructural details. The conclusion must be that the micrographs are representative of the material.

The problem of whether the sample preparation techniques have a delusive influence on the observed results is not expected to apply to the results obtained for the glass-ceramics of CA1(6) since no special treatments were used to prepare the specimens for SEM. The effect of the abrasion treatment used to standardise the surface of CA1(6) has already

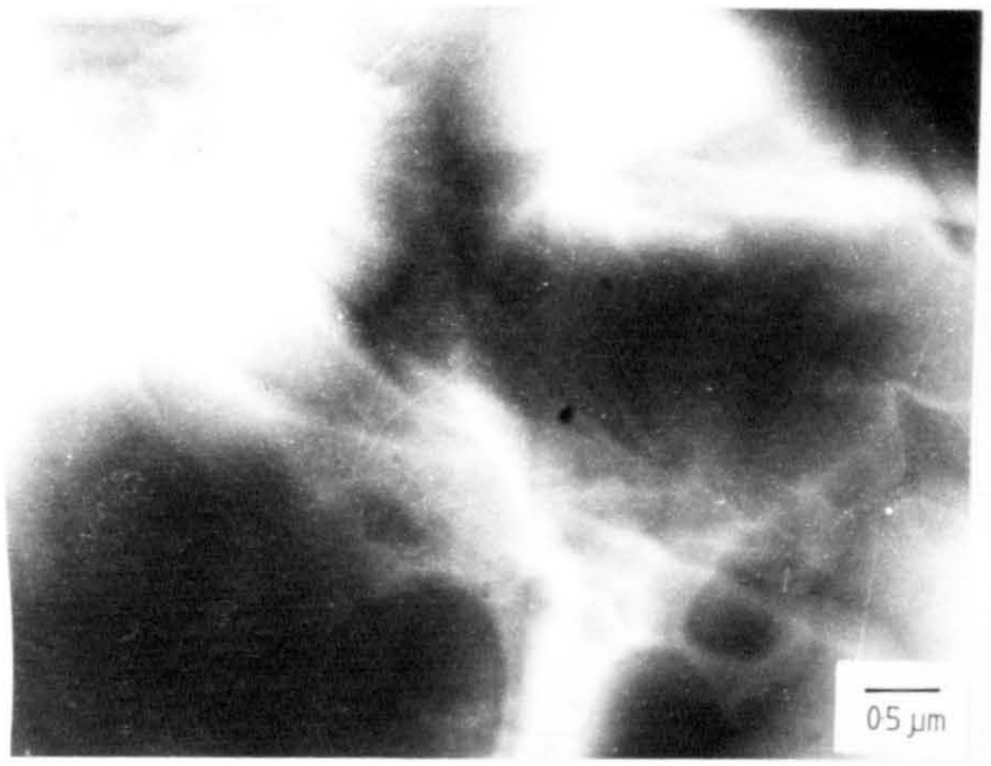

1hr.

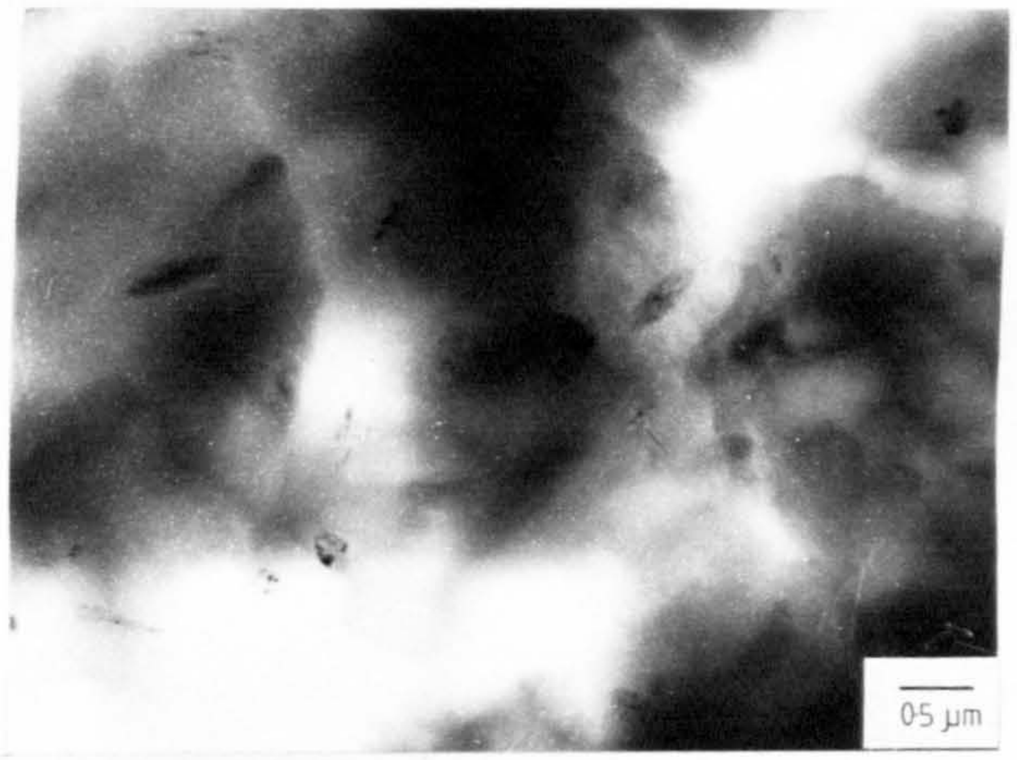

2 hrs.

3hrs.

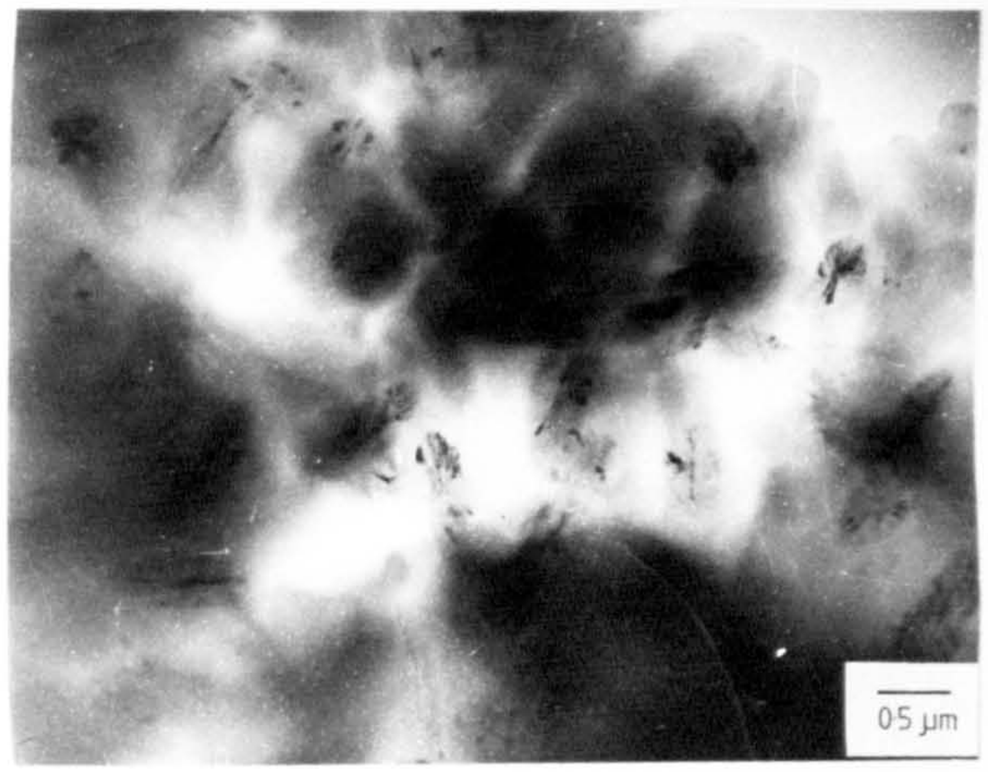

4 hrs.

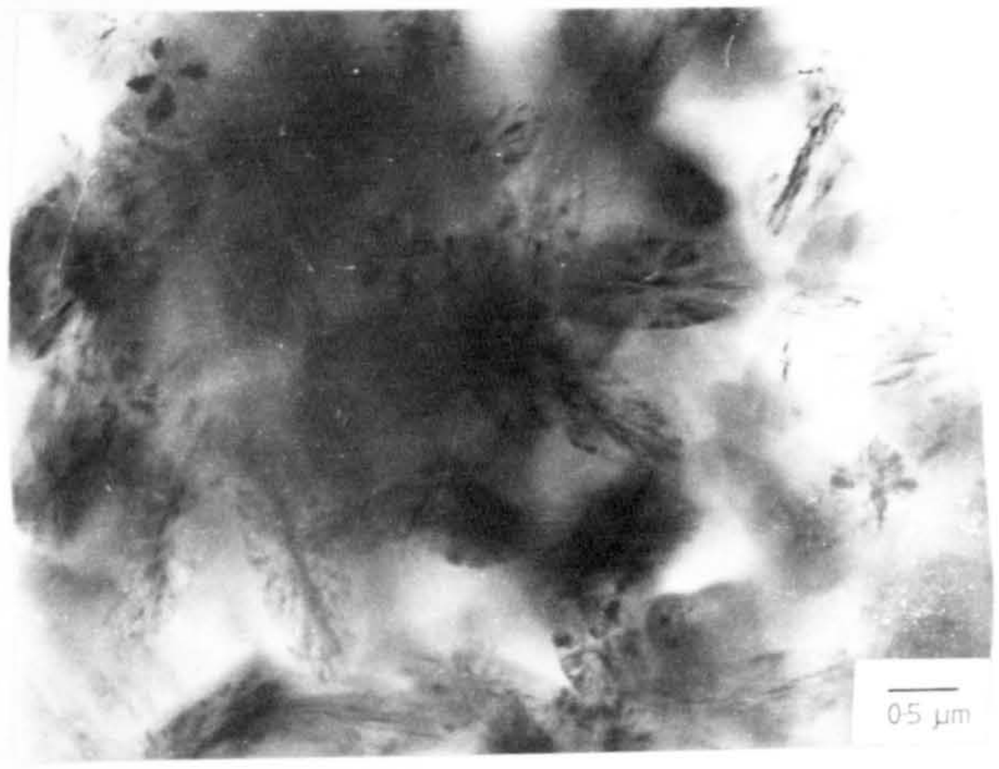

5hrs.

Figure 4.2.3

T.E.M. Micrographs of Mg B Al(3-2) heat treated at 670°C. for 4 hrs. and at 730°C. for various times.

been presented in figure 4.1.2, and figure 4.2.4 shows the surface condition with increasing heat treatment time. The surface can be seen to coarsen with time with the dimensions of the crystals reaching a few microns after 1 hour at 880°C. EDAX was carried out on the 1 hour specimen to identify any elemental differences between the protruding crystals and the surface, but no discernible difference was found. It was also observed that the condition of the surface did not change a great deal after 1 hour at 880°C. Figure 4.2.5 shows the depth profiles of samples of CA1(6) heat treated at 880°C for different times. The growth rate of the crystal layer seen here is relatively slow in the first 2 hours but increased more rapidly after that.

From the limited microscopy information available, the tentative picture suggested is that the crystals grow initially from nucleation sites present at the surface up to a point where they impinged on each other, say within the first 2 hours. This explains the observation that the surface condition did not change substantially after this time and that the crystal layer has remained at more or less the same thickness in this time (see figure 4.2.5). Beyond the point of impingement, the crystal layer formed proceeds to grow inwards which then explains the accelerated growth (in thickness) observed after 2 hours (see figure 4.2.6). The mechanism controlling growth is even less apparent, and the following deduction is of a speculative nature. It will be recalled from the DTA results that the transformation of CA1(6) may follow a first order reaction; that is with the Avrami exponent n=1. By referring to table 4.1.3, for n=1 and with the observed thickening of the crystal layer, a diffusion controlled growth mechanism is suggested for CA1(6).

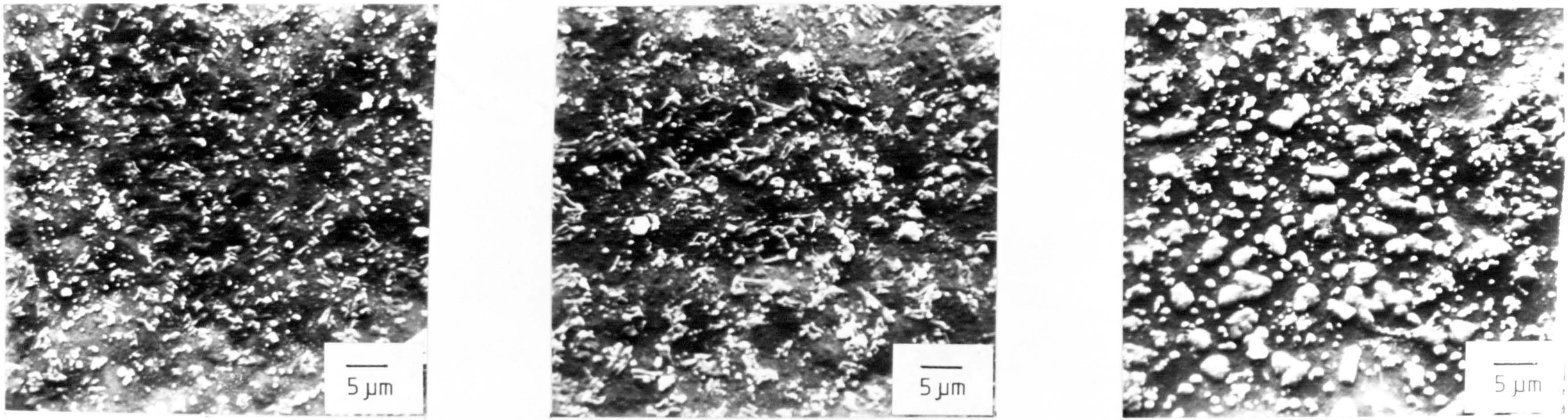

(a) (b) (c)

Figure 4.2.4

Surface conditions of CAl(6) having been abraded for 2hrs and heat treated at 880°c for a)$\frac{1}{4}$hr. b) $\frac{1}{2}$hr. c) 1hr.

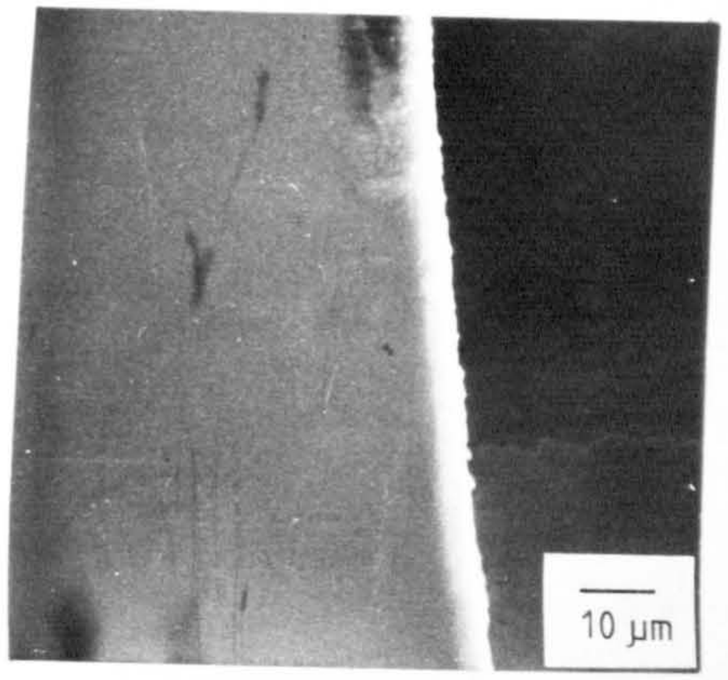

At 880°C 1hr.

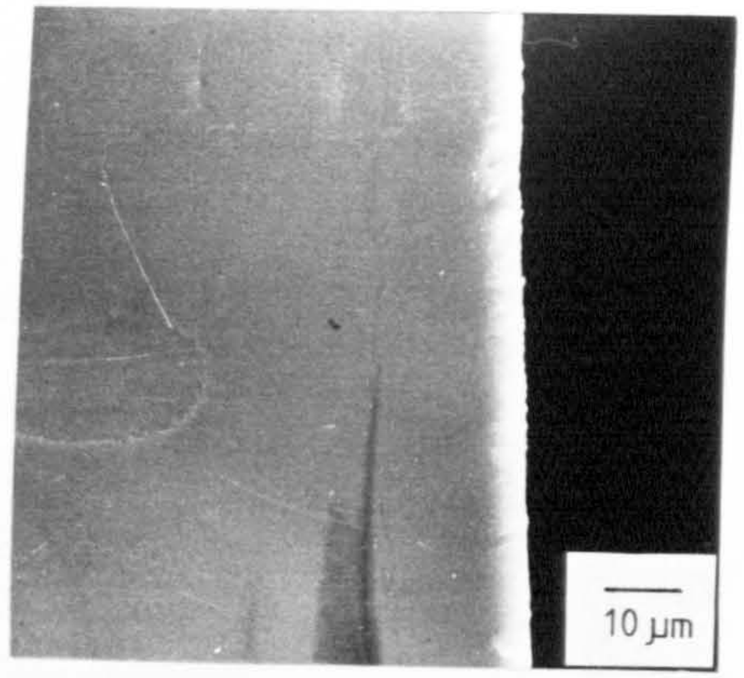

2hrs.

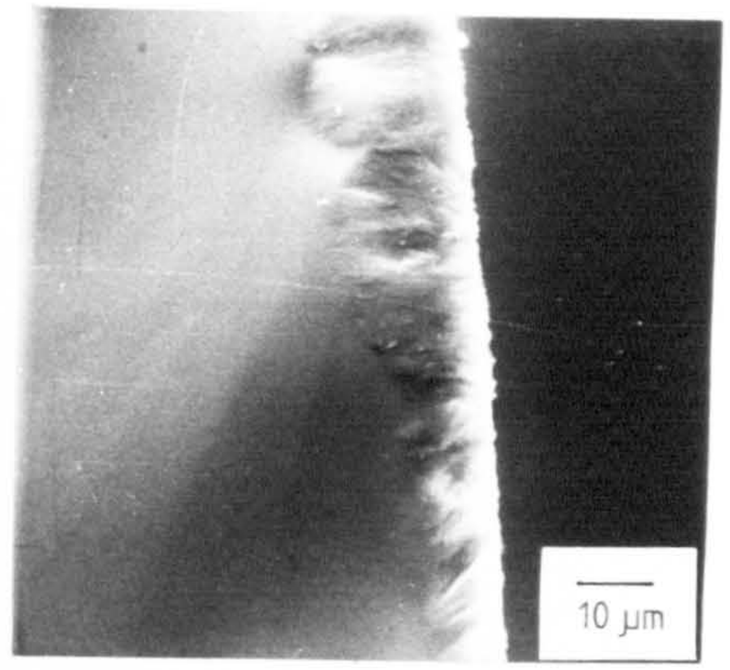

3hrs.

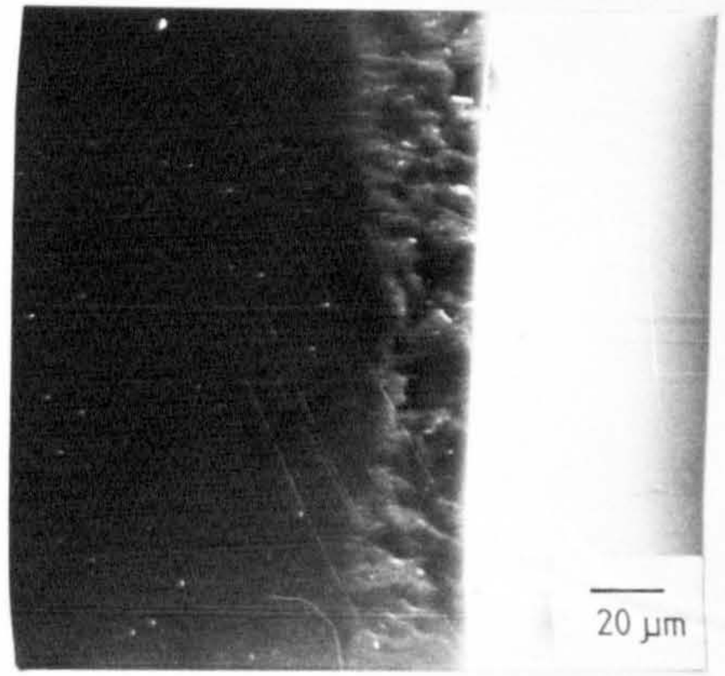

At 880°C 4hrs.

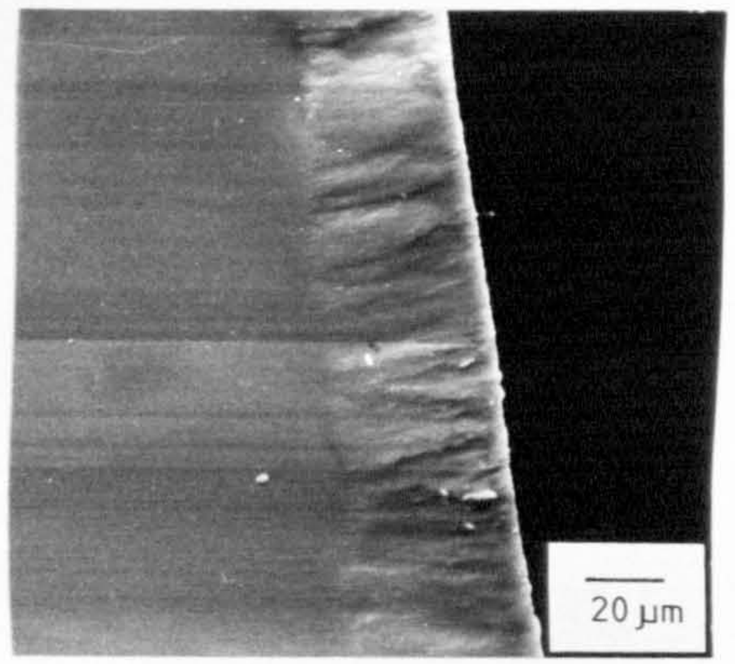

5hrs.

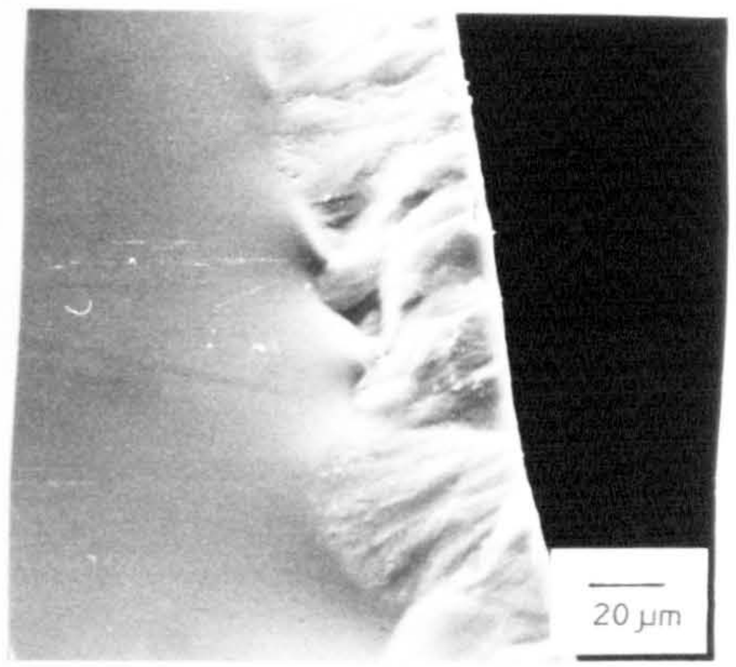

6hrs.

Figure 4.2.5

The thickening of the crystal layers in CAl(6) having been abraded for 2hrs and heat treated at 880°c for varying times.

4.2.2 Quantitative Analysis

From the SEM micrographs obtained for the glass-ceramics of MgBAl (3-2) the volume fractions of the α-phase crystals formed were measured using the point counting method described in section 2.4.2. The analysis was restricted to transparent specimens which had either been nucleated at 670°C for 4 hours or for 12 hours, and the results are presented in table 4.2.1.

In order to obtain reasonable statistics, the point counts were taken from between 10 to 12 different micrographs for each sample. For the purpose of calculating sectioning errors and errors associated with instrument resolution, the thickness of the etched layers were estimated from the micrographs and the quantity N_L (the number of grain boundaries per unit length) was obtained using lineal analysis. This was carried out by drawing 10 random lines (of known lengths) on each micrograph and then counting the number of boundaries crossing these lines. The errors due to finite number of sampling points, sectioning and instrument resolution quoted in table 4.2.1 were calculated using equations 2.4.2, 2.4.3 and 2.4.4 respectively. The final total error is the sum of these errors.

As can be seen from table 4.2.1, the largest source of uncertainty comes from the instrument resolution which, unfortunately, cannot be improved upon by better statistics. The volume fractions obtained by point counting can be compared with the results obtained for the amount of heat evolved [curves (A) and (C) of figure 4.1.1b] as it is directly proportional to the amount of crystals formed. Taking the error margins into consideration, the relative increase in volume fraction (by point counting) with heat treatment time is in reasonable agreement with the relative increase in heat evolved also as a function of heat treatment time.

		MgBAl(3-2). At 670°C for 4 hrs and at 730°C for			MgBAl(3-2). At 670°C for 12 hrs and at 730°C for		
		1 hr	2 hrs	3 hrs	1 hr	2 hrs	3 hrs
P_i	No. of points falling on phase α	36	302	1211	296	923	1355
P_o	Total no. of sampling points	3240	3888	3888	3888	3888	3240
N_L	No. of grain boundaries per micron	0.094	0.441	1.032	0.446	1.075	1.513
σ_{N_L}	Standard deviation of N_L	0.030	0.052	0.122	0.058	0.148	0.174
t	Estimated thickness of etched depth (μm)	0.1	0.15	0.4	0.1	0.25	0.3
Errors due to finite sampling points (%)		16.6	5.5	2.4	5.6	2.9	2.2
Sectioning errors (%)		31.9	11.8	11.8	12.9	13.8	11.5
Errors due to instrument resolution (%)		47	31	23	26	33	32
Total % error		95.5	48.3	37.2	44.5	49.7	45.6
True volume fraction (%)		0.63	4.99	10.51	5.37	10.26	19.10

TABLE 4.2.1

Volume fractions of transparent glass-ceramics of MgBAl(3-2).

The concept of a volume fraction is not strictly applicable to the glass-ceramics of CA1(6) since they exhibit surface crystallisation only. However, if the crystal layer is assumed to be 100% crystalline after a suitable time of heat treatment, then the thickness of the crystal layer formed after this time is a characteristic property of the material (provided the same abrasion and heat treatments were used). Although in practice 100% crystallinity is rarely achieved, this convenient assumption can be justified by observations made in the previous section, that there is complete impingement of the crystals formed at the surface before growth proceeds inwards, and that EDAX has shown no appreciable difference between the protruding crystals and the surface. The volume fraction in the crystal layer must therefore be fairly high.

The thickness of the crystal layer for each sample was measured from 3 different micrographs and the results are shown in figure 4.2.6. About 20 separate measurements were made for each data point and the error bars shown are the standard deviations. The thickness of the crystal layer can be seen to increase more or less linearly after the first 2 hours.

4.2.3 X-ray Diffraction

A Debye-Scherrer powder camera was used initially to identify the crystalline phases formed in the glass-ceramics of MgBAl (3-2). The diffraction patterns so obtained yielded a large number of lines, some of which were too diffuse to measure accurately. To ease this problem of identification, a diffractometer was used instead in the hope that the patterns might be better defined. The results are shown in figure 4.2.7. For the "fully crystallised" material, a different phase can be seen to emerge from that belonging to the transparent glass-ceramic.

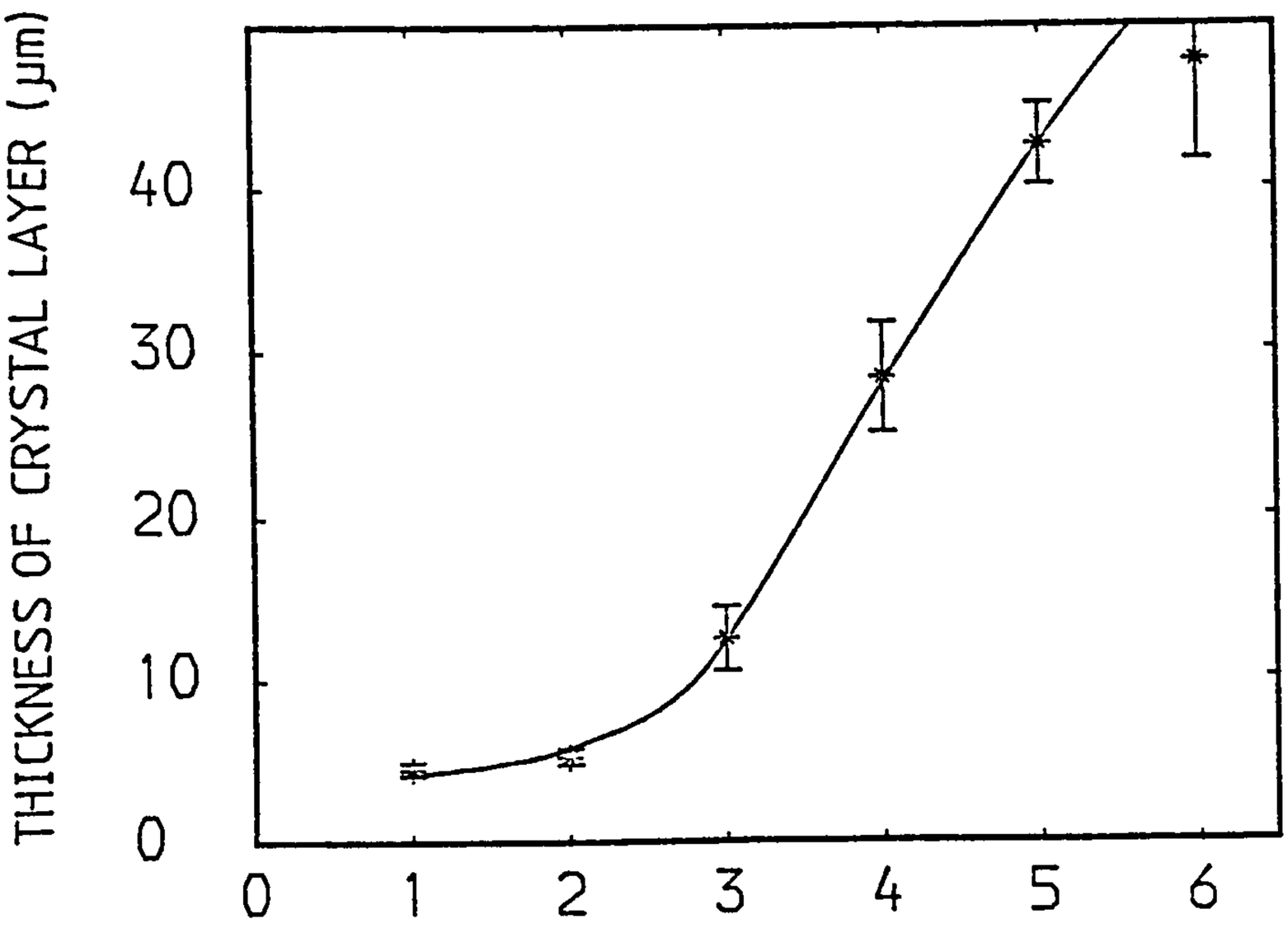

FIGURE 4.2.6

Thickness of crystal layer formed on CA1(6) having been abraded for 2 hrs. and heat treated at 880°C for varying times.

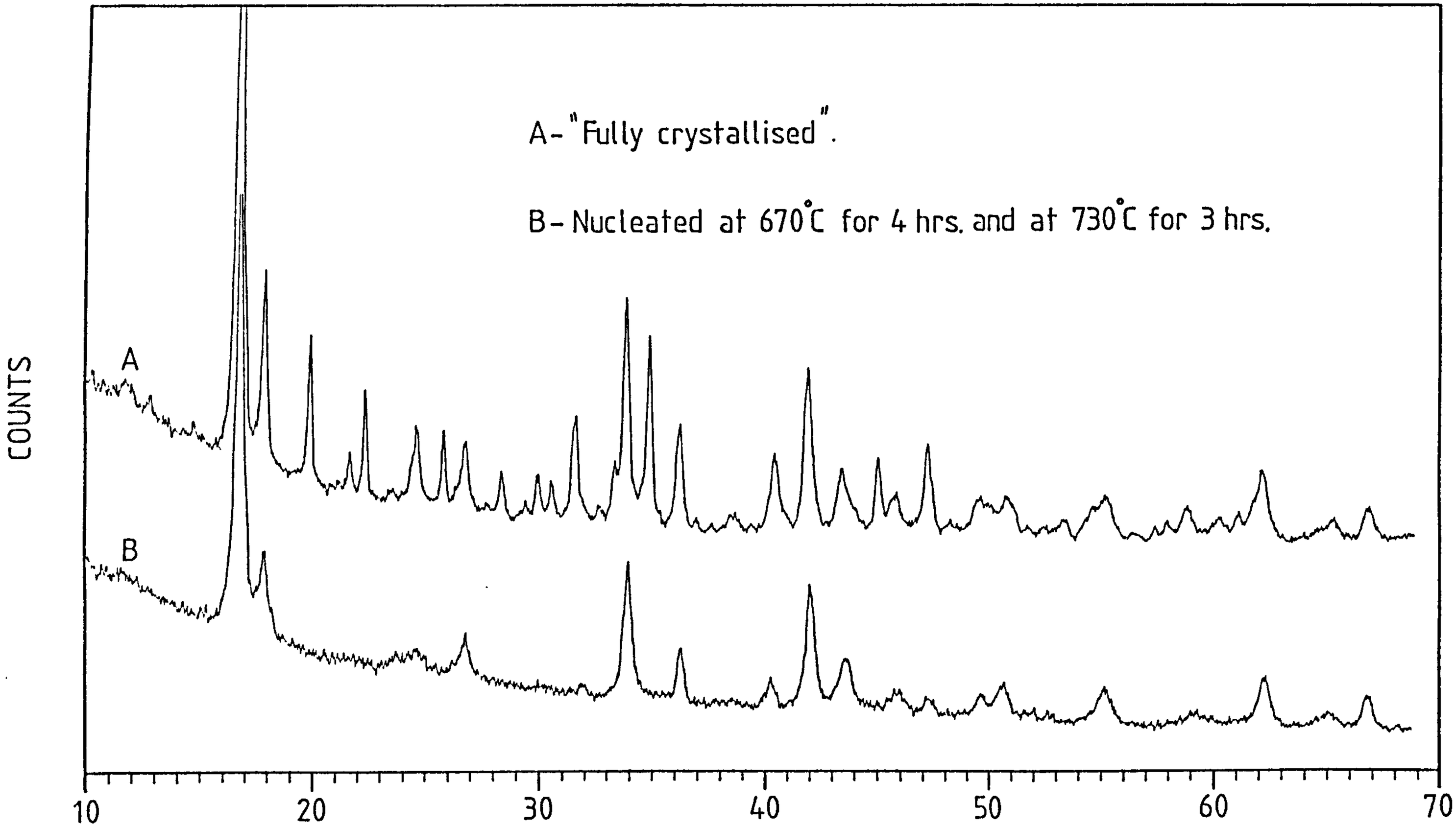

FIGURE 4.2.7

Diffraction patterns of glass-ceramics of MgBAl(3-2)

This corresponds to the "β-phase" or the "higher temperature phase" described in the DSC and DTA results respectively. It was identified to be $2MgO.B_2O_3$ from the A.S.T.M. powder data, card number 11-427. However the "α-phase" or the "lower temperature phase" could not be identified from the A.S.T.M. powder data (up to 1978). In fact, searches conducted through the usual literature failed to give any information on the system magnesium aluminoborate.

The identification of the crystalline phase formed in the glass-ceramic of CA1(6) was more straightforward. A powder camera was used to obtain the diffraction pattern and it was identified to be $12CaO.7Al_2O_3$ from the A.S.T.M. powder data, card number 9-413.

4.3 General Properties of Transparent Glass-Ceramics

4.3.1 Optical Transmission

As part of a programme to characterise some of the general properties of the glass-ceramics of MgBA1 (3-2) and CA1(6), the optical transmission was measured and the results are shown in figure 4.3.1.

In the case of MgBA1 (3-2), all the glass-ceramics formed during heat treatments at 730°C lasting up to 3 hours could transmit light, but became completely opaque for longer heat treatment times. It is worth noting, for specimens heat treated for the same length of time, but with different nucleation treatments, the transparency only differed marginally. Considering the specimens have very different volume fractions of crystals (see table 4.2.1), this implies the size of the crystals rather than the number of them that is important in obtaining transparency.

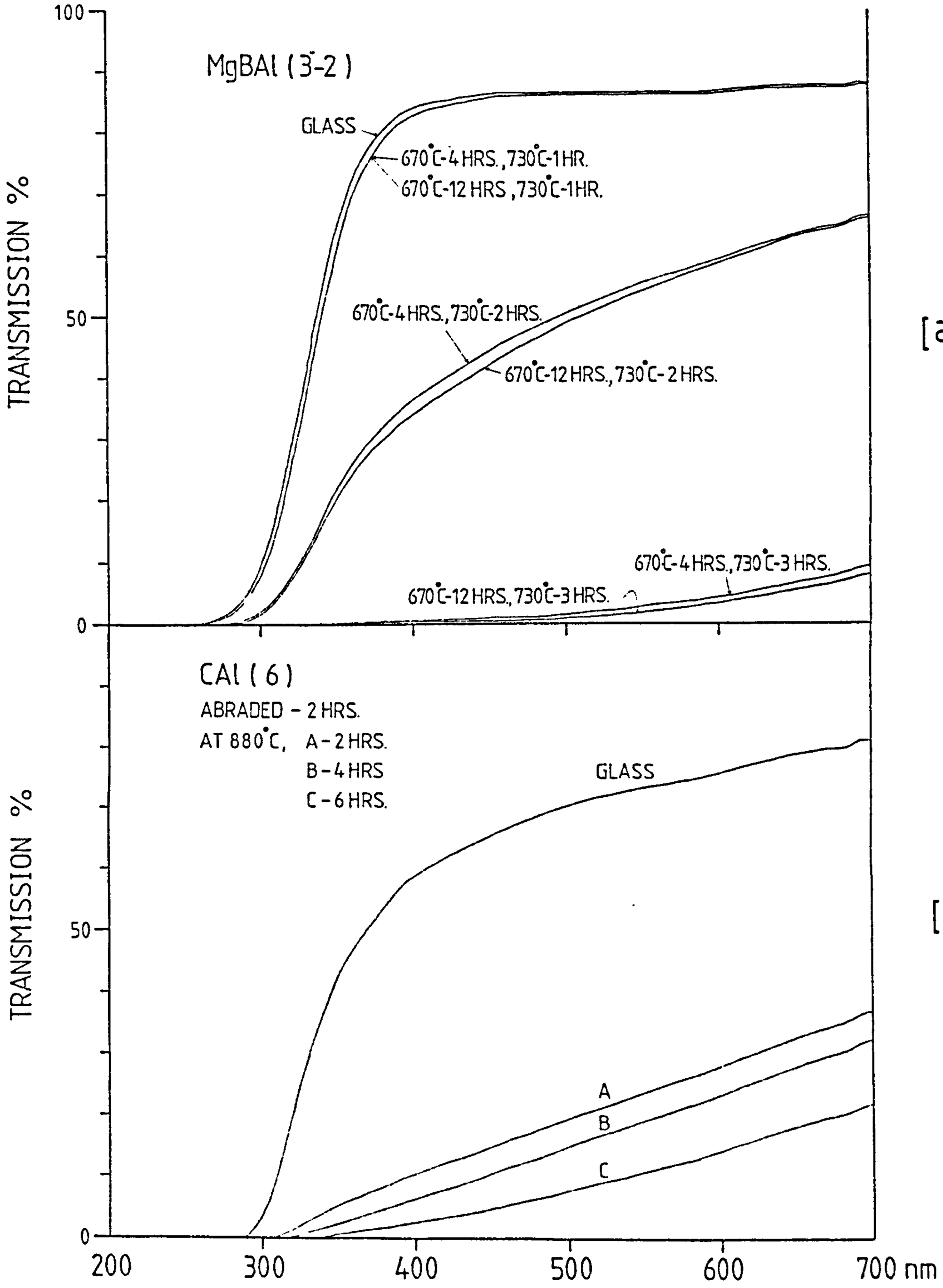

FIGURE 4.3.1

Transmission spectra for the glass-ceramics of [a] MgBAl(3-2) and [b] CAl(6). The thickness of the specimens used were 1.5 ± 0.1 mm.

All the glass-ceramics of CA1(6) were found to be translucent. This is a surprising result in view of the thickness of the crystal layers ~ 5-50 microns (see figure 4.2.6) which is much larger than the wavelength of light; one would expect strong scattering to occur and total opacity in the appearance of the samples. However, Burggraaf and Van Velzen (1968) have published figures of 1.60 and 1.62 for the refractive indices for the crystal $12CaO.7Al_2O_3$ and for the glass having the same composition respectively. It seems likely in the case of CA1(6) that there may be close matching of refractive indices between the crystal layer and the glass which would then explain the observed results.

A note of caution is due regarding these results. It will be recalled from the discussion in section 1.1.2, that the mechanism which causes the loss of transmitted intensity in a transparent glass-ceramic is due to the scattering of light by the crystals in the glassy matrix. According to equation 1.1.1, the scattered intensity, apart from the wavelength of light, the size of crystals and the ratio of the refractive index between the crystal and the glass, is also a function of the scattering angle and the distance from the scattering centre to the point of observation. This means depending on the kind of instrument used to measure the transmission, the relative position between the specimen and the detector along with the actual size of the detector will have an important bearing on the results. For this reason, the results presented here can only be treated on a qualitative basis.

4.3.2 Thermal Expansion and Mechanical Strength

The thermal expansion and the mechanical strength (by 4-point bending) for the glasses and glass-ceramics were measured and the results are presented in tables 4.3.1 and 4.3.2 respectively. Owing to the

Glasses and Glass-Ceramics	Thermal Expansion Coefficient ($\times 10^{-7}°C^{-1}$) R.T. → 550°C	300 - 550°C	Dilatometric Softening Pt. (°C)
MgBAl (3-2)	57.0 ± 1.0	62.5 ± 2.9	660
MgBAl (3-2) At 670°C for 4 hrs and at 730°C for 1 hr.	57.2 ± 1.6	62.6 ± 2.2	651
2 hrs	56.9 ± 1.0	62.6 ± 1.6	649
3 hrs	56.9 ± 0.6	62.8 ± 1.0	645
4 hrs	57.8 ± 1.4	64.0 ± 1.6	639
5 hrs	58.2 ± 1.1	64.5 ± 1.0	643
MgBAl (3-2) At 670°C for 8 hrs and at 730°C for 1 hr.	57.3 ± 0.5	63.2 ± 0.5	654
2 hrs	57.0 ± 1.3	63.1 ± 1.5	649
3 hrs	57.5 ± 1.4	63.4 ± 1.6	649
4 hrs	58.3 ± 1.5	64.5 ± 4.9	640
5 hrs	59.0 ± 3.0	65.3 ± 4.6	676
MgBAl (3-2) At 670°C for 12 hrs and at 730°C for 1 hr.	57.0 ± 0.5	62.8 ± 1.1	650
2 hrs	57.3 ± 0.2	63.5 ± 1.0	647
3 hrs	58.0 ± 0.5	64.0 ± 1.3	644
4 hrs	59.0 ± 0.6	65.2 ± 0.8	633
5 hrs	59.3 ± 3.3.	65.5 ± 3.7	> 740
CAl (6)	84.2 ± 2.7	88.9 ± 2.4	800

TABLE 4.3.1

Thermal expansion coefficients for the compositions MgBAl (3-2) and CAl (6).
Errors are quoted at 95% confidence level.

Glasses and Glass-Ceramics	Maximum Failure Stress (MNm^{-2})
"Float" glass	99.0 ± 7.0
MgBAl (3-2)	115.2 ± 13.0
MgBAl (3-2) At 670°C for 4 hrs and at 730°C for 1 hr	125.7 ± 9.0
2 hrs	117.0 ± 12.9
3 hrs	133.3 ± 7.9
4 hrs	159.5 ± 7.6
5 hrs	244.6 ± 17.9
MgBAl (3-2) At 670°C for 8 hrs and at 730°C for 1 hr	124.1 ± 9.0
2 hrs	104.9 ± 7.6
3 hrs	104.3 ± 10.6
4 hrs	180.9 ± 17.2
5 hrs	220.4 ± 24.4
MgBAl (3-2) At 670°C for 12 hrs and at 730°C for 1 hr	95.9 ± 9.0
2 hrs	111.2 ± 12.2
3 hrs	117.8 ± 9.3
4 hrs	189.7 ± 23.7
5 hrs	296.6 ± 17.7

TABLE 4.3.2

Mechanical strengths of the glass and glass-ceramics of MgBAl (3-2) by 4-point bending. Errors are quoted at 95% confidence level. All measurements were carried at between 50 - 60% relative humidity.

limited time available, it has not been possible to extend the measurements to the glass-ceramics of CA1(6).

From table 4.3.1, the expansion coefficients for all the glass-ceramics of MgBA1(3-2) can be seen to increase marginally with heat treatment time, but on the whole the thermal expansion is relatively insensitive to the changes in the microstructure. The only conclusion is that the α-phase has a similar expansion coefficient to that of the parent glass. More noticeable was the lowering of the dilatometric softening temperature with heat treatment time (up to about 4 hours). This implies as the α-phase is being crystallised out, the viscosity of the residual glass is decreased. From Appendix 1, by making use of the Stokes-Einstein relationship and substituting into the first exponential on the R.H.S. of equation A1.4, the rate of crystal growth becomes inversely proportional to the viscosity. It follows then that the lowering of the viscosity in the residual glass will tend to enchance the growth of the β-phase ($2MgO.B_2O_3$).

The mechanical strength measurements for the glass-ceramics of MgBA1(3-2) were found to be much more sensitive to changes in the microstructure (see table 4.3.2). However in the absence of a detailed analysis, the observed increase in strengths with heat treatment time could not be related to any specific properties of the materials. Qualitatively though, it is possible to connect these measurements to some of the features of the microstructures as observed by electron microscopy.

The mechanical strength data for some of the glass-ceramics of MgBA1(3-2) are shown graphically in figure 4.3.2 for clarity. Choosing the sample

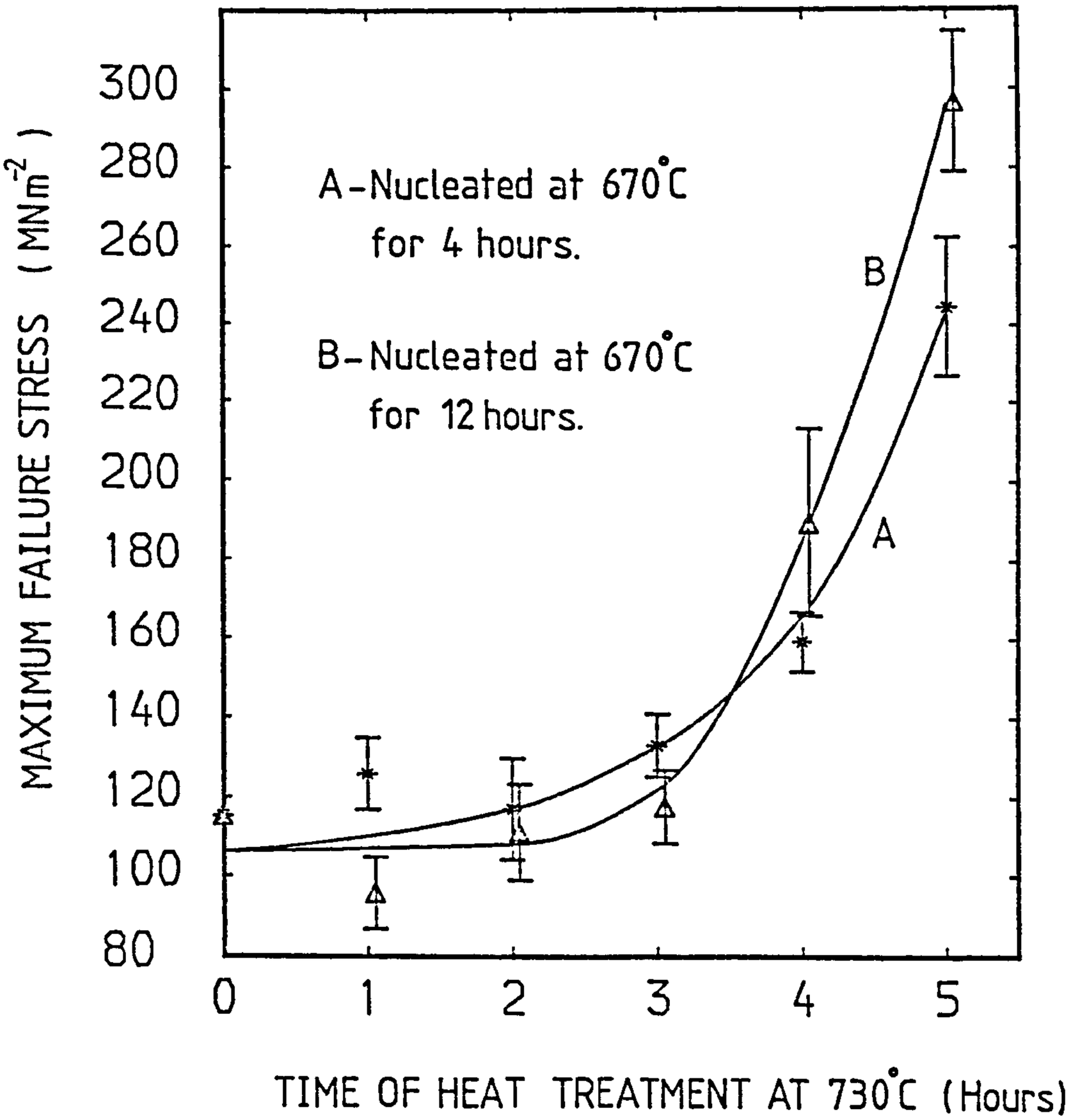

FIGURE 4.3.2

Maximum failure stress of glass-ceramics of MgBAl(3-2) by 4-point bending.

which had been nucleated for 12 hours as an example, the substantial increase in strength after 3 hours of heat treatment can be related to when the α-phase crystals impinged on each other to form an interlocking structure (shown in figure 4.2.2) and thereby improved the mechanical behaviour of the material.

CHAPTER 5: Results of the Interaction with Sodium Metal Vapour

The present chapter is concerned with the interaction of sodium metal vapour with the glasses given in table 2.2.1 and some of the transparent glass-ceramics derived from the composition MgBAℓ (3-2) and CAℓ (6) [described in chapter 4]. The chapter is divided into four sections. Under the heading of characterisation of discolouration, the first section describes the resistance of the various glasses and transparent glass-ceramics to sodium. The results of the reaction between sodium and these glasses investigated by DTA along with the identification of the reaction products by X-ray diffraction are the subjects of the second section. The third section deals with the results of the surface sensitive studies carried out in an attempt to reveal the nature of the discolouration and the mechanism by which the glasses are attacked. The last section gives the results of the investigation by ESR to detect the presence of any paramagnetic centres formed as a consequence of the glasses having been attacked by sodium.

5.1 Characterisation of Discolouration

A prominent feature of a glass having been attacked by sodium is the formation of a discoloured layer at the surface. The severity of the attack is indicated by the colour of the discolouration (see section 1.2) and this property was used in the present work as a means of gauging the resistance of the various glasses and transparent glass-ceramics towards attack by sodium. As already pointed out in section 3.3, the absorption band due to the discolouration (measured in the range 200-700 nm) could not be characterised simply. Instead an arbitrary method (described in detail in section 3.3) of plotting the absorption coefficient of the discolouration at 500 nm as a

function of temperature of exposure to sodium was used. The curve so obtained is then characteristic of the discolouration which in turn reflects the resistance of the material in question.

This method of describing the discolouration has several drawbacks as can be seen from either figure 3.3.1 or from figure 5.1.1 which shows the transmission spectra of vitreous silica having been exposed to sodium at various temperatures for different times. The absorption due to the discolouration increases monotonically with decreasing wavelength in some undetermined manner. Therefore by plotting the absorption coefficient at 500 nm alone against temperature of exposure the resultant curve does not give any information regarding the absorption at other wavelengths. The absorption of the discolouration also increases with the time of exposure to sodium, shown by curves B and C at 300°C and curves D and E at 350°C in figure 5.1.1. In order that valid comparison between different materials can be made, the time of exposure has to be standardised. In the present work, all the specimens were exposed to sodium for 3 hours; a time long compared with that required to reach thermal equilibrium after the sodium is introduced into the hot zone of the "bomb" (see section 3.2). The choice then of mapping the absorption coefficient at 500 nm as a function of exposure temperature and exposing the specimens to sodium for 3 hours is quite arbitrary. Furthermore, the curves obtained could not be related to any particular property of the materials under study. This method of characterising the resistance towards sodium however can be justified on the grounds that a comparison between the resistance of the materials is sought and that the results shown below are in agreement with the findings of previous authors (see section 1.2).

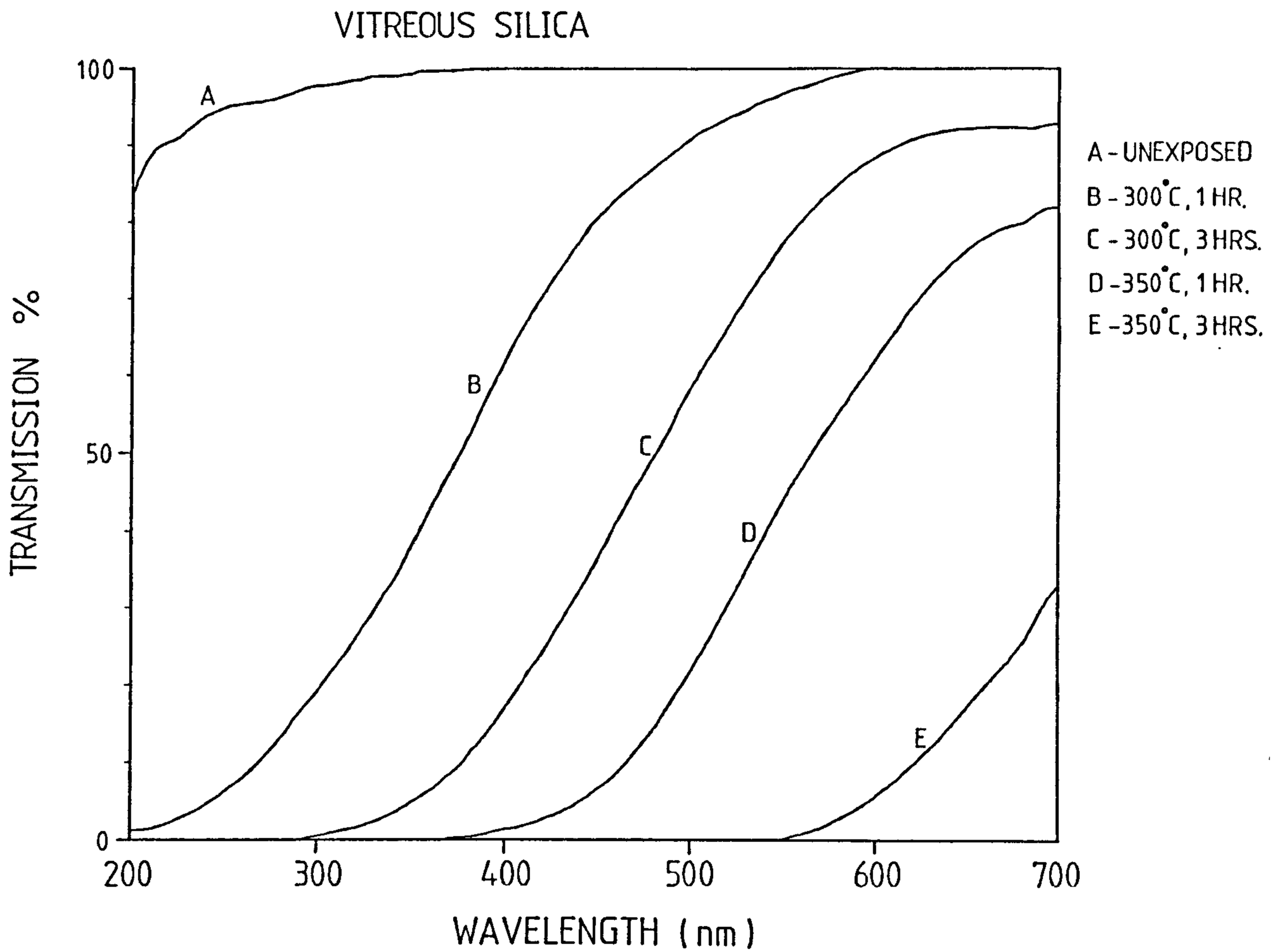

FIGURE 5.1.1

Transmission spectra of vitreous silica having been exposed to sodium at various temperatures for different times. The thickness of the samples were 1.00 $\pm$ .05 mm.

Figure 5.1.2a shows the curves of the absorption coefficient at 500 nm versus temperature of exposure for the simple silicate materials. For the one component systems, vitreous silica was severely discoloured at just over 300°C and was the least resistant of all the materials studied. Quartz (x-cut) on the other hand was amongst some of the most resistant of the silicate materials investigated and remained unaffected by sodium up to 350°C. Quartz crystals of a different orientation (z-cut) were also experimented with. The results were rather inconsistent due to the variable quality of some of the crystals. The overall impression was that the z-cut crystals were marginally less resistant to sodium than the x-cut crystals, but they showed a definite substantial improvement from vitreous silica. For the binary silicate glasses, the addition of 20 mole % soda to silica [NaS(1)] made very little difference to the resistance as compared with vitreous silica, but for a further 10 mole % increase in soda content [NaS(2)], the resistance to sodium was vastly improved.

Figure 5.1.2b shows the discolouration behaviour for the alumino-silicate glasses. The substitution of 5 mole % of alumina for silica in NaS(2) [NaSAℓ(1)] had a detrimental effect on the resistance, and this trend continued for NaSAℓ(2) where a further 5 mole % of alumina was substituted for silica. In the case of MgSAℓ(8B), the alumina content is about 13.3 mole % and it is therefore comparable to the alumina content of NaSAℓ(2) [10 mole %], yet the resistance to sodium is much lower. This suggests the replacement of soda by magnesia has a deteriorative effect on the resistance. These results are intuitively inconsistent with the fact that alumina and magnesia are known to be resistant to sodium, but they are in exact agreement with the findings

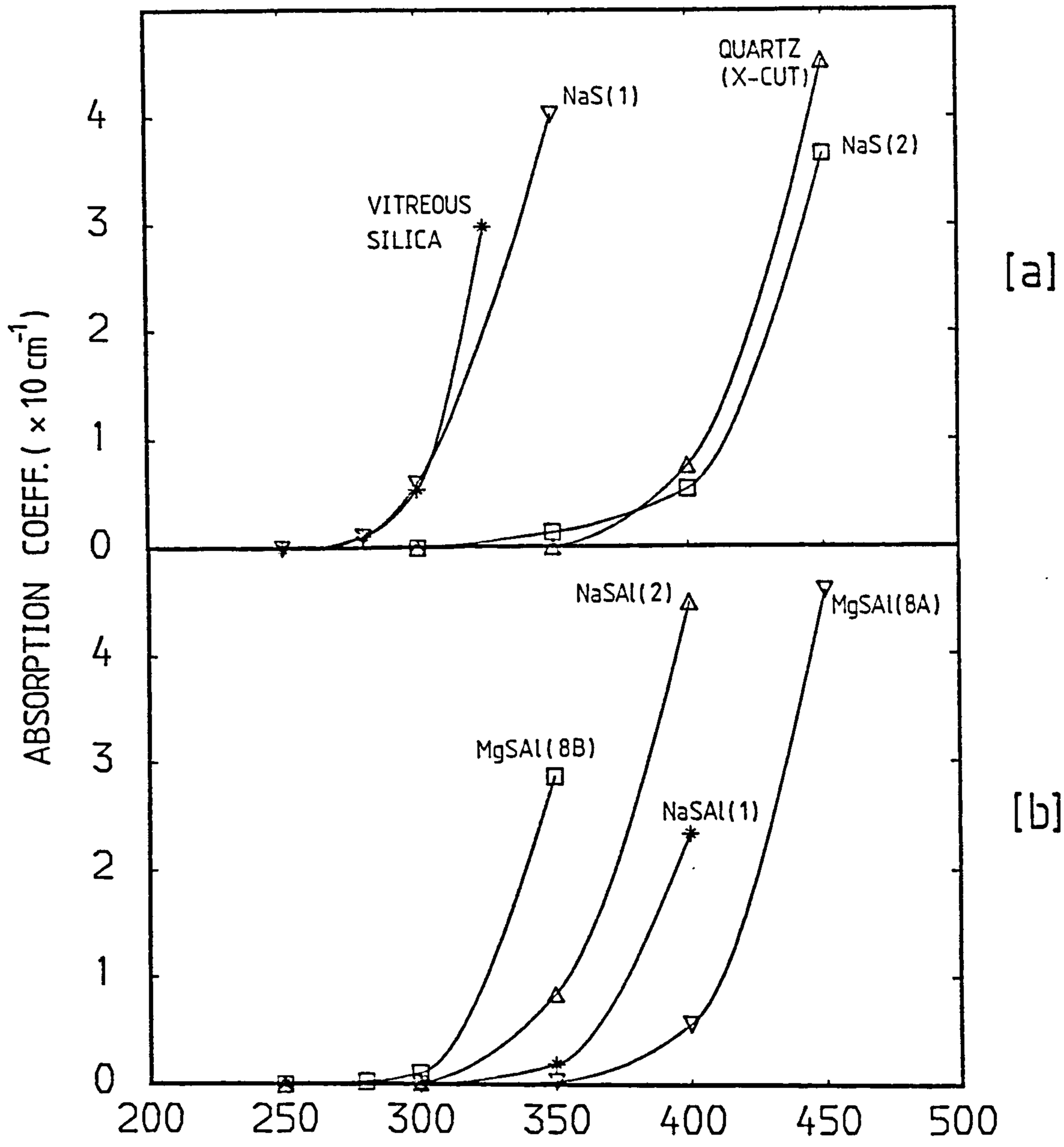

FIGURE 5.1.2

Absorption of the discolouration at 500 nm versus temperature of exposure to sodium for [a] one and two components silicates and [b] three components alumino-silicates. All samples were exposed to sodium for 3 hours.

of Elyard and Rawson (1962) who have observed the same results in simple borate and phosphate glasses. For glass MgSAℓ(8A) where the composition now contains a substantial proportion of magnesia (30 mole %) and alumina (20 mole %), it was found to be one of the most resistant of all the silicates studied. It is debatable whether this improvement in resistance is due to the increase in alumina and magnesia content or the fact that MgSAℓ(8A) has the lowest proportion of silica of all the silicates studied.

The results presented so far, namely that quartz showed a superior resistance to sodium relative to vitreous silica, that an increase in soda content retards the sodium attack and that the addition of alumina and magnesia in low proportions had a detrimental effect on the resistance are all in agreement with previous authors. Therefore the method chosen to describe the resilience of the materials towards sodium attack, although arbitrary, appears to give fairly reliable results.

Figure 5.1.3 shows the discolouration behaviour of the borates and the aluminates. Both NaB(1) [20 mole % soda] and NaB(2) [25 mole % soda] behaved very similarly and they were more resistant than any of the silicates studied. However, the low softening points of these glasses ($\sim 450^{\circ}C$) made it impossible to compare their behaviour with the alumino-borates at higher temperatures ($> 450^{\circ}C$) of exposure. MgBAℓ(8) was attacked more easily than MgBAℓ (3-2); as both glasses have about the same alumina content (20 and 21 mole % alumina respectively), the increase in resistance in MgBAℓ (3-2) can be attributed to the higher magnesia content of 37 mole % as compared with 30 mole % in MgBAℓ(8). Finally CAℓ (6) was found to be the

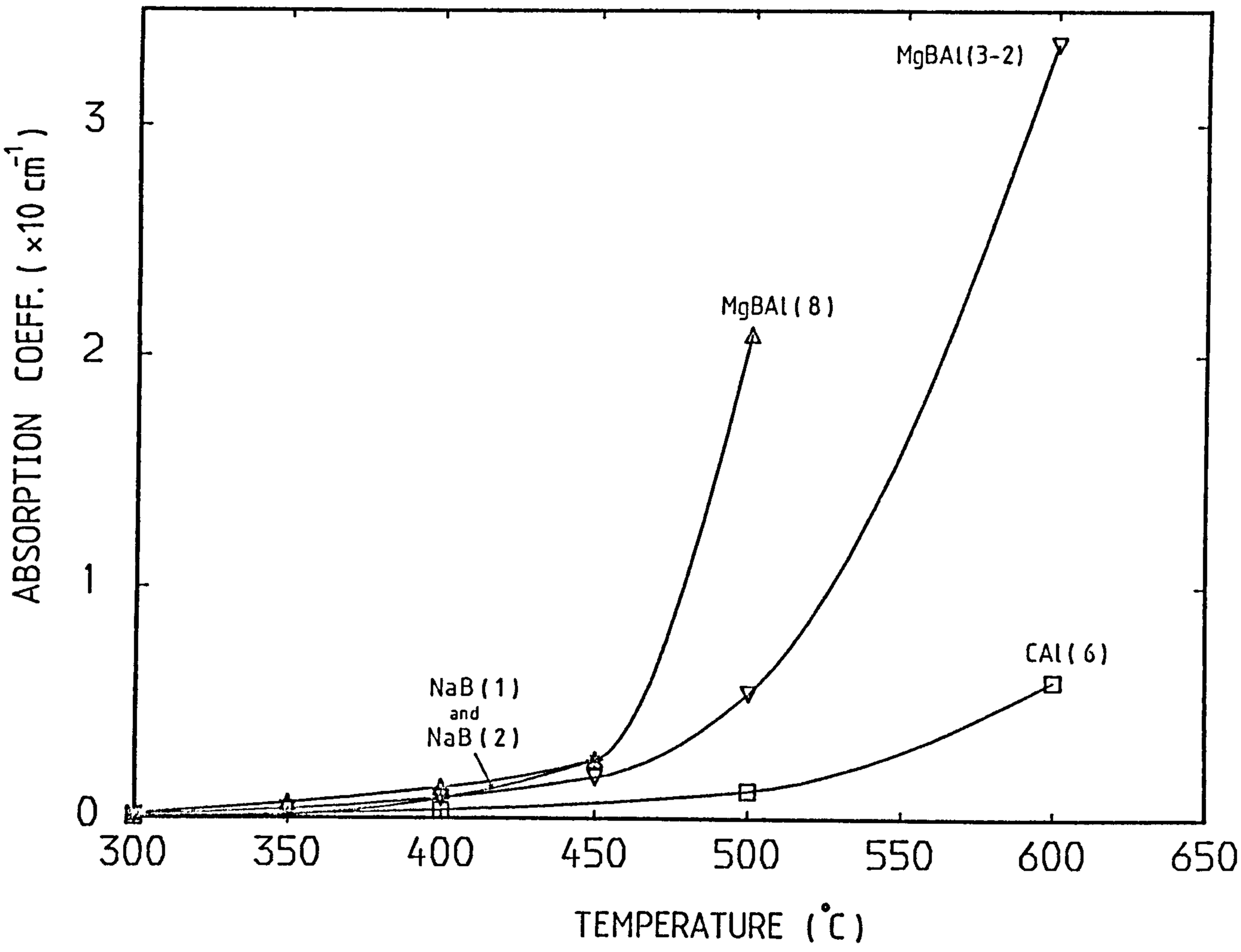

FIGURE 5.1.3

Absorption of the discolouration at 500 nm versus temperature of exposure to sodium for the borates and the aluminate. All samples were exposed to sodium for 3 hours.

most resistant of all glasses studied, in accordance with expectations since all the constituents of the glass (CaO, MgO and Al_2O_3) are known to be resistant to sodium.

The discolouration behaviour of a few of the transparent glass-ceramics are presented in figure 5.1.4. For the MgBAℓ (3-2) system, all the glass-ceramics showed a better resistance to sodium than the original glass and the resistance improved with increasing nucleation time (i.e. higher volume fraction of crystal phase). However, the increase in resistance is not as dramatic as in the case of vitreous silica and quartz. If indeed by altering the structure of a glass via crystallisation can improve the resistance; the marginal increase in resistance in the transparent glass-ceramics of MgBAℓ (3-2) is to be expected since the volume fractions of crystals formed are relatively low, about 5% and 10% (see table 4.2.1) for the specimens nucleated at 670°C for 4 hours and 12 hours respectively. For the CAℓ(6) system, it has not been possible to carry out exposures at temperatures higher than 600°C because of the limitations of the exposure apparatus. Despite this, the glass-ceramic can be seen to show a marked improvement from the original glass and the material was barely discoloured by sodium at 600°C. As discussed in section 4.2.1, for a sample of CAℓ(6) abraded for 2 hours and then heat treated at 880°C for 2 hours, this is the point where the crystals formed at the surface are beginning to impinge on each other and the resulting crystal layer (~ 5 microns thick) probably has a fairly high volume fraction. Since the discolouration process proceeds from the surface, the crystal layer effectively forms a protective skin for the material and hence the observed significant improvement to sodium.

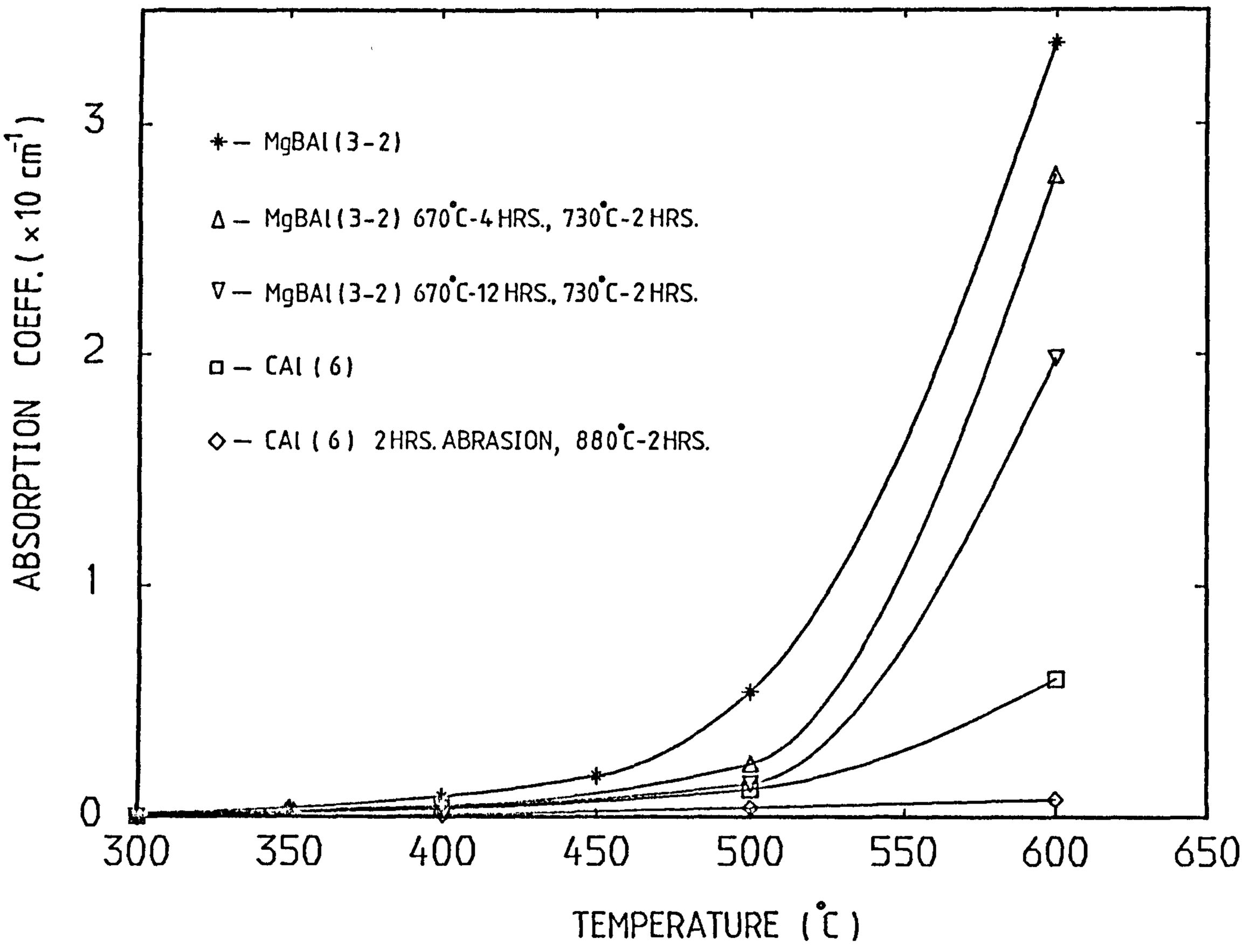

FIGURE 5.1.4

Absorption of the discolouration at 500 nm versus temperature of exposure to sodium for the transparent glass-ceramics of MgBAℓ(3-2) and CAℓ(6). All samples were exposed to sodium for 3 hours.

The general picture that has emerged from this investigation so far is that the glasses in increasing order of resistance to sodium are silicates, borates, aluminoborates and aluminates. The addition of refractory oxides such as magnesia and alumina in low proportions was found to have an adverse effect on the resistance, whilst substitution of these oxides in amounts greater than 20 mole % enchanced the resistance. Further improvements in the resistance to sodium other than by chemical substitution can be achieved by altering the structure of the glasses by crystallisation. In the case of crystallising the glasses in the bulk such that the resultant materials remain transparent (or translucent), the volume fraction of crystals formed is usually low (~ 10 - 20%) and therefore the improvement in resistance is only marginal. On the other hand, bearing in mind that the discolouration process is restricted to the surface regions, surface crystallising a glass represents a much more effective means of improving the resistance provided a "continuous" crystal layer can be formed; and at the same time, it is probably less difficult to achieve either transparency or translucency in the final material.

5.2 Thermal Investigation of the Reaction with Sodium Metal Vapour

5.2.1 Differential Thermal Analysis (DTA)

The principal objectives of this experiment were to investigate whether the glasses (listed in table 2.2.1) do indeed react with sodium by studying the heat changes involved and the possible effects of altering the composition of the glasses with respect to their reaction with sodium. The reaction of vitreous silica and α-quartz with sodium was also examined in the hope that an assessment of the applicability of equilibrium thermodynamics could be made.

In preparing the samples for DTA (described in section 3.4.2) considerable experimental difficulties were experienced with the sealing of the stainless steel capsules used for the containment of sodium and the glass specimen. Hence it has not been possible to carry out thermal analysis on all the glasses within the limited time available.

Figure 5.2.1. shows the DTA traces for the silicate materials. For α-quartz, a slow exothermic drift can be seen to begin from about 405°C until 527°C where a sharp exothermic peak occurred. In the case of vitreous silica, a more pronounced exothermic drift can be seen to initiate at about 440°C until 563°C where an equally sharp exothermic peak occurred. It is worth noting that the thermal analysis for vitreous silica was carried out at a higher rate of heating (~ 9.0°C/min) compared with that for α-quartz (~ 6.9°C/min). In DTA, the rate of reaction is dependent on the heating rate [Ware (1971)], and the effect of a faster heating rate is to promote the reaction to occur at a higher temperature. Therefore the difference in temperature between the exothermic peaks of vitreous silica and α-quartz is in fact less than that indicated. At temperatures below the occurrence of the exothermic peak (say 400 - 500°C), it is very likely that the materials had already been discoloured by sodium. The exothermic drift in both cases can be interpreted as being related to the situation when the materials were beginning to be attacked by sodium, corresponding to the discolouration phenomenon. The larger drift observed in vitreous silica indicates that the material is more prone to be discoloured by sodium than α-quartz, in accordance with the discolouration behaviour described earlier (see figure 5.1.2).

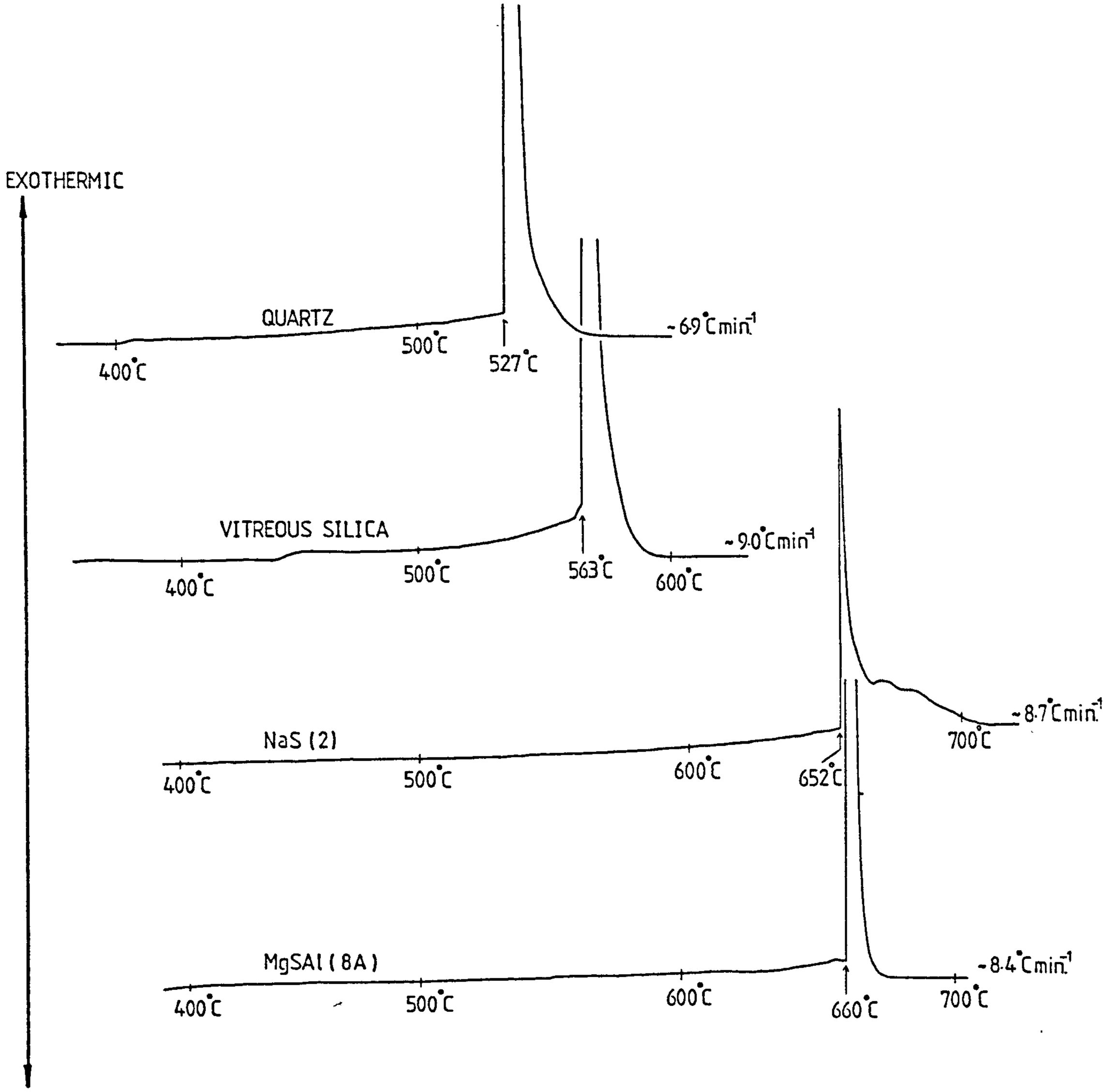

FIGURE 5.2.1

DTA traces of different silicates reacting with an excess of sodium. All specimens had the same particle size (100–150 microns), same weight (100 ± 0.2 mg) and all the traces were recorded on the same scale.

It is clear from the DTA traces shown so far that the determination of the temperature at which the exothermic drift first occurred and the magnitude of the drift can be very ambiguous, therefore DTA is not a particularly suitable technique for examining the discolouration behaviour. However, the traces do convey the information that at a certain temperature, the specimen and the sodium would react together to form some product as indicated by the appearance of the exothermic peak. This temperature in a sense represents the "top temperature limit" below which it is possible for the material to remain resistant to sodium.

In the case of NaS(2), a slow exothermic drift can be seen to begin at about 515°C until 652°C where a sharp exothermic peak occurred and the amount of heat evolved is much less than that for either vitreous silica or α-quartz. As will be shown in the following section, the exothermic peaks observed in vitreous silica, α-quartz and NaS(2) all correspond to the formation of the same crystalline compound ($Na_2O.SiO_2$). The fact that the exothermic peak for NaS(2) occurred at higher temperature than vitreous silica and α-quartz is indicative of the higher resistance of the material towards sodium. For MgSAℓ(8A), the reaction with sodium is similar to that for NaS(2) with the exothermic peak occurring at a marginally higher temperature of 660°C. The magnitude of heat evolved is much larger than that for NaS(2); although X-ray results shown in the next section are inconclusive, it is likely that a different crystalline compound (other than $Na_2O.SiO_2$) was being formed.

To summarise the results for the silicates studied: all were found to react exothermically with sodium, indicating that it is chemically favourable for them to be reduced by sodium. A common feature of their reaction with sodium is the sharpness with which the exothermic peaks occurred and there is as yet no apparent reason to explain this finding. The addition of substantial portions of oxides such as soda, magnesia and alumina has the effect of promoting the reaction to occur at higher temperatures, i.e. improving the resistance of the materials, in agreement with the results of section 5.1. Vitreous silica was found to behave in a very similar manner to α-quartz with respect to their reaction with sodium. The difference in thermodynamic properties between these two materials is therefore not significant enough to affect the overall reaction with sodium, thus offering more confidence in the use of equilibrium thermodynamics.

Figure 5.2.2 shows the DTA traces for the borates and the aluminate. Both NaB(1) and MgBAℓ (3-2) were found to react with sodium, but not as vigorously as the silicates and this is a reflection on their superior resistance to sodium. The thermal analysis of CAℓ(6) up to ~ 800°C revealed very little, indicating that the material did not react with sodium in any appreciable way. This is an interesting result in that the constituents of the glass were predicted to be resistant to sodium by an equilibrium thermodynamical argument [Singh (1976)], and the fusion of these oxides together has resulted in a glass which also exhibits a high resistance to sodium. If it is generally true that oxides which are predicted to be inert to sodium do indeed form glasses which are also resistant to sodium, then equilibrium thermodynamics can be used as a screening test in the

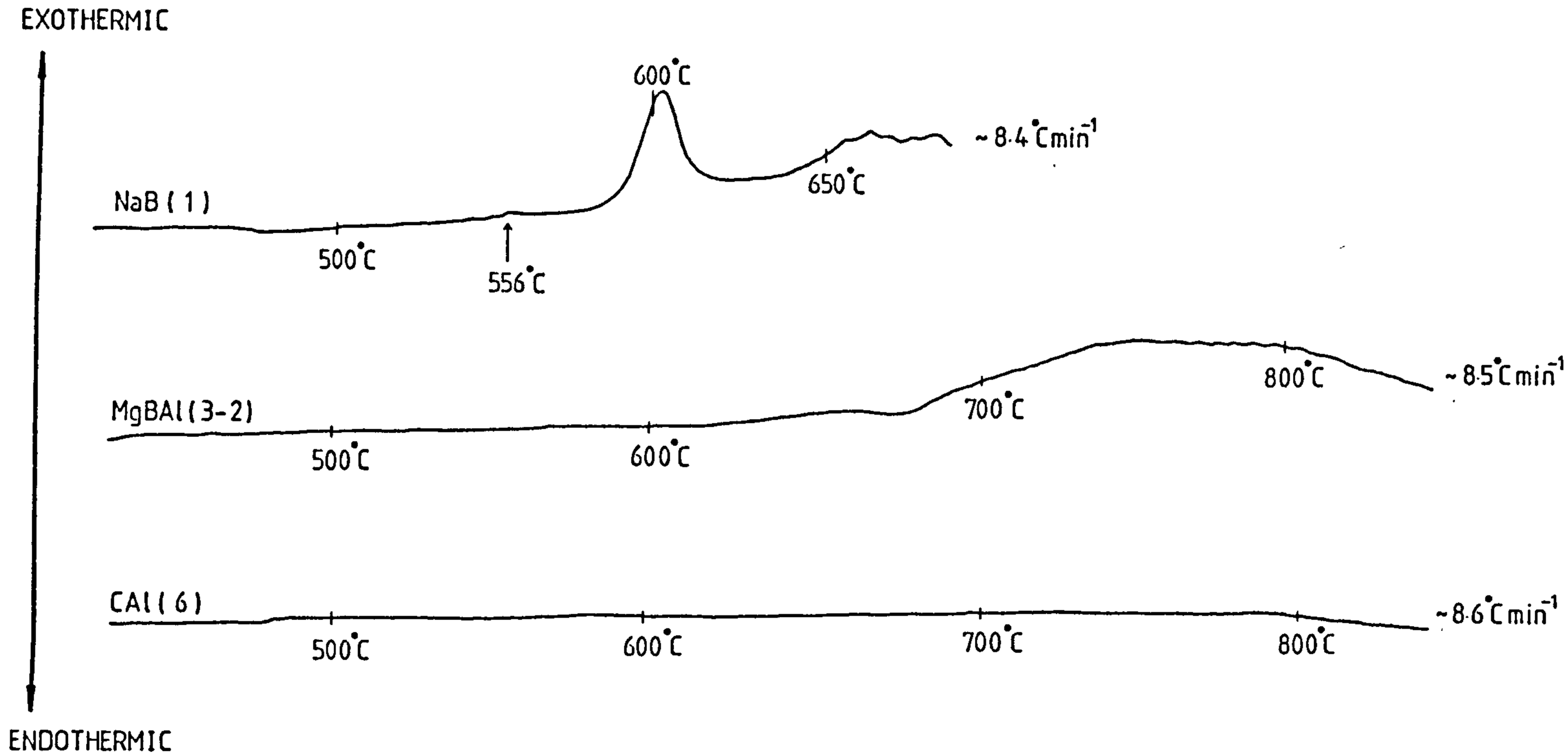

FIGURE 5.2.2

DTA traces of different borates and aluminate reacting with an excess of sodium. All specimens had the same particle size (100-150 microns), same weight (100 ± 0.2 mg) and all the traces were measured using the same scale as the previous figure (5.2.1).

initial selection of suitable constituents for making sodium resistant glasses.

5.2.2 X-Ray Diffraction

X-ray diffraction was used to identify the reaction products of the glasses and crystalline material after exposure to sodium. The information obtained then pinpoints which pathways the reactions have taken. The preparation of the specimens for X-ray diffraction has already been described in section 3.4.3, and the results are as follows.

Figure 5.2.3 shows the powder patterns for vitreous silica and α-quartz, each having been exposed to sodium at various temperatures for 3 hours. Vitreous silica can be seen to remain "disordered" after exposure up to around 400°C and a crystalline compound identified to be sodium meta-silicate $Na_2O.SiO_2$ (from A.S.T.M. powder data card number 16-818) was formed at about 450°C. The reaction of sodium with α-quartz was found to be very similar to that with vitreous silica. The crystal structure of α-quartz can be seen to remain relatively unaffected up to 400°C, but a new crystalline compound also identified to be $Na_2O.SiO_2$ emerged at around 450°C. Therefore the formation of $Na_2O.SiO_2$ from either vitreous silica or α-quartz occurred at nearly the same temperature, in close agreement with the DTA results (figure 5.2.1) where the exothermic peaks for both materials were also found to occur at roughly the same temperature, and naturally the occurrence of the exothermic peaks are associated with the formation of $Na_2O.SiO_2$.

By taking the case of α-quartz as an example, the above finding suggests that the reaction

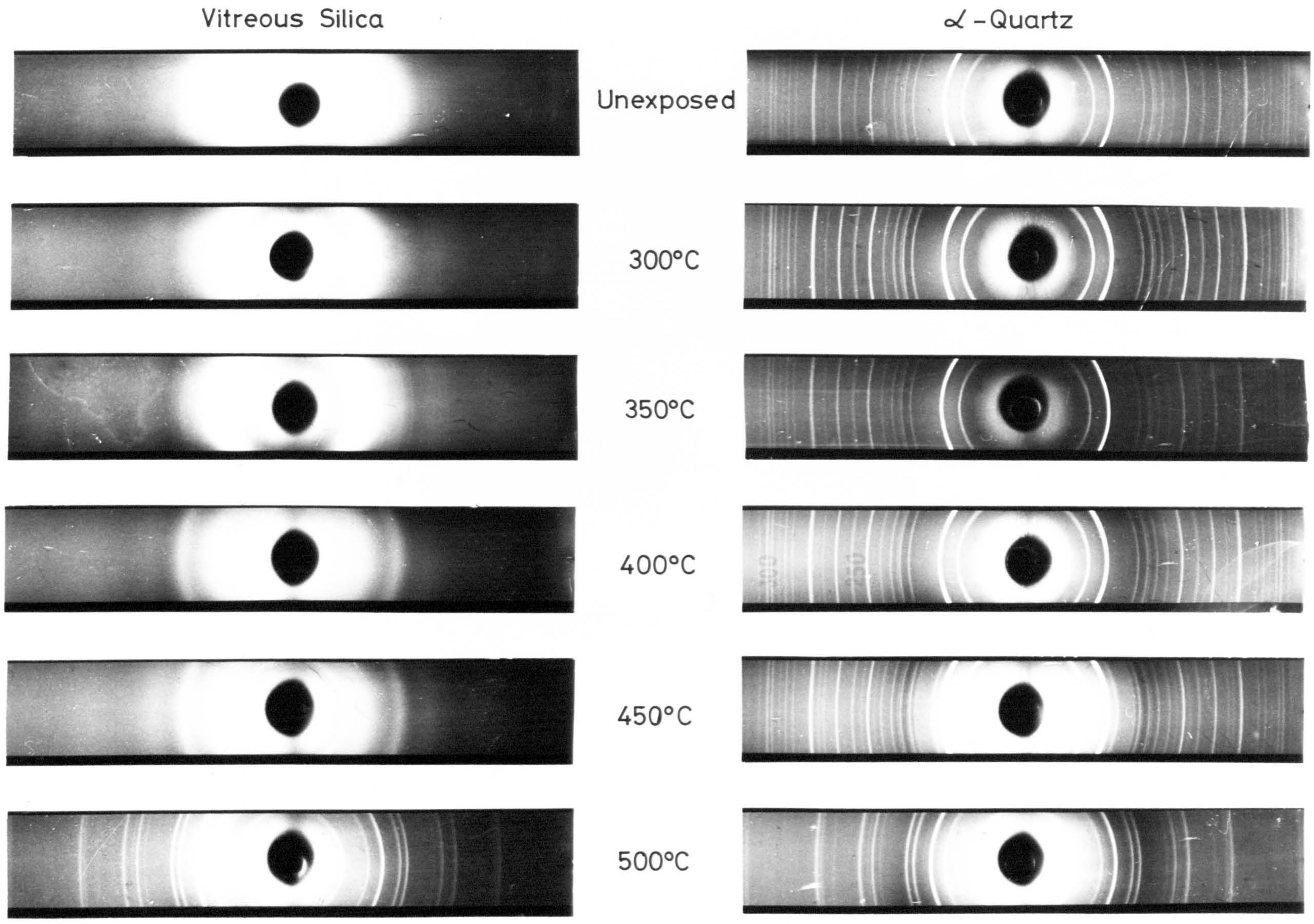

Figure 5.2.3

X-Ray powder diffraction patterns of vitreous silica and ∝-quartz having been exposed to sodium vapour at different temps. for 3hrs.

$$4Na + 3SiO_2 \xrightarrow{\sim 700K} 2Na_2SiO_3 + Si \qquad \Delta G = -77.0 kcal \qquad (5.2.1)$$
$$\Delta H = -95.7 kcal$$

has occurred. The change in free energy [from JANAF thermochemical tables edited by Stull and Prophet (1971)] is negative, therefore the reaction is favoured. Also the heat of reaction ΔH is large and exothermic, in agreement with the observed DTA results (figure 5.2.1).

The reaction indicated by equation 5.2.1 should be accompanied by the formation of silicon. Whether the silicon formed is in the crystalline or amorphous state is not known. However, the presence of crystalline silicon has not been confirmed from the diffraction patterns since the strongest diffraction lines of silicon (from the 111,220 and 311 planes with "d" spacings of 3.136, 1.92 and 1.64 Å respectively) were difficult to resolve from the slightly broadened $Na_2O.SiO_2$ diffraction lines (from the 111, 220 and 301 planes with "d" spacings of 3.04, 1.89 and 1.65 Å respectively). Another factor to bear in mind is that although the conditions of exposure to sodium were standardised as far as possible (section 3.2), it has not been possible either to control or to monitor the oxygen level in the exposure environment. A parallel reaction that can occur is

$$4Na + O_2 \xrightarrow{\sim 700K} 2Na_2O \qquad \Delta G = -154.0 \text{ kcal}, \ \Delta H = -201.4 \text{ kcal}$$

and then

$$2Na_2O + 2SiO_2 \xrightarrow{\sim 700K} 2Na_2SiO_3 \qquad \Delta G = -110.2 \text{ kcal}, \ \Delta H = -111.6 \text{ kcal}$$

Although the source of oxygen necessary for this reaction path is not particularly clear, oxygen is presumably present in the vacuum at $\sim 10^{-6}$ torr as well as in the sodium metal as an oxide. Therefore the amount of silicon formed, whether in the crystalline or amorphous

state could be less than that indicated by equation 5.2.1.

The X-ray results for the other glasses having been exposed to sodium under the same conditions as those of vitreous silica and α-quartz are presented in table 5.2.1 For NaS(1), NaS(2), NaSAℓ(1) and NaSAℓ(2), all were found to form crystalline $Na_2O.SiO_2$, and the temperatures at which the sodium meta-silicate phase appeared correspond very well with the discolouration behaviour (section 5.1), that is, the higher the temperature at which the crystalline phase emerged, the more resistant is the glass to discolouration. The reaction of these glasses with sodium is very similar to that of vitreous silica and α-quartz. However, the thermochemical tables necessary to illustrate fully the reaction pathway for these glasses were not readily available, apart from NaS(2) [with 30 mole % soda] which is close to the sodium disilicate composition. Therefore using the data for the sodium disilicate liquid and the results found for NaS(2) [table 5.2.1], the reaction with sodium can be written as

$$4Na + 3Na_2Si_2O_5 \xrightarrow{\sim 750K} 5Na_2SiO_3 + Si \qquad \Delta G = -81.2 \text{ kcal}, \quad \Delta H = -122.7 \text{ kcal}$$

and taking into account that oxygen may be present in the exposure environment, a parallel reaction that can occur is

$$Na_2O + Na_2Si_2O_5 \xrightarrow{\sim 750K} 2Na_2SiO_3 \qquad \Delta G = -57.0 \text{ kcal}, \quad \Delta H = -64.9 \text{ kcal}$$

The change in free energy in both cases is negative, so both reactions are favoured. The heat of reaction for the formation of one mole of Na_2SiO_3 in both of these reactions is considerably less than that in equation 5.2.1 (for α-quartz), and in accordance with the observed

	Temperature of Exposure to Sodium (°C)						
	300	350	400	450	500	550	600
Vitreous Silica				← $Na_2O.SiO_2$ →			
Quartz (X-cut)				← $Na_2O.SiO_2$ →			
NaS(1)					← $Na_2O.SiO_2$ →		
NaS(2)					← $Na_2O.SiO_2$ →		
NaB(1)			← $Na_2O.B_2O_3$ →				
NaB(2)			← $Na_2O.B_2O_3$ →				
NaSAℓ(1)					← $Na_2O.SiO_2$ →		
NaSAℓ(2)						← $Na_2O.SiO_2$	
MgSAℓ(8A)	← No crystalline product →						
MgSAℓ(8B)							$2Na_2O.Al_2O_3.2SiO_2$
MgBAℓ(8)					← Unidentified crystalline product		
MgBAℓ(3-2)						← Unidentified crystalline product	
CAℓ(6)	← No crystalline product →						

TABLE 5.2.1

Reaction products (identified using X-ray powder diffraction) of glasses and crystalline material after having been exposed to sodium for 3 hours.

DTA result for NaS(2) [figure 5.2.1] where the magnitude of the exothermic peak was found to be smaller than that for either vitreous silica or α-quartz.

As already hinted in the previous section, the magnesium alumino-silicates reacted with sodium in a different manner to the other silicates. The diffraction patterns of MgSAℓ(8A) did not yield "distinct" lines even after the highest temperature of exposure (600°C). There were signs however that the "halos" were becoming less diffuse and that a crystalline compound would have formed if the exposure temperature was raised further. Table 5.2.1 shows that MgSAℓ(8B) reacted with sodium to form $2Na_2O.Al_2O_3.2SiO_2$ (identified from A.S.T.M. powder data card number 10-31) and judging from the trend of the other silicates, it is possible to speculate that MgSAℓ(8A) would have also reacted with sodium to form $2Na_2O.Al_2O_3.2SiO_2$. The thermochemical data for these more complex glasses were not readily available. Therefore it has not been possible to describe their reaction with sodium any further or indeed make comparisons with the DTA results (section 5.2.1).

For the borates, NaB(1) and NaB(2) reacted with sodium to form sodium meta-borate $Na_2O.B_2O_3$ (identified from A.S.T.M. powder data card number 12-492). These simple borates reacted with sodium in a remarkably similar manner to the simple silicates in that NaB(1) and NaB(2) formed crystalline sodium meta-borate and NaS(1) and NaS(1) formed crystalline sodium meta-silicate. Taking NaB(2) as an example, since it is equivalent to the sodium hexaborate composition ($Na_2O.3B_2O_3$) for which thermochemical data is available (for the crystal only, but values for the liquid are expected to deviate by

by a few kcal only, judging from other sodium borate crystals and their equivalent liquids), the reaction with sodium can be written as

$$6Na + 2Na_2B_6O_{10} \xrightarrow{\sim 700K} 5Na_2B_2O_4 + 2B \qquad \Delta G = -143.0 \text{ kcal}, \quad \Delta H = -154.8 \text{ kcal}$$

and the parallel reaction that would have also occurred if oxygen was present can be written as

$$2Na_2O + Na_2B_6O_{10} \xrightarrow{\sim 700K} 3Na_2B_2O_4 \qquad \Delta G = -119.2 \text{ kcal}, \quad \Delta H = -110.8 \text{ kcal}$$

As the change in free energies is negative, so both reactions are favoured.

In the case of MgBAℓ(8), it is the borate analogue of MgSAℓ(8A), the crystalline compound formed after reacting with sodium is therefore likely to be $2Na_2O.Al_2O_3.2B_2O_3$ (the borate analogue of $2Na_2O.Al_2O_3.2SiO_2$). However searches through the current powder data files failed to give any information on this particular phase. MgBAℓ (3-2) reacted with sodium to form an indentical compound to that of MgBAℓ(8); and for CAℓ(6), the diffraction patterns did not show any distinct lines at all nor were there any signs that the "halos" were becoming less diffuse.

5.3 Surface Sensitive Studies

5.3.1 Electron Spectroscopy for Chemical Analysis (ESCA)

It was apparent from the literature survey (section 1.3) that many of the proposed possibilities concerning the nature of the discolouration of glasses by sodium are of a speculative nature.

The present work, necessarily restricted to the study of one of the simplest glass formers namely vitreous silica, was aimed at furnishing more information about changes in the chemical state of the glass after having been attacked by sodium. The experiment itself was mainly concerned with measuring the Auger parameter α^* or the modified Auger parameter α^{**} (see section 3.5.2) of the different elements in the glass, and a qualitative approach was adopted in the interpretation of the results which involved comparing the measured Auger parameters and those available in the current literature on well defined compounds.

Figure 5.3.1 shows the binding energy spectra of a sample of vitreous silica having been exposed to sodium at 280°C for 3 hours. Spectrum A was obtained on the "original surface", that is, apart from the exposure to sodium vapour (described in section 3.2), no further surface treatments were given. As can be seen, the sodium peaks [(KLL) Auger and (1S)] appeared very prominently whereas the oxygen peaks [(KLL) Auger and (1S)] are relatively weak as compared to spectrum B. It is interesting to note also the total absence of any silicon peaks and the appearance of two much smaller peaks attributed to C(IS) and Au(4f).

These observations can be explained bearing in mind that despite the precautions taken to prevent sodium vapour from condensing on the specimens at the end of an exposure, it is quite conceivable that some sodium vapour could still be deposited on the surface of the glass during cooling. Since sodium is very reactive, the high sodium concentration at the surface of the specimens would lead them to become extremely susceptible to contaminations. As it has not been

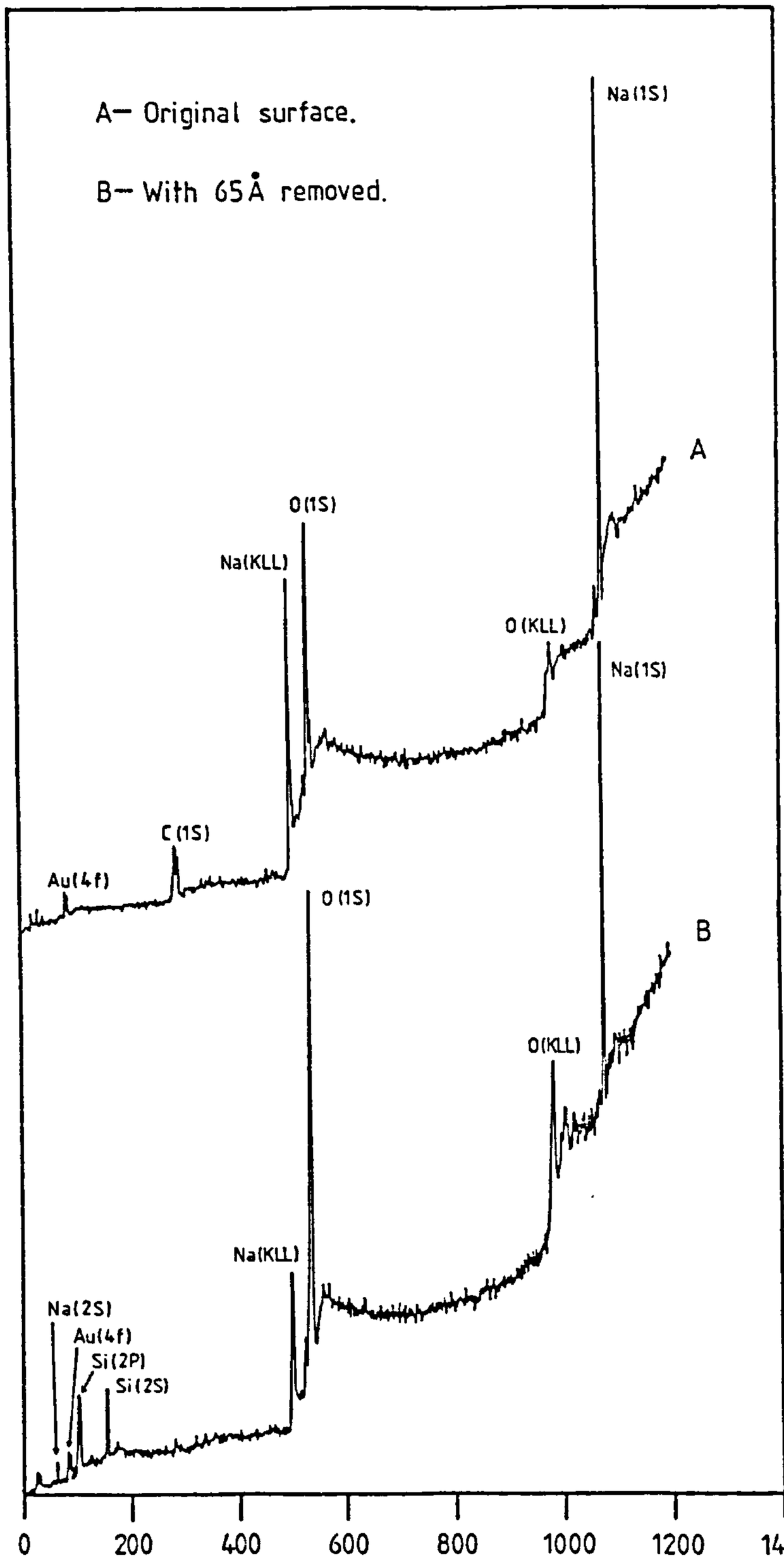

FIGURE 5.3.1

X-ray induced photoelectron spectra (in the binding energy scale) of vitreous silica having been exposed to sodium at 280°C for 3 hours. Spectrum A was obtained after the specimen was exposed to sodium vapour only, and spectrum B was obtained after ~ 65Å of the surface of the specimen was removed by argon ion bombardment.

possible to avoid completely the sodium exposed samples coming in contact with the atmosphere during the loading of the specimens into the ESCA spectrometer, the likely contaminants are water vapour, oxygen, carbon dioxide and carbon deposits from the pumping medium of the vacuum system. The contamination of the specimens would explain the observed features in spectrum A.

Therefore, to ensure that the surface of the specimens were "clean" such that a more representative analysis can be carried out, the specimens were etched with argon ions (in the preparation chamber of the spectrometer which was maintained at $\sim 10^{-6}$ torr) in ~ 30Å steps. The criterion used to determine whether the surface of the specimens was freed from contaminants was by monitoring the size of the C(1S) signal until it fell to a level comparable to the background. Spectrum B of figure 5.3.1 was obtained after ~ 65Å of the surface was removed. The intensity of the sodium peaks has decreased whereas those of oxygens have increased, and whilst the C(1S) peak has disappeared, the expected silicon [(2P) and (2S)] peaks have emerged. The small Au(4f) peak which appeared in both spectra (A and B) was due to the gold plated specimen holder.

The modified Auger parameters (α^{**}) of the different elements of the sodium exposed samples are presented in table 5.3.1. For sodium, α^{**}_{Na} was calculated (using equation 3.5.3) from the separation between the most intense Auger line (KL_2L_3) and the Na(1S) line; and for silicon, α^{**}_{Si} was calculated from the separation between the most intense Auger line (KL_2L_3) and the Si(2P) line. By comparing with the modified Auger parameters of various known sodium and silicon compounds (given in table 5.3.2), two salient features can be deduced from the

Modified Auger Parameter (eV)	Sodium Treatment 280°C 3 hrs	300°C 6 hrs	350°C 3 hrs	400°C 3 hrs
α^{**}_{Na}	2061.4	2061.4	2061.3	2061.3
α^{**}_{Si}	1711.8	1711.8	1711.7	1711.8

TABLE 5.3.1

Modified Auger parameter of samples of vitreous silica having been exposed to sodium. Error in α^{**} = ± 0.2 eV.

Element	Compound	Modified Auger Parameter (eV)
Na	Na	2066.3 (a)
	Na_2O	2062.5 (a)
	NaCℓ	2061.8 (b)
	Na_2SiO_3	2061.3 (d)
	$NaAℓSi_3O_8$	2061.1 (d)
Si	Si	1716.0 (c)
	SiO_2	1711.3 (d)
	Na_2SiO_3	1711.6 (d)
	$ZnSiO_3$	1711.8 (c)
	Zeolite (Na)	1711.8 (b)

TABLE 5.3.2

Modified Auger parameters of various sodium and silicon compounds. Data extracted from (a) Wagner (1977), (b) Wagner, Gale and Raymond (1979), (c) Castle and West (1979) and (d) Castle and West (1980).

results given in table 5.3.1. Firstly, sodium is present in vitreous silica in the ionic state since α^{**}_{Na} for the sodium exposed specimens is close to that of sodium silicate and albite, and definitely very different from metallic sodium. This result then totally discounts the possibility that the discolouration in vitreous silica may be due to sodium metal present in a colloidal form. The fact that sodium is present as an ion implies ionisation has taken place and it is possible that the released electron may take part in the formation of a colour centre. From tables 5.3.1 and 5.3.2, the second important feature to have emerged is that the chemical environment of the silicon atom resembles that of a silicate much more than elemental silicon. This result then also discounts the possibility that the discolouration may be due to the scattering of light by minute particles of silicon.

One further feature observed in this investigation was that the shape of the O(1S) peak was found to change with increasing temperature of exposure to sodium, and the results are shown in figure 5.3.2(a). Owing to the problem of charging associated with insulating specimens (see section 3.5.2), the O(1S) peaks for the different samples have slightly different binding energies (less than 1.5eV variation). Hence for the purpose of illustrating the gradual change in line-shape, the O(1S) peaks shown in figure 5.3.2(a) have been shifted to coincide with that obtained for the specimen which had been exposed to sodium at 400°C for 3 hours. As can be seen from the figure, the O(1S) peak broadened and became less symmetrical on the low binding energy side with increasing temperature of exposure. The shape of the O(1S) peak suggests that it could be composed of two separate line-shapes. To test out this hypothesis, the two line-shapes were assumed to be

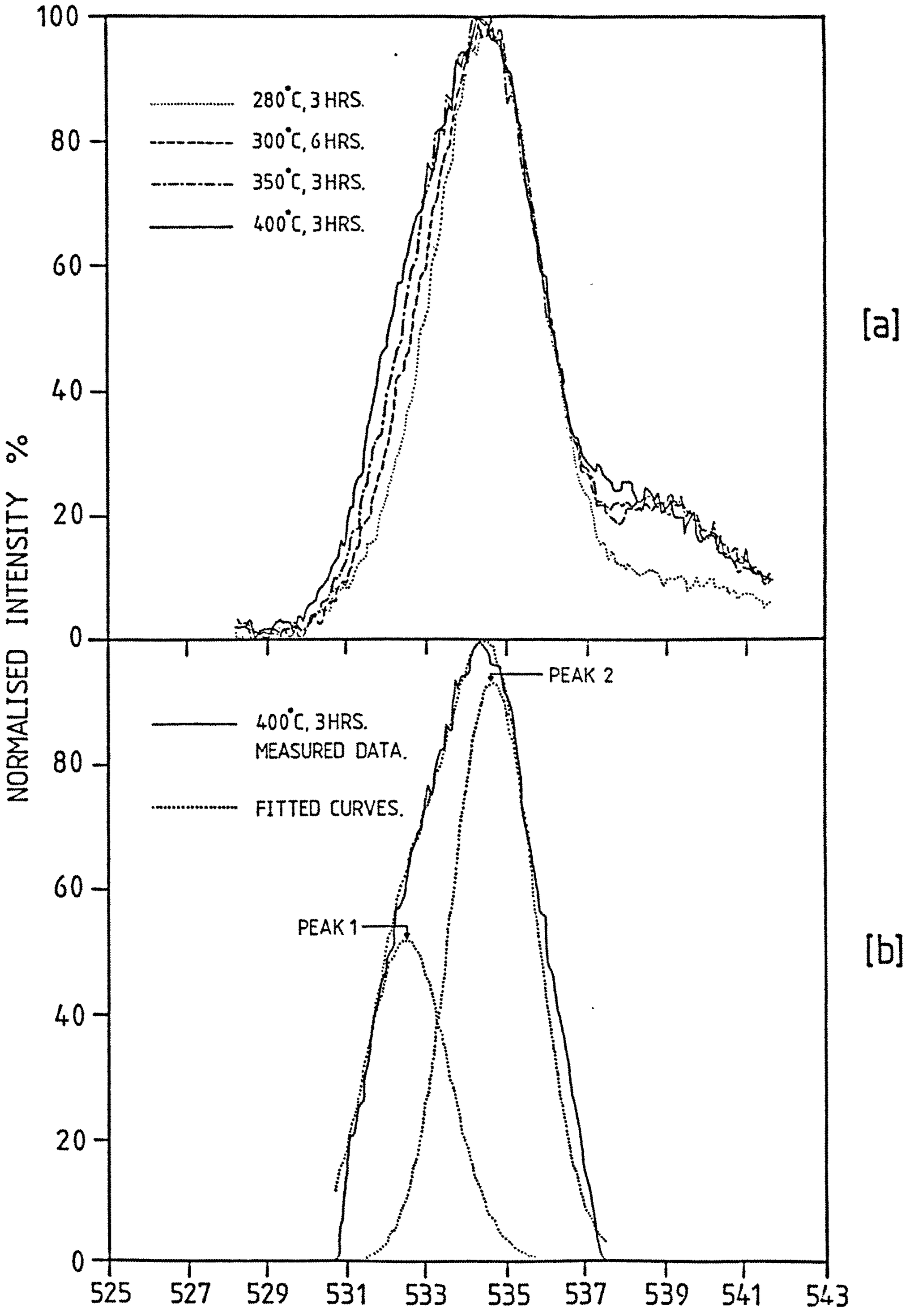

FIGURE 5.3.2

[a] Oxygen (1S) spectra for various sample of vitreous silica having been exposed to sodium.

[b] The fitting of two Gaussians to the O(1S) peak measured for the sample which had been exposed to sodium at 400°C for 3 hours.

Gaussians and they were adjusted to make a best fit to the measured data using a computer program available on the VG 3000 data system.

The results of the curve fitting are presented in table 5.3.3., and an example of one of the better fits to the measured data obtained from the specimen which had been exposed to sodium at 400°C for 3 hours is shown in figure 5.3.2(b). The assumed Gaussian line-shapes, which were labelled as peak(1) and peak(2) corresponding to the low and high binding energy peaks respectively, can be seen to fit the measured data fairly well, and although the results for the other specimens showed larger RMS deviations (see table 5.3.3), the fit was not considered unreasonable. Of course an intrinsic problem with this kind of curve fitting is that the initial assumption that the line-shapes are Gaussians may be incorrect and that the final fit to the data may not be unique. Therefore any conclusions drawn at this stage must be viewed with caution.

With regard to the significance of the two peaks, a clue was found in a paper by Bruckner, Chun and Goretzki (1978) who were investigating the structure of a series of sodium silicates by ESCA (or XPS). These authors have also observed the presence of two O(1S) lines, and the intensity of the line on the low binding energy side was found to increase with increasing soda content. This particular O(1S) line was attributed to oxygens in the non-bridging position (i.e. $Si-O^{-}$), whilst the other line-shape on the high binding energy side was attributed to oxygens in the bridging position (i.e. Si-O-Si). The separation in energy between these two peaks was found to vary from 2.0eV to 2.4eV for the high soda content silicates (33 to 40 wt.%), in good agreement with the results found in the present work (see table 5.3.3). This leads to the belief that two kinds of oxygens are

Sodium Treatment Given to Specimen	Separation in Energy between Peak (1) and Peak (2) (eV)	Relative Height of Peak (1) w.r.t. Peak (2) (%)	R.M.S. Deviation of Fit to Measured Data (%)
280°C, 3 hrs	2.4	27.9	8.15
300°C, 6 hrs	2.2	36.5	9.28
350°C, 3 hrs	2.1	45.2	13.49
400°C, 3 hrs	2.2	55.8	5.01

TABLE 5.3.3

Results of the fitting of two Gaussians labelled as peak (1) and peak (2) to the measured O(1S) line-shape.

being formed as a result of exposure to sodium, with peak (1) [see figure 5.3.2 (b)] corresponding to non-bridging oxygens and peak (2) corresponding to bridging oxygens. From table 5.3.3., the relative intensity of peak(1) increased with respect to peak (2) with increasing temperature of exposure to sodium, that is, more non-bridging oxygens were being formed, or to be more specific, the Si-O-Si bonds were progressively broken to form Si-$\bar{O}$ with increasing temperature of exposure to sodium.

5.3.2 Infra-Red Reflection Spectroscopy (IRRS)

The present work constitutes the second part of the surface sensitive investigation aimed at gaining more insight into the nature of the discolouration. All the glasses (listed in table 2.2.1) and the glass-ceramics (described in Chapter 4) were examined by IRRS (see section 3.5.3) before and after exposure to sodium. The information used to interpret the reflection spectra was drawn from major reviews on the subject [Simon (1960), Condrate (1972) and Wong and Angell (1970, 1976)]. In cases where the spectra were open to interpretation and where there is a general consensus regarding the assignments of the particular vibrational modes, it has been possible to infer some structural alterations in the materials as a result of the sodium treatment.

Figure 5.3.3 shows the reflection spectra obtained for vitreous silica. Spectrum A is for the unexposed specimen, the prominent peaks at $\sim$ 8.9 μm and at $\sim$ 21.0 μm are generally agreed to be due to the asymmetric stretching of the Si-O bond and the "rocking" or bending of the Si-O bond respectively. It appears that little is known about the shoulder at $\sim$ 8.1 μm [Simon (1960)], and the hump

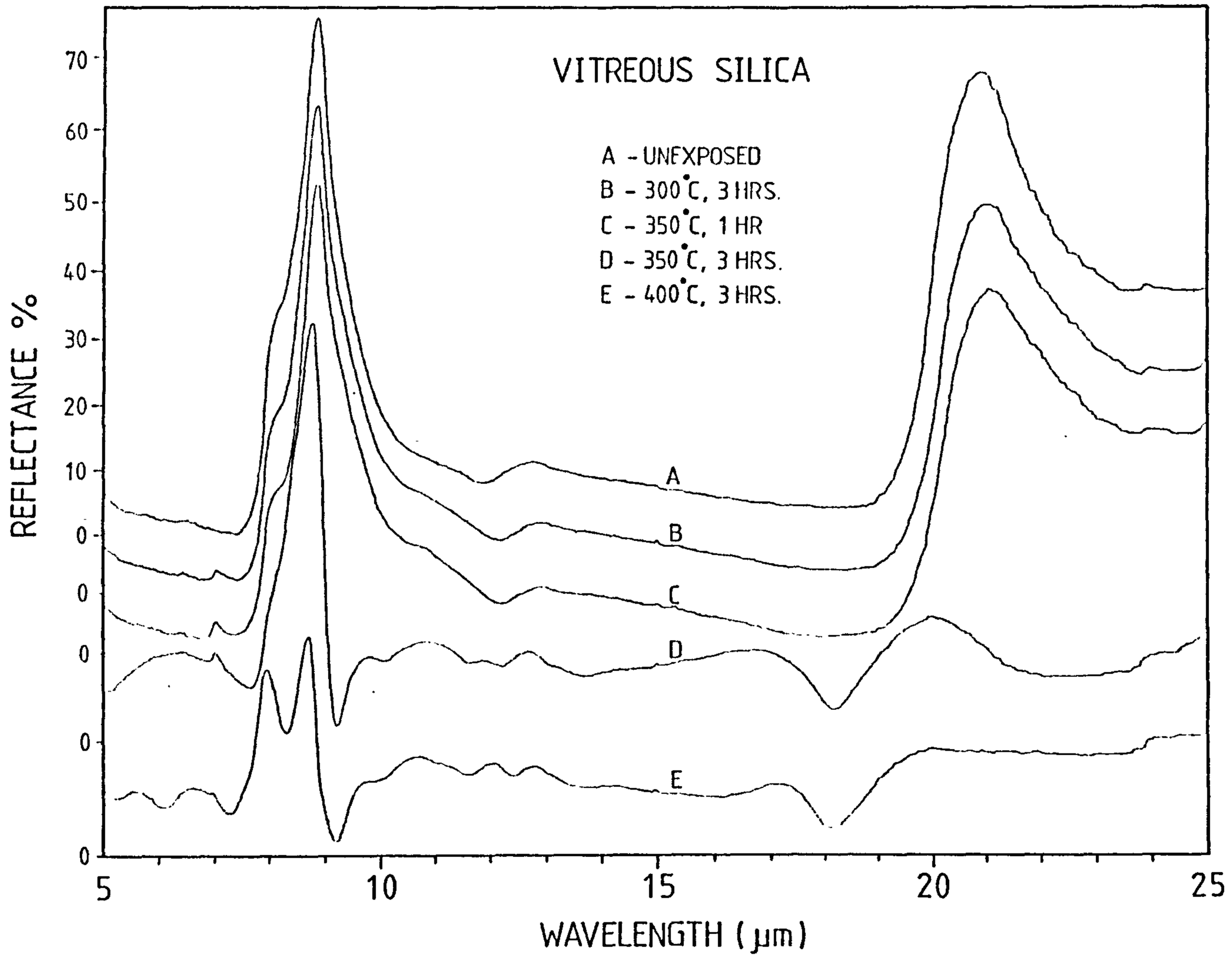

FIGURE 5.3.3

Reflection spectra of vitreous silica after having been exposed to sodium at various temperatures for different times.

between 12.5 to 13.0 μm is thought to originate from the vibration of the SiO_4 tetrahedra in a ring formation [Matossi (1949)]. After the specimens had been exposed to sodium, a new shoulder emerged at ~ 10.9 μm (spectra B and C) which increased in magnitude with increasing temperature of exposure whilst the Si-O stretching and bending modes decreased in intensity. The shoulder at around 10.9 μm is associated with the $Si-\bar{O}$ stretching mode [Jellyman and Procter (1955), Sanders, Person and Hench (1974)], the $\bar{O}$ being a non-bridging oxygen.

This particular finding adds strong support to the previous ESCA result (section 5.3.1) where it was thought two kinds of oxygens (bridging and non-bridging) might have been found. Since the principles behind the two surface sensitive techniques are very different and yet both experiments have yielded similar evidence, the conclusion that Si-O-Si bonds in vitreous silica are broken to form $Si-\bar{O}$ when exposed to sodium can therefore be viewed with confidence.

As the temperature of exposure to sodium is raised to 350°C and beyond, as shown in spectra D and E, drastic changes have occurred and the spectra became difficult to interpret. However, the interference fringes (between 5-7 μm) which can be seen clearly suggest the formation of a thin film which has a very different character to the substrate. The thickness of this film can be estimated using a simple equation of the form [Jenkins and White (1957)]

$$d = \frac{m\lambda}{2n \cos\phi} \qquad (5.3.1)$$

where d is the thickness of the film, m the order of the fringe, λ is the wavelength at minimum, n is the refractive index and cosϕ is the angle of refraction. By choosing n = 1.5 and cosϕ = 1, the thickness of the films were estimated to be $\sim$ 5 μm and $\sim$ 14 μm for spectra D and E respectively.

Figure 5.3.4 shows the reflection spectra of quartz (x-cut). Spectrum A obtained for the unexposed specimen is in good agreement with that found by Sevchenko and Florinskaia (1956), and although the prominent bands appeared sharper than that of vitreous silica (spectrum A of figure 5.3.3) owing to the ordered structure of quartz, the essential features in the spectra are exhibited by both materials. For the sodium exposed specimens, at 450°C (spectrum B), there was a general lowering of intensity by about 5% but there were no other obvious changes in the spectrum. It will be recalled from figure 5.3.1 (a) that quartz subjected to the same exposure conditions was already severely discoloured. The lack of change in the reflection spectrum suggests either that the depth sampled (see section 3.5.3) by this technique is much greater than the thickness of the discoloured layer or that the discoloured layer has essentially the same structure as quartz. This latter possibility is unlikely as can be seen from spectrum C where the specimen had been exposed to sodium at 500°C and where substantial changes in the spectrum have occurred. It has not been possible to interpret the structural information contained in spectrum C, and in the absence of a full theoretical analysis, the interpretation is necessarily restricted to the observation that quartz is more resistant than vitreous silica since severe disruptions of the structure (as indicated by the reflection spectrum) occurred at a higher temperature.

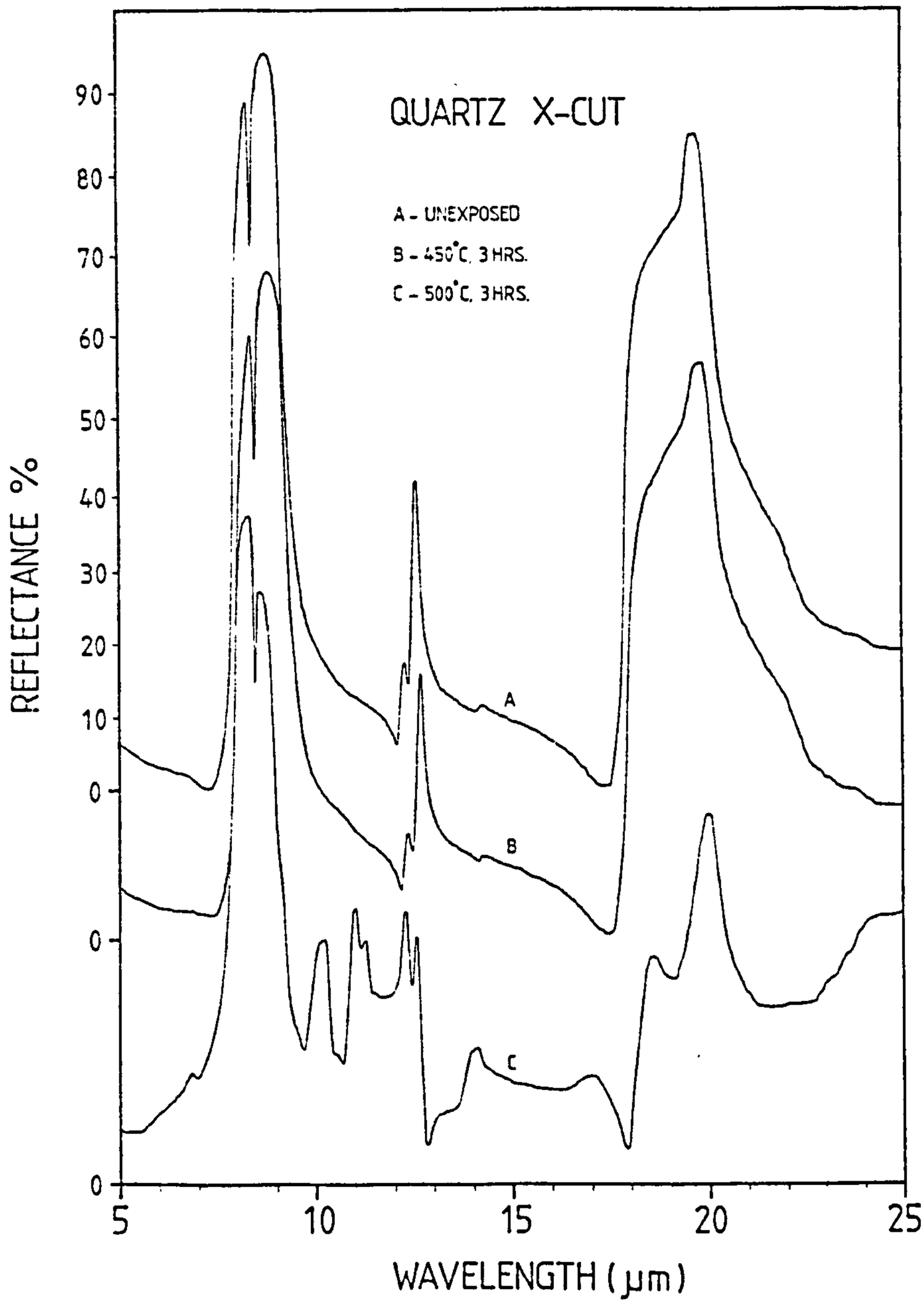

FIGURE 5.3.4

Reflection spectra of quartz (X-cut) after having been exposed to sodium at various temperatures for 3 hours.

Figure 5.3.5(a) shows the reflection spectra obtained for NaS(1). Spectrum A for the unexposed specimen is typical of that for a ~ 20 mole % sodium silicate [Florinskaya and Pechenkina (1963)]; the peak at 9.15 μm is associated with the Si-O stretching mode and the shoulder at ~ 10 μm is associated with the $Si-O^-$ stretching vibration. The broad peak at ~ 20 μm is attributed to the Si-O-Si bending mode. After exposure to sodium at 300°C (spectrum B), the intensity of the Si-O stretching mode has decreased, but the $Si-O^-$ vibration became more prominent and the peak has shifted to a longer wavelength of ~ 10.7 μm. Another feature is that the $Si-O^-$ vibration has broadened as compared with the unexposed specimen, an indication that the sodium exposed surface has become more disordered. At a higher exposure temperature of 350°C (spectrum C), a new band emerged at ~ 8.5 μm whilst the rest of the spectrum showed a remarkable resemblance to that for a 50 mole % sodium silicate glass [Sanders, Person and Hench (1974)]. The origin of the band at 8.5 μm is not known, and as can be seen from spectrum D, it persisted even when the exposure temperature was raised to 400°C. The remaining features in spectrum D have not been reported in the current literature, hence no further interpretation was carried out.

Figure 5.3.5(b) shows the reflection spectra for NaS(2). Bearing in mind that this was one of the more sodium resistant silicates studied (see figure 5.1.2), the pattern of behaviour throughout the entire range of exposure temperatures (300 - 500°C) is similar to NaS(1) at the initial stages of being attacked by sodium [spectrum B of figure 5.3.5(a)]. That is; the intensity of the $Si-O^-$ vibration gradually increased and then broadened whilst the intensity of the Si-O stretching mode decreased. One further feature was the

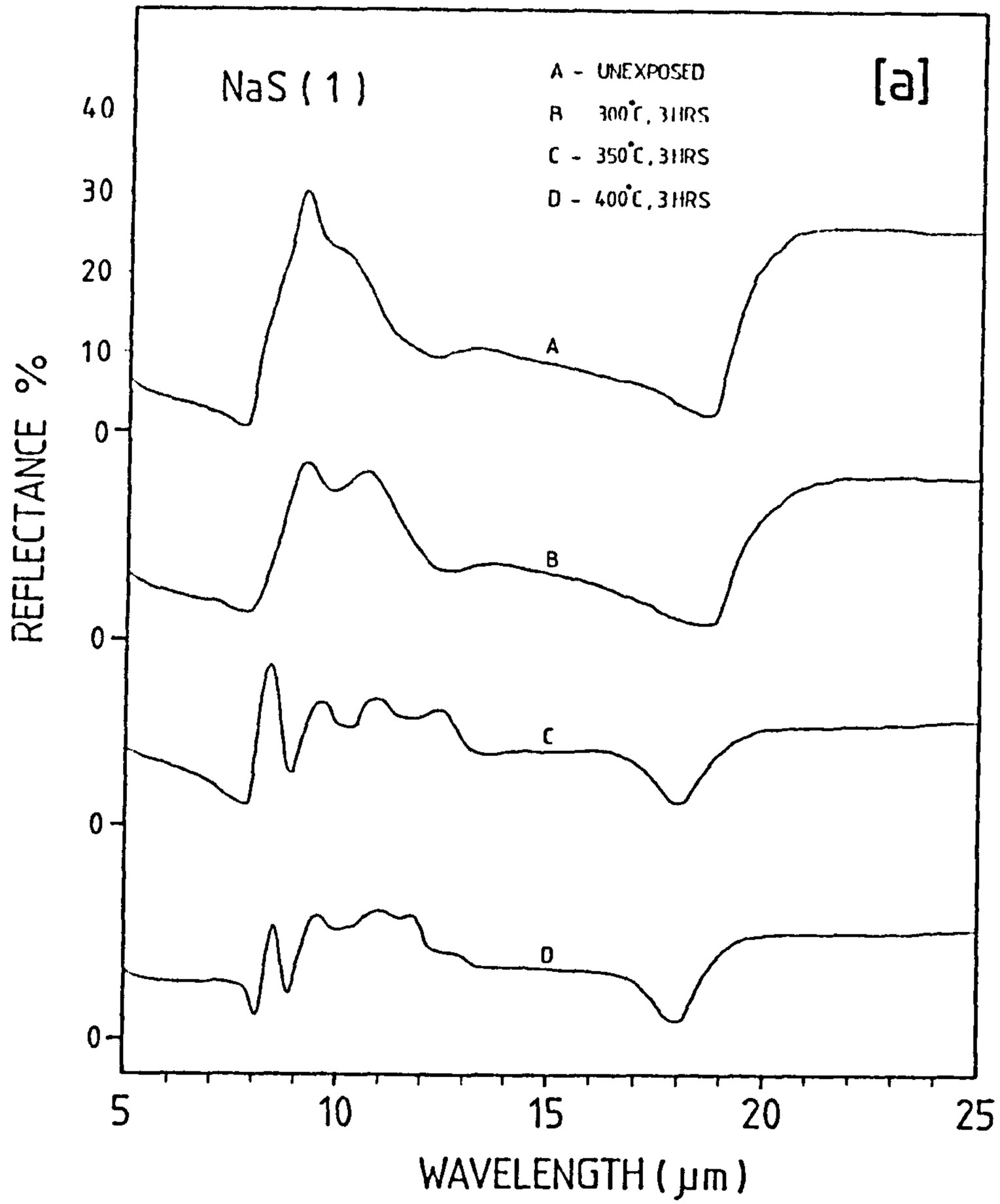

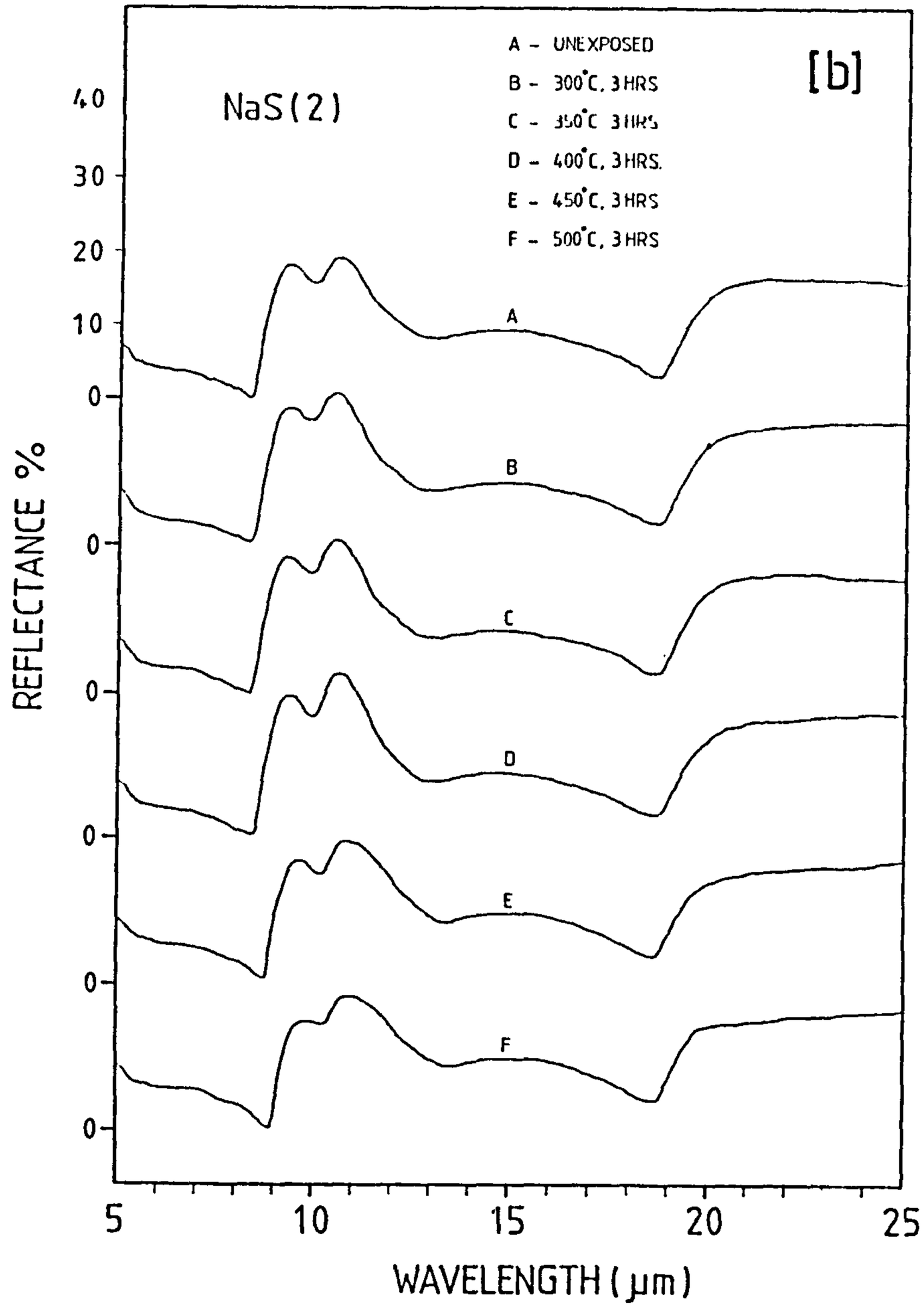

FIGURE 5.3.5

Reflection spectra of [a] NaS(1) (20 mole % soda) and [b] NaS(2) (30 mole % soda) after having been exposed to sodium at various temperatures for 3 hours.

shifting of the Si-O stretching mode to longer wavelengths from ~ 9.3 μm (spectrum A) to 9.8 μm (spectrim F), signifying a decrease in the force constant between the silicon and the oxygen atoms. A similar shift of this kind is also observed in sodium silicates as the soda content increases, and it is due to the interaction of the non-bridging oxygen of the $Si-O^-$ linkage with the sodium ion forming an ionic bond [Hanna and Su (1964)].

For the sodium alumino-silicate glasses, it is generally accepted that if the ratio of alumina to soda is less than 1, then alumina takes part in the glass network in the form of $A\ell O_4$ tetrahedra [Moore and McMillan (1956), Isard (1959)]. The formation of one of these $A\ell O_4$ units requires the donation of "half" an oxygen atom from the modifying oxide whilst the remaining oxygens (supplied by the modifier) are taken up by the glass network as non-bridging oxygens ($Si-O^-$). Therefore the effect of substituting alumina for silica while keeping the soda content constant [as in NaSAℓ(1) and NaSAℓ(2) where 5 and 10 mole % of alumina were substituted for silica respectively] is to reduce the number of non-bridging oxygens being formed in the glass network. This effect is clearly demonstrated in spectra A of figures 5.3.5(b), 5.3.6(a) and 5.3.6(b) where the intensity of the $Si-O^-$ stretching mode at ~ 10.5 μm decreased with increasing alumina content. Also a slight hump between 13.5 and 14.0 μm can be seen in spectrum A of figure 5.3.6(b), this is due to the presence of $A\ell O_4$ tetrahedra [Moore and McMillan (1956), Day and Rindone (1962)]. For the sodium exposed samples, NaSAℓ(1) behaved in a similar way to NaS(2) [see figures 5.3.6(a) and 5.3.5(b)] in that the peak corresponding to the $Si-O^-$ vibration increased in intensity and then broadened with

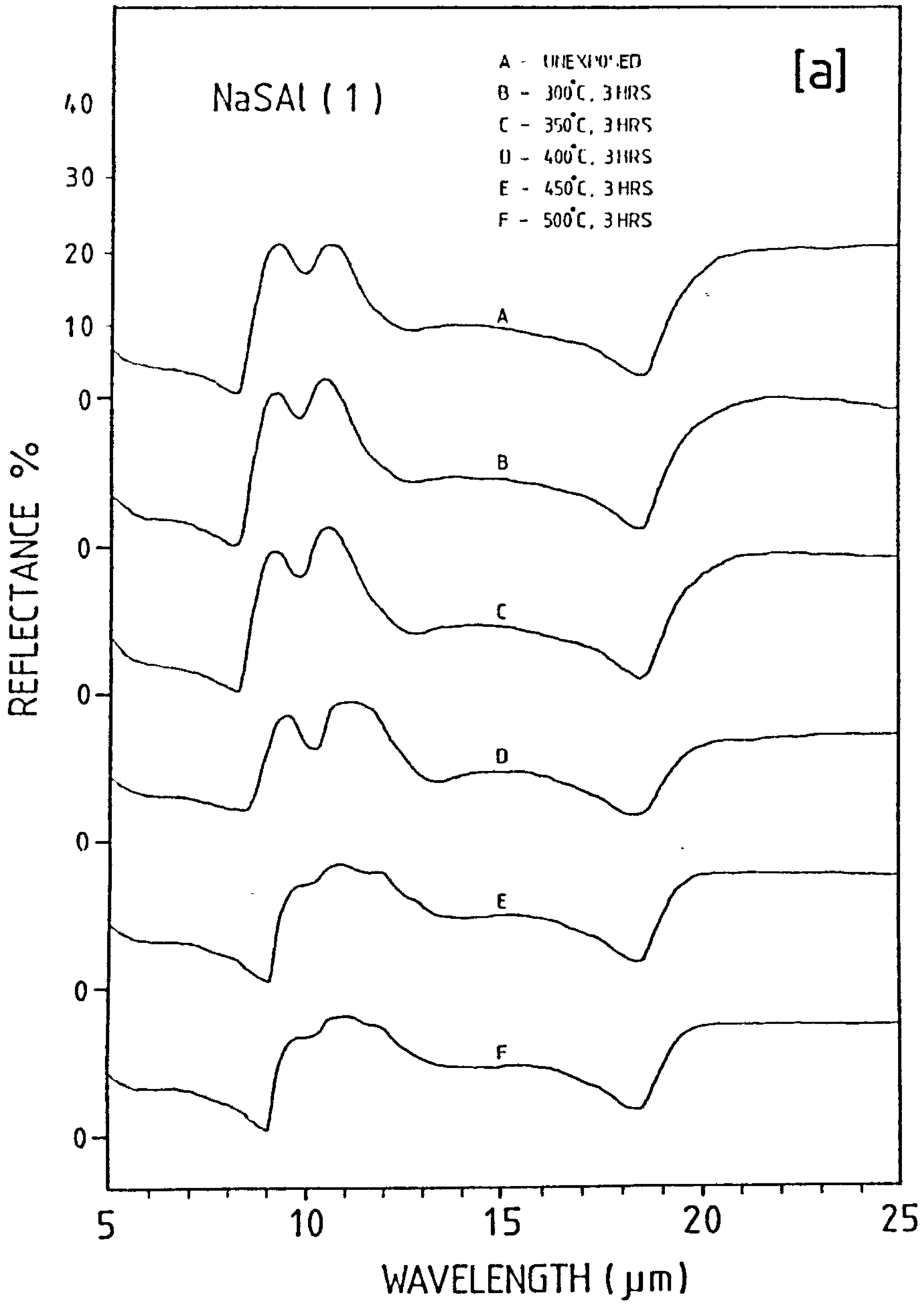

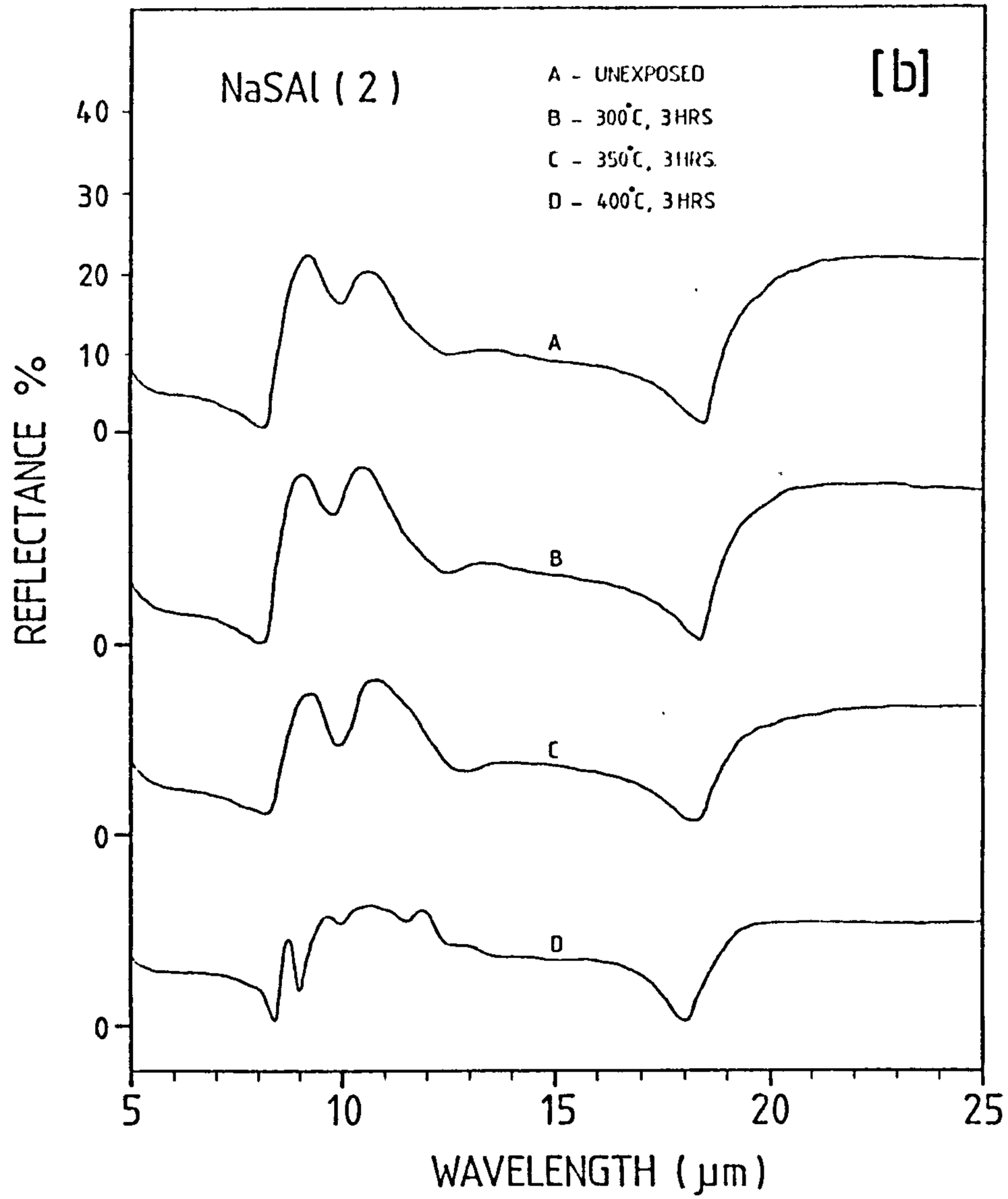

FIGURE 5.3.6

Reflection spectra of [a] NaSAℓ(1) and [b] NaSAℓ(2) after having been exposed to sodium at various temperatures for 3 hours.

increasing exposure temperatures except at the highest temperatures, where the spectra [E and F of figure 5.3.6(a)] resemble that of a 50 mole % sodium silicate glass [Sander, Person and Hench (1974)]. For NaSAℓ(2) [figure 5.3.6(b)], its behaviour with respect to sodium is comparable to that of NaS(1) in as far as the reflection spectra showed rapid changes with increasing exposure temperature, and at 400°C, spectra D of figures 5.3.6(b) and 5.3.5.(a) resemble closely to one another indicating that similar compounds were being formed on the discoloured surfaces of NaSAℓ(2) and NaS(1).

By combining the results of section 5.1 on the characterisation of the discolouration (see figure 5.1.2), the general pattern which has emerged from the present study of these simple silicates is that for the more sodium resistant silicates such as NaS(2) and NaSAℓ(1), the reflection spectra changed slowly with increasing exposure temperature. The change is centred around the $Si-O^-$ peak where its intensity increased slowly and then broadened whilst the Si-O stretching mode decreased in intensity. For the less resistant materials such as vitreous silica, NaS(1) and NaSAℓ(2), rapid changes occurred in the reflection spectra with increasing exposure temperature with the end result that either the spectra became too difficult to interpret or the spectra showed features similar to a 50 mole % sodium silicate glass. The fact that the results of section 5.1 can be used to categorise these IRRS results adds further credibility to the method used to assess "the order of resistance" of the materials towards sodium attack. Furthermore, the exposure temperatures at which the reflection spectra showed drastic changes (as compared to the unexposed specimens) correspond closely to the exposure temperatures where the glasses

showed a high absorption coefficient i.e. severe discolouration (see figure 5.1.2). This correlation suggests that the discolouration phenomenon is intimately linked to the disruption of the glass network observed in the reflection spectra.

For the magnesium alumino-silicates, apart from the paper by Gregory and Veasey (1973) on the crystallisation of cordierite glass, no other infra-red work on this system has been found in the current literature. Therefore interpretation of the reflection spectra was based mainly on experience with the other silicates presented earlier. For MgSAℓ(8A) [figure 5.3.7(a)], spectrum A for the unexposed specimen showed two peaks at ~ 9.3 and ~ 10.9 μm, they are associated with the Si-O and $Si-O^-$ stretching modes respectively. This spectrum showed a rather unusual feature in that the Si-O stretching mode has a lower intensity than the $Si-O^-$ vibration. The structural implication of this result is not clear but the behaviour of the sodium exposed specimens is somewhat different to the relatively sodium resistant silicates such as NaS(2) and NaSAℓ(1). Instead of a gradual increase in the Si-O peak with exposure temperature, the reflection spectra B and C of MgSAℓ(8A) did not show any appreciable change until at 400°C (spectrum D) where the Si-O stretching mode diminished and the $Si-O^-$ vibration broadened and shifted to a shorter wavelength of ~ 10.6 μm. Beyond 400°C, spectra E and F became impossible to interpret, but the presence of interference fringes (between 5 to 9 μm) suggests the formation of a thin film of a very different character to the original glass. Using equation 5.3.1, the thicknesses of the film were estimated to be ~ 10 μm and 40 μm for spectra E and F respectively. For MgSAℓ(8B) [figure 5.3.7(b)], the material was found to behave in

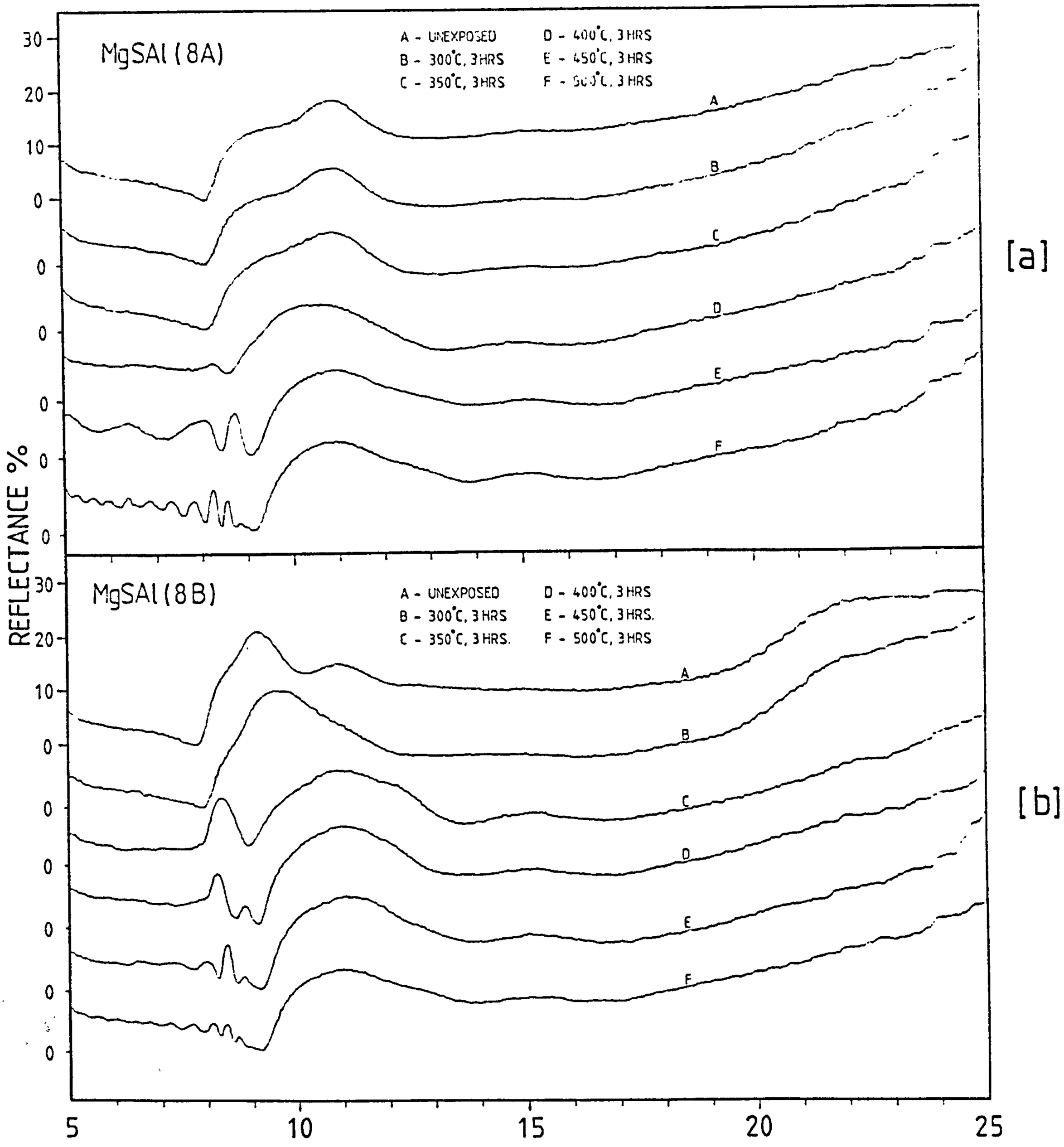

FIGURE 5.3.7

Reflection spectra of [a] MgSAℓ(8A) and [b] MgSAℓ(8B) after having been exposed to sodium at various temperatures for 3 hours.

a similar manner to MgSAℓ(8A) except the disappearance of the Si-O stretching mode occurred at a lower exposure temperature (spectrum C). This implies MgSAℓ(8B) has a lower resistance towards sodium attack, consistent with the characterisation results shown in figure 5.1.2. The reflection spectrum at high exposure temperatures was identical to that found for MgSAℓ(8A) indicating the same kind of compound was being formed at the surface; and from the interference fringes of spectrum F, the thickness of the surface film was estimated (using equation 5.3.1) to be ~ 60 μm.

With regard to the simple borate glasses [NaB(1) and NaB(2)], it was found that the reflection spectra for the sodium exposed specimens were not reproducible. This is probably due to the extreme reactivity of the exposed surfaces which resulted in a high level of contamination under the present routine of examination (see section 3.5.3). Further work on these glasses was therefore abandoned.

For the magnesium alumino-borate glasses (figure 5.3.8) and glass-ceramics (figure 5.3.9), no infra-red studies have yet been reported in the literature, and in the absence of any other structural information on these materials, it would have been imprudent to assign the reflection peaks to particular vibrational modes. This problem of interpretation does pose a serious limitation to the usefulness of IRRS with respect to unveiling any specific structural changes due to the sodium attack. However from the observed changes in the reflection spectra, the technique does enable one to assess the exposure temperature at which disruption of the network occurred. This temperature in turn gives a measure of the resistance of the material towards sodium attack.

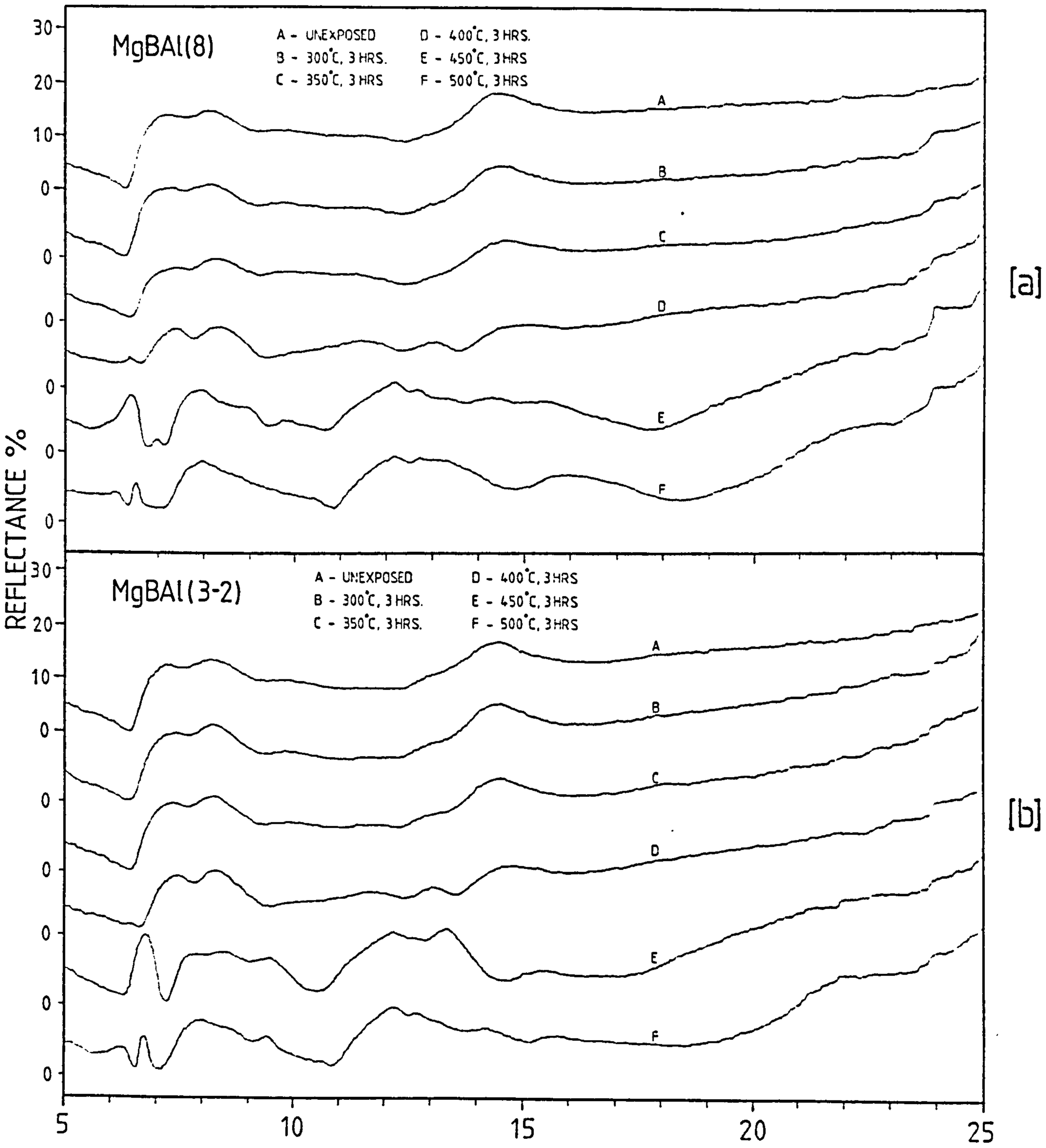

FIGURE 5.3.8

Reflection spectra of [a] MgBAℓ(8) and [b] MgBAℓ(3-2) after having been exposed to sodium at various temperatures for 3 hours.

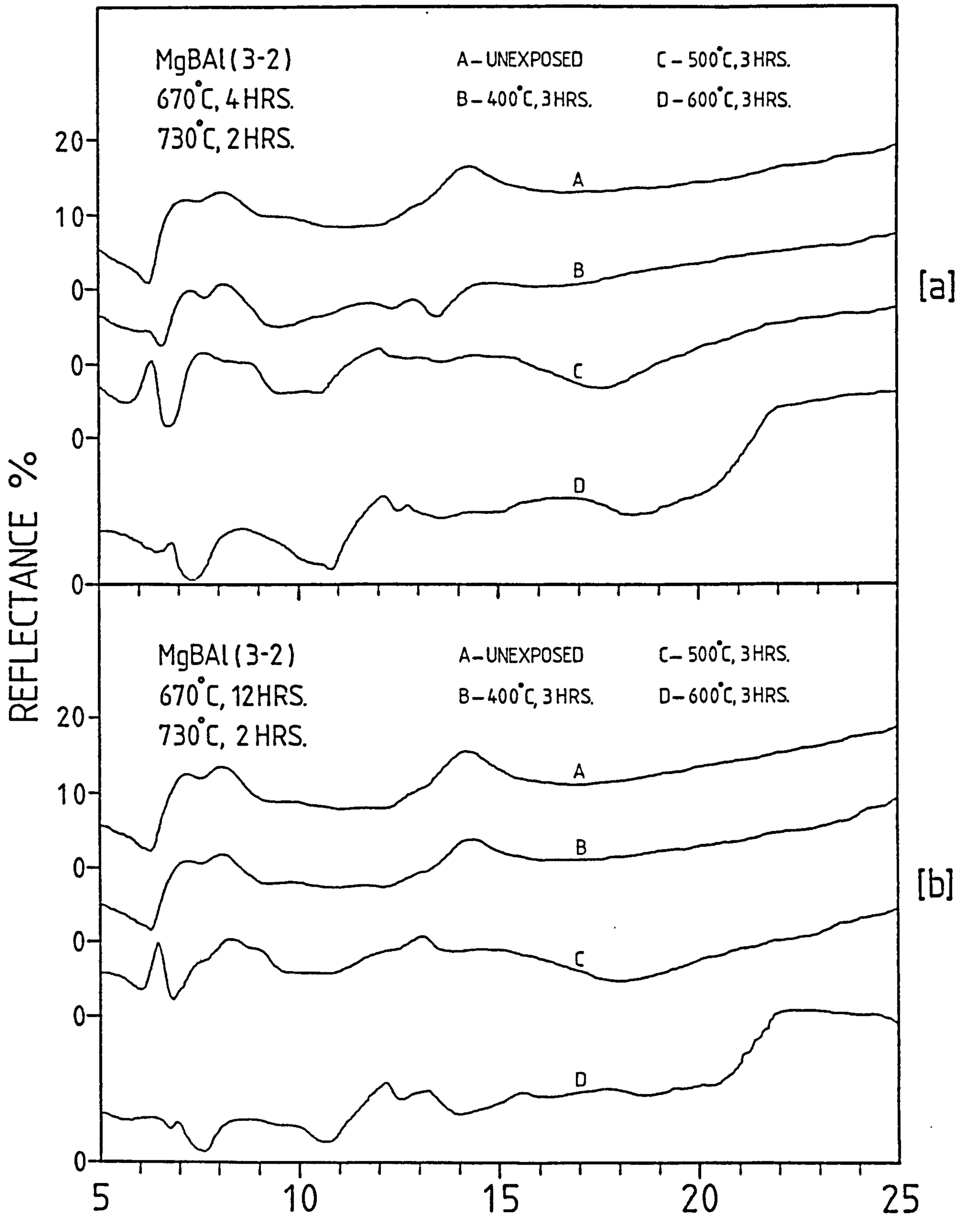

FIGURE 5.3.9

Reflection spectra of glass-ceramics of MgBAℓ(3-2) [a] nucleated at 670°C for 4 hours, [b] nucleated at 670°C for 12 hours and then heat treated at 730°C for 2 hours. All the samples were exposed to sodium at various temperatures for 3 hours.

Figure 5.3.8(a) shows the reflection spectra obtained for MgBAℓ(8). At 350°C (spectrum C), a lowering of intensity at the 7.3 μm and 8.3 μm peaks can be seen, and at 400°C (spectrum D), new bands at ~ 11.6 μm and 13.1 μm were beginning to emerge. For MgBAℓ (3-2) [figure 5.3.8(b)], no appreciable change was observed at 350°C (spectrum C), but new bands similar to those of MgBAℓ(8) can be seen at 400°C (spectrum D). These observations alone suggest that MgBAℓ (3-2) is marginally more resistant than MgBAℓ(8); in accordance with the results of section 5.1 (see figure 5.1.3). For the glass-ceramics of MgBAℓ (3-2) which had been nucleated at 670°C for 4 hours [figure 5.3.9(a)], changes in the reflection spectra can be seen at 400°C (spectrum B), whereas the glass-ceramic which had been nucleated at 670°C for 12 hours [figure 5.3.9(b)] showed little or no change at all at 400°C (spectrum B). Thus the material which had been nucleated for a longer time and hence a higher volume fraction of crystal phase (see table 4.2.1) is more resistant to sodium; in agreement with the optical results shown in figure 5.1.4.

For the calcium magnesium aluminate glass the glass-ceramics studied, the problem of interpreting the reflection spectra also applies, therefore no assignment of any kind was attempted. From figure 5.3.10(a) for the glassy specimens, apart from perhaps a slight change in shape on the low wavelength side of the 12.4 μm peak at 600°C (spectrum D), no substantial changes occurred in the reflection spectra throughout the entire range of exposure temperatures (300 - 600°C). The reflection spectra for the glass-ceramics of CAℓ(6) [figure 5.3.10(b)] differ significantly from that of the glass owing to the crystallisation of the 12 $CaO.7Al_2O_3$ phase (see section 4.2.1 and 4.2.3) at the surface. For the sodium exposed

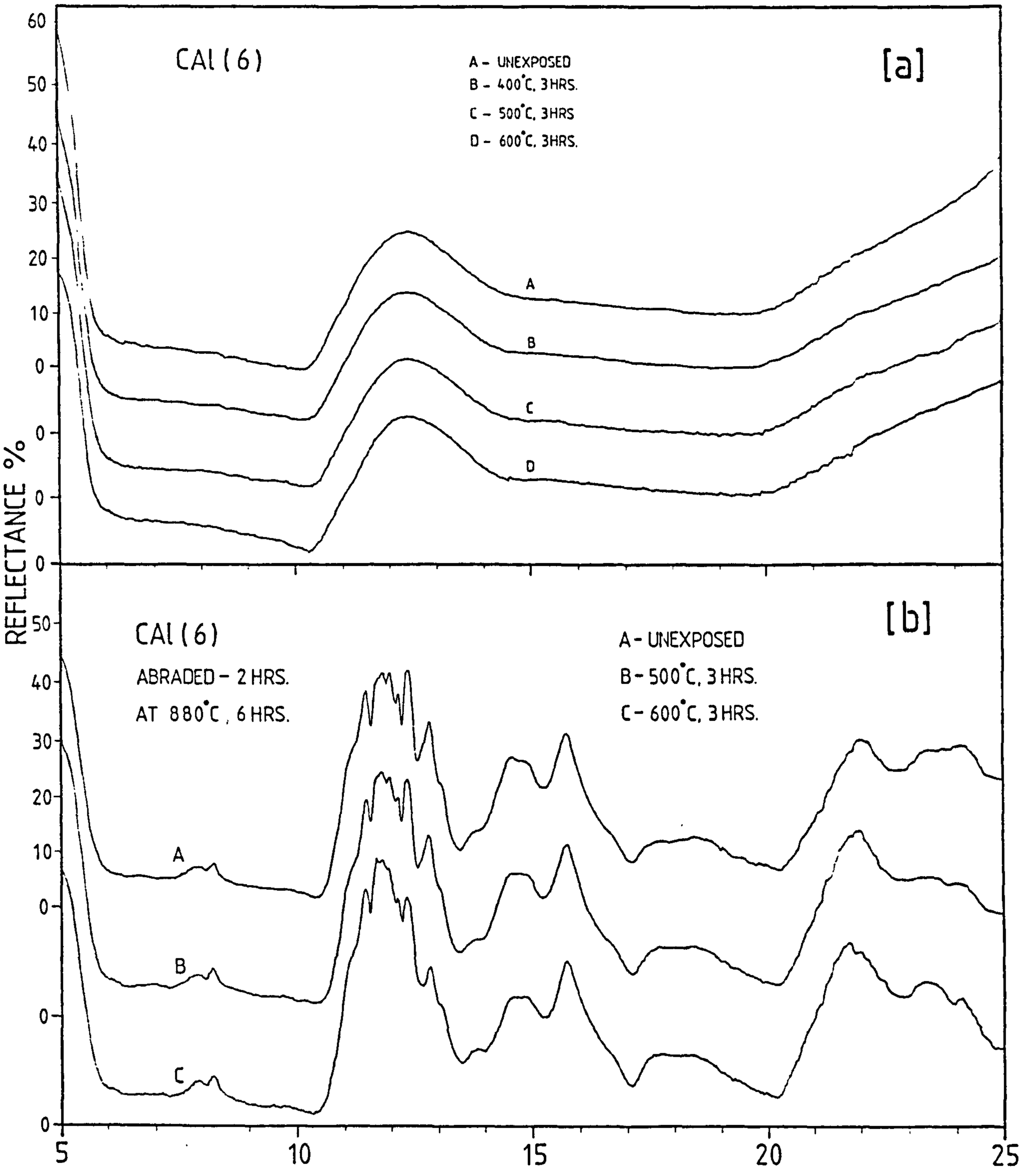

FIGURE 5.3.10

Reflection spectra of [a] CAℓ(6) and [b] glass-ceramics of CAℓ(6) having been abraded for 2 hours and then heat treated at 880°C for 6 hours. All the samples were exposed to sodium at various temperatures for 3 hours.

samples, no change whatsoever was observed in the reflection spectra, indicating an even higher resistance to sodium than found for the glass.

5.4 Electron Spin Resonance (ESR)

The present work constitutes the final part of a programme of investigation into the nature of the discolouration. The experiment was aimed at studying the possibility of colour centre formation [as proposed by Stryjak and McMillan (1979), also see section 1.3] in the sodium attacked surfaces. Although ESR is not a surface sensitive tool, the high sensitivity ($\sim 10^{-8}$ to 10^{-9} mole) of the technique does enable the surface to be probed. All the silicate glasses listed in table 2.2.1 were studied, but owing to the limited time available for this work, it has not been possible to undertake a full theoretical analysis of the ESR spectra. Instead, the results are treated qualitatively at present, their implications however will be the subject of discussion in the next chapter. Typical ESR spectra obtained are presented in figures 5.4.1 to 5.4.3 for the various materials studied, and since all the spectra exhibited similar features, they will be discussed collectively.

Apart from vitreous silica, all the glasses showed an asymmetric resonance at $g = 4.3 \pm 0.1$. This is due to the presence of Fe^{3+} ions [Castner, Newell, Holten and Slichter (1960)] present in the glasses as an impurity. All the glasses which had been exposed to sodium showed a symmetric resonance at $g = 2.002 \pm 0.001$, corresponding closely to the free electron value. The presence of this resonance implies paramagnetic centres of the free electron type were being formed as a result of the sodium treatment. The magnitude of the resonance (or peak to peak amplitude in the derivative spectrum) at $g = 2.002$, as can be seen from figures 5.4.1 to 5.4.3, increased with increasing temperature of

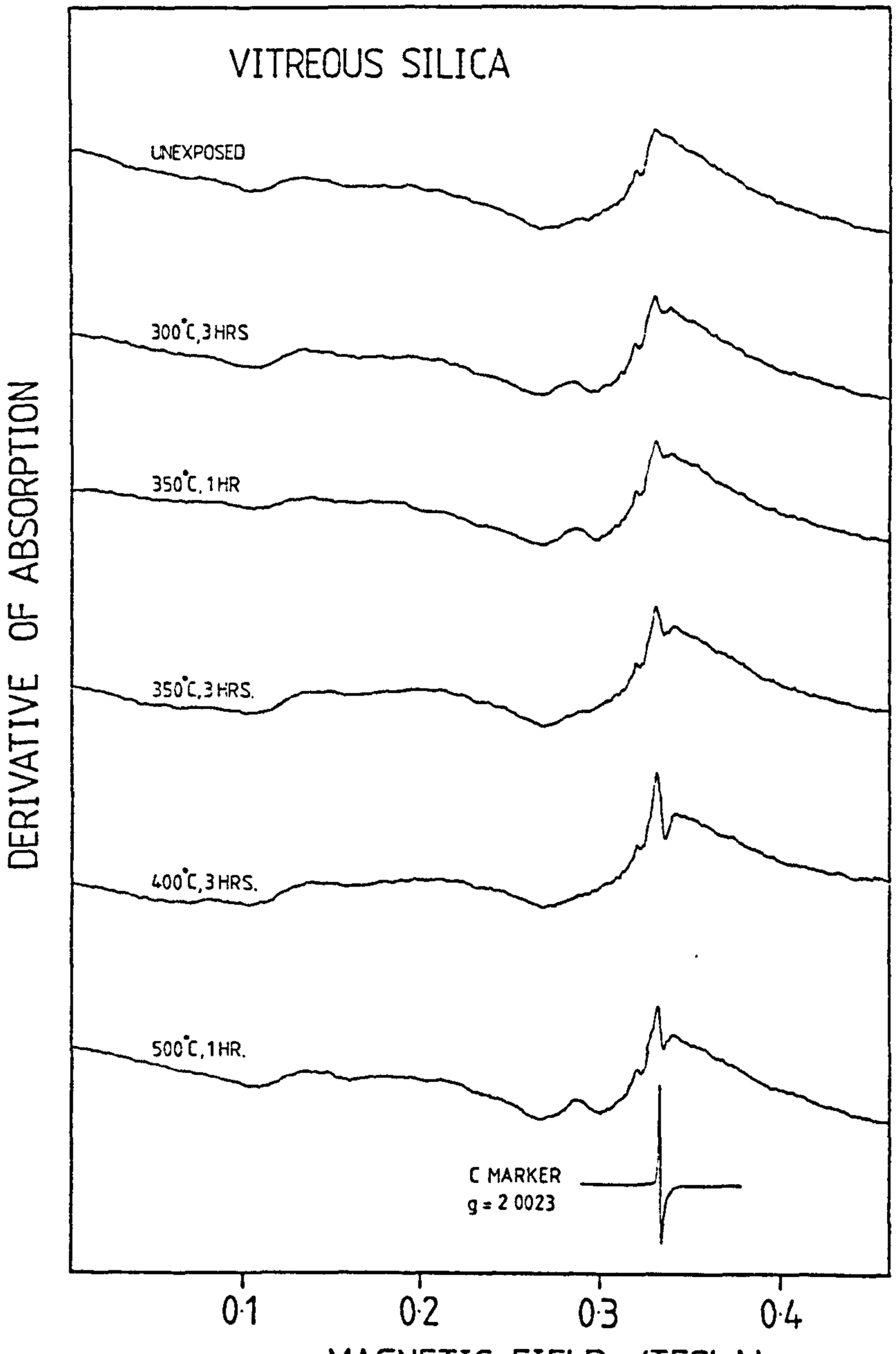

FIGURE 5.4.1

Room temperature ESR spectra of vitreous silica after having been exposed to sodium at various temperatures for different times.

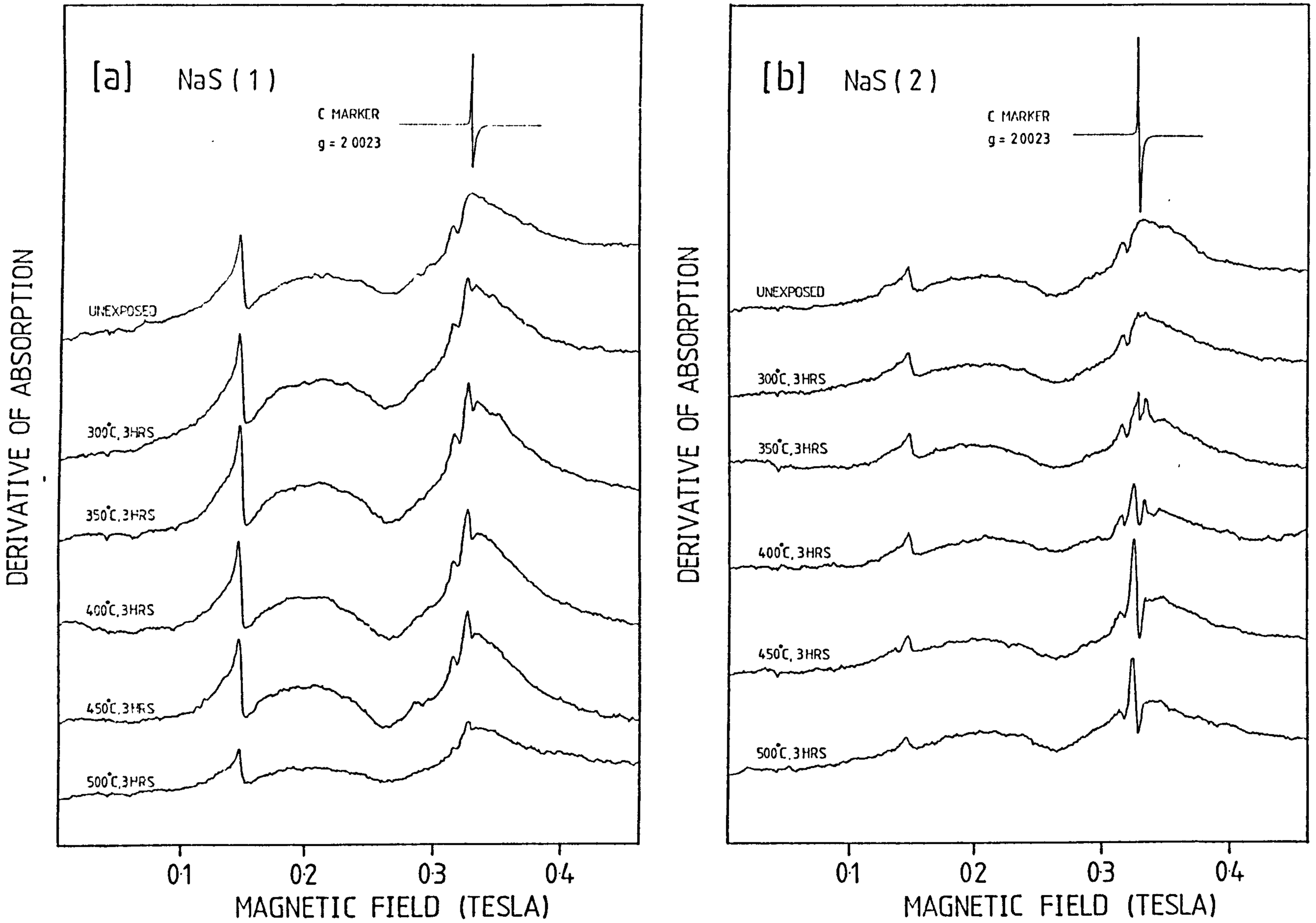

FIGURE 5.4.2

Room temperature ESR spectra of [a] NaS(1) and [b] NaS(2) after having been exposed to sodium at various temperatures for 3 hours.

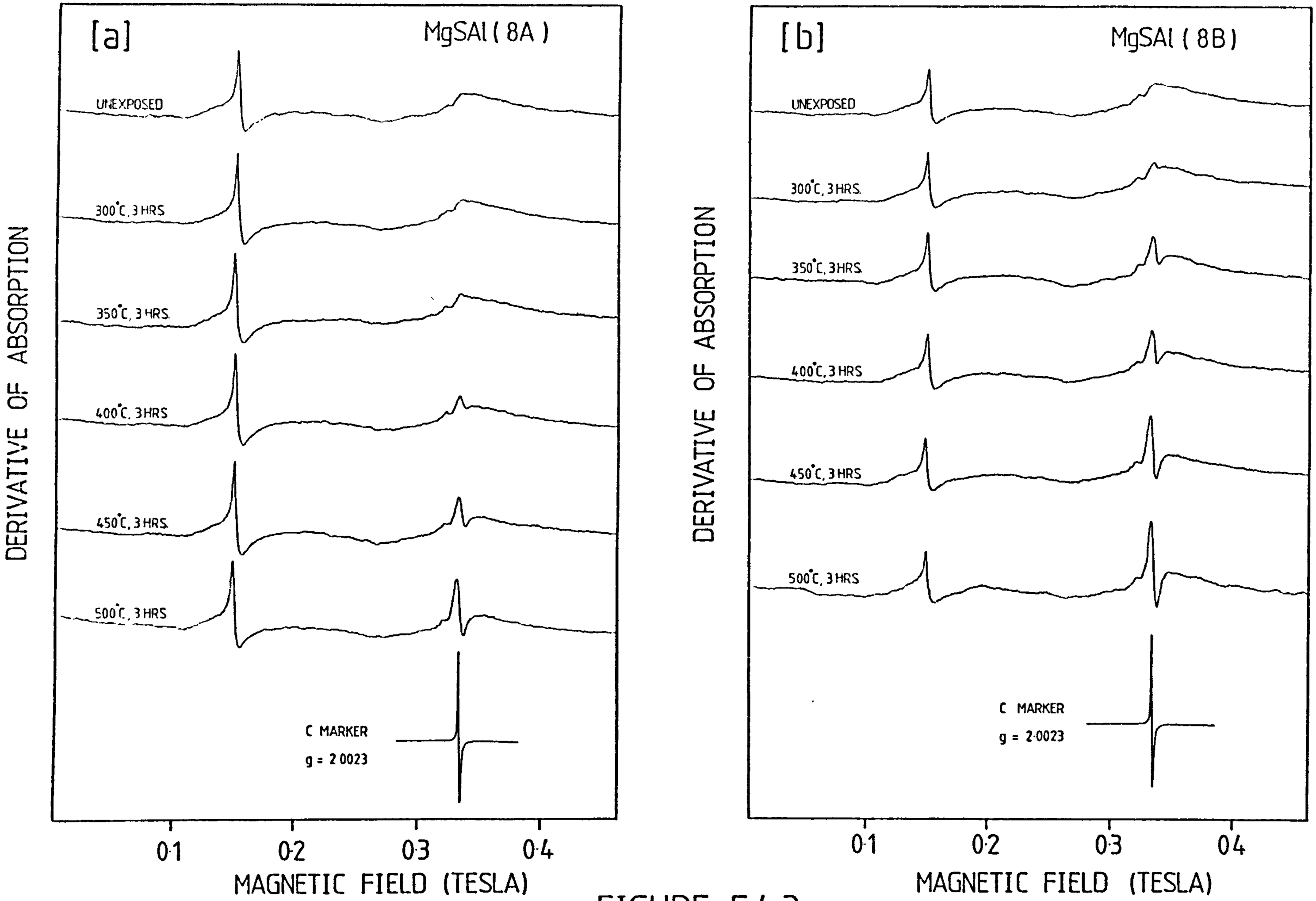

FIGURE 5.4.3

Room temperature ESR spectra of [a] MgSAℓ(8A) and [b] MgSAℓ(8B) after having been exposed to sodium at various temperatures for 3 hours.

exposure. For the less sodium resistant glasses such as vitreous silica, NaS(1) and MgSAℓ(8B), detectable resonance signals emerged at low exposure temperatures (~ 300 to 350°C), whereas for the more resistant glasses such as NaS(2) and MgSAℓ(8A), the g = 2.002 signal emerged at higher exposure temperatures (350°C upwards), in accordance to expectations. Furthermore, at exposure temperatures where large resonances were observed, these temperatures correspond to the condition where severe discolouration has occurred (see section 5.1) or where disruption of the glass network has reached an advanced stage (see section 5.3.2).

Another feature was that the g = 2.002 resonance was found to be quite broad, of the order of 30 to 40 gauss at 9.27 GHz (from peak to peak separation in the derivative spectrum) depending on the exposure temperature. This is much wider (by a factor of ~ 2 to 10) than resonances due to defect centres in glasses which have been irradiated with ionising radiation [Wong and Angell (1976)]. The fact that the spectra were measured at room temperature would contribute to the broadening, but other plausible explanations are that the sodium attacked surfaces have a distribution of defect sites such that the "free" electron can be coupled to the lattice in varying degrees. This will lead to a spread in the g values and hence a broadened absorption line. Another explanation could be that the colour centres are present in such high concentrations in the sodium attacked surface that there is a strong coupling between spins. In such situations where there is a strong spin-spin interaction, broadening of the absorption line will also occur [Orton (1968)]. This latter explanation could also account for the decrease in magnitude in the peak to peak amplitude (in the derivative spectrum) observed in some

of the glasses [such as vitreous silica and NaS(l)] at high exposure temperatures between 450 to 500°C.

CHAPTER 6: Discussion

6.1 Introduction

The present chapter is devoted to discussing the interaction of sodium with glasses and glass-ceramics from both atomic and macroscopic standpoints using the findings described in the previous chapters. The first section will be involved with examining the experimental evidence to support the model proposed by Stryjak and McMillan (1979) on the origin of the discolouration as well as the implications of this model. After dealing with the details of the discolouration phenomenon, the technologically important questions such as whether a glass or a glass-ceramic will be attacked by sodium and what are the criteria for selecting suitable materials will also merit particular consideration. The second section attempts to answer these questions from a thermodynamic viewpoint and brief mention will also be made concerning the kinetic factors. Finally, the last section is devoted to a critical assessment of the utility of the materials developed during this work.

6.2 Discolouration by Sodium

The model proposed by Stryjak and McMillan (1979) is central to the present discussion and it is therefore worthwhile recapitulating the salient features of this model. When a silicate glass is exposed to sodium, the authors suggested that sodium atoms diffuse or penetrate into the glass network causing the breakage of Si-O bonds, thus giving rise to the formation of non-bridging oxygens and negative ion vacancies (see figure 6.2.1). The electrons from the sodium atoms would tend to localise around the oxygen vacancies thus forming

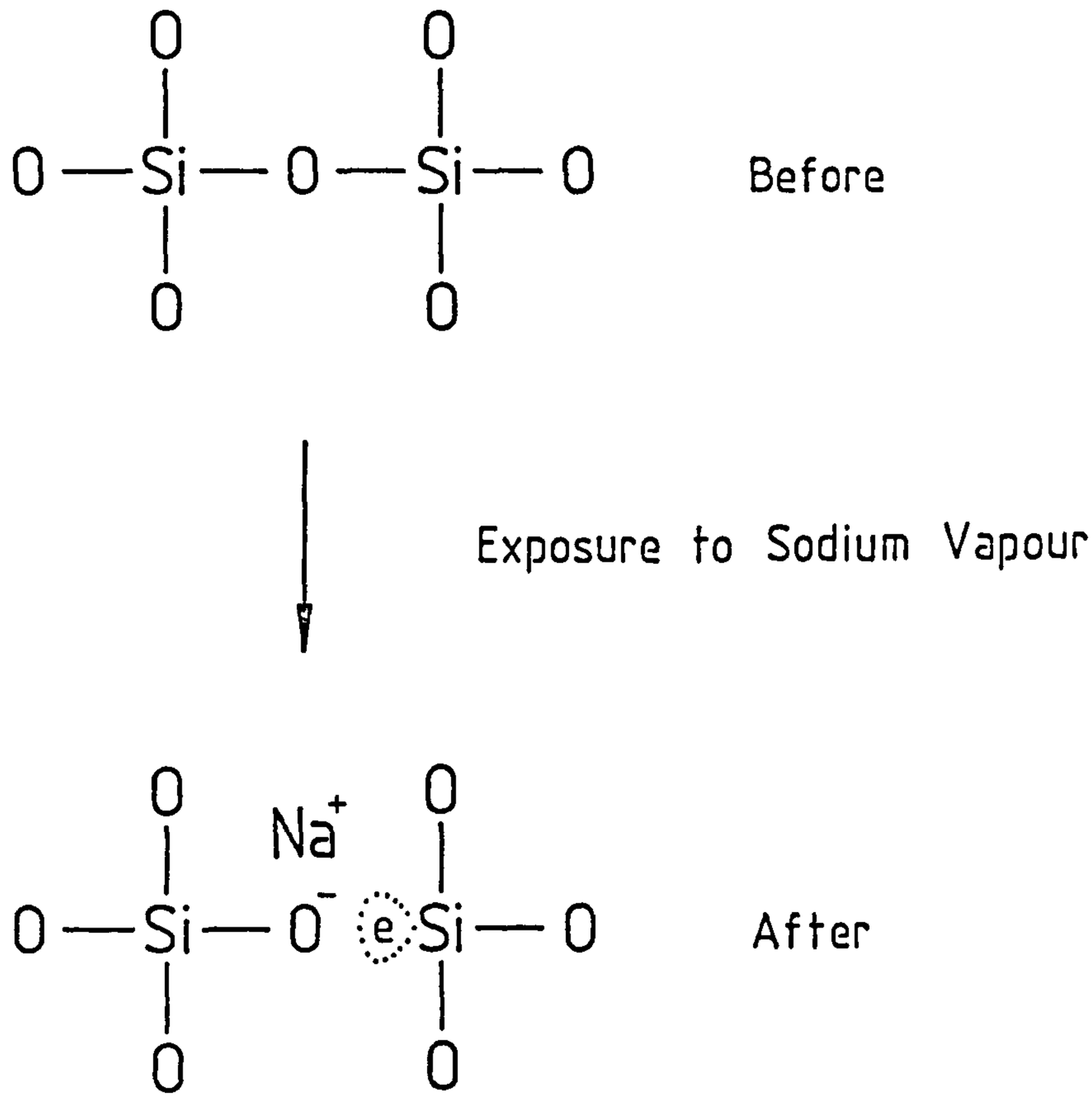

FIGURE 6.2.1

Model of discolouration of a silicate by sodium proposed by Stryjak and McMillan (1979).

defect centres similar to the E'-centre, whilst the remaining sodium ions reside near the non-bridging oxygens to maintain charge neutrality.

From the present study, the experimental evidence pertinent to this model was found to be fairly consistent. Starting from the ESCA results on vitreous silica (section 5.3.1), sodium which has diffused into the surface of the glass was found to be in the ionic state. This implies ionisation has taken place or the electrons liberated are available to form defect centres. From the deconvoluted oxygen (1S) spectra (figure 5.3.2), non-bridging oxygens were thought to be formed and their number was found to increase with increasing exposure temperature (see table 5.3.3). The IRRS results (section 5.3.2) have also suggested the formation of non-bridging oxygens as a consequence of the sodium exposure; in fact this result was found for all the silicate glasses studied. Finally from the ESR investigation (section 5.4), a resonance at $g = 2.0023$ of the free electron type was found for all the silicate glasses, and the intensity of this resonance increased with increasing exposure temperature.

The formation of non-bridging oxygens and paramagnetic centres with g-value close to the free electron value are consequences predicted by the proposed model, and the results described in the previous chapter have tended to confirm this. Therefore the situation envisaged when sodium is exposed to a silicate glass is as follows. At low exposure temperatures ($\sim 300^{\circ}C$), sodium atoms diffuse into the glass network; the driving force is presumably provided by the concentration gradient which exists between the sodium vapour environment and the glass interface. The sodium atoms which have

diffused into the glass interact with the silicate network in the way suggested by the model. There is as yet no experimental evidence to show whether the sodium atoms become ionised before interacting with the network (by breaking Si-O bonds) or vice versa. However the interaction arises because it is energetically favourable for the sodium atoms and the glass network to assume the configuration suggested by the model (i.e. an overall lowering of the energy of the system), and the exothermic drift observed in DTA (see section 5.2.1) supports this. At prolonged exposures, more sodium atoms would diffuse into the glass to react with the network thus creating more defect centres. This can be seen from figure 5.1.1 where the optical absorption was found to increase with increasing time of exposure. At higher exposure temperatures ($\sim$ 400 - 500°C), more and more Si-O bonds would be broken until a point is reached where the network could acquire sufficient "freedom" for reconstruction, provided the thermodynamic conditions are favourable. This was demonstrated by the X-ray results (section 5.2.2) where all the simple silicates were found to react with sodium to form crystalline sodium meta-silicate at sufficiently high exposure temperatures. At even higher exposure temperatures of around 700-800°C, (this was carried out by heating a small amount of sodium sealed inside an evacuated silica ampoule using a bunsen flame and then analysing the reaction product by X-ray diffraction) there is evidence to show that a further reaction occurred and that the metasilicate was reduced to silicon. This result is in agreement with the findings of Hoffman (1933) and Ihnat (1962).

Therefore the interaction of sodium with a silicate glass is seen as one continuous process of sodium entering the glass and

reacting with the network by breaking Si-O bonds to lower the overall energy of the system. Depending on the thermodynamic conditions such as temperature and pressure, the broken network is able to reconstruct to lower the energy of the system even further. It so happens that for the silicate glasses studied, their interaction with sodium resulted in the formation of sodium metasilicate at intermediate exposure temperatures ($\sim$ 400 - 500°C) and at a sufficiently high exposure temperature, the formation of silicon would presumably result.

Although the experimental results presented offer strong support for the proposed model of the sodium discolouration, it would be imprudent to regard the validity of the model as being irrefutable since there are observations which are as yet unexplained. It will be recalled that the discolouration phenomenon is ascribed to defect centres similar to the E' centres produced by irradiation (with either neutrons or γ-rays). To be more specific, two types of E' centres have been established from irradiation studies [Wong and Angell (1976)], the E'_1 centre where an electron is trapped at an oxygen vacancy, and the E'_2 centre where an electron is trapped at an oxygen vacancy in the near vicinity of a proton or an alkali ion. Both of these centres which are applicable to the proposed model have been found to show distinct absorption bands at 212 nm and 235 nm for the E'_1 and E'_2 centres respectively. For the sodium exposed glasses, no such distinct bands have been observed; although at low exposure temperatures, particularly in the case of vitreous silica (see figure 5.1.1), the optical absorption reached a maximum at $\sim$ 200 - 230 nm. The reason for the discrepancy in the absorption spectra between the sodium exposed glasses and the irradiated glasses is not clear.

The problem however can be approached in another way. If sodium is replaced by soda, the interaction with a silicate glass certainly will not result in any discolouration. The discolouration phenomenon then is really due to the absence of oxygens. So instead of comparing defect centres produced by irradiation, the comparison can be made between defect centres caused by oxygen deficiency. Hickmott (1969, 1971) has studied the ESR and optical properties of oxygen deficient silica glass films deposited by R.F. sputtering. He found that the optical absorption of the films was somewhat variable depending on the depositing conditions. In some cases, the optical absorption of the R.F. sputtered films bore a close resemblance to the irradiated fused silica, and in some cases the sputtered films showed a broad absorption over the entire visible region rather similar to that found for the sodium exposed glasses. It would appear then that different methods of producing the same kind of defects can lead to different absorption spectra.

Other aspects concerning the defect centres caused by sodium exposure such as whether the colour centres can be thermally bleached, or whether they can be suppressed, e.g. by doping the glasses with Ce^{4+} ions, have not been delved into in any serious way owing to the limited time available. This is an obvious area for future work where perhaps a better understanding of the nature of the discolouration can be gained. Despite these unexplored grounds, the present findings (as well as speculations) can be used to explain why some of the simple silicates discolour more easily than others. It will be recalled from the ESCA (section 5.3.1) and IRRS (section 5.3.2) studies that non-bridging oxygens or $Si-O^-$ bonds were being formed as sodium attacked the silicate network. The number of $Si-O^-$ bonds was found

to increase with exposure temperature whilst the number of Si-O bonds decreased, at least up to temperatures around 400 - 500°C depending on the glass. The fact that the number of $Si-O^-$ bonds increased (at the expense of the Si-O bonds) suggests they are more stable in the presence of sodium, otherwise the number of bridging and non-bridging bonds should decrease together as they are attacked by sodium. Hence a glass possessing a greater number of $Si-O^-$ bonds should be less susceptible to attack by sodium; or if R is expressed as the ratio of $Si-O^-$ bonds to Si-O bonds, the resistance to sodium should increase as R increases.

According to the above argument then, R = 0 for vitreous silica and it should be the least resistant to sodium. For the sodium silicates, R increases with soda content and so the resistance should increase correspondingly. For the glass NaS(1) [with 20 mole % soda] R = 0.143, and for the glass NaS(2) [with 30 mole % soda] R = 0.273, therefore NaS(1) should be less resistant than NaS(2). Upon the substitution of "small" amounts of alumina for silica in the sodium silicates, alumina would enter the glass as AlO_4 units, thereby reducing the number of oxygens available for the formation of $Si-O^-$ bonds. The resistance to sodium then should decrease as the alumina content increases. For the glass NaSAl(1) [with 5 mole % Al_2O_3 in NaS(2)] R = 0.238, and for the glass NaSAl(2) [with 10 mole % Al_2O_3 in NaS(2)] R = 0.2. Therefore NaSAl(1) should be more resistant than NaSAl(2), furthermore the resistance of these two alumino-silicate glasses should fall in between those of NaS(1) and NaS(2). As can be seen from figure 5.1.2, all these predictions are in perfect accord with the observed results. For the glass MgSAl(8A) and MgSAl(8B), the role played by magnesia in these glasses is not particularly clear and it has not been possible to

calculate the ratio of non-bridging oxygen bonds to bridging oxygen bonds. However, from figure 5.3.7(a) for the glass MgSAℓ(8A), the intensity of the $Si-O^-$ reflectance peak was found to be higher than that corresponding to the Si-O vibration. This would suggest that the ratio R is greater than 1, and from figure 5.1.2, MgSAℓ(8A) was found to be one of the most resistant silicates studied.

The model proposed by Stryjak and McMillan (1979) was used to describe the origin of the discolouration in silicates; the fact that a similar pattern of behaviour was found for the simple borates raises the question whether this model can be extended to describe the borates. For example, from X-ray studies (section 5.2.2), it was found that the simple borates [NaB(1) and NaB(2)] and silicates [NaS(1) and NaS(2)] reacted with sodium to form sodium metaborate and sodium metasilicate respectively. It is also known [Greenwood (1973)] that the reduction of borax by sodium is a method of producing boron metal; comparable to the reduction of a silicate to silicon by sodium (see above). It appears then that sodium attacks the borates in a similar manner to the silicates. The way in which sodium attacks the borates will be complicated by the fact that boron can be co-ordinated by either three or four oxygens, some of which can be non-bridging oxygens. There is as yet no experimental evidence to suggest whether sodium attacks the B-O bonds in the BO_3 units in preference to the B-O bonds in the BO_4 units or vice versa. However, the fact that sodium metaborate is being formed when exposed to sodium at $\sim$ 400 - 500°C suggests the metaborate structure (a three co-ordinated boron with one non-bridging oxygen as the basic unit and arranged either in a chain formation or as six-membered rings) is stable to sodium at these temperatures. Figure 6.2.2 depicts

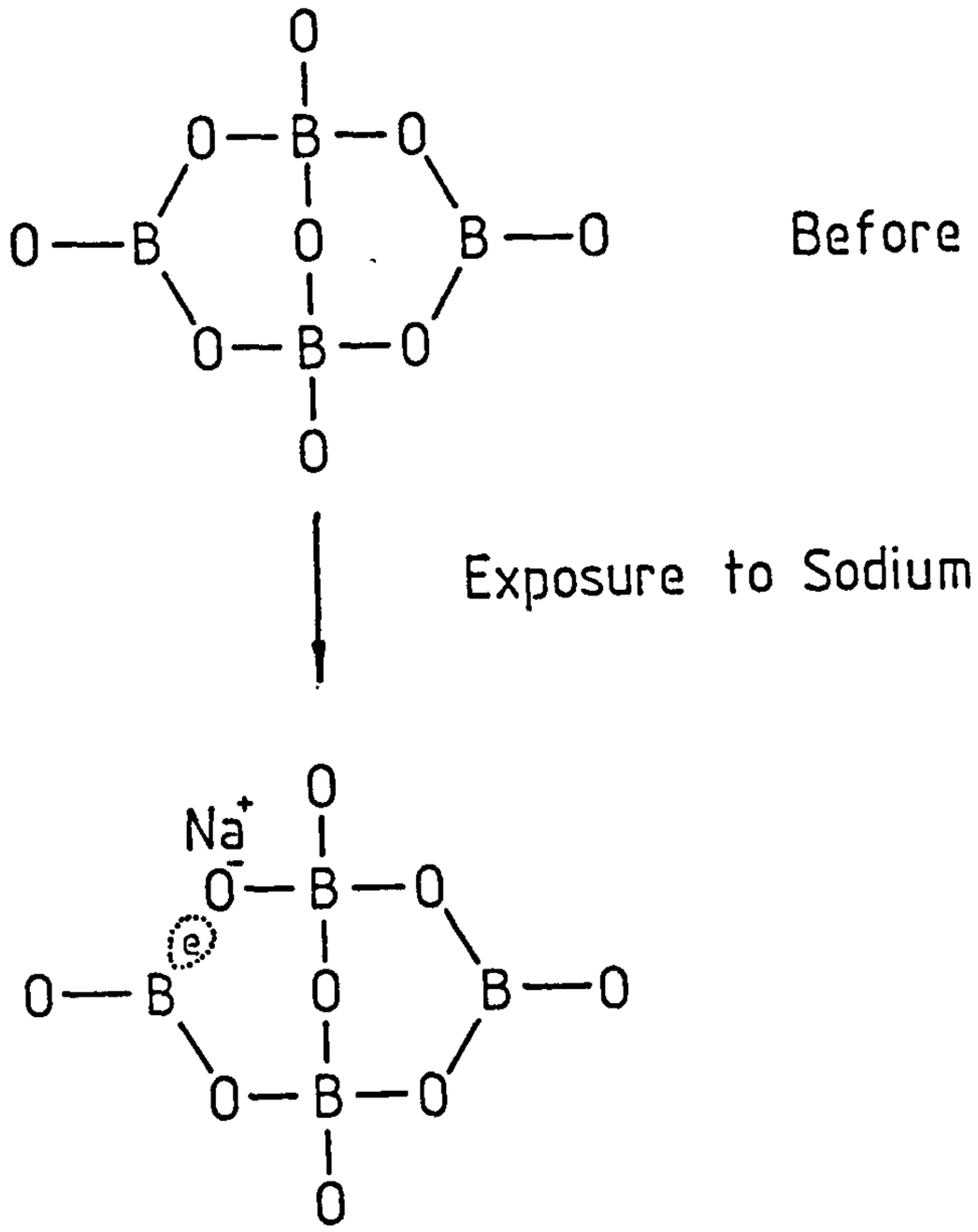

FIGURE 6.2.2

The discolouration of a diborate group by sodium. The different co-ordination of boron atoms in the structure can give rise to a variety of defect sites.

the simplest types of situations envisaged and it shows a diborate ring structure being attacked by sodium. As can be seen, there are a variety of defect sites all of which can give rise to discolouration; but in view of the lack of any experimental evidence, this picture presented remains, at best, speculative.

6.3 Factors which Influence the Resistance to Sodium

The discolouration of glasses by sodium vapour was examined in considerable detail, and some insight has been gained into the way sodium attacks the silicate glasses. This approach however was not sufficiently general to tackle technologically important questions such as whether a glass or a glass-ceramic will be attacked by sodium and what are the necessary criteria for selecting compatible materials for the containment of sodium. In an attempt to answer these questions, two other methods have been pursued, that is, by altering the chemical composition of the glasses and by rearranging the structure of the glasses via crystallisation. These two aspects of improving the resistance to sodium are discussed separately below.

To improve the resistance by changing the chemical composition, the constituents were chosen such that they would be resistant to sodium as well as having the ability to form a glass when fused together. To assess whether the components will be resistant, an equilibrium thermodynamic argument similar to that used by Elyard and Rawson (1962) and Singh (1976) is invoked. The simplest step is to consider a reduction reaction of the type

$$M_mO_x + 2x\,Na \rightarrow mM + x\,Na_2O \qquad (6.3.1)$$

where M_mO_x is the oxide under investigation and Na_2O being the most stable oxide compound of sodium. If the change in Gibbs free energy ΔG for the reaction is negative, then the reaction is favoured and the oxide will not be resistant to sodium.

A fundamental objection to this approach is the application of equilibrium thermodynamics to meta-stable or non-equilibrium systems such as glasses. Strictly speaking, equilibrium thermodynamics cannot be applied legitimately to glasses since the state parameters describing the glass are measured when the system is not in equilibrium, and they will therefore vary depending on the time scale of the measurement. However, if the deviation in the Gibbs free energy between the glassy state and its corresponding crystalline state is small as compared with the change in free energy in a reaction with sodium, then equilibrium thermodynamics is expected to be applicable providing this condition is satisfied. The difference in free energy between the glass and its corresponding crystalline solid can be estimated [Gutzow (1972)]. For most glasses, the deviation at Tg the glass transition temperature is $\sim$ 2/9 H_m, where H_m is the heat of crystallisation, and for most temperatures below Tg, the deviation is $\sim$ 1/4 H_m. Taking silica as an example, $H_m \sim 2$ kcal/mole, the difference in free energy between vitreous silica and quartz is therefore quite small. It is not surprising then to find that vitreous silica and quartz reacted with sodium in a very similar manner (sections 5.2.1 and 5.2.2).

Bearing the condition for the applicability of equilibrium thermodynamics in mind, an argument based on simple redox reactions is not an adequate criterion for selecting suitable components. As pointed out by Anderson (1977), who used "Lucalox" as an example, it is

necessary to consider all the possible chemical pathways since reactions to form mixed oxides may sometimes be much more favourable than the redox reaction. From the present work (see section 5.2.2), it has already been shown that vitreous silica, quartz, the simple silicates and borates do indeed form mixed oxides with sodium. Clearly though, it is not always possible to consider all reaction paths for each constituent of the glass owing to the lack of thermodynamic information, and the problem becomes intractable when dealing with a multi-component glass where one or more components of the glass may combine with sodium. In view of the absence of a more general approach, persistence with the above method of assessing the compatibility of the components can be justified on the grounds that it can be used as a screening test for oxides which are readily reduced by sodium (according to equation 6.3.1). The stability diagram for a few metal oxides has been calculated [data extracted from Weast (1977)] and their reaction with sodium is discussed below.

Figure 6.3.1 shows the stability diagram for some of the "better known" glass forming oxides and the most stable oxygen compound of sodium i.e. Na_2O. As can be seen, the free energy curve for P_2O_5 falls below that of Na_2O, therefore a simple redox reaction is favoured and phosphate glasses have been found to be the least resistant to sodium [Elyard and Rawson (1962)]. As for B_2O_3 and SiO_2, although the free energy curves lie above that of Na_2O indicating that the redox reaction is not favoured, it has already been shown (section 5.2) that they formed mixed oxides ($Na_2O.B_2O_3$ and $Na_2O.SiO_2$) with sodium. A similar situation is found for Al_2O_3 where the redox reaction is not favoured, but instead alumina combines with sodium

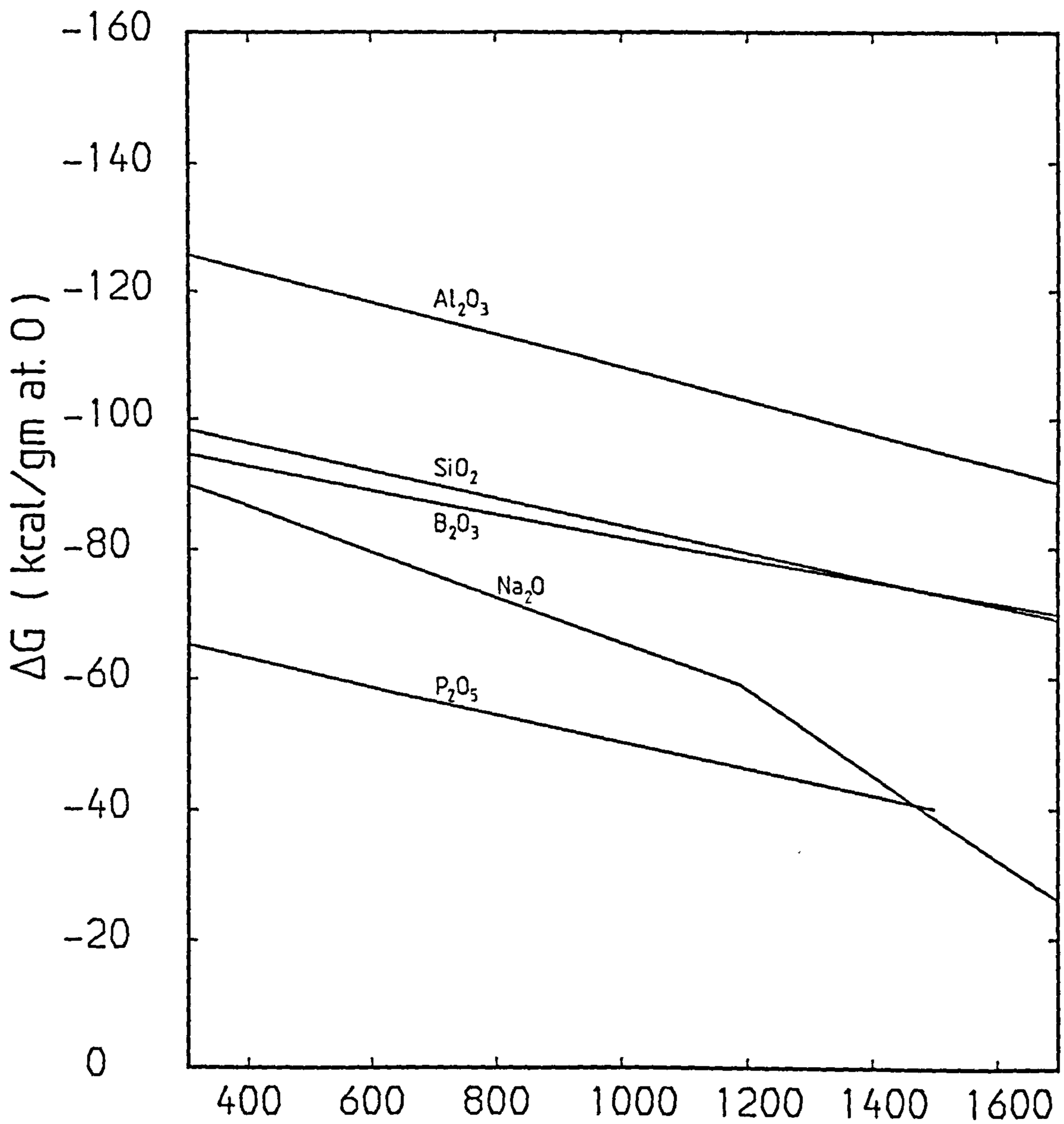

FIGURE 6.3.1

The stability diagram for a few glass forming oxides and Na_2O.

to form $Na_2O.Al_2O_3$ and β-alumina ($Na_2O.11Al_2O_3$) [Anderson (1977)].

Figure 6.3.2 shows the stability diagram for the alkali metal oxides. Apart from Li_2O, all the other alkali metal oxides can be reduced by sodium. From a thorough search through the current A.S.T.M. powder diffraction data file, which can be regarded as a fairly comprehensive source for most known compounds, the formation of mixed oxides between Li_2O and Na_2O having the general formula $aNa_2O.bLi_2O$ has not been reported. This suggests that there is a good chance that other reaction paths besides the redox reaction are also not favoured, and that Li_2O is inert to sodium.

Figure 6.3.3 shows the stability diagram for the alkaline earth metal oxides and, as can be seen, all the free energy curves lie above that for Na_2O. Therefore redox reactions according to equation 6.3.1 are not favoured; and from the A.S.T.M. data file, apart from beryllia which forms $3Na_2O.2BeO$, the formation of mixed oxides between the rest of the alkaline earth oxides and Na_2O has not been reported. Although it has not been possible to calculate ΔG for the reaction

$$5\ BeO + 6\ Na \rightarrow 3\ Na_2O.2BeO + 3\ Be$$

because of the lack of thermodynamic data, it is probably safe to conclude that the oxides MgO, CaO, SrO and BaO do not combine with Na_2O, and that they are resistant to sodium. It is worth noting that these resistant oxides (apart from SrO) are already being used in most of the commercial sodium resistant glasses [Volf (1961), Brit. Patent No. 1204670 (1970)].

The stability diagrams for the group 3B and group 4B metal oxides are shown in figures 6.3.4 and 6.3.5 respectively. The free energy

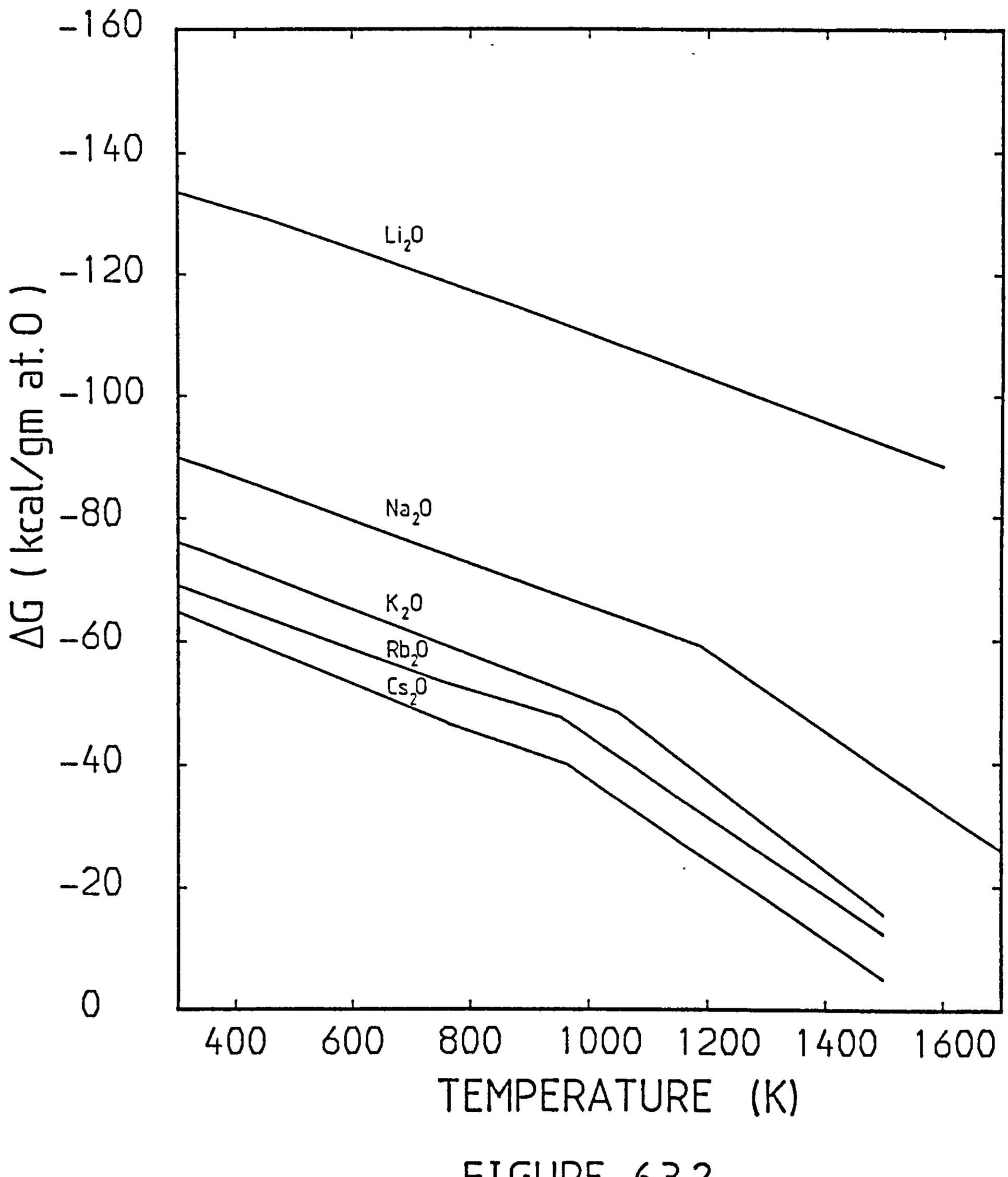

FIGURE 6.3.2

The stability diagram for the alkali metal oxides.

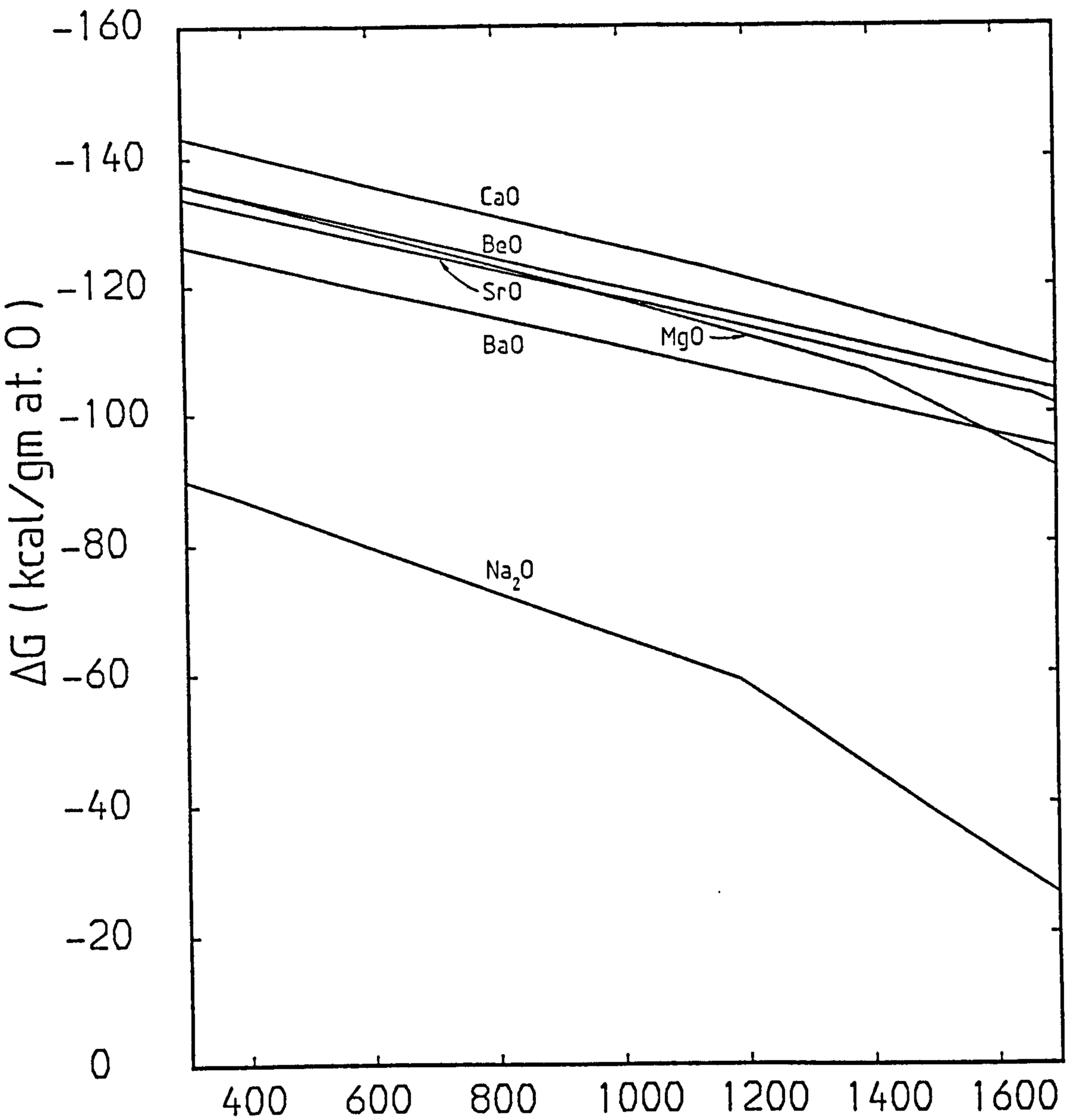

FIGURE 6.3.3

The stability diagram for the alkaline earth metal oxides and Na_2O.

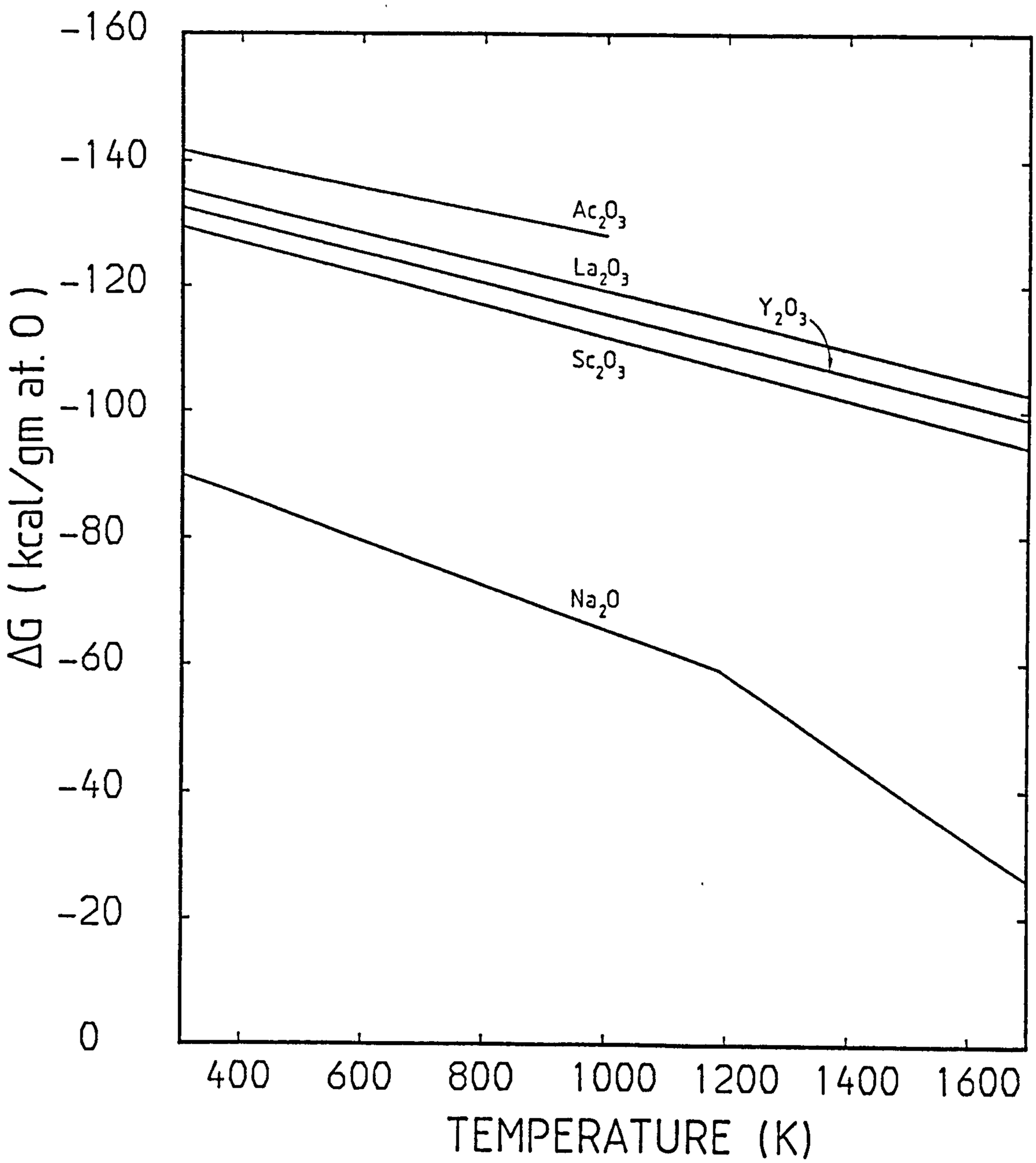

FIGURE 6.3.4

The stability diagram for the group 3B metal oxides and Na_2O.

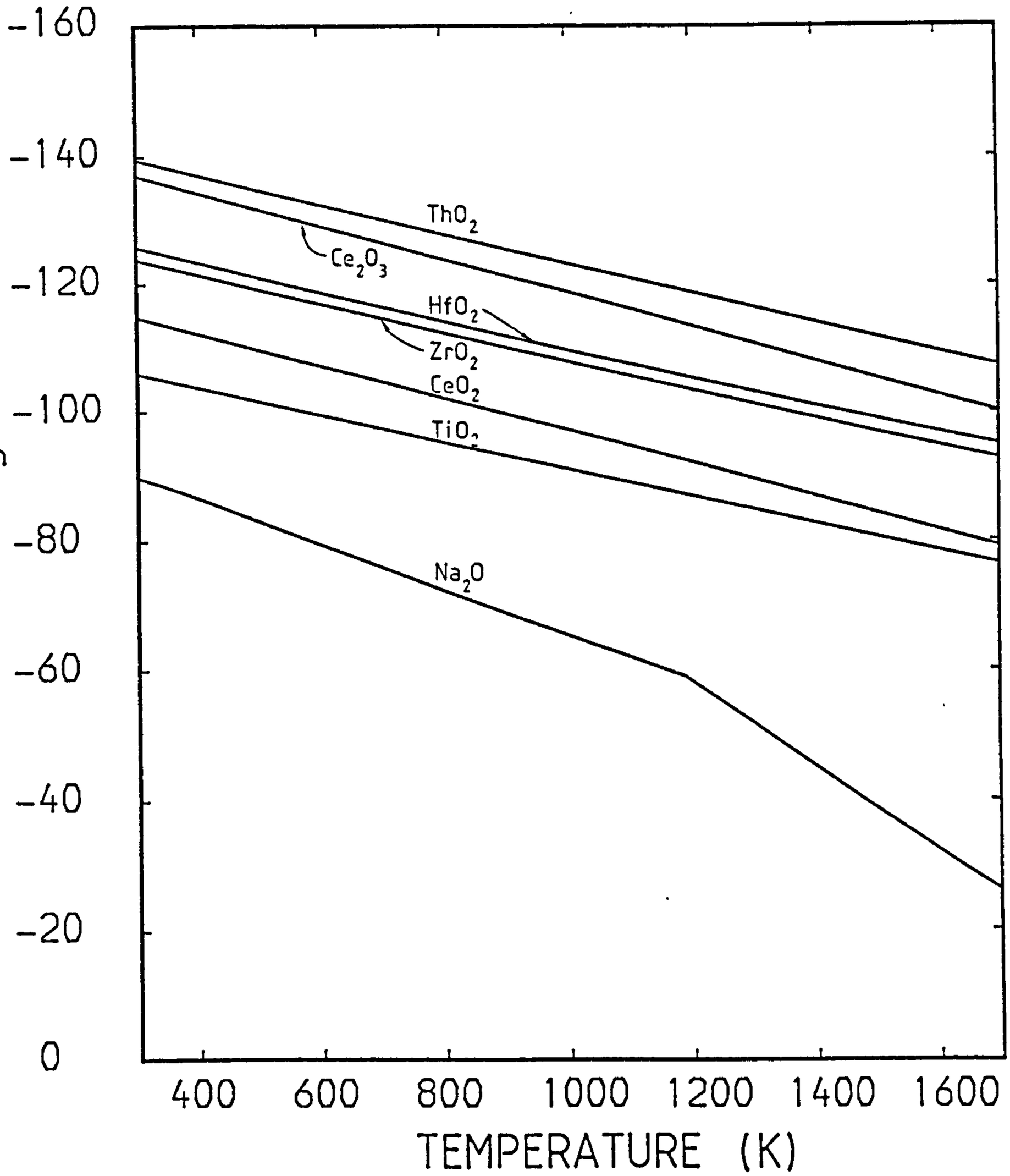

FIGURE 6.3.5

The stability diagram for the group 4B metal oxides and Na_2O.

curves for these two groups of metal oxides lie above that for Na_2O and therefore the redox reaction suggested by equation 6.3.1 is not favoured by these oxides. Of the group 3B metal oxides, only Sc_2O_3 has been found to form $Na_2O.Sc_2O_3$, and of the group 4B metal oxides, compounds of TiO_2, ZrO_2 and ThO_2 having the general formula $aNa_2O.bM_mO_x$ have been reported in the A.S.T.M. data file. The calculation of ΔG for these oxides is again limited by the availability of thermodynamic data, hence it is not possible to assess whether they are resistant to sodium. However, it is probably safe to conclude that alternative reaction paths for the rest of the oxides (Y_2O_3, La_2O_3, Ac_2O_3, HfO_2, CeO_2 and Ce_2O_3) to form compounds with the general formula $aNa_2O.bM_mO_x$ are not favoured since they have not been observed, and that these oxides are inert to sodium.

It has to be admitted that the above selection procedure for suitable materials is fairly crude, and limited to a large extent by the amount of information available. Therefore oxides which are suggested to be either resistant or non-resistant to sodium here can only be truly verified by experiments. It is interesting to add that TiO_2 and ZrO_2 which are suspected to react with sodium were used as nucleating agents in the glass MgBAℓ (3-2) [in 5 mole % additions], and that they were found to have a detrimental effect on the resistance of the glass. Bearing in mind the reservations regarding the present approach, the selection procedure can of course be applied to examining other metal oxides as well as for choosing materials which are resistant to other alkali metals such as lithium and potassium.

The connection between the formation of mixed oxides using the above thermodynamic approach and the discolouration phenomenon discussed in the previous section can be rationalised to some extent. It could be

argued that the discolouration, or the breaking of Si-O bonds to form $Si-O^-$ bonds and E' centres in the case of the silicates, is the incipient stage of the chemical reaction between the material and sodium. As the reaction proceeds towards equilibrium, the formation of a mixed oxide results. In other words, if a material was exposed to sodium at a certain temperature, the discolouration phenomenon would be observed first. At prolonged exposures, the formation of a mixed oxide would result.

Using the silicates studied as supporting evidence, the above suggestion follows from the observation that the discolouration phenomenon, which is a direct consequence of the breaking of Si-O bonds (see section 6.2), can usually be observed even at low exposure temperatures ($\sim 300^{\circ}C$) where the rate of reaction is comparatively show. However, the X-ray results (section 5.2.2) showed that the formation of a mixed oxide, which also requires the breaking of Si-O bonds, only occurred at medium to high exposure temperatures (from $\sim 450^{\circ}C$ upwards) where the rate of reaction is presumably faster.

The reason why the breaking of Si-O bonds occurred at all is because this would lead to an overall reduction in the energy of the system. The bond breaking process, from a macroscopic standpoint, can therefore be described by a negative change in the Gibbs free energy of the system. Hence by examining the change in free energies of the different components in a glass or glass-ceramic in their reaction with sodium, the question of whether the material will be attacked by sodium can be tackled.

The fact that ΔG for the reaction between sodium and the oxide being considered is negative can only mean that the reaction is

favoured, and it does not automatically exclude the material from being utilised. This is because a high energy barrier often exists between the initial and final states, or in other words, the reaction may take a "long time" to reach completion. Notable examples of this are "Lucalox" and some barium borate glasses [Henderson and Marsden (1972)] currently used in high and low pressure sodium lamps respectively, and these lamps have a life expectancy between 5000-10000 hours. The height of this energy barrier or the activation energy is intimately related to the structure of the material, and this was demonstrated clearly in the case of vitreous silica and quartz (see sections 5.1 and 5.3.2). In the present work, the effect on the resistance towards sodium of altering the structure of the glass MgBAℓ (3-2) and the glass CAℓ (6) via crystallisation was investigated.

The crystallisation of a glass would presumably lead to a closer packed arrangement thus increasing the activation energy for the reaction with sodium, or prolonging the time required for the reaction to reach equilibrium. Hence an increase in the resistance is expected and this was indeed observed (see sections 5.1 and 5.3.2). However, in preparing a transparent glass-ceramic suitable for lighting purposes via bulk crystallisation, the volume fraction of crystal phases developed as in the case of MgBAℓ (3-2) was necessarily small ($\sim$ 10 - 20%). Since the reaction with sodium proceeds from the surface, a substantial portion of the glassy phase will still be exposed to sodium, and the increase in resistance was therefore understandably small. To circumvent this problem of transparency or translucency and giving a substantial improvement in the resistance, it was found that surface crystallising a glass, as in the case of

CAℓ(6), where the surface crystal layer acted as a protective skin proved to be an effective solution.

It has to be emphasised that no detailed studies have been made during the course of the present work to relate the rate of reaction with sodium to structural factors such as the free volume available and the packing factor. It is suggested that future work in this area will be of value. Apart from the theoretical interest, a thorough understanding may benefit practical situations such as predicting the period of service that particular materials can provide before losing their integrity.

6.4 Assessment of Materials Developed

The glasses MgBAℓ (3-2) and CAℓ (6) and the transparent glass-ceramics derived from them were developed during the course of the present work, and this final section is devoted to assessing their properties as potential lamp materials. Only a limited number of properties are being considered, they are the chemical compatibility with sodium and the matching of thermal expansions with various metals with the view to forming hermetic glass-to-metal seals.

With regard to the chemical compatibility of MgBAℓ (3-2), it has been shown in section 5.2.2 that the material does indeed react with sodium at ~ 500°C, and from figure 5.1.3, the glass was noticeably discoloured at ~ 400 - 450°C. This however does not preclude the material from being considered since prolonged tests up to ~ 6000 hours carried out by exposing the specimens inside low pressure sodium lamps which operate at ~ 300°C have shown little or no discolouration. Also from figure 5.1.4, the transparent glass-ceramics of

MgBAℓ (3-2) showed marginally higher resistance to sodium than the glass. Therefore the suggested top temperature limits within which the glass and glass-ceramics of MgBAℓ (3-2) are durable to sodium would be ~ 300°C and ~ 350°C respectively. The glass CAℓ (6) did not react with sodium to form mixed oxides under the present exposure conditions (see section 3.2) up to temperatures around 600°C. The glass did however show signs of discolouration at ~ 500°C (see figure 5.1.3), but remained unaffected in prolonged tests at 300°C for ~ 2000 hours. From figure 5.1.4, the glass-ceramics of CAℓ (6) exhibited a substantial improvement from that of the glass and showed little sign of being discoloured at 600°C. In the absence of any further detailed testing, the top temperature limits within which the materials are durable to sodium are suggested as ~ 400°C for the glass and ~ 600°C (or beyond) for the glass-ceramic.

In addition to the chemical compatibility towards sodium, some specimens of MgBAℓ (3-2) which have stood in the laboratory environment for over two years were compared with some freshly prepared samples under a microscope. No observable differences were found, thus suggesting that the glass MgBAℓ (3-2) does not "weather" appreciably. On the other hand, the glass CAℓ (6) is sensitive to water and specimens which have been washed in "hot" water usually showed a thin surface film of calcium hydroxide.

Apart from the chemical compatibility, the ability to bond onto metals is another important aspect. In forming glass-to-metal seals, the close matching of thermal expansions is a basic requirement and deviations in the coefficients should ideally be less than 10%, with that of the metal being higher [Pask (1964)]. From table 4.3.1, the

expansion coefficients of the glass and transparent glass-ceramics of MgBAℓ (3-2) are ~ 5.7 x 10^{-6} $°C^{-1}$ in the range 25 - 550°C. Therefore suitable metals are molybdenum and "Kovar" (Ni-29, Co - 17, Fe - 54), both having a similar coefficient of ~ 5.5 x 10^{-6} $°C^{-1}$ in the range 25 - 500°C [Rulon (1972)]. For the glass CAℓ (6), the expansion coefficient is ~ 8.4 x $10^{-6}°C^{-1}$ in the range 25 - 550°C. Suitable metals are therefore niobium with a coefficient of ~ 7.9 x $10^{-6}°C^{-1}$ at 300°C [Kirby (1963)], rhodium and some nickel-iron alloys (e.g. Ni-46) with coefficients of 8.5 x $10^{-6}°C^{-1}$ and 9.2 x $10^{-6}°C^{-1}$ respectively in the range 25 - 500°C [Rulon (1972)]. It is possible to conclude then that there are a number of metals having similar expansion coefficients to the glasses and glass-ceramics developed. This is however only one aspect of forming glass-to-metal seals. The working ability or the viscosity characteristics of the glasses are also critical and this is an area which has not received much attention here. In order to make successful seals, it is almost certain that further development work will have to be carried out before these materials can be utilised.

To conclude, both the aluminoborates and the aluminates exhibited some advantages and disadvantages. The glass MgBAℓ (3-2) has a lower resistance towards sodium but showed a better working ability. On the other hand, the glass CAℓ (6) can resist sodium attack to higher temperatures, but showed a poor resistance to weathering and poorer working ability. Overall, the materials developed have been much more valuable in illustrating the effects of crystallisation and in particular surface crystallisation.

CHAPTER 7: Conclusions

7.1 General Conclusions

The general aims of this project have been to investigate the fundamental processes which are involved when glasses are brought into contact with sodium, and to examine the different methods of improving the resistance to sodium attack. From the work described in the previous chapters, many of these aims have been realised.

With respect to the discolouration phenomenon caused by exposure to sodium, the silicate glasses have been most intensely studied. From investigations carried out by ESCA, IRRS and ESR, it has been shown that $Si-O^-$ bonds were being formed as sodium attacks the glasses, and that sodium which has diffused into the glass is in an ionic state. Both of these experimental results substantiate the model proposed by Stryjak and McMillan (1979) on the origin of the discolouration. By combining the results from the IRRS and the X-ray studies, the mechanism by which sodium attacks the glasses is visualised as one continuous process of Si-O bonds being broken to form $Si-O^-$ bonds. At some stage when a sufficient number of bonds have been broken, the remaining network could acquire enough freedom to reconstruct to form crystalline compounds.

There are certain aspects of the discolouration phenomenon which have not been clarified such as the peculiar optical absorption and the thermal bleaching behaviour of the discolouration. Despite these shortcomings, the suggested mechanism by which sodium attacks the glasses can explain adequately the higher resistance shown by the sodium silicates and the deterioration in resistance upon small additions of alumina. It was found that the interaction of the simple

borates with sodium showed a striking similarity to that of the simple silicates. This suggests the same mechanism of sodium attack may also apply to the borates. By taking the diborate group as an example, possible models of the discolouration in borates have been suggested.

In attempting to alter the resistance towards sodium attack, two methods have been considered. The first is that of changing the chemical composition by choosing components of the glass which are inert to sodium. The procedure for selecting suitable components is based on an equilibrium thermodynamic argument similar to that used by Elyard and Rawson (1962), and Singh (1976). That is, by considering the change in Gibbs free energy for the possible reactions with sodium. Using this selection procedure, a number of materials have been suggested to be inert to sodium. Since the approach adopted is quite general, the procedure can be applied to selecting materials which are compatible with other alkali metals. With regard to the validity of equilibrium thermodynamics in its application to meta-stable systems, it has been shown, particularly in the case of vitreous silica and quartz, that providing the difference in free energy between the glassy state and its corresponding crystalline state is small as compared to the change in free energy in a reaction with sodium, then equilibrium thermodynamics is applicable.

The second method of altering the resistance towards sodium is by rearranging the structure of a glass via crystallisation. This is assuming that the closer packed structure in the glass-ceramic would lead to an increase in the activation energy, thus decreasing the rate of reaction with sodium. To this end a considerable amount of work

was devoted to studying the crystallisation behaviour and the microstructure of two compositions, MgBAℓ (3-2) and CAℓ (6). The glass MgBAℓ (3-2) was found to crystallise in the bulk and the volume fraction of crystal phases developed in the transparent glass-ceramics ranged from 0 - 20%. The glass CAℓ (6) showed surface crystallisation only, and depending on the heat treatment, the thickness of the surface crystal layer developed on the transparent glass-ceramics ranged from 5 microns upwards. The glass-ceramics of MgBAℓ (3-2) showed only a marginal improvement in the resistance towards sodium as compared with the glass, whilst in the case of CAℓ (6), a substantial increase in the resistance was observed. This is to be expected since the interaction with sodium takes place at the surface, consequently the crystal layer formed on the surface could act as a protective skin for the glass. The conclusion is that surface crystallisation is an effective means of improving the resistance of a glass.

Finally, the potential of the glasses and transparent glass-ceramics developed during the course of this work was assessed. Although the materials are promising in the respect of sodium resistance and having expansion coefficients close to several metals, further development work is necessary before they can be utilised in practical devices.

7.2 Suggestions for Future Work

Much insight has been gained into the fundamental processes which are involved when sodium interacts with a silicate. There are however areas such as the shape of the optical absorption spectrum and the thermal bleaching behaviour of the discolouration which require further clarification. Also, possible models of the discolouration in borates

have been suggested which will require further substantiation. These are obvious directions which future investigations can take.

Of perhaps greater interest, and an area which has not been studied in the present work, is the kinetics of the reaction with sodium. So far, the relationship between the activation energy or the rate of reaction and structural parameters such as the packing factors and free volume available has not been established. Apart from the fundamental interest, work of this kind can be valuable in an applied situation such as predicting the serviceable life time of a material operating under a particular condition. An ideal system for initiating further work will be for example, vitreous silica and the various modifications of silica such as quartz, coesite and stishovite where essentially the same chemical compound possesses a series of different structures. The rates of the reaction could be studied by more direct means such as monitoring the penetration of sodium into the material by Auger electron spectroscopy or secondary ion mass spectrometry, or by less direct means such as measuring the heat evolved in the reaction by DSC.

On an even more applied note, a number of refractory oxides have been suggested to be inert to sodium. It remains to be seen whether these materials can form practical glasses as well as glass-ceramics, or indeed remain resistant to sodium. In view of the commercial interest which could be generated, this is an area of future work which might prove to be rewarding.

APPENDIX I

Theory of Nucleation and Crystal Growth in a Supercooled Liquid

When a glass is heated above its transformation temperature, but below its liquidus temperature, it can be considered as a supercooled liquid. Since the crystallisation of glasses occurs in this temperature range, the classical theories of nucleation and crystal growth are applicable to glasses. The following is a brief outline of the classical theories. However, more comprehensive treatments can be found in Christian (1975), Rawson (1967), Turnbull and Cohen (1960), Bergeron (1972) and McMillan (1979).

The crystallisation of a supercooled liquid is generally thought of as a two step process, the homogeneous or heterogeneous nucleation of stable nuclei of a thermodynamically stable phase and the subsequent growth of these nuclei.

Consider the homogeneous nucleation of a solid phase in a supercooled liquid at constant temperature and pressure. The stability of the solid nuclei depends on the energy balance between the lowering of the energy of the system due to the formation of an equilibrium phase and the energy required to form an interface between the liquid and solid phases. For a spherical particle, the change in free energy can be expressed by

$$\Delta F = 4\pi r^2 \sigma_{Ls} - \frac{4}{3}\pi r^3 \Delta f_v$$

where ΔF is the change in free energy due to the formation of the particle, r is the radius of the particle, σ_{Ls} is the surface free energy per unit area between the liquid and the solid, and Δf_v is the change in volume free energy per unit volume associated with the liquid to solid transformation.

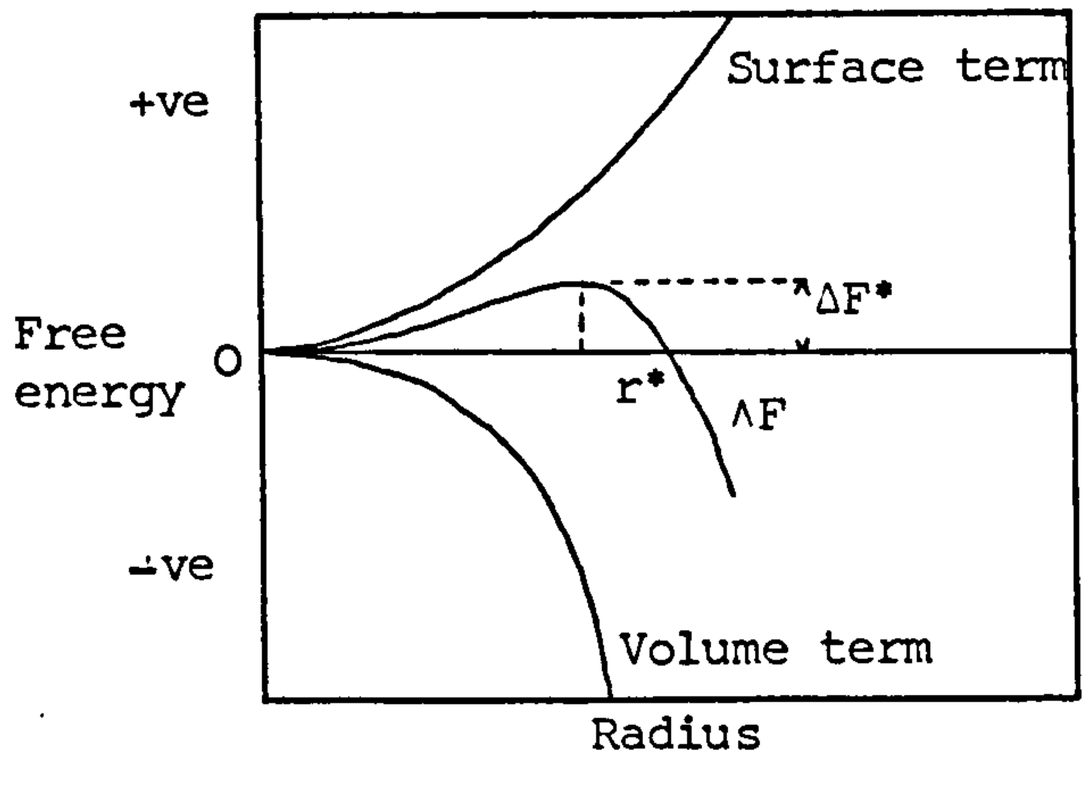

Figure A1.1 Free energy of formation of a spherical solid particle in a supercooled liquid versus the radius of the nucleus.

A critical radius r* exists when

$$\frac{\partial \Delta F}{\partial r} = 0$$

$$\rightarrow \quad r^* = -\frac{2\sigma_{Ls}}{\Delta f_v}$$

From figure A1.1, particles of radius smaller than r* called "embryos" are unstable owing to the decrease in size with the lowering of free energy. Particles of radius greater than r* are called "nuclei" and they are stable since growth is accompanied by a decrease in free energy.

Owing to thermal fluctuations, there is a distribution of particles of different sizes in the supercooled liquid. The probability of the number of particles n_r with a certain radius r being formed is given by

$$n_r = n \exp\left[-\frac{\Delta F}{kT}\right]$$

where n is the total number of atoms or molecules in the liquid. It follows

$$n_{r^*} = n \exp\left[-\frac{\Delta F^*}{kT}\right]$$

and

$$\Delta F^* = \frac{16\pi \sigma_{Ls}^3}{3\Delta f_v^2}$$

where n_{r^*} is the number of particles of critical size and ΔF^* is the change in free energy at the critical radius. The term exp $[-\Delta F^*/kT]$ is called the thermodynamic barrier to nucleation.

Another factor which contributes to the nucleation is that embryos may grow to form nuclei by the addition of atoms or molecules from the surrounding liquid. An atom must acquire an activation energy Q in order to detach itself from the liquid and move to the_solid. The number of times the atom attempts to cross the interface is given by the vibrational frequency υ_o and the probability P of that atom having energy Q is given by

$$P = \exp\left[\frac{-Q}{kT}\right]$$

Only atoms adjacent to the interface can attach themselves to the embryo. If this number is n_s, then the number of atoms crossing the interface per unit time is

$$\frac{dn_i}{dt} = n_s \upsilon_o \exp\left[\frac{-Q}{kT}\right]$$

The term exp [-Q/kT] is called the kinetic barrier to nucleation.

The rate of nucleation I at temperature T is the product of the number of critical size nuclei present per unit volume and the rate at which atoms are attached to the embryos.

$$I = nn_s \upsilon_o \exp\left[\frac{-\Delta F^*}{kT}\right] \exp\left[\frac{-Q}{kT}\right] \qquad (A1.1)$$

The nucleation rate I is very sensitive to variations in temperature. This can be illustrated by considering the free energy of the transformation Δf_v from the liquid to the solid. At constant pressure and assuming the entropy of fusion remains constant with temperature, the variation of Δf_v with temperature is given by

$$\Delta f_v = \Delta H_f \frac{(Tm - T)}{Tm}$$

where ΔH_f is the heat of fusion and Tm is the melting temperature. Therefore,

$$\Delta F^* = \frac{16\pi\sigma_{Ls}^3 \, Tm^2}{3 \, \Delta H_f^2 \, (Tm-T)^2}$$

and

$$I = nn_s \upsilon_o \exp \left[- \frac{16\pi\sigma_{Ls}^3 T_m^2}{3kT\ \Delta H_f^2\ (T_m - T)^2} \right] \exp \left[- \frac{Q}{kT} \right]$$

The dependence of I with $(T_m - T)$ the degree of undercooling is shown in figure A1. 2

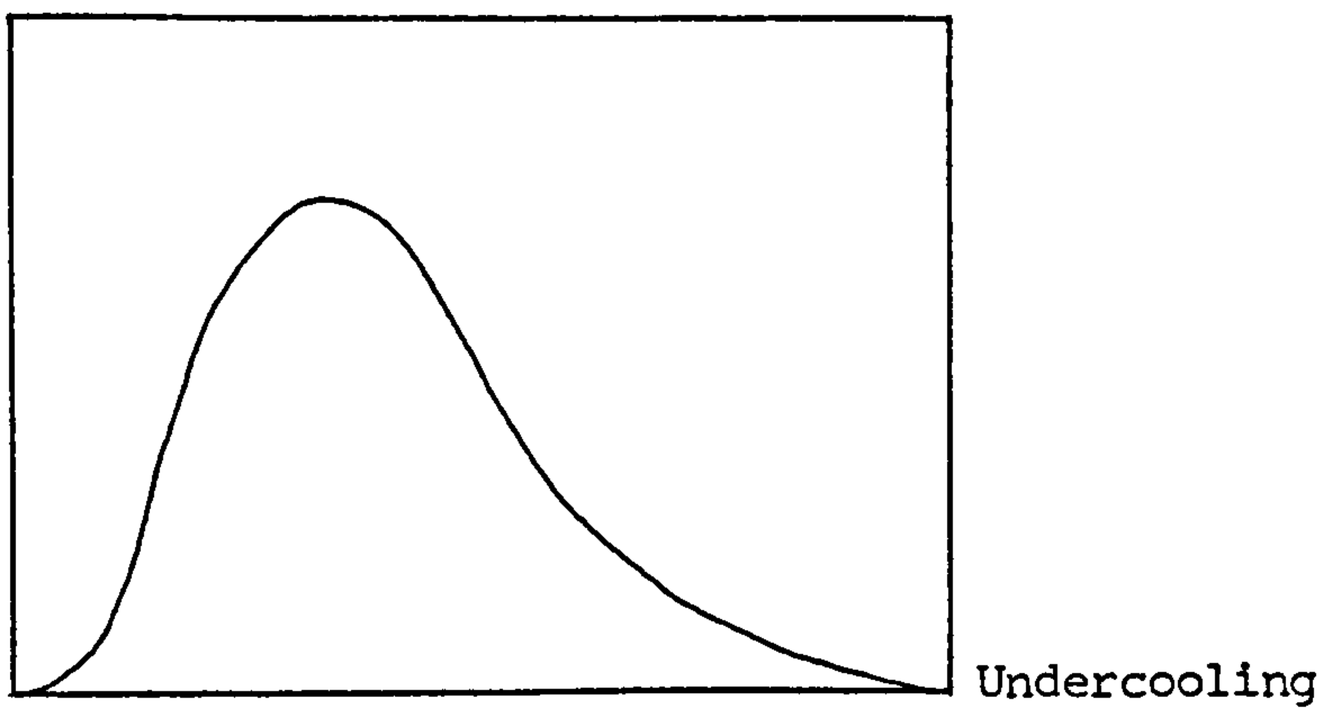

FIGURE A1.2 Variation of rate of nucleation with undercooling.

At small values of undercooling, the first exponential dominates, I increases rapidly due to the change in Δf_v with temperature. With large undercooling, the second exponential dominates and the nucleation rate is controlled by the rate at which atoms arrive at nucleus. This gives rise to a maximum rate of nucleation.

In the case of heterogeneous nucleation, consider the formation of a crystal nucleus in the form of a spherical cap on a solid substrate in contact with a supercooled liquid phase. The free energy change associated with the formation of the two new interfaces is

$$\Delta F_s = \sigma_{Lx} A_{Lx} + \pi r^2 (\sigma_{xs} - \sigma_{Ls})$$

where σ is the free surface energies of the respective interfaces as shown in figure A1.3 and A_{Lx} is the area of the liquid - crystal interface.

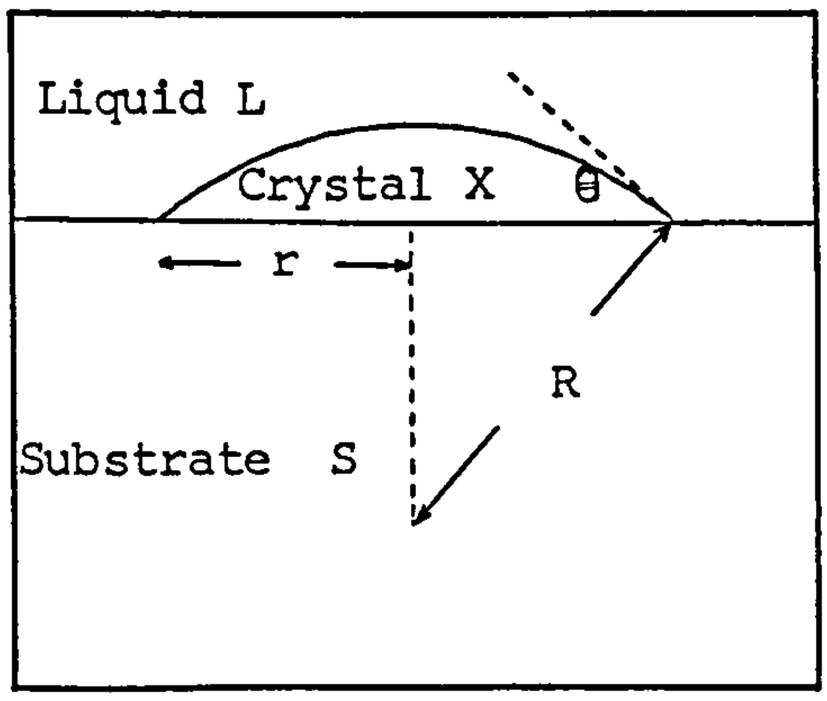

FIGURE A1.3 Schematic representation of a spherical cap formed on a solid substrate within a liquid phase.

If $\sigma_{Ls} > \sigma_{xs}$, then $\Delta F_s < \sigma_{Lx} A_{Lx}$, and the total surface energy required to form the nucleus on the substrate is less than that required for homogeneous nucleation.

The relationship between the contact angle θ and the interfacial energies is

$$\cos\theta = \frac{\sigma_{Ls} - \sigma_{xs}}{\sigma_{Lx}}$$

hence

$$\Delta F_s = \sigma_{Lx} A_{Lx} - \pi r^2 \sigma_{Lx} \cos\theta$$

The volume of the spherical cap is

$$V = \pi r^3 \left[\frac{2 - 3\cos\theta + \cos^3\theta}{3} \right]$$

and the surface area of the cap is

$$A_{Lx} = 2\pi R^2 \ (1-\cos\theta)$$

where

$$r = R \sin\theta$$

The free energy change associated with the transformation of a liquid to a crystal of volume V is

$$\Delta f = V \Delta f_v$$

As before, in the case of homogeneous nucleation

$$R^* = - \frac{2\sigma_{Lx}}{\Delta f_v}$$

$$\rightarrow \qquad r^* = - \frac{2\sigma_{Lx}\sin\theta}{\Delta f_v}$$

The total free energy change due to the formation of the nucleus is then

$$\Delta G^* = \sigma_{Lx} A_{Lx} - \pi r^2 \sigma_{Lx}\cos\theta + V\Delta f_v$$

$$\text{or} \qquad \Delta G^* = \frac{16\pi\sigma_{Lx}^3}{3\ \Delta f_v^2} \left[\frac{(2 + \cos\theta)(1 - \cos\theta)^2}{4} \right] \qquad \text{(A1.2)}$$

The first term on the R.H.S. of equation A1.2 is identical to that for the homogeneous case. When the contact angle is zero, i.e. complete wetting of the substrate by the crystal in the presence of the liquid phase, $\cos\theta = 1$ and $\Delta G^* = 0$. This implies there is no barrier to

nucleation. When the contact angle is π, the second term on the R.H.S. of equation A1.2 is 1 and the situation is identical to the homogeneous case.

Equation A1.2 implies that an effective nucleation catalyst involves a small contact angle and the nucleus-catalyst interfacial energy should be low. The form of the equation for the rate of heterogeneous nucleation is then

$$I = nn_s\upsilon_o \quad \exp\left[\frac{-\Delta G^*}{kT}\right] \exp\left[\frac{-Q}{kT}\right] \qquad (A1.3)$$

The crystallisation of glasses usually occurs by heterogeneous nucleation, proceeding from the surface or impurities or pre-existing surfaces such as container walls, boundaries of a phase separated glass etc.

Once a stable nucleus is formed, growth may proceed by a diffusion like process. Atoms or molecules in the liquid at the interface must acquire an activation energy Q in order to move to the crystal. Therefore, the rate of transfer of atoms from the liquid to the crystal is

$$\frac{dn_{Lx}}{dt} = n_s\upsilon_o \quad \exp\left[\frac{-Q}{kT}\right]$$

and the rate of transfer from the crystal to the liquid is

$$\frac{dn_{xL}}{dt} = n_s\upsilon_o \quad \exp\left[\frac{-(Q + V\Delta f_v)}{kT}\right]$$

The net rate of transfer from the liquid to the crystal is

$$\frac{dn}{dt} = \frac{dn_{Lx}}{dt} - \frac{dn_{xL}}{dt} = n_s\upsilon_o \exp\left[\frac{-Q}{kT}\right]\left[1 - \exp\left(\frac{-V\Delta f_v}{kT}\right)\right]$$

If λ is the increase in length due to the addition of atoms, then the linear growth rate of the nucleus is

$$U = \frac{dn}{dt}\ \frac{\lambda}{n_s} = \lambda \upsilon_o \exp\left[-\frac{Q}{kT}\right]\left[1 - \exp\left(\frac{-V\Delta f_v}{kT}\right)\right] \quad \text{(A1.4)}$$

In the situation where the undercooling is small, $V\Delta f_v$ is small and $-Q/kT$ remains more or less constant. The second exponential term in equation A1.4 can be expanded to first order. Then

$$U \sim \lambda \upsilon_o \exp\left[\frac{-Q}{kT}\right] \frac{V\Delta f_v}{kT}$$

or

$$U \sim \lambda \upsilon_o \exp\left[\frac{-Q}{kT}\right] \frac{\Delta f}{kT}$$

where Δf is the molar free energy change for the transition from the liquid to the solid. Using similar arguments as earlier, by assuming the entropy of fusion ΔS_f is independent of temperature and at constant pressure

$$\Delta f = \Delta S_f\ (Tm-T) = \Delta S_f\ \Delta T$$

where ΔT is the undercooling. Then U becomes

$$U \sim \lambda \upsilon_o \exp\left[\frac{-Q}{kT}\right] \frac{\Delta S_f \Delta T}{kT}$$

Hence for small undercooling, $U \propto \Delta T$.

In the case of large undercooling, Δf_v becomes large. Consequently the term

$$1 - \exp\left[\frac{-V\Delta f_v}{kT}\right] \rightarrow 1$$

then

$$U \sim \lambda \upsilon_o \exp\left[\frac{-Q}{kT}\right]$$

Hence for large undercooling $U \propto e^{1/T}$. The form of U versus temperature is shown in figure A1.4.

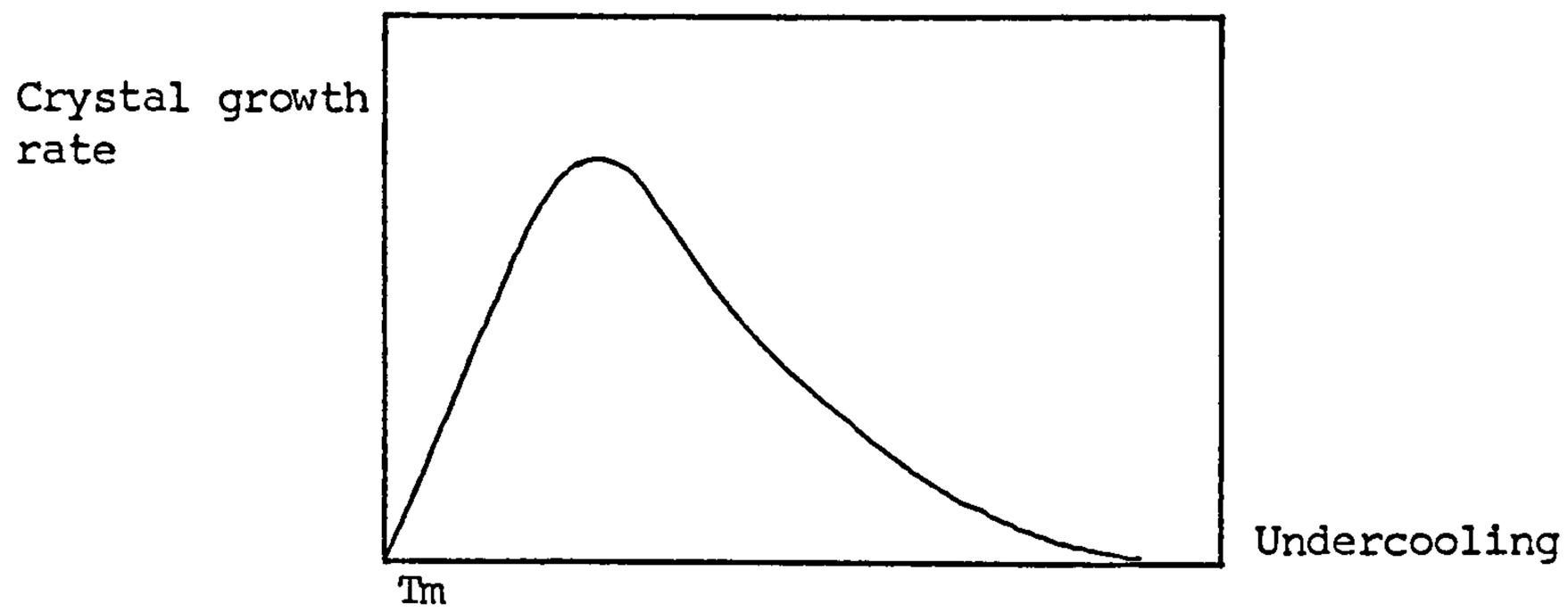

FIGURE A1.4 Variation of crystal growth rate with the degree of undercooling.

It can be seen that there is a maximum rate of crystal growth.

From the point of view of controlling the crystallisation of a glass, it is possible, in principle, to form a glass-ceramic with any desired microstructure by using a two stage heat treatment programme. The first stage of the programme is used to induce the formation of nuclei. By selecting a suitable temperature and heat treating for a convenient length of time, it is possible to control the number of nuclei. By suitable choice of temperature and heat treatment time, the size of the crystals formed can be controlled. In practice though, there is usually an overlap between the rate of nucleation and the crystal growth rate. This then limits the kind of microstructures that can be achieved.

REFERENCES

Akita K and Kase M. (1968), J. Phys. Chem. 72 (3), 906-913.

Andermann G., Caron A, and Dows D.A. (1965), J.O.S.A. 55 (10), 1210-1216.

Anderson N.C. (1977), J. Am. Ceram. Soc. 60, 95.

Andrade E.N. daC. and Tsien L.C. (1937), Proc. R. Soc. A159, 346-354.

Argon A.S. (1959), Proc. R. Soc. A250, 472-481.

Bagley B.G. and Vogel E.M. (1975), J. Non-Cryst. Solids 18, 29-32.

Bates C.W., Helmer J. and Wiechert N. (1972), Solid State Comm. 10, 847-851.

Beall G.H. and Duke D.A. (1969), J. Mat. Sci. 4, 340-352.

Bergeron C.G. (1972), "General Aspects of the Crystallisation of Glass" in "Introduction to Glass Science", 173-196, edit. L.D. Pye, H.J. Stevens and W.C. LaCourse, Plenum Press, New York.

Bishay A. (1970), J. Non-Cryst. Solids 3, 54-114.

Blank J.R. and Gladman T. (1970), "Quantitative Metallography" in "Tools and Techniques in Physical Metallurgy" Vol. 1, edit. F. Weinburg, Marcel Dekker, New York.

Born M and Wolf E. (1965), "Principles of Optics", Pergamon Press, New York.

Bowen D.K. and Hall C.R. (1975), "Microscopy of Materials", MacMillan, London.

Bruckner R., Chun H.U. and Goretzki H. (1978), Proc. Int. Conf. on X-ray and XUV Spectr., Jap. J. Appl. Phys. 17, Suppl. 17-2, 291-294.

Brundle C.R. (1974), J. Vac. Sci. Tech. 11 (1), 212-224.

Budd S.M. (1975), J. Non-Cryst. Solids 19, 55-64.

Burggraaf A.J. and Van Velzen H.C. (1968), J. Am. Ceram. Soc. 52 (5), 238-242.

Burns J.A. (1965), Glass Tech. 6 (1), 17-21.

Castle J.E. and West R.H. (1979), to be published in J.E.S.R.P. (1980), Private Comm.

Castner Jr. T., Newell G.S., Holton W.C. and Slichter C.P. (1960), J. Chem. Phys. 32, 668-673.

Chou C.C.P. and Turnbull D. (1975), J. Non-Cryst. Solids 17, 169-188.

Christian J.W. (1975), "The Theory of Transformations in Metals and Alloys" Part 1, 2nd ed., Pergamon Press.

Clark D.T. (1977), "ESCA Applied to Organic and Polymeric Systems" in "Handbook of X-ray Photoelectron Spectroscopy", 211-247, edit. D. Briggs, Heyden.

Condrate R.A. (1972), "The Infrared and Raman Spectra of Glasses" in "Introduction to Glass Science", 101-135, edit. L.D. Pye, H.J. Stevens and W.C. LaCourse, Plenum Press, New York.

Das G.C., Platakis N.S. and Dever M.B. (1974), J. Non-Cryst. Solids 15, 30-44.

Day D.E. and Rindone G.E. (1962), J. Am. Ceram. Soc. 45 (10), 489-496.

DeHoff R.T. and Rhines F.N. (1968), "Quantitative Microscopy", McGraw Hill, New York.

Delesse M. (1848), Ann. Mines 13, 379.

Donald I.W. and McMillan P.W. (1978), Part 1, J. Mat. Sci. 13, 1151-1176, Part 2, J. Mat. Sci. 13, 2301-2312.

Doremus R.H. (1962), "Diffusion in Non-Crystalline Silicates" in "Modern Aspects of the Vitreous State" Vol. 2, 1-71, edit. J.D. MacKenzie, Butterworths, London.

(1973), "Glass Science", John Wiley & Sons, New York.

(1977), J. Non-Cryst. Solids 25, 263-292.

Elyard C.A. and Rawson H. (1962), Adv. in Glass Tech., 6th Int. Congr. on Glass, Plenum Press, New York.

Ernsberger E.M. (1960), Proc. R. Soc. A257, 213-223.

(1962), Adv. in Glass Tech., 6th Int. Congr. on Glass, Plenum Press, New York.

Escard J.H. and Brion D.J. (1975), J. Am. Ceram. Soc. 58, 296-299.

Evans C.A. and Blattner R.J. (1978), Ann. Rev. Mat. Sci. 8, 181-214.

Feynman R.P. (1965), "Lectures on Physics" Vol. 3, Addison-Wesley, Reading, Mass.

Florinskaya V.A. and Pechenkina R.S. (1963), J. Struct. Chem. 4 (6), 850-860.

Fonda G.R. and Young A.H. (1934), General Electric Rev. 37, 331-337.

Gladman T. and Woodhead J.H. (1969), J.I.S.I. 194, 189.

Gordon J.E., Marsh D.M. and Parratt, M.E.M.L. (1959), Proc. R. Soc. A249, 65-72.

Greenwood N.N. (1973), "The Chemistry of Boron", Pergamon Press.

Gregory A.G. and Veasey T.J. (1972), J. Mat. Sci. 7, 1327-1341.

(1973), J. Mat. Sci. 8, 333-339.

Griffith A.A. (1920), Phil. Trans. R. Soc. A221, 163.

Griscom D.L. (1973/4), J. Non-Cryst. Solids 13, 251-285

(1973) , J. Non-Cryst. Solids 31, 241-266.

Gutzow I. (1972), "The Thermodynamic Functions of Supercooled Glassforming Liquids and the Temperature Dependence of their Viscosity" in "Amorphous Materials", 159-171, edit. R.W. Douglas and B. Ellis, Wiley Interscience, London.

Hanna R. and Su G-J. (1964), J. Am. Ceram. Soc. 47 (12), 597-601.

Hench L.L. (1975), J. Non-Cryst. Solids 19, 27-39.

Henderson S.T. and Marsden A.M. (1972), "Lamps and Lighting", Edward Arnold, London.

Hercules D.M. (1976), Anal. Chem. 48 (5), 294R-313R.

Herzberg G. (1945), "Infra-Red and Raman Spectra of Polyatomic Molecules", Van Nostrand, New York.

Hickmott T.W. (1969), Appl. Phys. Lett. 15, 232-234.

(1971), J. Appl. Phys. 42, 2543-2556.

Hilliard J.E. and Cahn J.W. (1961), Trans. A.I.M.E. 221, 344-352.

Hing P. and McMillan P.W. (1973), J. Mat. Sci. 8, 340-348.

Hoffman J. (1933), Z. Anorg. Chem. 211, 272-276.

Holloway D.G. (1973), "The Physical Properties of Glass", Wykeham Publ. Ltd., London and Winchester.

Houghton J.T. and Smith S.D. (1966), "Infra-Red Physics", O.U.P.

Ihnat M.E. (1962), Tech. Rept. RAD-TM-60-44.

Isard J.O. (1959), J. Soc. Glass Tech. 43 (211), 113-123T.

Jellyman P.E. and Procter J.P. (1955), Trans. Soc. Glass Tech. 39, T137.

Jenkins F.A. and White H.E. (1957), "Fundamentals of Optics" 3rd ed., p.262, McGraw Hill.

Jones G.O. (1971), "Glass" 2nd ed., Science Paperbacks and Chapman and Hall Ltd.

Kirby R.K. (1963), "Thermal Expansion" in "American Institute of Physics Handbook" 2nd ed., 4.65 - 4.76, McGraw Hill.

Klug H.P. and Alexander L.E. (1974), "X-ray Diffraction Procedures for Polycrystalline and Amorphous Materials" 2nd ed., Wiley.

Loudon R. (1973), "The Quantum Theory of Light", O.U.P.

MacKenzie J.D. (1960), "Modern Aspects of the Vitreous State", Vol. 1 - 3, Butterworths, London.

MacKenzie R.C. and Mitchell B.D. (1962), Analyst 87, 420-434.

McIntosh R.M., Turnock A. and Wilburn F.W. (1974), Trans. J. Brit. Ceram. Soc. 73 (4), 117-123.

McMillan P.W. (1979), "Glass-Ceramics" 2nd ed., Academic Press, London.

Matossi F (1949), J. Chem. Phys. 17 (8), 679-685.

Melling R., Wilburn F.W. and McIntosh R.M. (1969), Anal. Chem. 41 (10), 1275-1286.

Moore H. and McMillan P.W. (1956), J. Soc. Glass Tech. 40 (193), 97-138T.

Mott N.F. and Davis E.A. (1971), "Electronic Processes in Non-Crystalline Materials", O.U.P.

Nakamoto K. (1978), "Infra-Red Spectra of Inorganic and Co-ordination Compounds", 3rd ed., J. Wiley and Son, New York.

Nakayama J. (1959), J. Phys. Soc. Jap. 14 (8), 1107-1113.

Orton J.W. (1968), "Electron Paramagnetic Resonance", London Iliffe Books Ltd.

Pake G.E. (1962), "Paramagnetic Resonance", Benjamin, New York.

Pask J.A. (1964), "Glass-Metal Interfaces and Bonding" in "Modern Aspects of the Vitreous State" Vol. 3, 1-28, edit. J.D. MacKenzie, Butterworths, London.

Pickering F.B. (1975), "The Basis of Quantitative Metallography", published by Metals and Metallurgy Trust for the Inst. Met. Tech.

Pye L.D. (1972), "The Vitreous State" in "Introduction to Glass Science", 1-30, Plenum Press, New York.

Pye L.D., Stevens H.J. and LaCourse W.C. (1972), "Introduction to Glass Science", Plenum Press, New York.

Rao C.N.R. and Rao K.J. (1978), "Phase Transitions in Solids", McGraw Hill.

Rawson H. (1967), "Inorganic Glass-Forming Systems", Academic Press, London.

Rosiwal A (1903), Bull. Geol. Soc. Am. 14, 466.

Rulon R.M. (1972), "Glass to Metal Seals" in "Introduction to Glass Science", 661-704, edit. L.D. Pye, H.J. Stevens and W.C. LaCourse, Plenum Press, New York.

Sanders D.M., Person W.B. and Hench L.L. (1972), Appl. Spectros. 26 (5), 530 - 536. (1974), Appl. Spectors. 28 (3), 247-255.

Scott M.G. (1978), J. Mat. Sci. 13, 291-296.

Secrist D.R. and MacKenzie J.D. (1964), "Preparation of Non-Crystalline Solids by Uncommon Methods" in "Modern Aspects of the Vitreous State" Vol. 3, 149-165, edit. J.D. MacKenzie, Butterworths, London.

Sevchenko N.A. and Florinskaia V.A. (1956), Soviet Physics Doklady 1, 508-511.

Siegbahn K. (1967), "ESCA: Atomic Molecular and Solid State Structures by means of Electron Spectroscopy", Nova Acta Regiae Sci. Ups. Ser. 4, Vol. 20.

Simon I. (1959), J.O.S.A. 41, 336-345.

(1960), "Infra-Red Studies of Glass" in "Modern Aspects of the Vitreous State" Vol. 1, 120-151, edit. J.D. MacKenzie, Butterworths, London.

Singh R.N. (1976), J. Am. Ceram. Soc. 59 (3-4), 112-115.

Slichter C.P. (1963), "Principles of Magnetic Resonance", Harper and Row, New York.

Smith D.L. and Natesan K. (1974), Nuclear Tech. 22, 392-404.

Smothers W.J. and Chiang Y. (1958), "Differential Thermal Analysis: Theory and Practice", Chem. Pub. Co., New York.

Stryjak J.A. and McMillan P.W. (1978), J. Mat. Sci. 13, 1275-1281.

(1979), Glass Tech. 20 (2), 53-58.

Stull D.R. and Prophet H. (1971), JANAF Thermochemical Tables, 2nd ed., NBS, Washington, D.C.

Terai R. and Hayami R. (1975), J. Non-Cryst. Solids 18, 217-264.

Thakur R.L. and Thiagarajan S. (1966), Bull. Cent. Glass Ceram. Res. Inst. (Calcutta) 13 (2), 33-45.

Thornburg D.D. and Johnson R.I. (1975), J. Non-Cryst. Solids 17, 2-8.

Trickler M.J. et. al. (a. 1974), J. Non-Cryst. Solids 16, 303-307.

(b. 1974), J. Mat. Sci. 9, 1115-1122.

Turnbull D. and Cohen M.H. (1960), "Crystallisation Kinetics and Glass Formation" in "Modern Aspects of the Vitreous State" Vol. 1, 38-62, edit. J.D. MacKenzie, Butterworths, London.

Volf M.B. (1961), "Technical Glasses", Isaac Pitman and Sons, London, and SNTL, Publishers of Technical Literature, Prague.

Wagner C.D. (1977), "The Role of Auger Lines in Photoelectron Spectroscopy" in "Handbook of X-ray Photoelectron Spectroscopy", 249-272, edit. D. Briggs, Heyden.

Wagner C.D., Ashley Taylor J. (1979), submitted to J. Elect. Spectros. Relat. Phenom.

Wagner C.D. and Biloen P. (1973), Surf. Sci. 35, 82-95.

Wagner C.D., Gale L.H. and Raymond R.H. (1979), Anal. Chem. 51 (4), 466-

Ware R.K. (1971), "Thermal Analysis" in "Characterisation of Ceramics", 273-305, edit. L.L. Hench and R.W. Gould, Marcel Dekker, New York.

Weast R.C. (1977), "CRC Handbook of Chemistry and Physics" 58th ed., CRC Press.

Weeks R.A. and Nelson C.M. (1960), J. Am. Ceram. Soc. 43, 399-404.

Wheeldon J.W. (1959), Brit. J. Appl. Phys. 10 (6), 295-298.

Williams R.H. (1978), Contemp. Phys. 19 (5), 389-414.

Wong J. and Angell C.A. (1971), Appl. Spectros. Rev. Vol. 4, edit. E.D. Brame, Marcel Dekker, New York.

(1976), "Glass Structure by Spectroscopy", Marcel Dekker, New York.

Ziman J.M. (1964), "Principles of the Theory of Solids", C.U.P.